# ANTIMICROBIAL PEPTIDES FROM MARINE FISHES: MOLECULAR CHARACTERIZATION AND EVALUATION OF BIOACTIVE POTENTIAL

*Thesis submitted to*

*Cochin University of Science and Technology*

*in Partial Fulfilment of the Requirements for*

*the Award of the Degree of*

*Doctor of Philosophy*

*in*

*MARINE MICROBIOLOGY*

*Under the Faculty of Marine Sciences*

*By*

**AISHWARYA NAIR**

**Reg. No. 4539**

**DEPARTMENT OF MARINE BIOLOGY, MICROBIOLOGY AND BIOCHEMISTRY**

**SCHOOL OF MARINE SCIENCES**

**COCHIN UNIVERSITY OF SCIENCE AND TECHNOLOGY**

**KOCHI –682 016, INDIA**

**March 2018**

# Antimicrobial Peptides from Marine Fishes: Molecular Characterization and Evaluation of Bioactive Potential

*Ph.D. Thesis in Marine Microbiology under the Faculty of Marine Sciences*

*Author*

**Aishwarya Nair**
Research Scholar
Department of Marine Biology, Microbiology and Biochemistry
School of Marine Sciences
Cochin University of Science and Technology
Kochi – 682 016

*Supervising Guide*

**Dr. Rosamma Philip**
Professor
Department of Marine Biology, Microbiology and Biochemistry
School of Marine Sciences
Cochin University of Science and Technology
Kochi – 682 016

Department of Marine Biology, Microbiology and Biochemistry
School of Marine Sciences
Cochin University of Science and Technology
Kochi – 682 016

March 2018

*Dedicated to...*

*My family.....*

**Department of Marine Biology, Microbiology and Biochemistry**
**School of Marine Sciences**
**Cochin University of Science and Technology**
**Kochi – 682 016**

**Dr. Rosamma Philip**
Professor

# Certificate

This is to certify that the thesis entitled **"Antimicrobial Peptides from Marine Fishes: Molecular Characterization and Evaluation of Bioactive Potential"** is an authentic record of research work carried out by **Ms. Aishwarya Nair** under my supervision and guidance in the Department of the Marine Biology, Microbiology and Biochemistry, School of Marine Sciences, Cochin University of Science and Technology, in partial fulfilment of the requirements of the degree of **Doctor of Philosophy** in **Marine Microbiology** under the Faculty of Marine Sciences of Cochin University of Science and Technology, and no part thereof has been presented for the award of any other degree, diploma or associateship in any University or Institution. All the relevant corrections and modifications suggested by the audience during the pre-synopsis seminar and recommended by the Doctoral Committee have been incorporated in the thesis.

Kochi - 16
March 2018

**Prof. (Dr.) Rosamma Philip**
(Supervising Guide)

# *Declaration*

I hereby declare that the thesis entitled **"Antimicrobial Peptides from Marine Fishes: Molecular Characterization and Evaluation of Bioactive Potential"** is a genuine record of research work done by me under the supervision and guidance of **Dr. Rosamma Philip**, Professor, Department of Marine Biology, Microbiology and Biochemistry, Cochin University of Science and Technology and no part thereof has been presented for the award of any other degree, diploma or associateship in any University or Institution earlier.

Kochi - 16
March 2018

**Aishwarya Nair**

# Acknowledgement

*Prima Facie, I am grateful to God for the good health and wellbeing that were necessary to complete this thesis.*

*This Ph.D. thesis represents not just the work on the keyboard but rather is an accomplishment of a long cherished dream right from the start of my graduation degree. Many have been part of this milestone and I truly wish to share my success with them. Without them, my work would have never been completed in no more than five years. I thank and respect them throughout my life.*

*At this moment of fulfilment, I am greatly indebted to my advisor and research guide, Prof. Dr. Rosamma Philip, for being an incredible mentor to me. Dear Mam, it is so difficult to convey in short words what you have done for me. As customary in Indian tradition, I take this opportunity to touch my dear mentors feet and seek blessings for not only helping me in the past few years but also for all the years to come. The joy and enthusiasm you have shown for the research was contagious and motivational for me, even during the tough times of my Ph.D. pursuit. I successfully have overcome many difficulties and learnt a lot under your guidance. I honestly value all your contributions of time and ideas to make my Ph.D. experience productive and stimulating. I am also thankful for the excellent example you have provided as a successful woman scientist and professor. Your advice on both research as well as on my life have been priceless. You have taught me another aspect of life, that, "goodness can never be defied and good human beings can never be denied". I am glad that I could be one among the many students who has enjoyed the comfort under your guidance. For all these, I sincerely thank you from the bottom of my heart and will be truly indebted to you throughout my life time.*

*I would like to express my special appreciation and thanks to Dr. I. S. Bright Singh, Coordinator, UGC-BSR- Faculty and Former Coordinator, National Centre for Aquatic Animal Health, for his guidance, encouragement and help and for the requisite institutional facilities throughout my research tenure. I am also grateful for his positive appreciation and counsel throughout the course of the investigations which led to the successful completion of the research work.*

*My sincere gratitude to Dr. Sajeevan T. P., Assistant Professor, National Centre for Aquatic Animal Health, for the enough kindness offered and for his valuable advice, constructive criticism, and encouragement.*

*No research is possible without the required infrastructure, resource and funding. For this, I extend my sincere thanks to - Basic Scientific Research wing of University Grants Commission, Delhi and Cochin University of Science and Technology for providing me research fellowship to carry out my research.*

*I would like to express my sincere thanks to The Head, Department of Marine Biology, Microbiology and Biochemistry, for all the help and support extended to me throughout the research period. I also express my heart felt gratitude to the Dean and Director, School of Marine Sciences, CUSAT for all the help rendered and facilities provided for research.*

*I am grateful to all my beloved teachers in the Dept. for their care and encouragement. I thank (Prof.) Dr. Babu Philip (Rtd.), (Prof.) Dr. A.V. Saramma (Rtd.), (Prof.) Dr. A. A. Mohamed Hatha, (Prof.) Dr. Aneykutty Joseph, (Prof.) Dr. S. Bijoy Nandan, Dr. Swapna P. Antony, Dr. Priyaja P. and Dr. K. B. Padmakumar, for their valuable advice, suggestion and support. I am also greatly indebted to all my teachers in the past who have built self-discipline in me and have continually inspired me to do my best and have helped me strive my goals.*

*All the Non-teaching staffs (library staffs, lab assistants and technical staffs) of the Dept. of Marine Biology, Microbiology and Biochemistry have helped me and thanks are due to all of them for their timely contributions in particular, Section officer- Asha Madam, Jismon Chettan, Laly chechi, Saify Chettan and Lakshmi Chechi, who have been supportive in every way they could.*

*A big thanks goes to Dr. Swapna P. Antony. She was always there to meet and talk about my ideas, to proofread and to mark up my papers and chapters in the thesis. Her own zest for perfection, passion and conviction has always inspired me to do more in research. Special thanks to Dr. Jayesh P. not only for his insightful comments and encouragement, but also for the hard questions which incented me to widen my research. I am grateful to him for teaching me the basics of real time expression analysis. I also acknowledge him for showing me different ways to approach a research problem and the need to be persistent to accomplish any goal.*

*My time at CUSAT was made enjoyable at large due to many friends and groups that became a part of my life. I greatly appreciate and acknowledge the support of members of the RP's cavalry, including Dr. Swapna P. Antony, Dr. Chaithanya E. R., Dr. Naveen Sathyan, Dr. Afsal V. V., Anilkumar P.R., Jini Jacob, Sruthy K. S., Archana K., Neema Job, Divya T. Babu, Jayanath G., Wilsy Munna, Deepthi Augustine, Sephy Rose Sebastian, Bhavya K., Manomi S., Jimly C. J. and Ramya K. D. Other past and present group members that I*

*have had the pleasure to work with or alongside of are Dr. Smitha C. K., Dr. Preetha Shenoy, Dr. Anju Antony, Anju M. V., Dhanya Kesavan., Athira P. P., Anooja V. V and Revathi M. R. They have contributed immensely to both my personal and professional time at CUSAT. The group has been a source of friendship as well as good advice and collaboration.*

*It's my fortune to gratefully acknowledge my senior AMP team members, Swapna Chechi, Chaithanya, Naveen Chettan and Afsal Chettan for their support and generous care. They were the ones who introduced me to the molecular biology lab and the AMP research world. I thank all of them for the sleepless nights we were working together before deadlines, and for the stimulating discussions. I also owe many thanks to them for making the lab a wonderful workplace and a second home for me. My experience at CUSAT has been nothing short of amazing because of the companionship of Sruthy, whom I consider my best friend, ever since my first day at lab. Though she was younger to me, she was indeed the most mature and responsible person who led our group. She was also the care taker of my health who always insisted me to drink more water during my work hours and who kept track of my health. She was always beside me during the happy and hard moments to push me and motivate me.*

*A journey becomes a lot easier when you travel together. Interdependence is certainly more valuable than independence. I owe a special mention to Neema Chechi for sharing her experience of the thesis writing endeavour with me, for listening to my complaints and frustrations, and for believing in me. Thanks a lot for being a true elder sister for me.*

*I am also grateful for the time spent with my fellow mates (Anju, Dhanya, Anooja, Dr. Priyaja and Dr. Smitha B. R) for all the fun we had during our cruise trip. I would definitely miss our interesting and long-lasting chats. Thanks for providing me fond memories to cherish for ever.*

*Special thanks are extended to the UGC-BSR fellow members, Reshma Silvester, Jabir, Lakshmi and Sreelakshmi for all the support and help offered.*

*I would like to acknowledge all research scholars of Marine Biology Department for their co-operation and support. Also I like to extend my gratitude to research scholars of NCAAH, especially to Dr. Shalini, Ramya Chechi, Soumya, Bhoopal and Vinusree for their help and assistance.*

*Special thanks are extended to Rithin Raj for designing the cover page of the thesis and Mr. Binoop Kumar, Indu Photos, for the thesis outlay and for his excellent professional work. I also recognize the support from Mr. Vishnu,*

*Technical Staff, Maharajas College, for his help in taking the Electron Microscope images of the bacterial samples.*

*Words fail me to express my gratitude to my family, where the most basic source of my life energy resides. I especially thank my Achan and Amma, Mr Vijayan P. Nair and Mrs Ambika Vijayan, for being unique in many ways and for being a stereotype of a perfect family. I bow before u for the selfless love, care, pain and sacrifice you underwent to shape my life. You were all eager to know what I was doing and how I was proceeding, though you hardly understood what I researched on. I still cherish your screams of joy whenever a significant momentous was reached. I love you a lot and I doubt whether I will ever be able to pay back the love and affection showered upon by you. Also I express my thanks to my dear brother, Mithun, for his sincere support and valuable prayers. I am also grateful to all my Kalangad and Vijayamangalam family members for making an amazing family. I especially like to thank my (eternal) Gopalakrishnan ammavan, Aravindakshan ammavan, Sudhakaran ammavan, Vijayan ammavan, Shyamala velyamma, Jayan ammavan, Anil ammavan, Pushpa ammayi and my wonderful dear cousins for their moral support, affection, and blessings.*

*My heart felt regards goes to my in-laws, Mr Aravindan N.S, Mrs Rajalakshmy Aravindan, Vinod P and Anju Vinod and the little Adi, who supported me in every way possible to see the completion of this work. I am extremely grateful for the blessings of my beloved Muthazhee (Janakiamma), who have completed 9 decades recently. I consider myself the luckiest in the world to have such a lovely and caring family, standing beside me with their love and unconditional support.*

*Finally, I owe, thanks to the most special person in my life, my husband, Ajith, for his continued unfailing love and support. His support and understanding have truly made the completion of this thesis possible. He was there for me when I thought it was impossible to continue and his help to keep things in perspective is highly treasured. I greatly value your contribution and deeply appreciate his belief in me.*

*Last but not the least; I thank all the people who have supported me to complete the research work directly or indirectly.*

*Aishwarya Nair*

# Contents


*Chapter* 1

**GENERAL INTRODUCTION..... 01 - 37**

1.1 Introduction ..... 01
1.2 Classification of AMPs ..... 03
1.2.1 AMPs with an α-helical structure ..... 03
1.2.2 AMPs with β sheet structure ..... 04
1.2.3 AMPs with a looped structure ..... 05
1.2.4 AMPs with an extended structure ..... 05
1.3 Physicochemical parameters of AMP ..... 06
1.3.1 Charge (Q) ..... 06
1.3.2 Length ..... 07
1.3.3 Amphipathicity (A) and hydrophobic Moment ($M_H$) ..... 07
1.3.4 Hydrophobicity (H) ..... 08
1.3.5 Polar angle (θ) ..... 08
1.4 Mechanistic classes of AMPs ..... 09
1.4.1 Membrane active AMPs ..... 11
14.2 Non-membrane active AMPs ..... 12
1.5 Multifaceted roles of AMPs ..... 14
1.5.1 Antibacterial Peptides ..... 14
1.5.2 Antiviral Peptides ..... 15
1.5.3 Antifungal Peptides ..... 17
1.5.4 Antiparasitic Peptides ..... 17
1.5.5 Anticancer and Antitumor peptides ..... 18
1.6 Resistance mechanisms against AMPs ..... 19
1.7 Strategies for the production of AMPs ..... 20
1.8 Marine fish AMPs and their importance ..... 23
1.8.1 Families of fish AMPs ..... 24
1.8.1.1 Piscidins ..... 25
1.8.1.2 β-defensins ..... 27
1.8.1.3 Cathelicidins ..... 29
1.8.1.4 Hepcidins ..... 31
1.8.1.5 Histone derived peptides ..... 32
1.8.2 Fish AMPs in therapeutics ..... 33
1.9 Significance and objectives of the study ..... 35

*Chapter* 2

**MOLECULAR CHARACTERIZATION, RECOMBINANT PRODUCTION AND FUNCTIONAL ANALYSIS OF A NOVEL HEPCIDIN FROM *LEIOGNATHUS EQUULUS* ..... 39 - 111**

2.1 Introduction ..... 39

2.2 Materials and Methods ..... 47
2.2.1 Experimental organism ..... 47
2.2.2 Precautions for RNA preparation ..... 47
2.2.3 Tissue processing ..... 49
2.2.4 RNA isolation ..... 49
2.2.5 Determining quality and quantity of RNA ..... 50
2.2.6 cDNA synthesis ..... 50
2.2.7 PCR amplification ..... 50
2.2.8 Agarose gel electrophoresis ..... 51
2.2.9 Cloning of PCR product ..... 52
2.2.9.1 Ligation of the PCR product ..... 52
2.2.9.2 Competent cell preparation ..... 53
2.2.9.3 Transformation into *E. coli* DH5α ..... 53
2.2.9.4 Confirmation of gene inserts ..... 54
2.2.9.5 Plasmid extraction ..... 54
2.2.10 Plasmid sequencing ..... 55
2.2.11 Sequence characterization and phylogenetic analysis ..... 56
2.2.12 Selection of target gene for recombinant expression ..... 58
2.2.13 Details of expression vector: pET-32a(+) ..... 58
2.2.14 Designing of primers for cloning into expression vector ..... 59
2.2.15 PCR amplification of mature peptide ..... 60
2.2.16 Restriction digestion ..... 60
2.2.17 Purification of restriction digested insert and expression vector ..... 61
2.2.18 Construction of recombinant expression vector and transformation into *E. coli* DH5α competent cells ..... 62
2.2.19 Plasmid extraction and sequencing ..... 62
2.2.20 Transformation into expression host, *E. coli* Rosetta-gami™ B (DE3) pLysS ..... 63
2.2.20.1 Selection and characteristics of expression host ..... 63
2.2.20.2 Transformation into expression host ..... 64
2.2.21 Induction and expression of fusion protein ..... 64
2.2.22 SDS-PAGE analysis of the recombinant protein ..... 65
2.2.23 Western blotting ..... 66
2.2.24 Scale-up production of r*Le*-Hepc mature peptide ..... 67
2.2.25 Affinity purification of recombinant protein ..... 67
2.2.26 Concentration and re-folding of the recombinant protein ..... 68
2.2.27 Quantification of recombinant protein ..... 68
2.2.28 Haemolytic activity of recombinant proteins ..... 69
2.2.29 *In vitro* cytotoxicity assay ..... 70

2.2.30 Antimicrobial assay ..... 71
2.2.30.1 Broth microdilution assay ..... 72
2.2.30.2 Bactericidal assay ..... 73
2.2.30.3 Bacterial membrane permeability assay/ (Propidium Iodide (PI) uptake assay) ..... 73
2.2.30.4 Scanning electron microscopy imaging ..... 74
2.3 Results ..... 75
2.3.1 Molecular characterization of hepcidin from *Leiognathus equulus* ..... 75
2.3.1.1 PCR amplification, TA cloning and sequencing of *Le*-Hepc ..... 75
2.3.1.2 Sequence characterization and phylogenetic analysis using bioinformatics tools ..... 77
2.3.2 Recombinant production and functional characterization of *mLe*H ..... 87
2.3.2.1 PCR amplification and cloning of the target gene with restriction sites ..... 87
2.3.2.2 Restriction enzyme digestion and cloning of target gene into pET-32a(+) expression vector ..... 88
2.3.2.3 Recombinant expression of *mLe*H as fusion protein ..... 90
2.3.2.4 Purification, refolding and quantification of the recombinant protein ..... 92
2.3.2.5 *In vitro* cytotoxicity and haemolytic activity of the recombinant proteins ..... 93
2.3.2.6 Antimicrobial activity ..... 95
2.3.2.7 PI staining ..... 99
2.3.2.8 SEM analysis ..... 101
2.4 Discussion ..... 102

*Chapter* 3
**MOLECULAR CHARACTERIZATION, RECOMBINANT PRODUCTION AND FUNCTIONAL ANALYSIS OF HISTONE DERIVED PEPTIDE FROM *MUGIL CEPHALUS* ..... 113 - 162**
3.1 Introduction ..... 113
3.2 Materials and Methods ..... 121
3.2.1 Experimental organism ..... 121
3.2.2 Precautions for RNA preparation ..... 121
3.2.3 Processing of the tissue ..... 121
3.2.4 RNA isolation ..... 122
3.2.5 Determining quality and quantity of extracted RNA ..... 122
3.2.6 cDNA synthesis ..... 122
3.2.7 PCR amplification ..... 122

3.2.8 Agarose gel electrophoresis ..... 123
3.2.9 Cloning of PCR product ..... 123
3.2.10 Sequence characterization and phylogenetic analysis ..... 124
3.2.11 Selection of active peptide region for recombinant expression ..... 124
3.2.12 Designing of primers for cloning into expression vector ..... 124
3.2.13 PCR amplification of mature peptide ..... 125
3.2.14 Restriction digestion ..... 125
3.2.15 Purification of restriction digested insert and expression vector ..... 126
3.2.16 Construction of recombinant expression vector and transformation into *E. coli* DH5α competent cells ..... 126
3.2.17 Plasmid extraction and sequencing ..... 127
3.2.18 Transformation into expression host ..... 127
3.2.19 Induction and expression of pET-*Mc*-His fusion protein ..... 127
3.2.20 SDS-PAGE analysis of the recombinant protein ..... 128
3.2.21 Western blotting ..... 128
3.2.22 Scale-up production of r*Mc*-His fusion protein ..... 128
3.2.23 Affinity purification of recombinant *Mc*-His ..... 128
3.2.24 Concentration and re-folding of recombinant *Mc*-His ..... 129
3.2.25 Quantification of recombinant *Mc*-His ..... 129
3.2.26 Haemolytic activity of recombinant *Mc*-His ..... 129
3.2.27 *In vitro* cytotoxicity assay ..... 129
3.2.28 Antimicrobial assay ..... 129
3.3 Results ..... 130
3.3.1 Molecular characterization of a histone derived peptide from *Mugil cephalus* ..... 130
3.3.1.1 PCR amplification, TA cloning and sequencing ..... 130
3.3.1.2 Sequence characterization and phylogenetic analysis ..... 131
3.3.2 Recombinant production and functional characterization of *Mc*-His ..... 139
3.3.2.1 PCR amplification and cloning of *Mc*-His with restriction sites ..... 139
3.3.2.2 Restriction enzyme digestion and cloning into pET-32a(+) expression vector ..... 140
3.3.2.3 Recombinant expression of *Mc*-His as fusion protein ..... 142
3.3.2.4 Purification, refolding and quantification of the recombinant protein ..... 143
3.3.2.5 *In vitro* cytotoxicity and haemolytic activity of r*Mc*-His ..... 144
3.3.2.6 Antimicrobial activity ..... 146
3.3.2.7 PI staining ..... 150
3.3.2.8 SEM analysis ..... 151
3.4 Discussion ..... 153

*Chapter* 4
**MOLECULAR CHARACTERIZATION AND FUNCTIONAL ANALYSIS OF HISTONE H2A DERIVED SYNTHETIC PEPTIDE OF *ETROPLUS MACULATUS* .....163 - 218**
4.1 Introduction ..... 163
4.2 Materials and Methods ..... 170
4.2.1 Experimental organism ..... 170
4.2.2 Precautions for RNA preparation ..... 170
4.2.3 Processing of the tissue ..... 170
4.2.4 Total RNA isolation ..... 171
4.2.5 Quality assessment and quantification of RNA ..... 171
4.2.6 cDNA synthesis ..... 171
4.2.7 PCR amplification ..... 172
4.2.8 Agarose gel electrophoresis ..... 172
4.2.9 TA cloning of amplicons and sequencing ..... 172
4.2.10 Sequence characterization and phylogenetic analysis ..... 173
4.2.11 Peptide synthesis ..... 173
4.2.12 Mass spectrometry analysis of the synthetic peptide ..... 174
4.2.13 Purity determination of synthetic peptide using HPLC ..... 174
4.2.14 Haemolytic activity ..... 175
4.2.15 Antimicrobial activity ..... 175
4.2.16 DNA binding assay ..... 175
4.2.17 Anticancer activity ..... 176
4.2.17.1 *In vitro* cytotoxicity assay ..... 176
4.2.17.2 Gene expression analysis using real-time reverse-transcription polymerase chain reaction (RT-PCR) ..... 177
4.3 Results ..... 180
4.3.1 PCR amplification and TA cloning and sequencing ..... 180
4.3.2 *In silico* sequence analysis and characterization ..... 182
4.3.3 Peptide synthesis and functional characterization of *Em*-His2 ..... 189
4.3.4 Molecular mass determination and purity check of synthetic *Em*-His2 ..... 189
4.3.5 Haemolytic activity ..... 191
4.3.6 Antimicrobial activity ..... 191
4.3.7 PI staining ..... 196
4.3.8 SEM analysis ..... 198
4.3.9 DNA Binding assay ..... 200
4.3.10 *In vitro* cytotoxicity assay ..... 200
4.3.11 Anticancer activity ..... 202

4.3.11.1 Relative gene expression analysis of cancer related genes in *Em*-His2 treated NCI-H460 cell line ..... 202
4.3.11.2 Relative gene expression analysis of cancer related genes in *Em*-His2 treated HEp-2 cell line ..... 205
4.4 Discussion ..... 207

*Chapter* **5**
**MOLECULAR CHARACTERIZATION AND FUNCTIONAL ANALYSIS OF HISTONE H2A DERIVED SYNTHETIC PEPTIDE OF *HIMANTURA PASTINACOIDES* ..... 219 - 263**
5.1 Introduction ..... 219
5.2 Materials and Methods ..... 223
5.2.1 Peptide used for the study ..... 223
5.2.2 *In silico* analysis of the properties of the synthetic peptide *Hp*-His ..... 224
5.2.3 HPLC purity determination of synthetic peptide ..... 224
5.2.4 Mass spectrometry analysis of the synthetic peptide ..... 225
5.2.5 Haemolytic activity of the synthetic peptide ..... 225
5.2.6 Antimicrobial activity ..... 225
5.2.7 DNA binding assay ..... 226
5.2.8 Anticancer activity ..... 226
5.2.8.1 *In vitro* cytotoxicity assay ..... 226
5.2.8.2 Relative gene expression analysis using real-time reverse-transcription polymerase chain reaction (RT-PCR) ..... 226
5.3 Results ..... 227
5.3.1 *In silico* analysis of the histone based synthetic *Hp*-His peptide ..... 227
5.3.2 Purification and molecular mass determination of synthetic *Hp*-His ..... 232
5.3.3 Haemolytic activity ..... 234
5.3.4 Antimicrobial activity ..... 234
5.3.5 PI staining ..... 239
5.3.6 SEM analysis ..... 241
5.3.7 DNA Binding assay ..... 243
5.3.8 *In vitro* cytotoxicity assay ..... 244
5.3.9 Anticancer activity ..... 246
5.3.9.1 Gene expression profile of cancer related genes in *Hp*-His treated NCI-H460 cancer cells ..... 246
5.3.9.2 Gene expression profile of cancer related genes in *Hp*-His treated HEp-2 pharyngeal cancer cells ..... 249
5.4 Discussion ..... 251

*Chapter* 6
**SUMMARY AND CONCLUSION** ..... **265 - 271**

**REFERENCES** ..... **273 - 332**

**GenBank Submission** ..... **333**

**Publications** ..... **335 - 357**

# List of Tables


Table 2.1 List of primers used. ..... 56

Table 2.2 Sequence of restriction primer designed for *Leiognathus equulus* hepcidin mature peptide. ..... 60

Table 2.3 Microbial strains used to test the antibacterial activity of the peptides. ..... 72

Table 3.1 List of primers used in the study. ..... 123

Table 3.2 Restriction primers designed for *Mc*-His. ..... 125

Table 4.1 Primer sequence and details of primer used in the present chapter. ..... 172

Table 4.2 List of primers of the various genes used for real time qPCR analysis ..... 179

# List of Figures


Figure 1.1 Molecular models of different structural classes of antimicrobial peptides. (A) β-sheeted peptide, (B) α-helical peptide, (C) looped structure peptide and (D) extended peptide (Adopted from Hancock, 2001). ..... 06

Figure 1.2 Proposed mechanism of action of membrane active and non-membrane active AMPs (Adopted from Mai et al., 2017). ..... 10

Figure 1.3 Models explaining the mechanisms of membrane permeabilization (A) barrel- stave (B) carpet-like (C) wormhole or toroidal and (D) aggregate channel model. When the peptide reaches a threshold concentration at the outer surface of the membrane, they can insert themselves into the membrane and eventually form peptide lined pores according to the barrel-stave model; create micellar structures with the membrane by interacting with its lipids, in the carpet model; form peptide-and-lipid lined pores according to the toroidal pore model or; generate a non-bilayer intermediate form according to the aggregate channel model (Modified after Bahar and Ren, 2013) ..... 12

Figure 1.4 Various intracellular targets of different non-membrane active AMPs (Adopted from Brogden, 2005). ..... 13

Figure 1.5 Characteristics of the major expression systems used for heterologous production of AMPs (Adopted from Parachin et al., 2012). ..... 22

Figure 1.6 Schematic illustration of the antimicrobial defence mechanism present in the fish. When chemical or mechanical injury occurs, *via* bacteria or viruses, the epithelial cells start to release cytokines such as IL-1β, which attract neutrophils and T cells to the superficial parts of the epidermis. Simultaneously, the mucous goblet cells start to secrete mucus, which contains antimicrobial peptides (AMPs). AMPs like hepcidins are involved in the immune response to bacteria, whereas AMPs such as cathelicidins directly opsonize bacteria (Modified after Rakers et al., 2010). ..... 24

Figure 2.1 Experimental organism used for the study, common pony fish, *Leiognathus equulus* ..... 47
Figure 2.2 Vector Map: pGEM®-T Easy cloning vector (Promega, USA). ..... 52
Figure 2.3 Vector circle map of the expression vector pET-32a(+) showing the multiple cloning sites (Novagen, UK). ..... 59
Figure 2.4 Agarose gel of PCR amplification of *Le*-Hepc. Lane M: 100 bp DNA marker, Lane 1: *Le*-Hepc amplicons of 261 bp. ..... 76
Figure 2.5 Agarose gel (a) colony PCR of *Le*-Hepc. Lane M: 100 bp DNA ladder, Lane 1: ~ 400 bp amplicon obtained with vector specific primers and Lane 2: 261 bp amplicon obtained using gene specific primers (b) Plasmid isolated from positive clones of pGEMT-*Le*-Hepc vector constructs. Lane M: 1 kb DNA marker, Lane 1: pGEMT plasmid with *Le*-Hepc insert. ..... 76
Figure 2.6 Nucleotide and deduced amino acid sequences of *Leiognathus equulus* hepcidin, *Le*-hepc (GenBank ID: KM034809). The single letter amino acid code is shown below the corresponding nucleotide sequences. The start and stop codons are highlighted in red bold letters. Region highlighted in turquoise colour specifies the 24 amino acid signal peptide. The yellow coloured region indicates the propeptide domain and the mature peptide region is highlighted in green colour. ..... 77
Figure 2.7 (a) Signal peptide analysis and (b) Propeptide analysis of *Le*-Hepc (GenBank ID: KM034809) as predicted by the SignalP 4.1 and ProP 1.0 server respectively. ..... 78
Figure 2.8 Kyte-Doolittle plot showing hydrophobicity of *Le*-Hepc (GenBank ID: KM034809). The peaks above the score (0.0) indicate the hydrophobic nature of the predicted peptide. ..... 79
Figure 2.9 mRNA structure of *Leiognathus equulus* hepcidin, *Le*-Hepc drawn using RNA fold server. The different regions of mRNA are appropriately marked. ..... 80

Figure 2.10 (A) ClustalW multiple alignment of *Leiognathus equulus* hepcidin, *Le*-Hepc with other reported fish and non-fish vertebrate hepcidins obtained using BioEdit software. The relative positions of signal peptide, propeptide and mature peptide of all the sequences are marked. The identical residues are highlighted with background colours. (B) WebLogo visualization of the consensus motif based on multiple alignments of hepcidins. (a) Sequence logo of the signal peptide region, (b) sequence logo of the pro-peptide region and (c) sequence logo of the mature peptide region. The height of the letters indicates the relative frequency of the letter at that position and the overall height of the stack indicates the sequence conservation in terms of information content in bits. ..... 81

Figure 2.11 A bootstrapped Maximum Likelihood tree obtained using MEGA version 6.0.6, illustrating the phylogenetic relationship of *Leiognathus equulus* hepcidin, *Le*-Hepc with pre-prohepcidins of fishes as well as representatives from other vertebrate classes obtained from GenBank. The numbers shown at the branches denote the bootstrap majority consensus values of 1000 replicates. ..... 83

Figure 2.12 (a) Secondary structure annotation of *Leiognathus equulus* hepcidin, *Le*-Hepc predicted using POLYVIEW 2D. The α-helix region is shown in zig zag red lines, β-strand is shown in green arrows, and the coil region is shown in blue lines. The conserved cysteine residues are highlighted in blue colour. (b) Secondary structure wiring diagram of the mature peptide of *Le*-Hepc as predicted by PDBsum. The residues or motifs forming the β hairpins, β turns and the γ turns are shown. The cysteine residues forming the four disulphide bonds are also indicated. ..... 85

Figure 2.13 Spatial structure of *Le*-Hepc constructed by homology modelling using PyMOL software using the PDB ID: 1S6W, obtained from SWISS-MODEL server. The two antiparallel β-pleated structures are seen as yellow coloured ribbons. Cysteine residues that participate in disulphide bonds which stabilize the β -hairpin are highlighted. ..... 86

Figure 2.14 Agarose gel of PCR amplified mature peptide region of *Le*-Hepc with restriction primers. Lane M: 100 bp ladder, Lane 1-2: PCR amplified product (100 bp). ..... 88

Figure 2.15 Agarose gel image of colony PCR. Lane M: 1 kb ladder, Lane 1-2: amplicon (241 bp) of PCR using vector specific primers, Lane 3-4: amplicon (~100 bp) obtained for PCR with insert specific primers. ..... 88

Figure 2.16 Agarose gel image of plasmids digested with Nco1 and HindIII restriction enzymes. (a) Lane M: 1kb ladder, Lane 2: Restriction enzyme digested pGEMT-*mLe*H plasmid with released insert, Lane 3: Un-digested pGEMT-*mLe*H plasmid (b) Lane 1: restriction enzyme digested linearized pET-32a(+) vector, Lane 2: Un-digested pET-32(a+) vector ..... 89

Figure 2.17 (a) Agarose gel image of colony PCR of pET-32a(+) vector construct with *mLe*H insert using T7 forward and T7 reverse primers. Lane M: 1 kb DNA marker, Lane 1 and 2: 850 bp amplicons of PCR performed using vector specific primers, Lane 3 and 4: 100 bp PCR amplicons amplified using insert specific primers. (b) Plasmid gel image of the recombinant plasmid and the control pET plasmid. Lane 1: pET-32a(+) plasmid with the *mLe*H insert, lane 2: pET plasmid without any insert. ..... 90

Figure 2.18 Tricine SDS-PAGE analysis of recombinant expression of *mLe*H, before and after IPTG induction on a time-course basis. Lane M: Low-range protein ladder, Lane 1: uninduced control (before IPTG induction), Lane 2: recombinant cells at the time of induction; Lane 3-9: IPTG induced cells after 1-7 hours of induction. ..... 91

Figure 2.19 Tricine SDS-PAGE analysis of recombinant expression of Thioredoxin, Trx, before and after IPTG induction on a time-course basis. Lane M: High-range protein ladder, Lane 1: un-induced control (before IPTG induction), Lane 2-6: IPTG induced cells after 0-4 hours of induction. ..... 92

Figure 2.20 (a) Tricine SDS-PAGE analysis of Ni-NTA purified proteins. Lane M: Low range weight protein marker, Lane 1: purified recombinant *mLe*H (22.7 kDa), Lane 2: purified recombinant Trx (20.4 kDa) (b) Western blot showing the purified recombinant proteins, Lane M: Mid-range coloured marker, Lane 1: purified rTrx, Lane 2: purified r*mLe*H. ..... 93

Figure 2.21 *In vitro* cytotoxicity of the recombinant peptides r*mLe*H, rTrx and mellitin in NCI-H460 cells at various concentrations. ..... 94

Figure 2.22 Haemolytic activity of the recombinant peptides r*mLe*H, rTrx and mellitin in human RBCs at various concentrations ..... 94

Figure 2.23 (a-k) Antimicrobial activity of r*mLe*H against various bacteria at different concentrations..... 99

Figure 2.24 Fluorescent microscopy images of bacterial cells stained with propidium iodide without peptide treatment and after incubation with r*mLe*H peptide. ..... 100

Figure 2.25 SEM images of representative members of pathogens, control-untreated and r*mLe*H peptide treated pathogens..... 101

Figure 3.1 Experimental organism used for the study, flathead grey mullet, *Mugil cephalus.* ..... 121

Figure 3.2 Agarose gel of PCR amplification of *M. cephalus* HDAP gene. Lane M: 100 bp DNA marker, Lane 1: 243 bp amplicon of *M. cephalus* HDAP gene. ..... 130

Figure 3.3 (a) Colony PCR gel image of *M. cephalus* HDAP gene amplicon obtained from the recombinant pGEMT vector. Lane M: 100 bp DNA ladder, Lane 1: 384 bp amplicon obtained with vector specific primers and Lane 2: 243 bp amplicon obtained using gene specific primers (b) Plasmid extracted from positive clones of pGEMT vector with *M. cephalus* HDAP gene insert. Lane M: 1 kb DNA marker, Lane 1: pGEMT plasmid with *M. cephalus* H2A gene insert. ..... 131

Figure 3.4 Nucleotide sequence (grey colour) and deduced amino acid sequence (yellow and green) of histone H2A gene amplified from *M. cephalus*, (GenBank ID: MF966482). The highlighted region in yellow represents the biologically active peptide region (*Mc*-His). ..... 131

Figure 3.5 (a) ClustalW multiple alignment of *Mc*-His with previously reported histone H2A derived AMPs, from fishes, molluscs and crustaceans obtained using MEGA version 6.0.6 software. The highly conserved regions are marked with an asterisk. Gaps are inserted to obtain maximum homology (b) WebLogo visualization of the consensus motif based on multiple alignments of HDAPs. The relative heights of the amino acid symbols at each position represent the degree of sequence conservation at each of these positions based on information content in bits. ..... 133

Figure 3.6 Secondary structure of *Mc*-His precursor peptide predicted using POLYVIEW server. The alpha helical region is shown in zig zag red lines and the coiled region is shown in blue lines. ..... 134

Figure 3.7 Helical wheel diagram of *Mc*-His demonstrating its predictive α-helical amphipathic conformation. Helical wheel projects the positional arrangement of amino acids where hydrophobic and hydrophilic residues face opposite facets of the wheel. The values for hydrophobic moment displacement (5.16) and hydrophobic moment angle (12.9) are indicated respectively. .....135

Figure 3.8 Kyte-Doolittle plot showing the hydrophobic nature of *Mc*-His. The peaks above the score (0.0) indicate the hydrophobic nature of the predicted peptide. ..... 136

Figure 3.9 Predicted 3-dimensional structure of *Mugil cephalus* histone 2A constructed by homology modelling using PyMOL software (PDB ID- 3av1.1c) (b) Spatial structure of *Mugil cephalus* histone 2A with its proline hinge highlighted in blue colour. ..... 136

Figure 3.10 The mRNA structure of *Mc*-His predicted using RNA fold server. The MFE structure is coloured based on the base-pairing probabilities. Blue coloured bases denote the unpaired ones while red coloured bases denote the paired ones. ..... 137

Figure 3.11 Consensus neighbour-joining phylogenetic tree of *Mugil cephalus* histone H2A gene (GenBank ID: MF966482) with other vertebrates constructed using Mega 6.0.6. The values at the forks indicate the percentage of times in which this grouping occurred after bootstrapping (1000 replicates). ..... 138

Figure 3.12 (a) Agarose gel of selective amplification of *Mc*-His region with restriction primers, Lane M: 100 bp ladder; Lane 1: PCR amplified product (~ 160 bp) ; (b) Colony PCR gel image of amplicons obtained with pGEMT-*Mc*-His plasmid using vector and gene specific primers, Lane M: 100 bp ladder; Lane 1: ~300 bp amplicon obtained with vector specific primers and Lane 2: ~160 bp amplicon obtained with insert specific primers; (c) Recombinant pGEMT plasmids with *Mc*-His restriction primer amplified gene. ..... 140

Figure 3.13 (a) Agarose gel image of pGEMT plasmid containing *Mc*-His restriction primer amplified gene digested with BamHI and HindIII enzymes. Lane M: 100 bp ladder, Lane 1: ~150 bp released *Mc*-His insert, (b) Agarose gel image of pET-32a(+) vector restricted digested with BamHI and HindIII enzymes. Lane 1: Linearised pET vector after digestion, Lane 2: Uncut pET vector. ..... 141

Figure 3.14 (a) Colony PCR gel image of amplicons obtained with pET-*Mc*-His plasmid using vector and gene specific primers. Lane M: 100 bp ladder; Lane 1: ~900 bp amplicons obtained using vector specific primers, Lane 2: ~150 bp amplicons obtained using vector specific primers. (b) Plasmid gel image of the recombinant pET-32a(+)-*Mc*-His and the empty pET plasmid. Lane 1: control pET vector, Lane 2: pET plasmid with *Mc*-His insert. ..... 142

Figure 3.15 Tricine SDS-PAGE analysis of recombinant expression of *Mc*-His, before and after IPTG induction on a time-course basis. Lane M: Mid-range protein ladder, Lane 1: uninduced control (before IPTG induction), Lane 2: recombinant cells at the time of induction, Lane 3-8: IPTG induced cells from 1-6 h post induction. ..... 143

Figure 3.16 (a) Tricine SDS-PAGE analysis of Ni-NTA purified r*Mc*-His. Lane M: Mid-range protein marker, Lane 1: purified r*Mc*-His (25.5 kDa). (b) Western blot of purified r*Mc*-His. Lane M: mid-range coloured marker, Lane 1: purified r*Mc*-His. ..... 144

Figure 3.17 *In vitro* cytotoxicity of the recombinant peptides r*Mc*-His, rTrx and mellitin in NCI-H460 cells at various concentrations. ..... 145

Figure 3.18 Haemolytic activity of the recombinant peptides r*Mc*-His, rTrx against human erythrocytes. Five different concentrations have been tested, starting from 20 µM with successive dilutions. Melittin was used for comparison as a classical haemolytic peptide. ..... 145

Figure 3.19 (a-k) Antimicrobial activity of r*Mc*-His against various bacteria at different concentrations. ..... 150

Figure 3.20 Propidium iodide stained image of untreated control bacterial cells and recombinant r*Mc*-His treated cells taken using epifluorescence microscope. ..... 151

Figure 3.21 SEM images of r*Mc*-His treated *E. tarda*, *V. proteolyticus*, and *V. alginolyticus* showing a clear rough surface and collapsed membrane architecture in contrast to the respective control bacterial cells. ..... 153

Figure 4.1 Experimental organism used for the study Orange chromide, *Etroplus maculatus*. ..... 170

Figure 4.2 Agarose gel electrophoretogram of PCR amplification of *E. maculatus* H2A gene. Lane M: 100 bp DNA marker, Lane 1: 243 bp amplicon of *E. maculatus* HDAP gene. ..... 180

Figure 4.3 (a) Colony PCR gel image of gene amplicons obtained from the recombinant pGEMT vector. Lane M: 100 bp DNA ladder, Lane 1: 384 bp amplicon obtained with vector specific primers and Lane 2: 243 bp amplicon obtained using gene specific primers (b) Plasmid extracted from the recombinant clones of pGEMT vector with *E. maculatus* HDAP gene. Lane M: 1 kb DNA marker, Lane 1: pGEMT plasmid with *E. maculatus* H2A gene insert, Lane 2: control pGEMT vector without any insert. ..... 181

Figure 4.4 Nucleotide and deduced amino acid sequence of the HDAP from the haemocyte mRNA transcripts of *E. maculatus* (GenBank ID: MF966483). The nucleotide sequences are showed in green colour and the amino acid sequences are highlighted in both yellow and grey colour. The region highlighted in yellow represents the biologically active peptide region of *E. maculatus* HDAP, *Em*-His1, and the underlined area corresponds to *Em*-His2, the sequence similar to buforin II. ..... 181

Figure 4.5 (a) Multiple sequence alignment of *Em*-His2 (*Etroplus maculatus*) with Buforin I and II (*Bufo bufo gargarizans)*, Hipposin (*Hippoglossus hippoglossus*), Human H2A (*Homo sapiens*) Litopenaeus AMP (*Litopenaeus vannamei*), Scallop AMP (*Chlamys farreri*), Abhisin (*Haliotis discus*), Molluskin (*Crassostrea madrasensis*, *Saccostrea cucullata*, *Meretrix casta*, *Ficus gracilis*, *Bullia vittata)* and Himanturin (*Himantura pastinacoides*), created using BioEdit software. (b) The sequence consensus of the ClustalW alignment, obtained with WebLogo is shown in the lower panel ..... 184

Figure 4.6 ClustalW nucleotide sequence alignment of *Em*-His2 with Buforin II. The MSA of both the sequences illustrate a remarkable sequence variation. ..... 184

Figure 4.7 Secondary structure depiction of *Em*-His2 by POLYVIEW programme. The coiled regions are represented with blue lines and the α-helical regions as zig-zag lines in red. ..... 185

Figure 4.8 (a) Predicted 3-dimentional structural arrangement of *Em*-His2 generated using PyMol software using PDB ID: 2cv5 as the template; (b) Spatial structure representation of *Em*-His2. The proline hinge which confers structural flexibility to the peptide is also marked. ..... 186

Figure 4.9 Helical wheel representation of *Em*-His2. The helical wheel projection demonstrates the clustering of the hydrophobic residues into one side and the cationic residues into the other side of the wheel, indicating the strong amphipathic character of the peptide. ..... 186

Figure 4.10 Kyte-Doolittle plot showing hydrophobicity of *Em*-His2. The peaks above the score (0.0) indicate the hydrophobic nature of *Em*-His2 peptide. ..... 187

Figure 4.11 Predicted mRNA secondary structure of *E. maculatus* histone derived peptide*, Em*-His2 with minimum free energy. ..... 187

Figure 4.12 A bootstrapped neighbor-joining tree obtained using MEGA 6.0.6 illustrating the evolutionary relationship between the *E. maculatus* H2A (GenBank ID: MF966483) with other members of the vertebrate family. ..... 188

Figure 4.13 Electrospray ionization mass spectrum (ESI-MS) of *Em*-His2 shown as a function of abundance over the mass to charge ratio (m/z). ..... 190

Figure 4.14 HPLC chromatogram of synthetic *Em*-His2. ..... 190

Figure 4.15 Haemolytic activity of synthetic *Em*-His2 and mellitin against human RBCs at various concentrations. ..... 191

Figure 4.16 Antimicrobial activity of synthetic *Em*-His2 against various bacteria at different concentrations. ..... 195

Figure 4.17 PI stained image of untreated control pathogens and synthetic *Em*-His2 treated pathogens under FITC filter and PI filter. ..... 197

Figure 4.18 SEM image of untreated control pathogens and synthetic peptide, *Em*-His2 treated pathogens. The overall cell morphology appeared normal without apparent cellular debris, in the *Em*-His2 treated group. ..... 199

Figure 4.19 Agarose gel image of the DNA binding assay of synthetic *Em*-His2. Lane M: 1 kb ladder, Lane 1: Control pUC-18 plasmid, Lane 2-9: 1.625 µM to 200 µM concentration of peptide with 50 ng of pUC-18 vector. ..... 200

Figure 4.20 *In vitro* cytotoxicity of (a) the synthetic peptide, *Em*-His2 and (b) mellitin against NCI-H460 and Hep-2 cells at various concentrations. ..... 201

Figure 4.21 (a-e) Relative gene expression levels of different cancer related genes using quantitative real-time PCR in *Em*-His2 peptide treated NCI-H460 cell lines. ..... 204

Figure 4.22 (a-e) Quantitative gene expression levels of different cancer related genes using RT-PCR in *Em*-His2 peptide treated HEp-2 cell lines. ..... 207

Figure 5.1 Primary structure of the synthetic peptide, *Hp*-His. ..... 224

Figure 5.2 (a) Multiple sequence alignment of the amino acid sequence of *Hp*-His with different histone H2A derived peptides reported from various vertebrates and invertebrates. Identities are shaded dark with the same colour and the consensus residues are indicated with an asterisk. (b) WebLogo graphical representation of the sequence similarity and the consensus pattern within the multiple aligned sequence members. ..... 228

Figure 5.3 The helical wheel diagram demonstrating the probable amphipathic α-helical conformation of *Hp*-His. ..... 229

Figure 5.4 Schematic representation of the Kyte-Doolittle plot showing the hydrophobic nature of the predicted peptide of *H. pastinacoides, Hp*-His. The hydrophobic moieties clustered in the central region of the peptide are indicated by the peaks above the value (0.0). ..... 230

Figure 5.5 Secondary structure of *Hp*-His, predicted using POLYVIEW server. The α-helix regions are shown in red zig-zag lines and the coiled regions are shown in blue lines. ..... 231

Figure 5.6 (a) A ribbon view of the 3D structure of *Hp*-His based on homology modelling using the PDB ID: 2aro.1E, generated by SWISSMODEL server. (b) The spatial structure of *Hp*-His showing the conformationally important proline residue as a cyan stick. ..... 231

Figure 5.7 Chromatographic profile of synthetic peptide, *Hp*-His (RP-HPLC, Welchrom C18, 4.6×250 mm, flow rate: 1.0 ml/min). The chromatogram shows a major peak at retention time of 11.481 min. ..... 232

Figure 5.8 ESI Mass Spectrum of synthetic *Hp*-His. The most abundant ions in the spectrum is seen at m/z of 571.4 [M+5H]5+ followed by 476.4 [M+6H]6+. ..... 233

Figure 5.9 Haemolytic activity of the synthetic *Hp*-His and mellitin against human RBCs at various concentrations. ..... 234

Figure 5.10 Antimicrobial activity of synthetic *Hp*-His peptide against the bacterial pathogens at various concentrations. ..... 239

Figure 5.11 PI stained images of untreated control bacterial cells and synthetic *Hp*-His treated *V. vulnificus*, *V. alginolyticus* and *E. tarda* cells taken under FITC filter and PI filter ..... 241

Figure 5.12 Effects of synthetic peptide, *Hp*-His treatment on bacterial cell membranes observed using scanning electron microscopy. Untreated cells show a normal smooth surface, while cells treated with *Hp*-His reveal a disrupted cell membrane, except for *E. tarda*. ..... 243

Figure 5.13 Agarose gel image of the DNA binding assay of synthetic *Hp*-His. Lane M: 1 kb ladder, Lane 1: control plasmid, Lane 2-9: 1.625 µM to 200 µM concentration of peptide with 50 ng of pUC-18 vector. ..... 244

Figure 5.14 *In vitro* cytotoxicity of (a) synthetic *Hp*-His and (b) mellitin in HEp2 and NCI-H460 cells at various tested concentrations. ..... 245

Figure 5.15 (a-e) Gene expression pattern of different cancer related genes using real time PCR in *Hp*-His peptide treated NCI-H460 cell lines. ..... 248

Figure 5.16 (a-e) Relative gene expression profile of different cancer related genes in synthetic *Hp*-His peptide treated NCI-H460 cell lines. ..... 251

# List of Abbreviations

| | | |
|---|---|---|
| AMPs | – | Antimicrobial peptides |
| APD | – | Antimicrobial peptide database |
| BLAST | – | Basic Local Alignment Search Tool |
| bp | – | base pair |
| CD | – | Circular Dichroism |
| cDNA | – | complementary DNA |
| CFU | – | Colony forming unit |
| DNA | – | Deoxyribonucleic acid |
| dNTP | – | Deoxyribonucleotide triphosphate |
| *Em*-His1 | – | *Etroplus maculatus* histone H2A derived peptide 1 |
| *Em*-His2 | – | *Etroplus maculatus* histone H2A derived peptide 2 |
| EST | – | Expressed Sequence Tag |
| GRAVY | – | Grand average of hydropathicity |
| HAMP | – | Hepcidin antimicrobial peptide |
| HDAP | – | Histone derived antimicrobial peptide |
| HEPES | – | 4-(2-hydroxyethyl)-1-piperazineethanesulfonic acid |
| *Hp*-His | – | *Himantura pastinacoides* histone H2A derived peptide |
| hRBCs | – | Human red blood cells |
| HRP | – | Horseradish peroxidase |
| IPTG | – | Isopropyl β-D-1-thiogalactopyranoside |
| kb | – | kilobase |
| kDa | – | kilodalton |
| kV | – | kilovolt |
| LB | – | Luria Bertani |
| LEAP | – | Liver expressed antimicrobial peptide |
| *Le*-Hepc | – | *Leiognathus equulus* hepcidin |
| LPS | – | Lipopolysaccharide |
| µg | – | microgram |

| | | |
|---|---|---|
| MBC | – | Minimum Bactericidal Concentration |
| *Mc*-His | – | *Mugil cephalus* histone H2A derived peptide |
| MCS | – | Multiple Cloning site |
| MCT | – | Micro Centrifuge Tube |
| MEM | – | Minimum Essential Medium |
| mg/ml | – | milligram per millilitre |
| MIC | – | Minimum Inhibitory Concentration |
| ml | – | millilitre |
| *mLe*H | – | mature peptide of *Leiognathus equulus*, hepcidin (*Le*-Hepc) |
| mM | – | millimolar |
| MRSA | – | Methicillin-resistant *Staphylococcus aureus* |
| $NaH_2PO_4$ | – | Monobasic sodium phosphate |
| NCBI | – | National Centre for Biotechnology Information |
| nm | – | nanometer |
| OD | – | Optical Density |
| PBS | – | Phosphate Buffered Saline |
| PCR | – | Polymerase Chain Reaction |
| PI | – | Propidium Iodide |
| PVDF | – | Polyvinylidene difluoride |
| RNA | – | Ribonucleic acid |
| RNase | – | Ribonuclease |
| rpm | – | Revolutions per minute |
| RT- PCR | – | Reverse transcriptase polymerase chain reaction |
| SDS-PAGE | – | Sodium dodecyl sulphate polyacrylamide gel electrophoresis |
| SEM | – | Scanning Electron Microscope |
| Taq | – | *Thermus aquaticus* DNA polymerase |
| TCBS | – | Thiosulfate Citrate Bile Salts Sucrose |
| TFA | – | Trifluoroacetic acid |

| | | |
|---|---|---|
| Tris-HCl | – | 2-amino-2-(hydroxymethyl)-1, 3-propanediol hydrochloride |
| tRNAs | – | transfer RNAs |
| U | – | Unit |
| v/v | – | volume/volume |
| X-gal | – | 5-Bromo-4-Chloro-3-Indolyl β-D-Galactopyranoside |
| XTT | – | 2, 3-Bis-(2-methoxy-4-nitro-. 5-sulfophenyl)-2H-tetrazolium-5-carboxanilide |

.....ꕥ.....

# Chapter 1

# GENERAL INTRODUCTION

Contents


1.1 Introduction
1.2 Classification of AMPs
1.3 Physicochemical parameters of AMPs
1.4 Mechanistic classes of AMPs
1.5 Multifaceted roles of AMPs
1.6 Resistance mechanisms of AMPs
1.7 Strategies for the production of AMPs
1.8 Marine fish AMPs and their importance
1.9 Significance and objectives of study


## 1.1 Introduction

The marine ecosystem represents the greatest biodiversity as oceans comprise more than two-thirds of the earth's surface. In order to survive in a microbe laden environment, most aquatic animals ought to depend on a network of host defence mechanisms. The initial contact of fastidious microorganisms with the host usually occurs at inner or outer body surfaces; hence they are the primary site for an immune reaction to occur. Thus, innate immune responses refer to the first line of host defence which acts within a few hours after microbial exposure. Antimicrobial Peptides (AMPs) are one of the key elements directly implicated in the innate immune response of their hosts. In lower eukaryotes, mostly invertebrates, AMPs constitute the main component of their biochemical

defence, while these peptides ensure the first line of defence in vertebrates complementing the adaptive immune system (Hancock and Scott, 2000; Wiesner and Vilcinskas, 2010). AMPs are plethoric and represent a hyphen between innate and adaptive immunity (Iwanaga and Lee, 2005; Lawniczak et al., 2007).

AMPs are low molecular weight, biologically active peptides produced by wide variety of organisms ranging from microorganisms to superior mammals. AMPs are generally oligopeptides, comprising of approximately less than 50 amino acids. Most of them are cationic and amphipathic, though some AMPs consist of anionic peptides (Brogden et al., 2003). The fundamental role of AMPs is host defence by exerting its cytotoxic effect on the invading pathogenic microorganisms, though they also serve as immune modulators in higher organisms. Consequently, they have been termed as 'natural antibiotics', because they are active against a large spectrum of microorganisms, including bacteria, viruses and filamentous fungi, in addition to protozoan and metazoan parasites (Liu et al., 2000; Vizioli and Salzet, 2002). The smaller size of AMPs facilitate the rapid diffusion and secretion of peptide outside the cells, which is required for eliciting immediate defence response against pathogenic microbes (Nissen-Meyer and Nes, 1997). With the rise of antibiotic resistance, the search for alternative antibiotic chemotherapeutics has emerged as a priority to enable the treatment of imminent antibiotic resistance strains. As a result, the ability of these natural compounds to interact with microorganisms has raised interest for promising pharmacological and therapeutic applications (Falanga et al., 2016). Compared to antibiotics, these peptides kill bacteria rapidly, have broader

spectrum of activity and furthermore, they are not affected by resistance mechanisms since their mode of action is presumed to be substantially different from existing antibiotics.

## 1.2 Classification of AMPs

The diversity of antimicrobial peptides discovered is so vast that it is difficult to categorize them on the basis of origin, size, amino acid sequence, biological action etc., but can be broadly classified based on their secondary structure (Epand and Vogel, 1999; van't Hof et al., 2001). The principal structural characteristic of AMP is their ability to adopt a shape in which clusters of amphipathic and cationic amino acids are spatially arranged in discrete parts of the molecule. AMPs are grouped into four classes according to their secondary structure as proposed by van't Hof et al. (2001) (Fig. 1.1).

### 1.2.1 AMPs with an α-helical structure

One of the largest and most studied classes of antimicrobial peptides are those forming cationic amphipathic helices. These peptides adopt a disorganised structure in aqueous solution while assume an α-helical conformation upon interaction with hydrophobic solvents or lipid surfaces. Often, α-helical peptides are found to be amphipathic and possess a tertiary structure with a kink or a hinge in the middle (Gennaro and Zanetti, 2000; Tossi et al., 2000).

They can either absorb onto the membrane surface or insert into the membrane as a cluster of helical bundles. Majority of the cytotoxic amphipathic helical peptides are cationic and exhibit selective toxicity for

microbes. One of the best studied cationic, antimicrobial, amphipathic helical peptide is a 23 amino acid peptide, magainin, obtained from the skin of the African clawed frog, *Xenopus laevis* (Zasloff, 1987). Hydrophobic or slightly anionic α-helical peptides also exist. Typical example of a hydrophobic and negatively charged cytotoxic peptide is alamethicin, produced by the fungus, *Trichoderma viride* (Duclohier and Wroblewski, 2001; Kikukawa and Araiso, 2002).

### 1.2.2 AMPs with β sheet structure

In contrast to the linear α-helical peptides, β-sheet peptides are peptides conformationally constrained by one or more disulfide bonds. This group of peptides largely exist in the β -sheet conformation in aqueous solution that may be further stabilized upon interactions with lipid surfaces. Different mechanisms involving either the perturbation of lipid bilayers or the formation of discrete channels have been suggested for these peptides based on high resolution crystallography (Hill et al., 1991) and 2D-NMR studies (Zhang et al., 1992). Critical parameters associated with the antimicrobial action of these groups of peptides appear to be the maintenance of a certain hydrophilic-hydrophobic balance, cyclic structure and number of disulfide bridges (Matsuzaki et al., 1997b; Tamamura et al., 1998; Rao, 1999). Defensins represent the most characterized β-sheet-forming antimicrobial peptide (Hancock, 2001), while tachyplesins (Matsuzaki, 1999), protegrins (Harwig et al., 1995), and lactoferricin (Jones et al., 1994) constitute other noteworthy members of this group.

### 1.2.3 AMPs with a looped structure

In particular, proline-arginine-rich peptides cannot form stable amphipathic structures due to the incompatibility of high concentration of proline residues. Hence, such structures have been proposed to adopt a polyproline helical type-II structure (Boman et al., 1993; Cabiaux et al., 1994). Nisin, one of the lantibiotics, contain small ring structures enclosed by a thioether bond (Montville and Chen, 1998). Upon binding to lipid membranes the cyclic peptides can stack to form hollow, β-sheet-like tubular structures increasing membrane permeability. Owing to their very short size, easy to synthesize and stable nature, this class of peptides holds considerable potential in fighting existing and emerging infectious diseases.

### 1.2.4 AMPs with an extended structure

This group of peptides have an unusual amino acid composition and are often characterized by an overexpression of one or more specific amino acid. For example, the histatin peptide which is produced in the saliva, is highly rich in histidine residues (Brewer et al., 1998; Tsai and Bobek, 1998; Helmerhorst et al., 1999). The cathelicidin family of antimicrobial peptides produced by porcine neutrophils are very rich in proline and arginine or proline and phenylalanine and are termed PR-39 and prophenin, respectively (Zhao et al., 1995; Linde et al., 2001). Tryptophan rich peptides, tritrpticin (Lawyer et al., 1996) and indolicidin (Selsted et al., 1992) are generally noteworthy since tryptophan is not an abundant amino acid residue in peptides and their presence is important with regard to the partitioning of peptides into membranes because of its

propensity to position itself near the membrane/water interface (Persson et al., 1998; Yau et al., 1998).

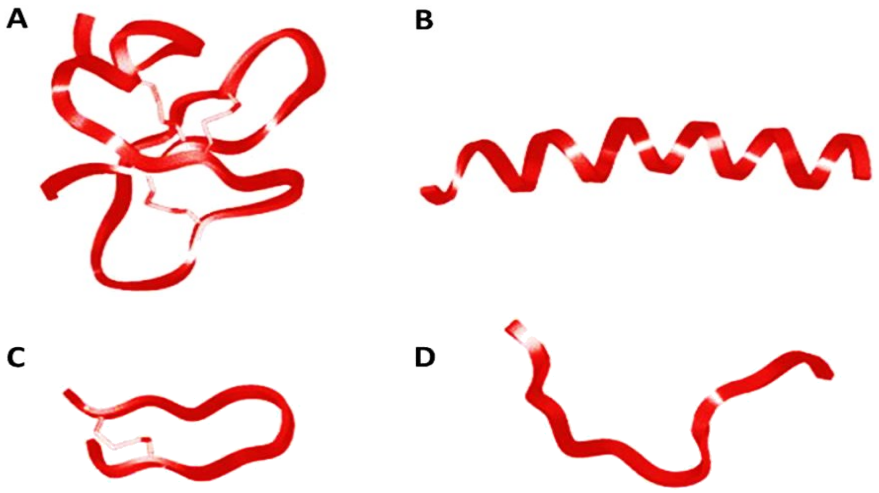


**Fig. 1.1** Molecular models of different structural classes of antimicrobial peptides. **(**A**)** β-sheeted peptide, (B) α-helical peptide, (C) looped structure peptide and (D) extended peptide (Adopted from Hancock, 2001).

## 1.3 Physicochemical parameters of AMP

Several structural factors affect the efficiency and activity of AMPs and many levels of interactions exist between these factors. Even a single change in primary sequence can affect many other physicochemical parameters which are often vital for the activity of an antimicrobial peptide and the range of target cells (Giangaspero et al., 2001; Dennison et al., 2010; Gomes et al., 2018).

### 1.3.1 Charge (Q)

Most of the cytotoxic peptides are positively charged due to the presence of lysine and arginine residues (and to a lesser extent, histidine)

in their sequences. The overall charge of an AMP is the sum of all charges of ionizable groups present in the peptide. Typically, the net charge of these molecules ranges from +2 to +9. The net charge of an AMP facilitates the binding of antimicrobial peptides to negatively charged membranes which could vary with pH as a result of the ionization state of various residues. However, when the positive charge becomes too high, the membrane activity of the peptides may decrease because the strong electrostatic interactions anchor the peptide to the lipid head group region (Dathe and Wieprecht, 1999). Moreover, the ability of amphipathic peptides to penetrate or disrupt the membrane is dependent on the charge and the size of the lipid head group (Wieprecht et al., 1997; Vogt and Bechinger, 1999; Lee et al., 2006).

### 1.3.2 Length

The length of an AMP is particularly vital for its activity since at least 7–8 amino acids are required to form amphipathic structures with hydrophobic and hydrophilic faces on opposite sides of a peptide molecule. For example, the size for an AMP to penetrate the lipid bilayer of bacteria in the barrel-stave model should be at least 22 amino acids for α-helical AMPs, while eight amino acids are needed for β-sheet AMPs (Westerhoff et al., 1989).

### 1.3.3 Amphipathicity (A) and hydrophobic Moment ($M_H$)

Amphipathicity is a measure for the relative abundance of hydrophilic and hydrophobic residues within the AMP. They are generally determined by calculating the hydrophobic moment which is the vector sum of the hydrophobicities of individual amino acid perpendicular to the axis of the

helix. Amphipathicity of AMP is essential for a strong partition into the membrane interface and is normally achieved *via,* a multitude of protein conformations, the simplest one being the amphipathic helix. It was further revealed that amphipathicity of the peptide was more decisive than its hydrophobicity for binding to microbial membranes (Mihajlovic and Lazaridis, 2012).

### 1.3.4 Hydrophobicity (H)

Hydrophobicity of an AMP is usually defined as the percentage of hydrophobic residues within a peptide (Eisenberg et al., 1984) and is typically 50 % for most AMPs. It governs the extent to which a peptide can partition into lipid bilayer. However, an increased level of hydrophobicity is strongly correlated with mammalian cell toxicity and loss of antimicrobial specificity (Javadpour et al., 1996; Skerlavaj et al., 1996). The decrease in antimicrobial activity when the hydrophobicity is increased could be attributed to the increased likelihood of dimerization, thereby preventing access of the peptide to the bacterial membrane. Also, the breach in the membrane discrimination mechanism with enhanced hydrophobicity of peptides may be due to their penetration deep into the hydrophobic core of the mammalian membrane (Chen et al., 2007; Yin et al., 2012).

### 1.3.5 Polar angle (θ)

Polar angle of an AMP represents the relative proportion of polar versus nonpolar facets of a peptide, standardized to an ideal amphipathic helix. A reduced segregation between these domains or an increased hydrophobic proportion of the helix would proportionately reduce the

polar angle. Antimicrobial peptides with smaller polar angle are directly associated with increased capacity to permeabilize the membranes (Dathe et al., 1997; Wieprecht et al., 1997; Uematsu and Matsuzaki, 2000). Furthermore, the polar angle has also been shown to correlate with the overall stability and half-life of peptide induced membrane pores. Peptides with smaller polar angles induced greater membrane permeabilization, translocation and pore formation rates (Uematsu and Matsuzaki, 2000). However, AMPs with smaller polar angles achieve less stable pore structures compared with those having larger polar angles. In general, peptides with relatively high cationicity, a large hydrophobic moment and a small hydrophilic angle tend to have higher activity against microbial membranes, low haemolytic activity, and a tendency for carpet-like mechanism of action. On the contrary, peptides possessing a low positive charge, a small amphipathic moment and high intrinsic hydrophobicity display higher activity to microbial as well as host membranes and have a preference to form barrel-stave-like pores (Shai, 1999).

## 1.4 Mechanistic classes of AMPs

Majority of the antimicrobial peptides studied so far, regardless of their size, sequence, charge, structure and diastereomerism, kill bacteria in the micromolar range supporting a non-receptor mediated mechanism for their mode of action (Prenner et al., 1999). The net positive charge of antimicrobial peptides promotes their preferential binding to more than one negatively charged target on bacteria, which may account for the selectivity of AMPs (Hancock and Scott, 2000). Likewise, it has also

been described that not only the nature of the peptide but also the characteristics of cell membrane, as well as the metabolic state of the target cells determine the mechanisms of action of antimicrobial peptides (Liang and Kim, 1999). Majority of antimicrobial peptides kill microbes by membrane depolarization and pore formation on a nanometer scale followed by membrane disruption. By way of action of AMPs, they can be broadly classified under two main heads: membrane active AMPs and non-membrane active AMPs (Fig. 1.2). The balance between these two modes of action depends mainly on the peptide concentration.

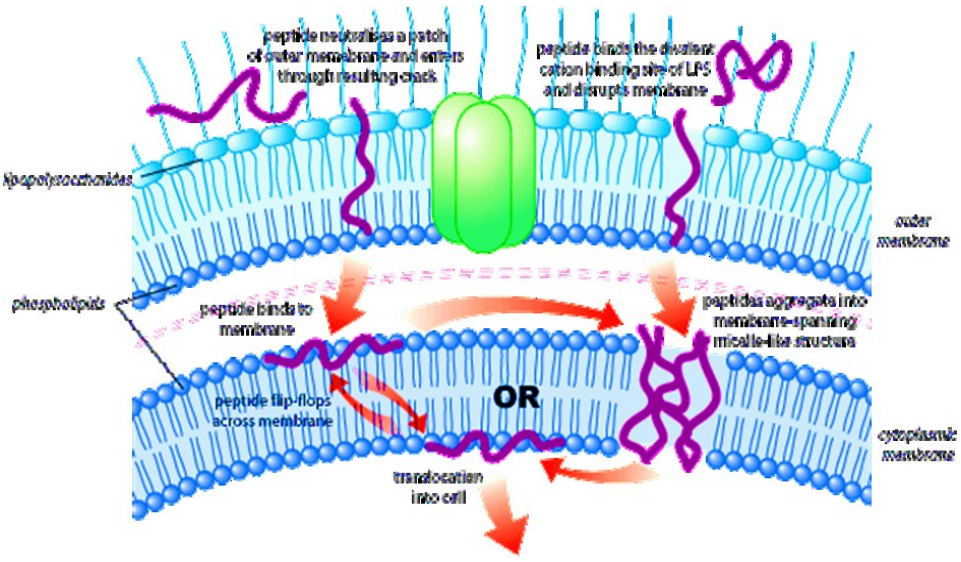


**Fig. 1.2** Proposed mechanism of action of membrane active and non-membrane active AMPs (Adopted from Mai et al., 2017).

### 1.4.1 Membrane active AMPs

One of the main modes of action of AMPs is their ability to interact with membranes, and the characteristic feature is membrane permeabilization. General model for mechanism of action of AMPs that target membrane follows three important consecutive steps: AMP-microbe membrane attraction, accompanied by attachment of the peptide onto the membrane and finally insertion of the AMP into the membrane causing its disruption. So far, α-helical peptides have been the most studied, whereas little is known in comparison about the mechanism of action by which β-sheet peptides use to permeabilize the membrane. The peptides possess hydrophilic positively charged domains, interact with the negatively charged microbial surfaces, and head groups of bilayer phospholipids (mainly by hydrophobic and ionic interactions) leading to cell membrane penetration. Further, the transmembrane potential and pH gradient are destroyed, the osmotic regulation is affected and respiration is inhibited. As indicated by the previous studies and the literature, peptide–membrane interactions play a crucial role in determining the activity of these membrane-active AMPs (Pandey et al., 2011). Several mechanistic models of membrane active AMPs have been proposed, *viz*., barrel-stave, carpet like, wormhole or toroidal and aggregate channel model and the mechanism of their actions are summarised in Fig. 1.3.

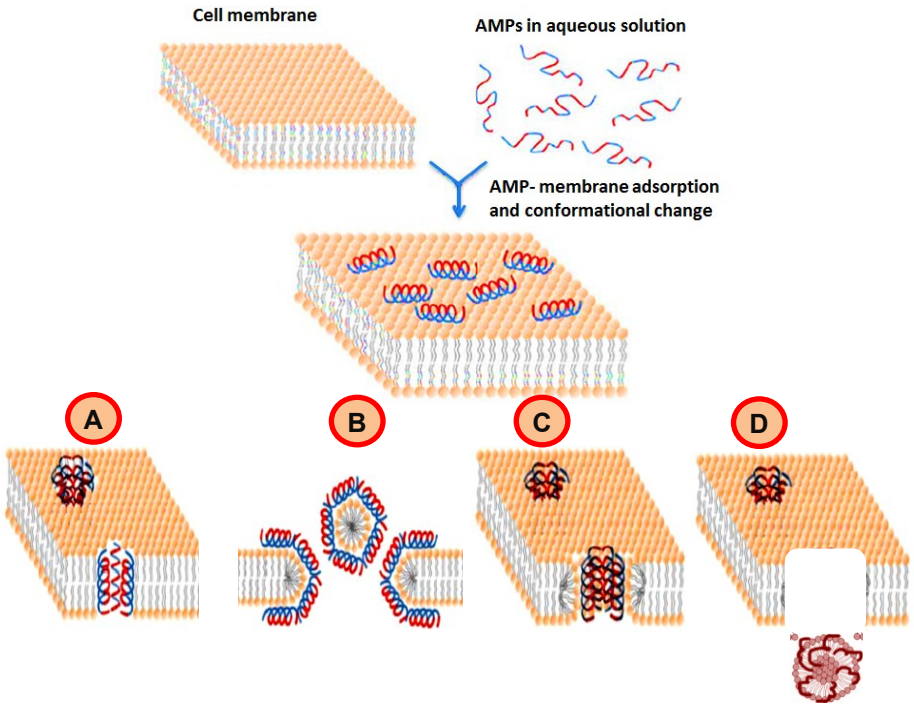


**Fig. 1.3** Models explaining the mechanisms of membrane permeabilization (A) barrel- stave (B) carpet-like (C) wormhole or toroidal and (D) aggregate channel model. When the peptide reaches a threshold concentration at the outer surface of the membrane, they can insert themselves into the membrane and eventually form peptide lined pores according to the barrel-stave model; create micellar structures with the membrane by interacting with its lipids, in the carpet model; form peptide-and-lipid lined pores according to the toroidal pore model or; generate a non-bilayer intermediate form according to the aggregate channel model (Modified after Bahar and Ren, 2013).

### 1.4.2 Non-membrane active AMPs

Besides the ability to interact with membranes, several metabolic as well as intracellular targets also have been described for AMPs (Fig. 1.4). AMPs have developed unique mechanisms to translocate to the cytoplasm, in order to alter the cytoplasmic membrane septum formation, inhibit cell-wall synthesis, nucleic acid synthesis, protein synthesis or inhibit enzymatic

activity (Cudic and Otvos, 2002; Brown and Hancock, 2006). AMPs rich in arginine are able to translocate across both the cellular and nuclear membranes, where they interact with DNA, RNA and/or proteins to inhibit synthesis pathways (Futaki et al., 2001). Cell penetrating property have been described for an increasing number of AMPs such as buforin II (Jang et al., 2015), PAF26 (Munoz et al., 2012) or histatin 5 (Orrapin and Intorasoot, 2014). Furthermore, peptides can interfere with bacterial cytokinesis by cell filamentation provoked by several types of AMPs *in vitro* or *in vivo*. Antimicrobial peptides such as those originally isolated from insects, drosocin, pyrrhocoricin, and apidaecin, act on heat shock proteins (DnaK and GroEL) and repress the stress response of cells (Otvos, 2000). Besides, some peptides can even use multiple antimicrobial mechanisms (Nguyen et al., 2011). This multiple-hit strategy may be effective in increasing antimicrobial efficiency and evading potential resistance mechanisms.

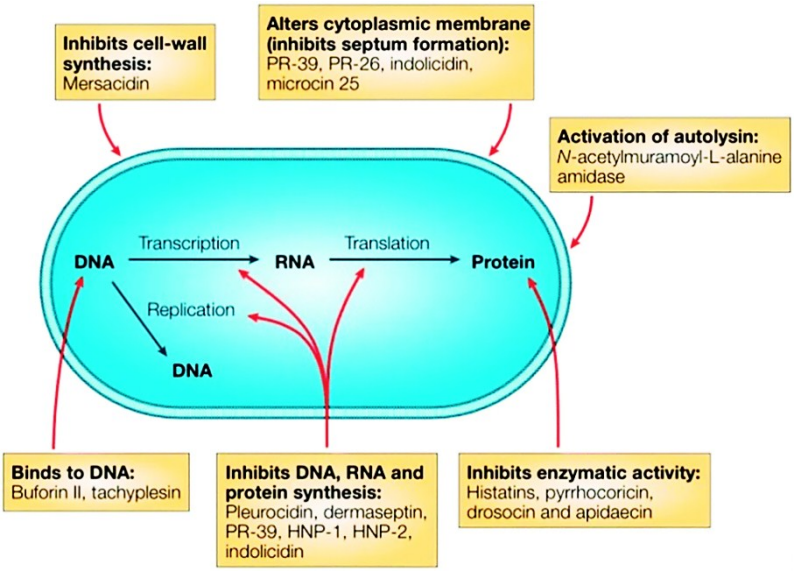


**Fig. 1.4** Various intracellular targets of different non-membrane active AMPs (Adopted from Brogden, 2005).

## 1.5 Multifaceted roles of AMPs

Ubiquitous in nature, AMPs typically have broad-spectrum activity against both bacteria and fungi. Moreover, their toxicity could also be seen extended towards enveloped viruses, exo- and endoparasites, and subsequently to cancerous cells (Li et al., 2012). Apart from its action against microorganisms, AMPs also have been shown to modulate the innate and adaptive immunity *via,* expression induction, modulation, or production of proinflammatory cytokines and chemokines, apoptosis, and gene transcription. Thus, recent findings have implicated AMPs as host defence peptides (HDPs) that also functions as immunomodulators, adding a layer of complexity to their functional role in defence against pathogens (Kumar et al., 2018; Semreen et al., 2018).

### 1.5.1 Antibacterial Peptides

Antibacterial AMPs are the most studied AMPs till date and most of them are cationic which target bacterial cell membranes without specifically interacting with the receptors (Shai, 2002; Zhang et al., 2001). The AMPs exploit the fundamental difference in design between the bacterial membrane and the membrane of multicellular animals. The outer leaflet of the bacterial lipid bilayer is largely composed of lipids with negatively charged head groups, such as phosphatidylglycerol and cardiolipin, while the outer monolayer of the animal membranes are rich in zwitterionic phospholipids such as phosphatidylcholine, sphingomyelin and other neutral constituents such as cholesterol (Zhang et al., 2001). More importantly, the outer surface of Gram-negative bacteria and Gram-positive bacteria contains lipopolysaccharide and teichoic acid, each conferring

overall net negative charge on the surface allowing the initial electrostatic attraction with cationic AMPs (Shai, 2002; Yeaman and Yount, 2003).

Upon interacting with the membranes, the peptide assumes an amphipathic conformation and the positive charges of AMPs cluster at the lipid–peptide interface establishing strong electrostatic interactions with the membrane of pathogens. The non-polar facets of the peptides will then insert into the membrane through hydrophobic interactions, and cause increased membrane permeability through different perturbation mechanisms (Papo and Shai, 2003; Bowdish et al., 2005; Teixeira et al., 2012). Antibacterial AMPs usually disrupt the cytoplasmic membrane, though some seem to merely pass the membrane to target intracellular processes such as DNA, RNA, and protein synthesis (Park et al., 1998; Krijgsveld et al., 2000; Xiong et al., 2002). Antimicrobial peptides exhibit selectivity against different microorganisms, of which the molecular basis is not fully understood. On the contrary, several antimicrobial peptides display broad-spectrum activity against Gram-negative bacteria and Gram-positive bacteria (Miyasaki and Lehrer, 1998). However, some peptides, e.g., andropin and insect defensins preferentially kill Gram-positive bacteria (Samakovlis et al., 1991; Meister et al., 1997), while others, e.g., apidaecin, drosocin and cecropin P1 preferentially kill Gram-negative bacteria (Boman et al., 1991; Casteels and Tempst, 1994; Bulet et al., 1996).

### 1.5.2 Antiviral Peptides

Antiviral peptides share the same biophysical properties as other AMPs, but have different mechanism of action towards the targets

(Jenssen et al., 2006). Antiviral AMPs can neutralize viruses by integrating into either the viral envelope or the host cell membrane. Studies reveal both enveloped RNA and DNA viruses can be targeted by antiviral AMPs (Bastian and Schäfer, 2001; Horne et al., 2005), with the exception of non-enveloped adenovirus (Bastian et al., 2001) and echovirus (Pietrantoni et al., 2006). Another mode of action of antiviral AMPs is to integrate into viral envelopes and cause membrane instability, rendering the viruses unable to infect host cells (Robinson et al., 1998; Sitaram and Nagaraj, 1999). Also, AMPs can reduce the binding of viruses to host cells preventing their entry into cells (Belaid et al., 2002). Some antiviral AMPs can prevent viral particles from entering host cells by occupying specific receptors on mammalian cells (Tamamura et al., 1996; Song et al., 2001; Gomes et al., 2017). For example, heparan sulfate is important for the attachment of HSV viral particles to the host cell surface (WuDunn and Spear, 1989). The heparan sulphate molecules are negatively charged glycosaminoglycan molecules (Laquerre et al., 1998). Some others do not compete with viral glycoproteins for binding to the heparin sulphate receptors on cell surface, instead, these antiviral AMPs can traverse the cell membrane and localize in the cytoplasm and organelles, causing changes in the gene expression profile of the host cells, which help the host defence system to fight against viruses or block viral gene expression. Representative member of this group of antiviral AMP is NP-1, an AMP from rabbit neutrophils that prevents Vero cell lines from infection by herpes simplex viruses type 2 (HSV-2), by preventing the migration of a major viral protein, VP16, into the nucleus (Liu et al., 1999; Sinha et al., 2003).

### 1.5.3 Antifungal Peptides

Similar to antibacterial AMPs, antifungal peptides can kill fungi by targeting either the cell wall (De Lucca et al., 1998; De Lucca and Walsh, 1999) or intracellular components (Lee et al., 1999). However, the contents of bacterial membrane and fungi cell wall are different. Some of antifungal peptides are capable of binding to chitin, which is one of the major components of fungal cell wall (Fujimura et al., 2004; Yokoyama et al., 2009; Pushpanathan et al., 2012). Cell wall targeting-antifungal AMPs kill the target cells by disrupting the integrity of fungal membranes (Lehrer et al., 1985; Terras et al., 1992), by increasing permeabilization of the plasma membrane (van der Weerden et al., 2010) or by forming pores directly (Moerman et al., 2002). Despite the fact that majority of antifungal AMPs have polar and neutral amino acids in their structures, there does not appear to be a fair correlation between the structure of an AMP and the type of cells that it targets (Jenssen et al., 2006).

### 1.5.4 Antiparasitic Peptides

Compared to the other three AMP classes, antiparasitic peptides form a smaller group. The first antiparasitic peptide reported is magainin, which is able to kill *Paramecium caudatum* (Zasloff et al., 1987). Later, a synthetic peptide was developed against *Leishmania* parasite (Alberola et al., 2004). Reports of fish derived AMPs with antiparasitic properties are considerably very less. One such example of antiparasitic peptide is cathelicidin, which kills *Caenorhabditis elegans* by forming pores in the cell membrane (Park et al., 2004). Another fish AMP, epinecidin-1, have also demonstrated antiparasitic activity against *Trichomonas vaginalis*

(Pan et al., 2009). The hybrid striped bass piscidin-2 synthetic peptide was also shown to be lethal to fish ectoparasites such as *Cryptocaryon irritans*, *Trichodina* sp., *Amyloodinium ocellatum* and *Ichthyophthirius multifiliis* (Colorni et al., 2008). Recently, two piscidins, piscidin-5 and piscidin-6, isolated from the white bass, *Morone chrysops*, were identified to have activity against the parasite *Tetrahymena pyriformis* (Salger et al., 2016). Even though some parasitic microorganisms are multicellular, the mode of action of antiparasitic peptides is the same as other AMPs. They kill cells by directly interacting with cell membrane (Park et al., 2004).

### 1.5.5 Anticancer and Antitumor peptides

Some cationic antibacterial peptides also exhibit a broad spectrum of cytotoxic activity against cancer cells. Three mechanisms have been proposed against cancer cells and they are namely: (1) lysis of the cell membrane, (2) activation of extrinsic apoptotic pathways, and (3) inhibition of angiogenesis. Most of the anticancer peptides (ACPs) adopt either a bioactive α-helical conformation or a β-sheet structure at the cell surface upon interacting with the membranes. The cancer cell selectivity of AMPs is mainly due to the phenotype of the membrane surface in cancer cells. The negatively charged lipid, phosphatidyl serine exposure, the presence of O-glycosylated mucins, sialylated gangliosides, and heparin sulfate, in conjugation with an increased transmembrane potential, surface area, and membrane fluidity (Schweizer, 2009; Hilchie et al., 2011), promote the specific activity of AMPs towards cancer cells without being affected by tumor heterogeneity (Kelly et al., 2016).

The antimicrobial peptides, magainins and their analogs have been found to lyse solid tumor and hematopoietic tumor cells displaying minimal toxicity against normal blood lymphocytes (Cruciani et al., 1991; Baker et al., 1993). Magainin was proposed to target cell membrane by a non-receptor pathway (Baker et al., 1993). As a matter of fact, certain fish AMPs have also demonstrated antitumor activity. Tilapia hepcidin, TH2-3 that showed potent activity against human fibrosarcoma cells seemed to target tumor on the basis of charge rather than cell growth (Chen et al., 2009a). While antitumor activity of piscidin family members appear to occur through membrane permeabilization and pore formation as well as the induction of reactive oxygen species and apoptotic pathways (Cho and Lee, 2011; Hilchie et al., 2011; Morash et al., 2011; Lin et al., 2012).

## 1.6 Resistance mechanisms against AMPs

Bacterial pathogens have developed various means to curtail the effect of antimicrobial peptides. There are mainly two different types of resistance mechanisms against AMPs: constitutive resistance and inducible resistance (Yeaman and Yount, 2003). The inducible resistance mechanisms include substitution (Lewis et al., 2009), modification (Gunn, 2001), and acylation (Guo et al., 1998) of the membrane molecules, activation of some proteolytic enzymes (Guina et al., 2000) and efflux pumps (Shafer et al., 1998), and modifications of intracellular targets (del Castillo et al., 2001). The constitutive resistance mechanisms comprise of electrostatic shielding (Campos et al., 2004), alteration of membrane potential during different stages of cell growth (Yeaman et al., 1998), and biofilm formation (Yeaman and Yount, 2003).

Direct degradation of antimicrobial peptides and modification of cell surface properties are two major strategies used by Gram-negative bacteria to resist the bactericidal activity of antimicrobial peptides. It has been found that *E. coli* outer membrane protease OmpT cleaves the antimicrobial peptide, protamine before it enters the bacterium (Stumpe et al., 1998). Resistance mechanisms established in *Salmonella typhimurium* are slightly different from those found in other bacteria. *Salmonella typhimurium* has a membrane bound lipid A modification system, which defend themselves against AMPs from the host (Miller et al., 1989). In this system, PhoQ is a membrane bound sensor kinase and PhoP is intracellular response regulator. PhoQ generally gets activated in the presence of high level positive charges outside the cells. It then phosphorylates the PhoP causing up-regulation of some genes including those related to AMP resistance. It is promising to observe that, although bacteria have diverse mechanisms of resistance to AMPs, the general lipid bilayer structure of bacterial membranes make it hard to develop a complete resistance against AMPs. Also, the resistance against AMPs reported to date is not as strong as seen against antibiotics and it only covers a limited number of AMPs.

## 1.7 Strategies for the production of AMPs

In order to become real alternatives for conventional antibiotics, it is essential that the cost of AMPs should be reduced significantly as long as cheap conventional antibiotics are in the market. Also, in order to better characterize a novel AMP, i.e., to determine its mechanism of action, to report the structure and function, or its potential use as a

pharmaceutical drug, a substantial amount of active purified molecule is needed.

In general, there are three different approaches that are employed to obtain a reasonable quantity of AMPs: direct isolation from natural sources, chemical synthesis, or recombinant expression (Li and Chen, 2008). However, as very low concentrations of AMPs are present in most organisms, direct isolation of peptides from natural sources is time consuming, environmentally hostile and involves a high-cost strategy (Li et al., 2010; Meneguetti et al., 2017). The chemical synthesis allows the production of both natural and synthetic AMPs. Chemical peptide synthesis using the established solid-phase techniques is faster, easy to automate, and requires only simpler purification steps. Besides, this technique enables studies on structure-activity relationships without biological restrictions due to toxicity. Also, it is possible to incorporate unnatural amino acids during synthesis (Nilsson et al., 2005). Nevertheless, high cost for large-scale peptide synthesis has been observed. Moreover, these costs can step-up especially for the synthesis of peptides that have disulphide bonds, which hampers the production of such molecules (Li et al., 2010). Therefore chemical synthesis of AMPs is restricted to smaller AMPs lacking post-translational modifications and low cysteine content. Considering the fact that AMPs are simple gene translation products, it is relatively simple to produce them by recombinant expression methods at the place of action, thus avoiding problems associated with proteolysis and rapid clearing. Moreover, peptide production using advanced molecular techniques can unfold its applications in different industrial sectors and increase the knowledge of the mechanism of action.

This technology has the advantage of cloning foreign genes in specific vectors for expression in prokaryotic and/or eukaryotic host cells. This has been considered the most effective method regarding time and production costs (Rao et al., 2005; Xu et al., 2007).

There are several expression systems available to produce heterologous peptides with different sizes, folds, and complexities. Among the various expression systems, bacteria, yeast, and plants are proposed as promising candidates for peptide production (Fig. 1.5). Several features that are to be carefully considered while selecting a host system for peptide production are their size, intracellular localization or secretion, proper folding, and glycosylation pattern (Desai et al., 2010). Bacteria and yeasts are regarded as the main hosts for AMP production, representing 97.4 % of the heterologously expressed AMPs (Li and Chen, 2008). Recently, plants also have emerged as a promising host for AMP production since transgenic plants can be directly used for microbial control by simply expressing the peptide in the desired crop without the need for purifying the peptide.

| Expression system | Promoter | Transformation | Selection | Functional expression | Purification | Time for recovery |
|---|---|---|---|---|---|---|
| Bacteria | Inducible | Heat shock/ Electroporation | Antibiotics | Highly achieved after isolation from the carrier protein | From cytoplasm, periplasm or supernatant fractions | 3-4 Days |
| Yeast | Inducible or constitutive | Electroporation | Antibiotics/ Auxotrophic | Usually achieved | Recovery from supernatant | 1- Week |
| Plant | constitutive | Biolistic/PEG/ Agrobacterium | Antibiotics/ Herbicides | Usually achieved | Cell lysis, recovery from media | 1-6 months |

**Fig. 1.5** Characteristics of the major expression systems used for heterologous production of AMPs (Adopted from Parachin et al., 2012).

## 1.8 Marine fish AMPs and their importance

Fishes live in a microbe-rich environment thus requiring to have a robust system of host defence. Fishes rely heavily on their innate immune defences for initial protection against pathogens invasion, both during the initial and later stages of their lives (Smith et al., 2000). During the early phase of their life, the adaptive immunity is ineffective and when they are completely developed the adaptive immune system display a scarce memory and short-lived secondary responses (Du Pasquier, 2001). Furthermore, specific immunity in fish is limited by environmental factors such as low temperature (Magnadóttir, 2006). Innate immunity may be of particular importance in suboptimal environments and included in the realm of innate defence components are antimicrobial peptides (Van Muiswinkel and Vervoorn-Van Der Waal, 2006).

A number of antimicrobial polypeptides and other defence components have been established in many fish species. Among them, the fundamental ones are apolipoproteins (Concha et al., 2003, 2004), permeability-increasing protein (Xu et al., 2005), a number of different isotypes of muramidase (lysozyme) (Aoki et al., 2002), Squalamine (Moore et al., 1993) and other miscellaneous antimicrobial factors (Ourth and Chung, 2004) (Fig. 1.6).

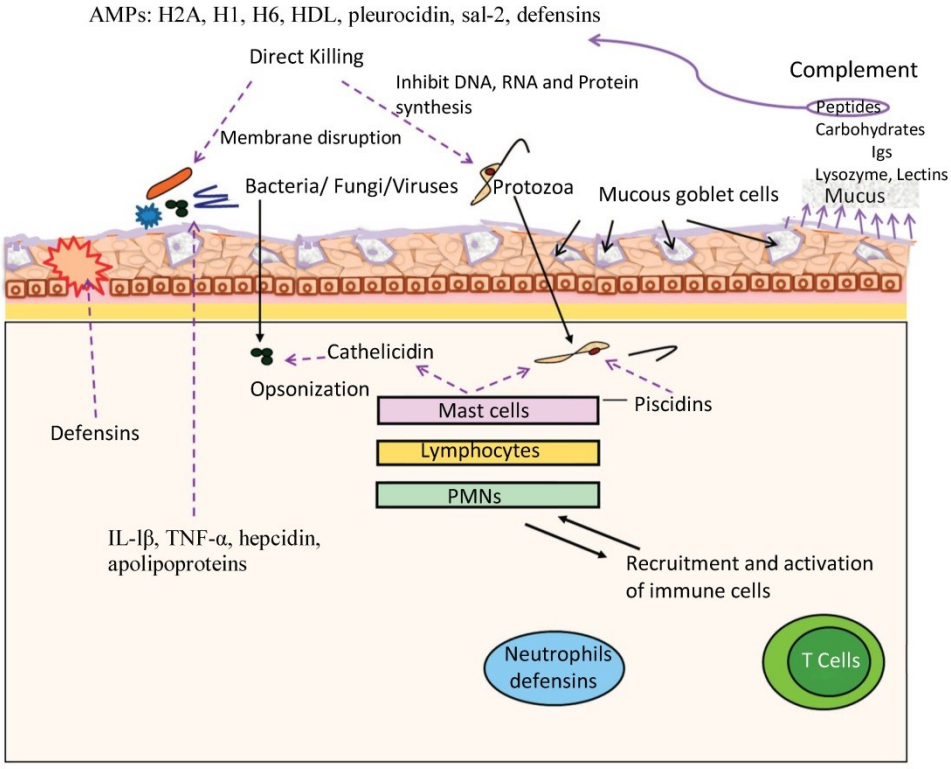


**Fig. 1.6** Schematic illustration of the antimicrobial defence mechanism present in the fish. When chemical or mechanical injury occurs, *via*, bacteria or viruses, the epithelial cells start to release cytokines such as IL-1β, which attract neutrophils and T cells to the superficial parts of the epidermis. Simultaneously, the mucous goblet cells start to secrete mucus, which contains antimicrobial peptides (AMPs). AMPs like hepcidins are involved in the immune response to bacteria, whereas AMPs such as cathelicidins directly opsonize bacteria (Modified after Rakers et al., 2010).

### 1.8.1 Families of fish AMPs

Reports of fish AMPs only began to emerge in the late 1990s, despite their identification in amphibians and humans in the late 1970s and early 1980s. The first fish AMP to be discovered was the α-helical pardaxins, isolated from the skin glands of red sea moses sole,

*Pardachirus marmoratus*, based on their cytotoxic and pore-forming activities (Lazarovici et al., 1986; Thompson et al., 1986). Till date, over 90 fish AMPs have been identified and fall into five major families based on their structure; fish specific piscidins, β-defensins, cathelicidins, hepcidins, and histone-derived peptides, each of which has got its own unique characteristics and properties. Despite the differences, these fish AMP families appear to retain an overall similar structure, broad-spectrum antimicrobial activity and immunomodulatory function to that of other vertebrate AMPs (Shabir et al., 2017). A brief description about each of the class and their biological activities are as follows.

**1.8.1.1 Piscidins**

Piscidins family of peptides represent an evolutionarily conserved family of peptides, unique to fish, which exhibits broad homology to the linear, amphipathic class of antimicrobial peptides (Tamang and Saier, 2006). The first member of the family to be discovered was a 25 residue peptide, isolated and characterized from skin mucous secretions of the winter flounder, *Pleuronectes americanus*, called pleurocidin (Cole et al., 1997). Other representative members of the piscidin family include misgurin (Park et al., 1997), moronecidin (Lauth et al., 2002), chrysophsin (Iijima et al., 2003), piscidin (Sun et al., 2007), dicentracin (Salerno et al., 2007), epinecidin (Pan et al., 2008), gaduscidin (Browne et al., 2011) and chionodracine (Buonocore et al., 2012). The diverse piscidin family members are classified under the same evolutionarily related group, based on the analysis of their gene structures (Salerno et al., 2007; Sun et al., 2007) as well as on the similarities of the mature peptide and predicted secondary structure (Syvitski et al., 2005; Peng et al., 2012).

Genomic organization of majority of the piscidin gene has a four-exon/three-intron gene structure (Cole et al., 2000; Lauth et al., 2002; Sun et al., 2007). However, deviations from the general gene organization exist and include a three-exon/two-intron structure in one piscidin gene from nile tilapia (*Oreochromis niloticus*) (Peng et al., 2012) and the yellow croaker (*Larimichthys crocea*) (Niu et al., 2013; Zhou et al., 2014), together with two epinecidin genes with a five-exon/four-intron structure in the grouper (*Epinephelus coioides*) (Pan et al., 2008). Piscidins are produced as a prepropeptide that undergoes proteolytic cleavage both at the N-terminus to remove the signal peptide and at the C-terminus to cleave away the prodomain, releasing an 18–26 amino acid mature peptide that is approximately 2.5 kDa (Cole et al., 1997; Cole et al., 2000; Peng et al., 2012). All members of the piscidin family are no more than 26 amino acids long with the exception of a novel type of piscidin isolated from hybrid striped bass, piscidin 4 that is 44 amino acids long with a size of 5.33 kDa (Noga et al., 2009). Little sequence homology could be seen amongst the mature peptides, although the members share a similar structure. Conventionally, the mature piscidin peptides assume an amphipathic α-helical conformation with the hydrophilic side being cationic, capable of interacting with pathogen membranes in a parallel fashion (Chekmenev et al., 2006; Bae et al., 2014; Olivieri et al., 2015). On the other hand, positive selection has been found to influence the evolution of these peptides, where the highest sequence diversity could be found in the mature peptide that suggest adaptation for attacking new pathogen strains (Tennessen, 2005; Fernandes et al., 2010).

Attractive features of piscidin includes their ability to retain antibacterial activity at high salt concentrations (Lauth et al., 2002), thermostability (Sun et al., 2012) while maintaining relatively low cytotoxicity against mammalian cells (Kim et al., 2010). Members of the piscidin family exhibit antimicrobial activity towards a wide array of Gram-negative and Gram-positive bacteria with varying bacterial selectivity in a time-dependent fashion and over a considerable temperature and salt range (Cole et al., 1997; Lauth et al., 2002; Douglas et al., 2003; Patrzykat et al., 2003; Chiou et al., 2006; Noga et al., 2009; Ruangsri et al., 2012; Acosta et al., 2013; Shin et al., 2017; Zhuang et al., 2017; Houyvet et al., 2018). Piscidins also exhibit anti-viral activity under a broad range of physiological conditions and temperatures (Chinchar et al., 2004), anti-fungal activity (Sung et al., 2008a; Sung et al., 2008b), anti-parasitic activity at physiological concentrations of piscidins found in fish (Colorni et al., 2008; Dezfuli et al., 2008; Park et al., 2011; Niu et al., 2013) and antitumor activity towards mammalian cells (Chen et al., 2009b; Lin et al., 2009; Hilchie et al., 2011; Lin et al., 2012). Studies on the mechanism of action about the anti-bacterial activity exhibited by piscidins reveal that they interact with acidic phospholipids to form toroidal pores in the membrane (Yoshida et al., 2001; Saint et al., 2002; Campagna et al., 2007). However, the extent of anti-fungal and anti-mammalian tumor activity varies with the piscidin genes expressed.

#### 1.8.1.2 β-defensins

Defensins display general conformation consisting of cysteine-stabilized α-helical and β-sheet folds. However in fish, sequence and structural analysis have revealed that fish defensins are solely β-defensin-

like including the conserved six cysteine motif (Cuesta et al., 2011; Zou et al., 2007; Falco et al., 2008). Fish defensins, resemble that of mammalian β-defensins and were first identified in zebrafish (*Danio rerio*), fugu (*Takifugu rubripes*) and tetraodon (*Tetraodon nigroviridis*) by a database mining approach (Zou et al., 2007). Gene duplication events have led to the existence of multiple copies and up to four genes and five isoforms of defensins have been found in a single species, olive flounder, *Paralichthys olivaceus* (Nam et al., 2010; Casadei et al., 2009; Zhu and Gao, 2013). Key features of the fish β-defensin family include their small-size, cationic and amphipathic nature with six conserved cysteine residues (Casadei et al., 2009; Cuesta et al., 2011; Zou et al., 2007). A negatively charged glutamic acid residue is also found conserved at the end of the loop.

The fish β-defensins are produced as a prepeptide and are cleaved to produce the mature peptide. The prepeptide is commonly synthesized as a precursor that is composed of a 18–24 amino acid leader signal sequence followed by a 39–45 amino acid mature peptide, with the exception of olive flounder which has a 15 amino acid proregion (Zou et al., 2007; Falco et al., 2008; Nam et al., 2010). The mature β-defensin peptides are small (4–6 kDa), with 6 conserved cysteine residues, the CPRRYK/R motif between the $4^{th}$ and $5^{th}$ cysteine and an overall cationicity between +1 and +7 (Casadei et al., 2009; Zhao et al., 2009; Chen et al., 2013). The β-defensins of fish seem to fall into two main groups; one having an overall three beta-strand secondary structure and the other possessing an extra alpha-helix at the N-terminus of the three-beta strand structure (Zou et al., 2007; Ruangsri et al., 2013).

Recombinant as well as synthetic fish defensins have demonstrated antimicrobial activity towards Gram-negative bacteria (Zhao et al., 2009; Nam et al., 2010; Cuesta et al., 2011; Chen et al., 2013; Zhu et al., 2017), Gram-positive bacteria (Wang et al., 2012; Dong et al., 2015) with moderate activity. Besides, fish defensins also inhibit the activity of various fish specific viruses such as *Singapore grouper irido* virus, *viral nervous necrosis* virus, *haemorrhagic septicaemia* virus, and the frog-specific *Rana grylio* virus (Guo et al., 2012; Jin et al., 2010; Falco et al., 2008). The antimicrobial activity was found to be dependent on the fish species and the defensin gene itself. However, fish β-defensins have not been tested against fungi, human viruses and parasites till date, thus representing an area of study that requires further investigation. Apart from their antimicrobial activities, fish β-defensins have shown to exhibit multiple immunomodulatory activities. The β-defensins from the gilthead seabream was shown to attract head-kidney leukocytes (Cuesta et al., 2011), while β-defensin from Atlantic cod was capable of stimulating antimicrobial activity in phagocytes (Ruangsri et al., 2013). Collectively, the studies suggest that fish β-defensins function similarly to their mammalian counterparts, contributing to the innate host defence in multiple ways.

#### 1.8.1.3 Cathelicidins

This family of peptides are constituted by peptides in which the C-terminus of the precursor form shares homology with a porcine serine protease known as cathelin, hence the name, cathelicidins (Zanetti et al., 1995). They were first identified in Atlantic hagfish, *Myxine glutinosa* (Uzzell et al., 2003). The majority of the cathelicidins possess a four-

exon/three-intron structure like that of mammalian cathelicidins (Maier et al., 2008; Chang et al., 2005). It has been proved that cathelicidins are produced as a pre-pro-protein, with a signal peptide at the N-terminus, a conserved cathelin-like domain and a variable C-terminal antimicrobial domain (Tomasinsig and Zanetti, 2005). The variable C-terminal domain contains a QKIRTRR elastase cleavage site and a unique cathelicidin mature peptide (Lu et al., 2011; Chang et al., 2006). When the signal sequence is cleaved off, the pro-protein is further cleaved by elastase or other proteases (Shinnar et al., 2003) to form the bioactive peptide. The mature peptide is formed of 47–69 amino acids, carrying a charge of +8 to +17 (Chang et al., 2005; Maier et al., 2008; Scocchi et al., 2009). Regarding the structure, fish cathelicidins are mainly composed of β-sheets and random coils (Zhang et al., 2015).

In contrast to the mammalian cathelicidins, a high degree of homology is maintained in the cathelin domain of the fish cathelicidins. Also a higher degree of sequence similarity of the mature peptide could be seen than observed in mammals (Scocchi et al., 2016). Thus, fish cathelicidins are subdivided into two classes: linear peptides, and those that exhibit a characteristic disulphide bond. Fish cathelicidins have broad-spectrum activity against Gram-negative bacteria, Gram-positive bacteria (Chang et al., 2005; Bridle et al., 2011; Lu et al., 2011; Li et al., 2013; Zhang et al., 2015), and fungi (Broekman et al., 2011; Li et al., 2013). Early studies in rainbow trout have demonstrated cathelicidins capability to bind LPS in a dose-dependent manner and exert their antimicrobial activity through membrane permeabilization. Deletion studies in rainbow trout have also showed that the N-terminus of the mature cathelicidin

domain is vital for its antimicrobial activity, although the extent of activity loss in these deletion mutants was found to be variable (Zhang et al., 2015). The activity profiles of cathelicidins are likely to be directed by the hypervariable nature of the mature cathelicidins, with structural differences at the C-termini (Tossi et al., 2017).

#### 1.8.1.4 Hepcidins

Hepcidins are cysteine rich antimicrobial peptides that were originally identified in humans (Krause et al., 2000; Park et al., 2001), since then they have been identified in a number of vertebrates (Fu et al., 2007; Hu et al., 2008; Hao et al., 2012). In mammals, hepcidins are expressed predominantly in the liver and plays an important role in maintaining iron homeostasis as well as possess direct antimicrobial activity towards pathogens *in vitro* (Shi and Camus, 2006). Basically, hepcidin gene has a conserved three-exon/two-intron structure in fishes (Chen et al., 2005; Rodrigues et al., 2006; Yang et al., 2007). Despite the fact that a single hepcidin gene exists in humans, whole genome duplications have led to some fish species having multiple gene copies of hepcidin in fishes. Fish hepcidins are encoded as prepropeptides having three main domains; a 22–24 amino acid leader domain, followed by a 40–47 amino acid proregion domain, tailed by a 20–26 amino acid mature peptide domain that contain the 6–8 cysteine residues that are vital for the formation of the 3–4 disulphide bridges (Chen et al., 2005; Chen et al., 2007; Huang et al., 2007; Wang et al., 2009; Srinivasulu et al., 2008; Lin et al., 2014). The sequences of the mature hepcidin peptides from mammals to fish show high conservation of the eight cysteine residues found within the

mature peptide, with one of the four disulphide bonds forming a vicinal disulphide bridge (Hunter et al., 2002; Chaturvedi et al., 2014). The mature hepcidin peptides are cationic and rich in β-sheets with a tendency to primarily form amphipathic molecules (Zhang et al., 2004; Zheng et al., 2006). Collectively, hepcidins of fish demonstrate antimicrobial activity towards a broad range of pathogens *in vitro*, including Gram-negative bacteria, Gram-positive bacteria, viruses, and parasites.

### 1.8.1.5 Histone derived peptides

Histone derived peptides are peptide fragments generated from the proteolytic cleavage of histones, which are basically a family of alkaline proteins involved in the packaging of DNA. Antimicrobial histone derived peptides have also been identified in fishes. Fish histone derived peptides have been discovered from both the N-terminus and C-terminus of H1 (Patrzykat et al., 2001; Fernandes et al., 2004; Luders et al., 2005) and H2A (Park et al., 1998; Birkemo et al., 2003) and have been reported to be present in the skin and skin mucus of several fish taxa (Smith and Fernandes, 2009). Few reports on fish histone peptides have revealed that they can originate in response to epidermal damage or LPS (Park et al., 1998) and have antimicrobial activity against a broad spectrum of Gram-positive and Gram-negative bacteria (Noga et al., 2011), dinoflagellates (Noga et al., 2001) and fungi (Robinette et al., 1998). Histone derived peptides in their active form are more structured, rigid and condensed than their inactive precursor peptides and they bind to anionic membranes (Patrzykat et al., 2001; Luders et al., 2005). However, some histone derived peptides bind and permeabilize the membrane (Bustillo et al., 2014;

Shamova et al., 2014), while others do not, suggesting that they require a binding partner to enter the cell (Patrzykat et al., 2001). Compared to other fish AMPs, there is relatively little information about the histone derived peptides in fish in terms of their distribution across species of fish, conservation of cleavage sites, the signal that triggers the cleavage of the histone-derived peptides from histones, their antimicrobial mechanism of action on pathogens and whether these peptides can act as host-defence peptides by modulating immune responses.

### 1.8.2 Fish AMPs in therapeutics

All AMPs share some common characteristics that support their development as therapeutic antimicrobials. One area where fish peptides may provide a value is in food preservation, as they are obtained from a natural food source, and thus may be more amenable to being consumed (Burrowes et al., 2004). For example, similar to other piscidins, pleurocidin retains its antibacterial activity even up to 300 mM NaCl (Cole et al., 1997; Lauth et al., 2002; Subramanian et al., 2009). Understanding the structural foundation that supports this salt-independency and activity could aid in the design of novel peptide mimetics that could address infections under a wide range of normal and abnormal salt concentrations, such as in serum, tear film hyperosmolarity or in saliva (da Silva et al., 2012; Mai et al., 2011; Oli et al., 2012).

Different applications of piscidins as antimicrobials have been promising. For example, epinecidin-1, when administrated orally or injected can significantly enhance survival in zebrafish and grouper that were challenged with *Vibrio vulnificus* (Pan et al., 2012). In conjunction

with this finding, electrotransfer of epinecidin-1 in zebrafish and grouper muscle showed significant reduction in *V. vulnificus* and *Streptococcus agalactiae* bacterial counts (Peng et al., 2010; Lee et al., 2013). Moreover, treatment of lethally challenged methicillin-resistant *Staphylococcus aureus* (MRSA) mice with epinecidin-1 enhanced the survivability of mice by lowering the bacterial counts, where also there was evidence of wound healing and angiogenesis enhancement (Huang et al., 2013).

In oral disease treatment, piscidins are propitious, due to the potent effect of chrysophsin-1, in killing the cariogenic pathogen *Streptococcus mutans* (Wang et al., 2012). Further, pleurocidin also demonstrated anti-cariogenic activity against both *S. mutans* and *S. sobrinus*, where killing of biofilms occurred in a dose-dependent manner. In addition, it retained its activity in physiological or higher salt concentration, and was found to be relatively stable in the presence of human saliva (Tao et al., 2011). Epinecidin-1 have shown to be a potential candidate for topical application that can prevent vaginal or skin infections due to the synergistic effect that it possessed with commercially available cleaning solutions. Moreover the response was not observed to be affected by low pH or storage at room temperature and at 4 °C for up to 14 days (Pan et al., 2010). Besides, antimicrobial surfaces have been created by the immobilization of chrysophsin-1 resulting in a surface with antibacterial activity capable of killing approximately 82% of *E. coli* (Ivanov et al., 2012).

Interestingly, fish AMPs have also been used to create inactivated virus for vaccination purposes. Huang et al. (2011) found that mice

injected with epinecidin-1-based inactivated Japanese Encephalitis Virus (JEV) displayed 100% survival, and its performance was better than the formalin-based JEV-inactivated vaccine. The effect was reported to be caused by the modulation of immune-related genes, including the augmentation of anti-JEV-neutralizing antibodies in serum, which subdued the multiplication of JEV in brain sections (Huang et al., 2011).

Fish hepcidins are also under trial for development as therapeutics. More assuring results have been demonstrated by tilapia hepcidin TH2-3, where injections with pre-incubated TH2-3 and *Vibrio vulnificus* for 30 min enhanced the survival of infected and re-infected mice, presenting up to 60% of survival with a dose of 40 μg/mice. Additionally, TH2-3 also exhibited significant prophylactic effect by administration prior to infection, where survival rate of 100% was recorded after 7 days of infection (Pan et al., 2012).

## 1.9 Significance and objectives of the study

Marine organisms, which regularly encounter extreme and stressful environments, are becoming a rich source of templates for the design of novel AMPs which could be developed into effective drugs for human and veterinary medicine. Serious problems caused by drug resistant bacteria have created an urgent need for the development of alternative therapeutics. Need to produce novel drugs with lesser chance of developing resistance has enhanced the interest towards molecules which target the cell membrane for which no resistance has been reported. In this regard, AMPs are considered as promising antimicrobial agents against emerging infectious diseases. AMPs have considerable advantages for

therapeutic applications, including broad-spectrum activity, rapid onset of activity, and relatively low propensity for emergence of resistance. In particular, marine AMPs have novel structures remarkably different from their terrestrial counterparts and are taxa-specific or even species-specific. In addition, they display a wide spectrum of anti-infective activities, a low bio-deposition rate in body tissues, and are highly specific to targets.

Biodiversity of marine environment and versatility of marine derived bioactive peptides are under-explored. Fishes still remain an undisclosed source of bioactive molecules for developing novel drugs, as relatively small number of peptides that have been isolated and only a low percentage have been studied to date for their potential as commercial products. Unique for the field of fish AMPs are their potential application in aquaculture. The constant risk of large-scale microbial infection that can lead to significant economic losses demands new strategies to prevent or treat these pathogens. Identification of AMPs from fishes provide valuable information regarding the innate defence mechanisms in fishes which in turn would help to improve the health management practices in aquaculture.

With the above mentioned viewpoints, the present study was undertaken with the following objectives:

- Bio-prospecting for novel Antimicrobial peptides (AMPs) from fishes using gene based approach
- Molecular and phylogenetic characterization of the AMPs
- Heterologous production of AMPs and its functional characterization.
- Structural and functional characterization of synthetic AMPs.

The thesis is presented in six chapters. Chapter 1 provides a general introduction about the research topic. Chapter 2 deals with the molecular characterization, recombinant production and functional analysis of a novel hepcidin from the common pony fish, *Leiognathus equulus.* Molecular characterization, recombinant production and functional analysis of histone derived peptide from flathead grey mullet, *Mugil cephalus* is presented in Chapter 3. Chapter 4 illustrates the molecular characterization of histone derived peptide from orange chromide, *Etroplus maculatus* and its functional analysis using the synthetic peptide. Structural and functional characterization of a synthetic peptide from the histone H2A peptide of *Himantura pastinacoides* is dealt in Chapter 5. The overall findings of the present work are summarized in Chapter 6, followed by References, GenBank accessions and Publications.

Chapter **2**

# MOLECULAR CHARACTERIZATION, RECOMBINANT PRODUCTION AND FUNCTIONAL ANALYSIS OF A NOVEL HEPCIDIN FROM *LEIOGNATHUS EQUULUS*

Contents


2.1 *Introduction*
2.2 *Materials and methods*
2.3 *Results*
2.4 *Discussion*


## 2.1 Introduction

Hepcidin represents a family of cysteine-rich antimicrobial peptides that are basically involved in the immunological processes and antimicrobial activity in several vertebrate species. They were first identified by two independent research groups as a circulating antimicrobial peptide predominantly expressed in the human liver. Originally it was isolated from human blood ultra-filtrate and was termed as Liver Expressed Antimicrobial Peptide (LEAP-1) (Krause et al., 2000). LEAP-1 was found to be active against Gram-positive bacteria, *Bacillus subtilis*; Gram-negative bacteria, *Neisseria cinerea* as well as the yeasts *Saccharomyces cerevisiae* (Krause et al., 2000). Simultaneously, it was also isolated by another group from human urine, and was named as hepcidin (Park et al., 2001). Later, it was renamed as hepatic antimicrobial peptide (HAMP). Soon

after, a hepcidin homologue was isolated from the gills of a teleost fish, the hybrid striped bass (*Morone saxatilis* x *Morone chrysops*) with antimicrobial functions (Shike et al., 2002). From then on, different full-length cDNA sequences of hepcidin genes were obtained from various teleosts. Currently, they are known by the term 'hepcidin', replacing the initially reported LEAP-1, in order to reflect its hepatic site of synthesis and the antimicrobial properties (Nemeth et al., 2004). Subsequent studies have identified their role also as an iron regulatory hormone involved in hereditary haemochromatosis and anaemia of chronic disease (Nicolas et al., 2002; Shi and Camus, 2006; Kwapisz et al., 2009).

The hepatic hepcidin synthesised as an 84 amino acid precursor peptide matures after two-stage enzymatic cleavage at the C terminus in the cytosol of hepatocytes. Initially, the 24 amino acid N-terminal signal peptide is cleaved from the prepropeptide followed by final processing to biologically active C-terminal 25 amino acid peptide by furin and other convertase enzymes (Krause et al., 2000; Park et al., 2001). In fishes, the hepcidin gene is organised as three exons separated by two introns (Douglas et al., 2003). Like the human hepcidin, the fish hepcidin gene also encodes for a prepropeptide (81–96 residues) which consists of a highly conserved signal peptide (~24 residues), a prodomain (38–40 residues), and a mature peptide (19–27 residues) (Pigeon et al., 2001; Chen et al., 2005; Rodrigues et al., 2006; Yang et al., 2007). Moreover, the gene structure and gene sequence were shown to be remarkably conserved, both within fishes and between fish and mammals (Robertson, 2009). The prepropeptide precursor contains the consensus furin cleavage site and the mature peptide contains the eight conserved cysteines and a conserved glycine residue.

In mammals a single hepcidin gene exists playing dual roles in both iron metabolism regulation and antimicrobial response, with mouse being the only known exception (Ilyin et al., 2003). They serve as a negative regulator of iron homeostasis by interacting with its receptor ferroportin, a transmembrane iron-export protein, inducing its internalization and degradation by lysosomes, leading to a decrease in iron-export (Nemeth et al., 2004). However, studies performed with other fish species have shown that many teleosts present multiple copies of hepcidin genes (Hilton and Lambert, 2008; Masso-Silva and Diamond, 2014) especially in Perciformes and Pleuronectiformes. These fish hepcidins are classified into two groups based on the degree of similarity of the predicted mature peptides, also on the overall cationicity and the presence or absence of the presumed iron binding motif QSHLS/DTHFP (Hilton and Lambert, 2008). HAMP1 like peptides are homologous to mammalian HAMP and are distributed in all groups of fishes, while HAMP2 like group are delineated only from acanthopterygian fishes (Hilton and Lambert, 2008) with a single exception (Chaithanya et al., 2013). The HAMP2-type isoforms, of which many copies exist, can present unique characteristics, suggesting a singular role in the immune response against a variety of pathogens. Therefore, hepcidins are considered as key regulators of systemic iron metabolism with its antimicrobial role being relegated to the background in mammals (Shi and Camus, 2006; Ramey et al., 2010). In a broader token, the diversity of hepcidin isoforms may be attributed to the diversity of aquatic environments with varying degree of pathogen challenge, oxygenation and iron concentration, factors known to affect hepcidin expression in mammals (Xu, 2008). Moreover, the evolution of

hepcidin gene was found to be influenced by the environment in which it is found (Lee et al., 2012).

Hepcidin genes have been identified in several species, including the mouse (Pigeon et al., 2001), dog (Fry et al., 2004), rat (Zhang et al., 2004), pig (Sang et al., 2006), and camel (Boumaiza et al., 2014). To date, hepcidins have been identified in at least 40 fish species. Recently they have been identified and functionally studied in many such as Black rockfish, *Seabastes schlegelli* (Kim et al., 2008); Mud loach, *Misgurnus mizolepis* (Nam et al., 2011); Mozambique tilapia (*Oreochromis mossambicus*) (Huang et al, 2007; Chen et al., 2009a; Hsieh et al., 2010; Chang et al., 2011); Javanese ricefish, *Oryzias javanicus* (Lee et al., 2011); Turbot (*Scophthalmus maximus*) (Chen et al., 2007; Pereiro et al., 2012; Zhang et al., 2014); Miiuy croaker, *Miichthys miiuy* (Xu et al., 2012); Orange-spotted grouper, *Epinephelus coioides* (Zhou et al., 2011; Qu et al., 2013); Medaka, *Oryzias melastigmus* (Cai et al., 2012); Blunt snout bream, *Megalobrama amblycephala* (Liang et al., 2013); Common carp, *Cyprinus carpio* (Li et al., 2013; Yang et al., 2014); Blotched snakehead, *Channa maculata* (Gong et al., 2014); Zebrafish, *Danio rerio* (Shike et al., 2004; Lin et al., 2014); Snow trout, *Schizothorax richardzoni* (Chaturvedi et al., 2014); Spinyhead croaker, *Collichthys lucidus* (Sang et al., 2015); European sea bass, *Dicentrarchus labrax* (Neves et al., 2015; Álvarez et al., 2016); Convict cichlid, *Amatitlania nigrofasciata* (Chi et al., 2015); Chinese rare minnow, *Gobiocypris rarus* (Ke et al., 2015); Spotted scat, *Scatophagus argus* (Gui et al., 2016); Hamilton, *Tor putitora* (Chaturvedi et al., 2016); Siberian taimen, *Hucho taimen* (Wang et al., 2016); Yellow catfish, *Pelteobagrus fulvidraco* (Shen et al., 2009; Ren et al., 2014; Liu

et al., 2017), Mudskipper, *Boleophthalmus pectinirostris* (Li et al., 2016; Chen et al., 2017); Roughskin sculpin, *Trachidermus fasciatus* (Liu et al., 2017); Jewfish, *Argyrosomus regius* (Campoverde et al., 2017) and Grass carp, *Ctenopharyngodon idellus* (Wei et al., 2018).

The tissue distributions of fish hepcidins are not consistent across various species. In general, fish hepcidins, like mammalian hepcidins are predominantly expressed in the liver. Nevertheless, hepcidin mRNA has also been detected in other tissues such as spleen, head kidney, gill, intestine and skin (Douglas et al., 2003; Bao et al., 2005; Chen et al., 2005; Feng et al., 2009; Robertson, 2009). In black porgy, hepc6 mRNA was expressed at a higher level in head kidney than in the liver (Yang et al., 2011) whereas in channel catfish, LEAP-2 levels were higher in muscle than in any other tissues (Bao et al., 2005). Also, hepcidin transcripts were found to be abundant in the liver, oesophagus, and cardiac stomach of winter flounder and in the liver, blood, muscle, gill, and skin of Atlantic salmon (Douglas et al., 2003). In ayu, hepcidin mRNA was mainly expressed in the liver, spleen, kidney, heart, and muscle (Chen et al., 2010). Besides, relative expression levels of hepcidin in the Pacific mutton hamlet, showed high basal values in liver and muscle (Masso-Silva et al., 2011). The red banded seabream encodes four different hepcidin genes, each with different expression patterns. HAMP1 was expressed predominantly in kidney and spleen, while the HAMP2 isotype was predominately expressed in kidney, spleen, and intestine. In addition, the HAMP3 and HAMP4 were mainly expressed in liver (Martin-Antonio et al., 2009). Considering, the wide tissue distribution of the different hepcidin isoforms, Neves et al. (2015) suggested that each

hepcidin isoform may assume a different biological role, depending on the tissue in which it is expressed. Fish hepcidins have been demonstrated to respond to a number of infectious stimuli, such as Gram-negative and Gram-positive bacteria (Shike et al., 2002; Rodrigues et al., 2006; Chen et al., 2007; Cuesta et al., 2008; Kim et al., 2008; Cho et al., 2009; Yang et al., 2011; Zhou et al., 2011; Pereiro et al., 2012; Pridgeon et al., 2012; Li et al., 2013; Liang et al., 2013; Wei et al., 2018), viruses (Cho et al., 2009; Zhou et al., 2011), parasites (Mohd-Shaharuddin et al., 2013; Zheng et al., 2018), LPS (Hirono et al., 2005; Huang et al., 2007; Martin-Antonio et al., 2009; Wang et al., 2009; Barnes et al., 2011; Nam et al., 2011) and in infection and inflammation (Chiou et al., 2007). HAMP-2 type of hepcidin transcription was significantly up-regulated in the skin of the common carp (Yang et al., 2014); in the intestine of rainbow trout (Zhang et al., 2004) and in the liver of grass carp (Liu et al., 2010). Interestingly, qPCR studies performed by Pridgeon et al. (2012) analysed the relative transcriptional levels of seven channel catfish antimicrobial peptide genes (NK-lysin type 1, NK-lysin type 2, NK-lysin type 3, bactericidal permeability-increasing protein, cathepsin D, hepcidin and liver-expressed AMP-2) in response to *Edwardsiella ictaluri* infection, and observed that hepcidin was the only one that was significantly upregulated at 4, 6 and 12 h post-infection. In some cases, different isoforms exhibit varying expression patterns (Hirono et al., 2005; Huang et al., 2007; Cho et al., 2009; Neves et al., 2011; Zhou et al., 2011; Liang et al., 2013). These patterns of differential induction of HAMP-2 isoform upon bacterial challenge indicate that its expressions may be species-specific in fish. Various other studies have investigated the effects of iron overload in hepcidin showing its involvement

in the control of iron levels in fish (Hirono et al., 2005; Rodrigues et al., 2006; Huang et al., 2007; Cho et al., 2009; Neves et al., 2011; Zhou et al., 2011; Pereiro et al., 2012).

Hepcidin does not show sequence similarity to any of the known antimicrobial-peptides. However, structurally it resembles other β-sheet peptides like defensins, tachyplesins and protegrins due to the four disulfide bridges in its tertiary structure. The structure of fish hepcidin has been well defined as a small cationic and cysteine-rich peptide, as it is in mammals (De Domenico et al., 2014). Furthermore, based on research conducted in sea bass, it was noted that the mature synthetic hepcidin peptide exhibited a similar three-dimensional structure and have the same disulphide-bonding pattern to human hepcidin (Lauth et al., 2005). It forms a simple hairpin structure with 8 cysteines in a ladder-like configuration, where the two arms are linked by disulfide bridges. Studies with trout hepcidin have proved that disulphide bridges and oxidized state of hepcidin peptides are vital for its optimal conformation and antimicrobial activity (Hocquellet et al., 2012; Alvarez et al., 2014). Additionally, a study conducted using a series of synthetic peptides suggested that the five N-terminal hepcidin amino acids are critical for its function (Pospisilova et al., 2006).

Biological activities of AMPs are diverse, in particular, hepcidins. An increasing number of studies have showed that HAMP-2 types exhibit broad range of bactericidal activities against Gram-positive and Gram-negative bacteria. Recently, Siberian taimen (*Hucho taimen),* hepcidin-2 displayed antimicrobial activities against *E. coli, Micrococcus lysodeikticus*

and *Staphylococcus aureus* (Wang et al., 2016). Synthetic hepcidin-2 of orange-spotted grouper, *Epinephelus coioides* inhibited the growth of *Vibrio vulnificus* and *S. aureus*. At the functional level, synthetic trout hepcidin showed antimicrobial activity against *Piscirickettsia salmonis,* which is a bacterial pathogen causing an epizootic disease in salmonid fishes. Also, antifungal activity of marine fish hepcidin has been described against the fungi *Aspergillus niger*, *Fusarium graminearum* and *Fusarium solani* (Wang et al., 2009). Also, fish hepcidins display agglutination activities against a number of bacteria. Roughskin sculpin hepcidin was capable of agglutinating the Gram-negative *Pseudomonas aeruginosa*, *Vibrio anguillarum*, *E. coli* and Gram-positive *Bacillus thuringiensis*, *Bacillus subtilis* and *S. aureus* (Liu et al., 2017). Apart from the antimicrobial and agglutination activities, hepcidin-2 also possess antiviral (Zhou et al, 2011; Zhang et al., 2014; Gui et al., 2016) and antitumor activities (Chen et al., 2009a; Chang et al., 2011; Cai et al., 2012; Qu et al., 2013; Hassan et al., 2015).

*Leiognathus equulus,* known as the common pony fish are normally found in the estuaries and rivers. They constitute the only other species of Leiognathidae family**,** along with *Leiognathus robustus,* that possess a non-sexually dimorphic light organ system. Being delicious, *L. equulus* finds great demand in Indian as well as foreign markets mostly in the dried and fresh forms. Although, a number of hepcidin isoforms have been reported from various fish species, to our knowledge, there are no reports of hepcidin genes identified from Leiognathidae family. Therefore, the aim of this study was to sequence and characterize *L. equulus* hepcidin cDNA and to describe its antimicrobial activity using the recombinant peptide, r*mLe*H.

## 2.2 Materials and Methods

### 2.2.1 Experimental organism

The experimental organism used for the study was the common pony fish, *Leiognathus equulus* belonging to the class Actinopterygii (Fig. 2.1). The species is a part of the order Perciformes and is included in the family Leiognathidae. Live specimens of *Leiognathus equulus* were caught from Cochin estuary along the Vypeen coast of Kerala, India. The samples were transported to the laboratory in small tanks by providing aeration.

**Fig. 2.1** Experimental organism used for the study, common pony fish, *Leiognathus equulus*

### 2.2.2 Precautions for RNA preparation

The quality and quantity of extracted RNA greatly affects the fidelity of cDNA preparation. Ribonucleases (RNases) are enzymes that cleave and degrade the RNA. Moreover, they are ubiquitous, stable and difficult to inactivate. Hence great care was taken to create a ribonuclease-free environment, which can otherwise negatively impact the resulting analysis. The precautions that were taken for maximizing the yield and quality of

sample RNA during sample collection, storage, and RNA isolation procedures includes:

a) All the accessories/utensils used for RNA extraction were made freed of RNase by treating with Diethyl pyrocarbonate (DEPC). Treatment with DEPC involved overnight incubation of glass wares, homogenizers, scissors and forceps with 0.1 % DEPC at room temperature. The residual DEPC was removed by autoclaving at 15 lbs pressure for 1 hour. The procedure yields RNase free materials as all the DEPC would get evaporated as ethanol and $CO_2$. These utensils were further autoclaved at 15 lbs pressure for 15 min to ensure a sterile condition.

b) Gloves and mask were worn throughout the experiment to prevent contamination from RNases found on human hands and saliva.

c) Dedicated set of pipettes that are only used for RNA related works were used.

d) Sterile, disposable plastic wares (filter tips and tubes) that are tested and certified to be RNase free were used whenever possible to prevent the cross-contamination of RNA samples and

e) RNase-free chemicals and reagents that are reserved for RNA applications were used to avoid the introduction of RNases. These were stored separate from chemicals for other uses.

### 2.2.3 Tissue processing

Live samples of *Leiognathus equulus* were killed humanely. Tissue samples such as gills, liver, kidney, muscle and intestine were dissected out and transferred to TRI™ reagent (Sigma). Blood was collected from the lamellar artery near the gill region and transferred to TRI™ with a syringe that was pre-rinsed with anticoagulant (RNase free, 10 % sodium citrate, pH 7.0). The samples were stored in TRI™ reagent (Sigma) at -20° C until processed.

### 2.2.4 RNA isolation

Total RNA was isolated from the gills preserved in TRI™ reagent, following manufacturer's instructions. Briefly, the tissue was homogenised in 1 ml TRI™ with a tissue homogenizer. The samples were allowed to stand for 5 min at room temperature to ensure complete dissociation of nucleoprotein complexes. To the homogenate 0.2 ml chloroform was added and shaken vigorously for 15s. The reaction mixture was allowed to stand at room temperature for 15 min and then centrifuged at 12,000 x g for 15 min at $4^{o}$ C. Centrifugation separated the mixture into three phases: a red organic phase (containing protein), an interphase (containing DNA) and a colorless upper aqueous phase (containing RNA).

The aqueous phase was transferred to a fresh micro centrifuge tube (MCT) and added 0.5 ml of 2-propanol per ml of TRI Reagent used, and mixed well. The sample was allowed to stand for 5–10 min at room temperature and centrifuged at 12,000 x g for 10 min at 4 °C. The precipitated RNA in the form of a pellet was washed twice by adding 1 ml 75 % ice cold ethanol. The samples were vortexed and centrifuged at

7500 x g for 5 min at 4° C. The RNA pellets thus obtained were dried for 10 min and dissolved in RNase free water by repeated pipetting with a micropipette. For complete dissolution the pellet was kept at 55° C for 5 min.

### 2.2.5 Determining quality and quantity of RNA

Purity and quality of RNA was checked on 0.8 % agarose gel. RNA was quantified spectrophotometrically by measuring the optical density (O.D) at 260 and 280 nm in a UV Spectrophotometer (U-2900, Hitachi). Only good quality RNA with absorbance ratios (A260:A280) greater than 1.8 were used for cDNA synthesis. For one cm path length an absorbance of 1 unit at 260 nm corresponds to 40 µg of RNA per ml. Hence RNA concentration was calculated as:

RNA concentration (µg/ml) = OD at 260 nm × Dilution factor × 40

### 2.2.6 cDNA synthesis

Single stranded cDNA was synthesized from total RNA using specific oligo-d(T20) primers. First strand cDNA was generated in a 20 µl reaction volume containing 5 µg total RNA, 1X RT buffer, 2 mM dNTP, 2 mM oligo $(dT)_{20}$, 20 U of RNase inhibitor and 100 U of MMLV Reverse transcriptase (New England Biolabs, USA). The reaction was conducted at 42 °C for 1 h followed by an inactivation step at 85 °C for 15 min. The synthesized cDNA was stored at -20 °C for further use.

### 2.2.7 PCR amplification

The PCR amplification of cDNA was initially carried out with β-actin primers as an internal control to verify reverse transcription and

thereafter using hepcidin primers (Ren et al., 2006). Primer sequences used for β-actin and hepcidin genes are given in the Table 2.1.

The PCR amplification of both the genes were carried out in 25 µl total reaction volume containing 1X standard Taq buffer (10 mM Tris-HCl, 50 mMKCl, pH 8.3), 3.5 mM $MgCl_2$, 200 mM dNTPs, 0.4 mM each primer and 1U Taq DNA polymerase (New England Biolabs). The PCR condition involved an initial denaturation of 95 °C for 2 min followed by 35 cycles of 94 °C for 15 s, 60 °C for 30 s and 72 °C for 30 s and a final extension at 72 °C for 10 min.

### 2.2.8 Agarose gel electrophoresis

PCR products were analysed by electrophoresis in 1.5 % agarose gel prepared in 1X TBE buffer (Tris-base– 10.8 g, 0.5 M EDTA– 4ml, Boric acid– 5.5 g, double distilled water– 100 ml, pH– 8.0). To the melted agarose, 2 µl ethidium bromide (1 mg/ml stock) was added. After cooling down to ear bearing temperature, the agarose was poured on to gel tray and was allowed to solidify. The solidified agarose gel was then submerged in 1X TBE buffer, filled in a buffer tank of electrophoresis unit. About 10 µl PCR product was mixed with 2 µl of 6X gel loading buffer (1 % bromophenol blue– 250 µl, 1 % xylene cyanol– 250 µl, glycerol– 300 µl, double distilled water– 200 µl) and loaded into the well. Electrophoresis was carried out at a constant voltage of 3-5 volt/cm until the dye front is approximately 75-80 % of the way down the gel. The gel was visualized on a UV transilluminator using the Gel-DOC$^{TM}$ XR+ imaging system (BioRad, USA).

### 2.2.9 Cloning of PCR product

The purified PCR products were cloned into pGEM®-T Easy cloning vector (Promega, USA) using the TA-cloning technique. pGEM®-T Easy Vectors are linearized vectors with a single 3´-terminal thymidine at both ends that provides a compatible overhang for PCR products generated by some thermostable polymerases (Fig. 2.2**).** PCR products are usually amplified using Taq DNA polymerase which preferentially adds an adenine to the 3' end of the product. Moreover, the T-overhangs at the insertion site enhance the efficiency of ligation of PCR products by preventing recircularization of the vector.

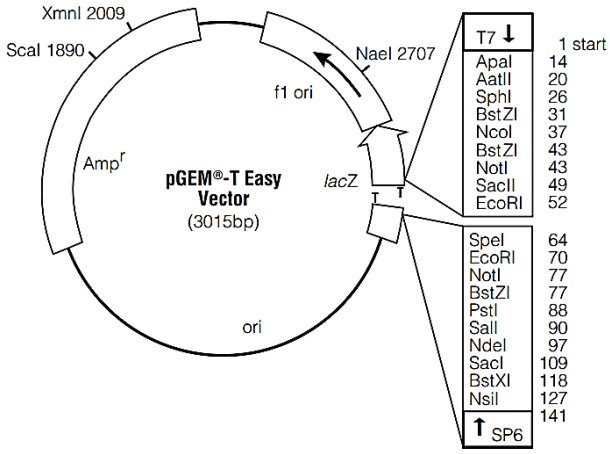


**Fig. 2.2** Vector Map: pGEM®-T Easy cloning vector (Promega, USA)

#### 2.2.9.1 Ligation of the PCR product

The reaction mix for ligation (10 µl) consisted of 5 µl ligation buffer (2X), 0.5 µl of the vector (50 ng/µl), 3.5 µl PCR product (600 ng/µl) and 1 µl of T4 DNA ligase (3 U/µl). The ligation mix was incubated at 4 °C for 12 h.

### 2.2.9.2 Competent cell preparation

*E. coli* DH5α cells were used as the competent cells for transformation of pGEM-T Easy vector with the insert. The competent cells were prepared as follows. Briefly, a single colony of *E. coli* DH5α was inoculated into 10 ml LB media and incubated overnight at 37 °C at 150 rpm. An aliquot of 5 ml of the overnight culture was seeded into 50 ml LB broth and incubated at 37 °C for 2 h at 250 rpm. The cells that are in their logarithmic phase were centrifuged at 6000 rpm for 20 min at 4 °C (Hitachi, Japan). The supernatant was decanted. The cell pellet was then re-suspended by gentle vortexing with 50 ml ice-cold 100 mM $CaCl_2$. The suspended cells were kept in ice for 1 h with intermittent swirling and mixing. The cells were then centrifuged at 6000 rpm for 20 min at 4 °C. The supernatant was decanted and cell pellet was again re-suspended using 1 ml of 100 mM $CaCl_2$. Competent cells thus prepared was aliquoted to a 1.5 ml MCT (80 µl) and added 20 µl of sterile 60 % glycerol. The cells were stored at -80 °C for further use.

### 2.2.9.3 Transformation into *E. coli* DH5α

Transformation of the ligated cloning vector into *E. coli* DH5α competent cells was carried out using heat-shock method. In brief, the frozen competent cells of *E. coli* DH5α were thawed in ice for 5 min. The ligation mix was gently spun down and 5 µl was mixed with 50 µl of competent cells in a 1.5 ml MCT. It was then incubated on ice for 30 min. The cells were given a heat-shock for 60 s in a water-bath at 42 °C without shaking. Immediate to the heat shock, the tubes were returned to ice for 2 min. To the transformation tube, 450 µl of LB broth was added

at room-temperature and incubated for 1.5 h at 37 °C with shaking (~150 rpm). The transformation mixture was then spread plated onto LB agar plates supplemented with ampicillin (100 µg/ml), IPTG (100 mM) and X-gal (80 µg/ml). The plates were incubated at 37 °C for 16 h and the recombinant clones with the inserts were selected by blue white screening. Only the white colonies that appeared on the plate were selected and patched onto fresh LB + Ampicillin + X-gal + IPTG plates and incubated overnight at 37 °C.

**2.2.9.4 Confirmation of gene inserts**

The transformed cells were screened for the presence of the insert DNA by colony PCR using both vector, (T7 and SP6) as well as gene specific primers (Table 2.1). The PCR was carried out in 25 µl total reaction volume containing 1X standard Taq buffer (10 mM Tris-HCl, 50 mM KCl, pH 8.3), 200 µM dNTPs, 0.4 µM each primer and 1U Taq DNA polymerase. The PCR programme used involved an initial denaturation of 95 °C for 5 min followed by 35 cycles of 94 °C for 15 s, annealing at 57 °C for 30 s, extension at 72 °C for 30 s and a final extension at 72 °C for 10 min. The PCR products were then analysed by electrophoresis in 1.5 % agarose gel. Positive clones with the required size insert were selected for plasmid isolation.

**2.2.9.5 Plasmid extraction**

Plasmid extraction was carried out using GenElute ™ HP Plasmid Miniprep Kit (Sigma) as per manufacturer's protocol. For this purpose, the positive clone was inoculated into LB broth supplemented with ampicillin (100 µg/ml) and incubated at 37 °C with shaking at 150 rpm

for 16 h. The culture was pelletized at 12,000 x g for 1 min. The pellet thus obtained was resuspended in 200 µl resuspension solution containing RNase A. The suspended cells were then lysed to release the cell contents by adding 200 µl of the lysis buffer. The contents were mixed gently by inverting the tubes until the mixture becomes clear and viscous. An aliquot of 350 µl neutralization solution was then added and centrifuged at 12,000 x g for 10 min to remove the cell debris.

Meanwhile, the GenElute HP Miniprep binding column was activated by adding 500 µl of column preparation solution. The solution was then allowed to pass through the column by centrifugation at 12000 x g for 1 min. The cleared cell lysate from the neutralization step was loaded to the prepared column. The column was washed twice to remove any unbound materials and other contaminants with wash solution I and II, supplied with the kit, respectively. The flow through was discarded. The column was given an additional centrifugation at 12000 x g for 1 min to eliminate any residual ethanol from wash solution II. Plasmid DNA was eluted by centrifuging at 12000 x g for 1 min using 100 µl of elution buffer (10 mM Tris-HCl). The eluted plasmid DNA was stored at -20 °C. The plasmid DNA thus obtained was analyzed for the presence of the target insert by agarose gel electrophoresis.

### 2.2.10 Plasmid Sequencing

Plasmids with the insert were sequenced with an ABI Prism Sequencing kit (Big-Dye Terminator Cycle) on an ABI Prism 377 DNA sequencer (Applied Biosystem) using primers T7 F and Sp6 R, at SciGenom sequencing facility, Kochi, Kerala, India.

**Table 2.1** List of primers used.

| Target gene | Sequence (5'-3') | Product size (bp) | Annealing Temp. (°C) |
|---|---|---|---|
| **Hepcidin** | F: cgaagcagtcaaaccctcctaagatg | 275 | 60 |
| | R: gaacctgcagcagacaccacatccg | | |
| **β-actin** | F: gatcatgttcgagaccttcaacac | 400 | 60 |
| | R: cgatggtgatgacctgtccgtc | | |
| **T7** | F: tgtaatacgactcactataggg<br>R: ctagttattgctcagcggtg | 750 | 57 |
| **SP6** | R: gatttaggtgacactatag | _ _ | 57 |

### 2.2.11 Sequence characterization and phylogenetic analysis

The nucleotide sequences were analysed, trimmed and assembled using GeneTool software. The assembled nucleotide sequence was translated to their respective amino acid sequence using ExPASy translate tool (http://web.expasy.org/translate/). Homology searches of nucleotide and the deduced amino sequences were performed using BLASTn and BLASTp algorithm of National Centre for Biotechnology Information (http://www.ncbi.nlm.nih.gov/). The enzyme cleavage sites, signal peptide and processing sites for pro-peptidases were determined using the PeptideCutter tool (http://web.expasy.org/peptide_cutter/), SignalP 3.0 server (http://www.cbs.dtu.dk/services/SignalP-3.0/) and ProP 1.0 server (http://www.cbs.dtu.dk/services/ProP) respectively. The N-terminal transmembrane sequence was determined by DAS transmembrane prediction program (http://mendel.imp.ac.at/sat/DAS/DAS.html). Characteristic domains or motifs in the peptide were identified using PROSITE profile database (http://prosite.expasy.org/scanprosite/). Physico-chemical characteristics of the peptide and its mature peptide were analysed separately using ExPASy

ProtParam and APD programs (http://cn.expasy.org/cgi-bin/protparam; http://aps.unmc.edu/AP/main.php). Hot spots of aggregation and the aggregation propensity of the mature peptide were predicted using AGGRESCAN (http://bioinf.uab.es/aggrescan/). Amphipathicity and helical characters of the peptide were represented by Heliquest online tool (http://heliquest.ipmc.cnrs.fr/cgi-bin/ComputParamsV2.py). In order to analyse the stability of the mRNA, the cDNA sequence of the peptide was converted into their corresponding RNA sequence using Sequence editor (http://www.fr33.net/seqedit.php). The converted RNA sequence was then submitted to RNA fold server (http://rna.tbi.univie.ac.at/cgi-bin/RNAfold.cgi) and the structure of RNA was predicted with minimum free energy (MFE).

Conserved domains and residues were identified by multiple alignments with other similar sequences retrieved from the GenBank database using Clustal W algorithm of BioEdit software. The visualization of the consensus motif was performed with WebLogo (http://weblogo.berkeley.edu/logo.cgi). Phylogenetic analyses were carried out using MEGA version 6.0.6. The phylogenetic tree was constructed by the maximum likelihood (ML) method based on the Jones–Taylor–Thornton (JTT) model with complete deletion of gaps. The reliability of the resultant phylogenetic tree was examined using 1000 bootstrap replications. The antimicrobial property of active mature peptide was predicted using antimicrobial peptide database (APD) (http://aps.unmc.edu/AP/main.php). Furthermore antimicrobial domains within the peptide were predicted by various algorithms of Collection of Antimicrobial Peptides ($CAMP_{R3}$) database (http://www.camp.bicnirrh.res.in/#).

Annotation of the secondary structure of the peptide from the sequence profile was carried out using POLYVIEW-2D online tool (http://polyview.cchmc.org/). The secondary structure of the peptide was generated by SWISS-MODEL server (Guex and Peitsch, 1997; Schwede et al., 2003; Arnold et al., 2006). The PDB data thus obtained was used to visualise the spatial structure and bonding patterns of the residues in the structure using Python-enhanced molecular (PyMOL) viewer. The choice of homology model template was validated using PDBsum online tool (http://www.ebi.ac.uk/thornton-srv/databases/pdbsum/).

### 2.2.12 Selection of target gene for recombinant expression

The bioactive domain of the precursor peptide i.e., the mature peptide region (target gene) was selected for recombinant expression. The recombinant production of the target gene was accomplished using pET-32a(+) and *E. coli* Rosetta-gami™ B (DE3) pLysS expression system.

### 2.2.13 Details of expression vector: pET-32a(+)

The pET-32a(+) vector series are designed for cloning and high-level expression of peptide sequences fused with the 109 amino acid Trx•Tag™ thioredoxin protein. Wide choices of cloning sites are available for the production of fusion proteins containing cleavable His•Tag® and S•Tag™ for efficient detection and purification. The Trx•Tag™ expressed from the vector not only enhances the solubility of many target proteins, but also catalyses the formation of disulphide bonds in the cytoplasm of *trx*B mutants. The sequences are numbered by the pBR322 convention and the unique sites in the vector are shown on the circle map (Fig. 2.3).

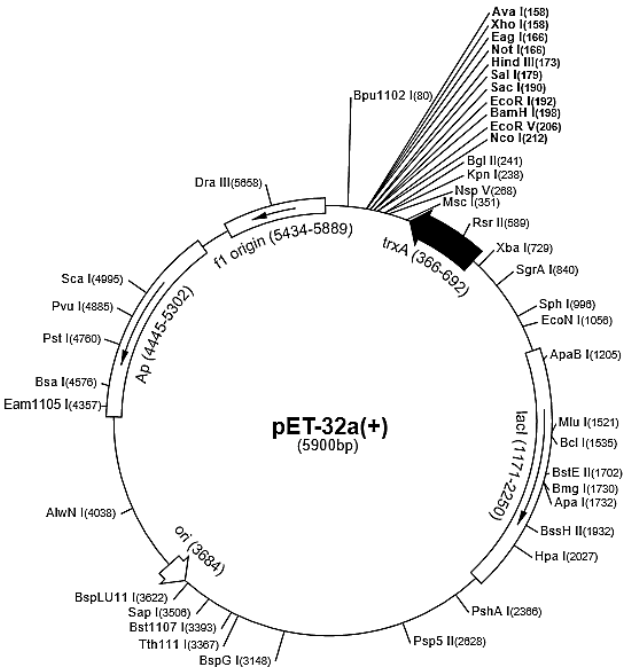


**Fig. 2.3** Vector circle map of the expression vector pET-32a(+) showing the multiple cloning sites (Novagen, UK).

## 2.2.14 Designing of primers for cloning into expression vector

Primers for restriction cloning were designed by adding suitable restriction sites to the 5' end of PCR primers. The restriction primers used for amplifying the mature peptide region of *Leiognathus equulus* hepcidin contained NcoI (CCATGG) restriction sequence in the forward primer and HindIII (AAGCTT) restriction site in the reverse primer. Choice of the restriction site from multiple cloning site (MCS) of vector was made based on the absence of that particular restriction sequence in the target gene. The details of the restriction primers used for *Leiognathus equulus* hepcidin are given in Table 2.2. Hence, for direct cloning, restriction sites of NcoI and HindIII enzymes were introduced at the 5' and 3' ends of the mature peptide sequence respectively.

**Table 2.2** Sequence of restriction primer designed for *Leiognathus equulus* hepcidin mature peptide.

| Target gene | Sequence (5'-3') |
|---|---|
| pET *Le*-Hepc F | 5' TAAGCACCATGGGCCACAGCAATGCTGCTGGC 3' |
| pET *Le*-Hepc R | 5' CGAAGCTTTCAGAACCTGCAGCAGAC 3' |

*** Colour definitions**

Nucleotide bases included to ensure enzyme digestion.
Nucleotide bases added to make the frame correct
Restriction enzyme site: NcoI in F and HindIII in R primer
Target gene sequence

### 2.2.15 PCR amplification of mature peptide

The mature peptide region of *Le*-Hepc was amplified using the designed restriction primers mentioned in section 2.2.14. The PCR amplification was performed in a 25 µl reaction volume containing 1X standard Taq buffer (10 mM Tris HCl, 50 mM KCl, pH 8.3), 3.5 mM $MgCl_2$, 200 µM dNTPs, 0.4 µM each primer and 1U Taq DNA polymerase. pGEMT-*Le*-Hepc was used as the template for the reaction. The thermal profile used was 95 °C for 2 min followed by 35 cycles of 94 °C for 15 s, 60 °C for 30 s and 72 °C for 30 s and a final extension at 72 °C for 10 min. Amplicons were analysed by electrophoresis in 1.5 % agarose gel stained with ethidium bromide and visualized under UV light.

### 2.2.16 Restriction digestion

Double digestion of both the expression vector pET-32a(+) (Novagen, UK) and the PCR products flanked by restriction sites was performed so that the gene was inserted in the correct orientation and in frame with the transcription promoter of the vector. Restriction digestion was carried out

in separate reactions by using the restriction enzymes NcoI and HindIII (FastDigest restriction enzymes, Thermo Fisher Scientific). For restriction digestion, 50 µl of PCR product was incubated with 5 µl of 10X reaction buffer and 0.5 units each of NcoI and HindIII and kept for 1 h at 37 °C followed by an inactivation at 65 °C for 20 min. Subsequently, the restriction digested products was resolved by agarose gel electrophoresis.

### 2.2.17 Purification of restriction digested insert and expression vector

The restriction digested insert and the expression vector, pET-32a(+) were purified using GenJET™ Gel Extraction Kit (Thermo Scientific, USA) following manufacturer's instructions. Briefly, the DNA fragment of appropriate sizes were excised from the agarose gel using a sterile scalpel and transferred to 1.5 ml pre-weighed vials. The excised gel was solubilized completely in binding buffer by incubating the gel mixture at 60 °C with intermittent inversion. 1X gel volume of 100 % isopropanol was added to the solubilized gel solution and mixed well till it became homogenous. The homogenous gel solution was then loaded onto the binding column and centrifuged at 12000 x g for 1 min. The column was washed twice with 700 µl of wash solution and centrifuged at 12000 x g for 1 min. The empty purification column was given an additional centrifugation for 1 min to remove the residual wash buffer. Finally the purified insert and vector were eluted from the column by centrifugation with 25 µl of elution buffer in a fresh 1.5 ml MCT. The purified DNA was stored at -20 °C for further use. The purified products were visualized by agarose gel electrophoresis and the concentration was measured spectrophotometrically at 260/280 nm in a UV-VIS spectrophotometer (U2800, Hitachi, Japan).

### 2.2.18 Construction of recombinant expression vector and transformation into *E. coli* DH5α competent cells

The recombinant expression vector was constructed by ligating the purified restriction digested target gene to the digested pET-32a(+) vector (Novagen, UK) following manufacturer's instructions. The ligation reaction was effected by T4 DNA ligase (Thermo Fisher Scientific).

Briefly, 10 µl ligation mixture contained 1 µl pET-32a(+) vector (50 ng/µl), 4 µl target gene, 1 µl ligation buffer (10X), 1 µl T4 DNA ligase (1U/µl ) and 3 µl MilliQ. The ligation mixture was incubated overnight at 4 °C. The ligated products were then transformed to *E. coli* DH5α competent cells as discussed in section 2.2.9.3. Selected recombinant clones were then streaked on to LB/ampicillin (50 µg/ml) plates. Further, all individually streaked colonies were subjected to colony PCR using vector specific primers *viz*., T7 forward and T7 reverse primers (Table 2.1) as well as insert specific restriction primers (Table 2.2) to confirm the presence of vector with insert. The colony PCR was carried out in 25 µl total reaction volume containing 1X standard Taq buffer (10 mM Tris-HCl, 50 mM KCl, pH 8.3), 200 µM dNTPs, 0.4 µM each primer (T7 forward and T7 reverse) and 1U Taq DNA polymerase. The thermal profile used for colony PCR was an initial denaturation at 95 °C for 5 min followed by 35 cycles of denaturation at 94 °C for 15 s, annealing at 60 °C for 30 s and extension at 72 °C for 1 min and a final extension at 72 °C for 10 min. The amplicons were examined by electrophoresis in 1.5 % agarose gel.

### 2.2.19 Plasmid extraction and sequencing

Positive clones with the required size insert were selected for plasmid isolation. For this purpose, a single colony was inoculated into

10 ml LB broth supplemented with 50 µg/ml ampicillin and incubated at 37 °C with shaking at 250 rpm for 16 h. Plasmid extraction was carried out as discussed in section 2.2.9.5. The recombinant plasmids were sequenced with an ABI Prism Sequencing kit by T7 F and T7 R sequence at SciGenom, Kochi, India. The sequences were analyzed using GeneTool software to ensure that the reading frame of pET-32a(+) expression vector and that of the target gene are preserved.

### 2.2.20 Transformation into expression host, *E. coli* Rosetta-gami™ B (DE3) pLysS

#### 2.2.20.1 Selection and characteristics of expression host

*E.coli* Rosetta-gami™ B (DE3) pLysS was selected as the expression host for heterologous production of *Le*-Hepc mature peptide. Rosetta-gami™ B strains combine the basic features of BL21, Origami, and Rosetta to enhance the expression of eukaryotic proteins. Also, by virtue of *trx*B/*gor* (thioredoxin reductase/glutathione reductase) mutation it effectively mediates the formation of target protein disulfide bonds in the bacterial cytoplasm. Besides, this strain, expresses six rare tRNAs (AGG, AGA, AUA, CUA, CCC, GGA) which facilitates the expression of genes that encode rare *E. coli* codons. Furthermore, this strain is a BL21 *lac*ZY deletion mutant which allows production of protein from target genes cloned in pET vectors by induction with IPTG. pLysS strain expresses T7 lysozyme, which further suppresses basal expression of T7 RNA polymerase prior to induction, thus stabilizing pET recombinants encoding target proteins that affect cell growth and viability. An additional feature of this strain includes deficiency in *lon* and the *omp*T outer membrane proteases that can degrade proteins during purification. All the above said features

of *E.coli* Rosetta-gami™ B (DE3) pLysS enable successful expression of a eukaryotic gene (in particular, rich in disulphide bonds) in a prokaryotic cell.

### 2.2.20.2 Transformation into expression host

*E. coli* Rosetta-gami™ B (DE3) pLysS competent cells were purchased from Novagen, UK and stored at -80 °C until use. About 5 µl of the recombinant pET-32a(+) plasmids with insert and control vector pET-32a(+) without insert were transformed to the competent cells using heat shock method as explained in section 2.2.9.3. The transformation mixture (200 µl) was plated on to LB agar plates, containing the antibiotics ampicillin (50 µg/ml), kanamycin (15 µg/ml), chloramphenicol (34 µg/ml) and tetracycline (12.5 µg/ml). The plates were then incubated overnight at 37 °C for the development of colonies. Colonies obtained were patched onto fresh LB plates supplemented with ampicillin, kanamycin, chloramphenicol and tetracycline. Positive clones were determined by colony PCR with vector specific as well as gene specific primers.

## 2.2.21 Induction and expression of fusion protein

Single colonies of transformed expression host cells containing recombinant pET-32a(+) plasmid with *Le*-Hepc mature peptide insert and empty pET-32a(+) vector without insert (negative control) were selected for heterologous expression of the fusion protein. These transformed bacteria were cultured overnight in 10 ml LB broth containing antibiotics *viz*., ampicillin (50 µg/ml) and kanamycin (15 µg/ml) at 37 °C with shaking at 250 rpm. One ml of this overnight culture was then propagated in fresh 100 ml LB broth (culture conditions provided as explained above) until

$OD_{600nm}$ reaches 0.6–0.8. Immediately, the cells were induced for expression with the inducer, IPTG. The effective IPTG concentration used for induction of the culture was 0.1mM. Uninduced culture, taken prior to IPTG induction, served to get track on the basal level expression of the recombinant protein. Both the culture sets (induced and the uninduced) were further incubated at 37 °C with shaking at 250 rpm for 4–8 h. On a time-course basis, 2 ml aliquot from both the sets were collected and centrifuged, upto seven hours. The cell pellet was stored at -20 °C for SDS-PAGE analysis.

### 2.2.22 SDS-PAGE analysis of the recombinant protein

Tricine–sodium dodecyl sulphate polyacrylamide gel electrophoresis (SDS-PAGE) was carried out to check the level of expression of recombinant *Le*-Hepc mature peptide and control, thioredoxin (Trx) protein. The cell pellets (negative control, uninduced and induced cells taken at various time intervals) were boiled for 10 min with 100 µl of sample buffer containing 150 mM Tris-Cl (pH 7), 12 % SDS, 30 % glycerol, 6 % mercaptoethanol and 5 % coomassie brilliant blue R-250 (CBB). The samples were centrifuged and the supernatant was loaded onto SDS-PAGE gel. Electrophoresis was carried out on a 4 % stacking and 16 % resolving gel using 4-gel Mini-PROTEAN® Tetra cell protein electrophoresis unit (BioRad, USA). 1X Tris (pH 8.9) and 1X Tris-tricine (pH 8.3) was employed as the anode and cathode buffer respectively. The samples were run at a voltage of 50 V for stacking gel and 120 V for resolving gel. After electrophoretic separation of proteins, gels were stained in staining solution (0.5 % coomasie brilliant blue R-250, 40 %

methanol and 10 % acetic acid in distilled water) and de-stained using de-staining solution (10 % methanol and 10 % acetic acid in distilled water). Finally, the gel was documented using Gel-DOC™ XR+ imaging system (BioRad, USA). BioLit low molecular weight protein ladder (3 – 40 kDa) was used for determining the molecular weight. Recombinant protein expression was confirmed by the presence of band at the expected size range.

### 2.2.23 Western blotting

Western blotting was carried out to demonstrate the ability of anti-His tag antibody to detect hexa-histidine tagged fusion protein. For this, SDS-PAGE of recombinant proteins (r*Le*-Hepc mature peptide and rTrx) was performed as explained in the previous section. BioLit low range protein molecular weight standard (3–40 kDa) was used for determining the molecular weight. The cell pellets were boiled for 10 min in sample buffer and then electrophoresed on 16% SDS–PAGE gel. After electrophoresis the gel was transblotted onto a 0.2 mm PVDF membrane at 100 V for 1 h in Mini-PROTEAN® Tetra cell protein electro blotting unit (BioRad, USA). The membrane was blocked for 1 h in a 5 % non-fat dry milk solution in TBS-Tween20.

The membrane was then washed and incubated overnight at 4 °C in His-Tag Mouse mAb (HRP conjugate) horseradish peroxidase-labelled anti-His tag antibody (Cell Signaling Technology® Inc.) at 1:1000 dilution in blocking buffer. After incubation, the membrane was rinsed in TBS-Tween20 buffer for 30 min. Finally, the membrane was incubated in 1–Step™ Chloronaphthol reagent (Thermo Scientific, USA) for 10 min

and observed for blue colour development. The blue colour developed was documented using Gel-DOC$^{TM}$ XR+ imaging system (BioRad, USA).

### 2.2.24 Scale-up production of r*Le*-Hepc mature peptide

To study the bioactive potential of r*Le*-Hepc mature peptide, the mass production of the recombinant peptide was carried out in 2 litre culture medium as explained in section 2.2.21. Cell pellet with r*Le*-Hepc was collected and stored at -20 °C for SDS-PAGE analysis and purification.

### 2.2.25 Affinity purification of recombinant protein

Purification of the 6x-histidine tagged recombinant r*Le*-Hepc mature peptide and Trx from bacterial pellet was accomplished with immobilized metal affinity chromatography (IMAC) using nickel-nitrilotriacetic acid spin columns (Qiagen®). The peptides were purified under denaturing condition following manufacturer's protocol. Briefly, cell lysates were prepared by mixing the thawed cell pellets with 700 µl of buffer B (7 M Urea, 100 mM $NaH_2PO4$, pH 8.0) and was vortexed for 15 min. It was then centrifuged at 6000 x g for 30 min. The supernatant thus formed was collected and stored at -20 °C. The Ni-NTA spin columns were equilibrated with 600 µl of buffer B followed by centrifugation at 2900 rpm for 2 min. These equilibrated columns were loaded with 600 µl of cleared lysate containing 6x histidine tagged fusion proteins and centrifuged at 1600 rpm for 10 min at room temperature. The columns were washed twice with 600 µl buffer C (8 M Urea, 100 mM $NaH_2PO4$, pH 6.3) and centrifuged at 2900 rpm for 2 min to remove unbound and untagged proteins. The recombinant protein was eluted by centrifugation (2900 rpm for 2 min) using 400 µl buffer E (elution buffer- 8 M urea,

100 mM $NaH_2PO_4$, pH 4.5). The flow through after each step was collected for SDS-PAGE analysis to check the binding efficiency of the column. The purification steps were repeated a number of times to obtain sufficient quantities of protein for various assays. The eluted protein was stored at -20 °C for further use.

### 2.2.26 Concentration and re-folding of the recombinant protein

The Ni-NTA column purified samples were concentrated by centrifugation (5000 x g, 30 min) to one tenth the original volume using Millipore's Amicon Ultra-Centrifugal 3 kDa cut-off membrane. The 3 kDa cut-off membrane allows the passage of low molecular weight proteins through the filter while high molecular weight fusion proteins will be retained by the filter. The concentrated samples were then reconstituted to the original volume using the refolding buffer (50 mM Tris-Cl (pH 8)) and centrifuged at 5000 x g for 30 min. The concentrated samples were given repeated washes with refolding buffer to remove the denaturing salts (especially urea); thereby refolding the protein to its native form. The concentrated sample was finally constituted in refolding buffer to a desired volume.

### 2.2.27 Quantification of recombinant protein

The concentration of recombinant proteins (r*Le*-Hepc mature peptide and control-Trx protein) was quantified with Quant-iT$^{TM}$ protein assay kit using Qubit fluorometer (Invitrogen, UK) following manufacturer's protocol. Briefly, the Quant-iT working solution was prepared by diluting the Quant-iT protein reagent in Quant-iT protein buffer (1: 200) and mixed well. About 190 µl of Quant-iT working solution was aliquoted to

fresh and clean 0.5 ml tubes. To this, 10 µl of the recombinant peptides were added and mixed by mild vortexing. The tubes were incubated for 15 min at room temperature. The concentrations of the recombinant proteins were measured using the Quant-iT protein programme and the readings were recorded in µg/ml. The sample concentration was calculated using the following equation:

Concentration of sample = QF value x (200/X)

Where, QF value = the value given by the Qubit fluorometer,

X = volume of sample (in microliters) added to the assay tube.

### 2.2.28 Haemolytic activity of recombinant proteins

The ability to differentiate between bacterial and mammalian cells is an important characteristic of an ideal antimicrobial peptide. The cytotoxicity of the recombinant proteins was therefore determined using haemolytic assay. Haemolytic activity of the recombinant proteins was measured using human red blood cells (hRBCs) with a modified protocol of Onuma et al. (1999). In brief, freshly packed human erythrocytes were washed three times in 0.01M Tris–HCl (pH 7.4) buffer containing 0.15 M NaCl until the supernatant was colorless. A 1:10 dilution of washed erythrocytes was prepared in the same buffer and about 100 µl was dispensed to 0.5 ml micro centrifuge tubes. An equal volume of recombinant proteins (serially diluted in Tris buffer) were added to the 1 % erythrocyte suspension. The final volume in each tube was 200 µl; 100 µl of a given peptide dilution plus 100 µl of the cell suspension. The tubes were incubated for 1 h at 37 °C. Samples were centrifuged at 3000 rpm for 5 min and 100 µl aliquots of the supernatants were transferred into

96-well microtiter plates. Absorbance at 405 nm was determined using an ELISA plate reader (Tecan, USA). The 100 % lysis reference was 100 µl of 1 %(v/v) Triton X-100 added to 100 µl of the cell suspension; the 0 % reference was 100 µl of the cell suspension plus 100 µl of the Tris buffer. The assay was performed in triplicate. Concentration of the peptides that caused 50 % haemolysis of the cells was determined.

Percentage haemolysis was calculated by the following formula:

$$\text{Percentage haemolysis} = 100\ [(A_s - A_0) / (A_t - A_0)]$$

where As represents absorbance of peptide sample at 405 nm and $A_0$ and $A_t$ represent zero % and hundred % haemolysis determined in Tris buffer and 1 % Triton X-100, respectively.

### 2.2.29 *In vitro* cytotoxicity assay

Cytotoxicity of peptides against human cancer cells NCI-H460 was measured using the standard XTT assay in microtitre plates. About, $1\times10^6$ human lung cancer cells NCI-H460 were inoculated into each well of a 96 well tissue culture plate containing minimal essential medium (MEM). The plates were then incubated for 12 h at 37 °C. Following incubation, the cells were washed with phosphate buffered saline (PBS) and the medium was exchanged with fresh MEM containing a series of two fold dilutions of r*Le*-hepc mature peptide. Cytotoxic AMP, Mellitin was used as the positive control and MEM without peptide served as the negative control. Cells were treated with peptides and incubated for another 24 h at 37 °C. Subsequently, morphological changes of the cells were observed under inverted phase contrast microscope (Leica, Germany). The medium

was removed and 50 µl of 2, 3-bis[2-methyloxy-4-nitro-5-sulfophenyl]-2H-tetrazolium-5-carboxanilide (XTT) solution (1 mg/ml in RPMI 1640 medium) was added to each well and incubated for 2 h at 37 °C in a $CO_2$ incubator (Scudiero et al., 1988). All the experiments were performed in triplicate. The absorbance of each well was measured at 450 nm against a reference at 690 nm using Microplate reader (TECAN Infinite M200, Austria). Metabolically active cells cause the cleavage of the yellow tetrazolium salt XTT to form an orange formazan dye. The results are expressed as percentage of the inhibition rate for viable cells in the peptide treated group versus the control group. Cytotoxicity ($IC_{50}$ value) was recorded as the lowest concentration of the protein that resulted in at least 50 % cell death.

### 2.2.30 Antimicrobial assay

The antimicrobial activity of the recombinant protein was examined against a panel of Gram-negative and Gram-positive bacterial pathogens. Microbial strains used to test the antibacterial activity of r*Le*-Hepc mature peptide are listed in Table 2.3. For the assay, bacterial strains were tested for purity by repeated streaking on sterile nutrient agar plates. The relationship between absorbance at 600 nm and colony-forming units (CFUs) was determined for each micro-organism by spreading serial dilutions of the cell suspension onto Nutrient agar or TCBS plates (for vibrios). All bacteria were grown aerobically and cultured at different temperatures: 28 °C for vibrios and 37 °C for rest of the organisms.

**Table 2.3** Microbial strains used to test the antibacterial activity of the peptides.

| Gram reaction | Micro-organism | Strain description |
|---|---|---|
| Gram-positive | *Bacillus cereus* | MCCB 101 |
| | *Staphylococcus aureus* | MTCC 3061 |
| Gram-negative | *Edwardsiella tarda* | MTCC 2400 |
| | *Pseudomonas aeruginosa* | MCCB 119 |
| | *Aeromonas hydrophila* | MCCB 113 |
| | *Escherichia coli* | MTCC 483 |
| | *Vibrio cholerae* | MCCB 129 |
| | *V. vulnificus* | WV13 |
| | *V. proteolyticus* | M10W1 |
| | *V. alginolyticus* | VKF44 |
| | *V. parahaemolyticus* | MCCB 133 |

### 2.2.30.1 Broth microdilution assay

Antimicrobial activity of the peptides was assayed using broth microdilution method as described by Park et al. (2000) with minor modifications. Briefly, single colonies of bacteria were inoculated into the appropriate medium, and cultured overnight at 37 °C (28 °C for vibrios). Aliquots of each culture were transferred to 10 ml of fresh medium and incubated for an additional 2-4 h to obtain mid- logarithmic phase cells. The cells were then washed and resuspended in 50 mM 4-(2-hydroxyethyl)-1-piperazine ethane sulfonic acid (HEPES) buffer, pH 7.4. The cell suspension was diluted to $10^4$ CFU/ml with 50 mM HEPES buffer. 10 µl of the diluted cell suspension and 10 µl of serially diluted peptide samples were added to 96 well propylene microtiter plates (Costar, Cambridge, MA, USA). After incubation for 2 h at room temperature, Muller Hinton broth was added to the mixture and incubated at 37 °C or 28 °C (vibrios) for an additional 16 h. The inhibition of growth was determined by measuring absorbance at

600 nm with a Microplate reader (Tecan, USA). Peptides were substituted by HEPES buffer / diluent for the negative control whereas bacteria treated with thioredoxin fusion protein served as the negative control. Percentage of microbial growth inhibition was calculated using the following formula:

Inhibition % = 100 – Growth percentage.

Where, Growth % = (OD of Test / OD of Control) × 100.

Minimal Inhibitory Concentration (MIC) of the peptides was determined and was defined as the lowest concentration of the peptide that completely inhibited the growth of the microorganism. Three replicates of each MIC determination were performed.

#### 2.2.30.2 Bactericidal assay

The bactericidal activity of the peptide was determined according to Steinberg and Lehrer (1997) with slight modifications. Bacterial pathogens were treated similarly as discussed in the previous section. After incubation, bactericidal effect of the peptide was determined by streaking a 10 µl aliquot of the microtiter plate reaction mixture onto Muller Hinton agar plate for the three serial dilution wells above the determined MIC. MH agar plates were incubated overnight at 37 °C and observed for the development of colonies. The minimal bactericidal concentration (MBC) of the peptide for a given bacterial strain was defined as the lowest concentration of the peptide that killed the bacteria.

#### 2.2.30.3 Bacterial membrane permeability assay (Propidium Iodide (PI) uptake assay)

The integrity of the microbial membrane treated with r*Le*-Hepc mature peptide was determined by measuring the influx of Propidium

Iodide (PI) using a modified method of Wang et al. (2013). Bacterial pathogens found sensitive when treated with the recombinant mature peptide of *Le*-Hepc were analysed by the assay. Membrane permeability of r*Le*-Hepc mature peptide with the treated cells was finally visualized by epifluorescence microscopy. Briefly, bacterial suspension was prepared as discussed in previous sections and treated with peptide at the minimum inhibitory concentration obtained for that pathogen. The mixture was then incubated at 37 °C for 2 h followed by centrifugation at 5000 rpm for 5 min. The pellet thus obtained was re-suspended and washed in PBS. 200 µl of propidium iodide (PI, Sigma-Aldrich, 50 µg/ml) in PBS was added to the washed cell pellet and mixed well. After incubation at room temperature in dark for 5 min, cells were centrifuged and washed twice with PBS. Treated cells were spread in a glass slide and covered with a coverslip. Meanwhile, a bacterial suspension without peptides was included as the control. The influx of PI into bacterial cells was observed using a Fluorescence microscope (Leica DMRA, Heidelberg, Germany). Images were obtained by Leica DMDL digital camera and LEICA FISH software. Fluorescence of PI was observed using an excitation filter with wavelength of 540 - 580 nm and an emission filter of 600 - 660 nm.

**2.2.30.4 Scanning electron microscopy imaging**

Scanning electron microscopy (SEM) was performed to observe the morphological changes in bacteria after treatment with r*Le*-Hepc mature peptide. Bacteria in the mid-exponential growth phase were prepared and were diluted with distilled water to an $OD_{600nm}$ of 1. Microbial inoculum was treated with double the MIC of peptides to mediate the killing of higher number of microbes. After incubation of pathogens with peptide at

37 °C for 1 h, cells were centrifuged (5000 rpm for 5 min). The resulting pellet was washed twice with sterile 0.1 M sodium phosphate buffer and then fixed in 2.5 % glutaraldehyde for 2 h at room temperature. The cells were washed again, fixed with 1 % Osmium tetroxide for 30 min at 4 °C. Further, the cells were dehydrated in a graded series of ethanol solutions until a final concentration of 100 % ethanol was achieved. After critical point drying and sputter-coating with gold, the bacteria were observed with VEGA3 TESCAN Scanning electron microscope at a voltage of 10 kV. Bacterial cells that were not treated with the peptide were used as the control.

## 2.3 Results

In the present study, a novel HAMP2 isoform of an antimicrobial peptide, hepcidin could be identified, cloned and characterized from the common pony fish, *Leiognathus equulus*.

### 2.3.1 Molecular characterization of hepcidin from *Leiognathus equulus*

This section deals with the molecular and phylogenetic characterisation of hepcidin from *Leiognathus equulus* by various bioinformatics tools. The HAMP2 isoform of *L. equulus* hepcidin, hereafter would be designated as *Le*-Hepc.

#### 2.3.1.1 PCR amplification, TA cloning and sequencing of *Le*-Hepc

A 261-bp fragment cDNA with a complete coding sequence for 86 amino acids was obtained from the gill mRNA transcripts of *L. equulus via,* RT-PCR (Fig. 2.4). The amplicons were then cloned into pGEM®-T Easy cloning vector and insert was confirmed using vector-specific and gene specific hepcidin primers by colony PCR (Fig. 2.5a). Recombinant pGEMT-

*Le*-Hepc plasmids isolated from the white colonies were sequenced and analysed (Fig. 2.5b). The *Le*-Hepc cDNA sequence and deduced amino acid sequence (Fig. 2.6) has been submitted to the NCBI GenBank under the accession number **KM034809**.

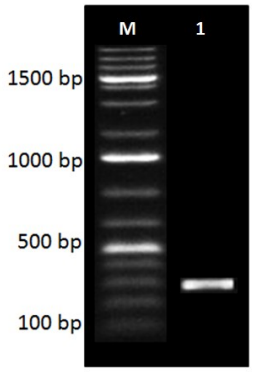


**Fig. 2.4** Agarose gel of PCR amplification of *Le*-Hepc. Lane M: 100 bp DNA marker, Lane 1: *Le*-Hepc amplicons of 261 bp.

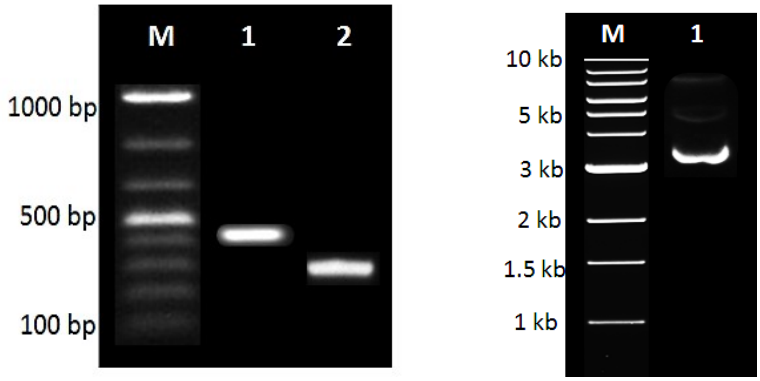


**(a)** **(b)**

**Fig. 2.5** Agarose gel (a) colony PCR of *Le*-Hepc. Lane M: 100 bp DNA ladder, Lane 1: ~ 400 bp amplicon obtained with vector specific primers and Lane 2: 261 bp amplicon obtained using gene specific primers (b) Plasmid isolated from positive clones of pGEMT-*Le*-Hepc vector constructs. Lane M: 1 kb DNA marker, Lane 1: pGEMT plasmid with *Le*-Hepc insert.

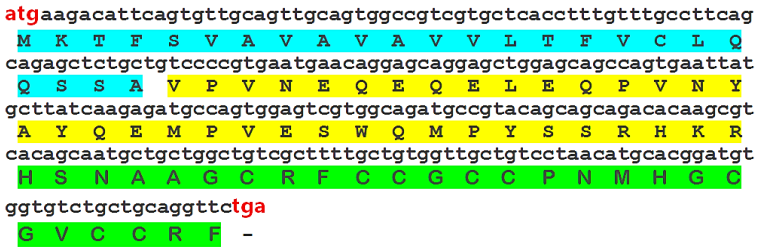


**Fig. 2.6** Nucleotide and deduced amino acid sequences of *Leiognathus equulus* hepcidin, *Le*-hepc (GenBank ID: **KM034809).** The single letter amino acid code is shown below the corresponding nucleotide sequences. The start and stop codons are highlighted in red bold letters. Region highlighted in turquoise colour specifies the 24 amino acid signal peptide. The yellow coloured region indicates the propeptide domain and the mature peptide region is highlighted in green colour.

### 2.3.1.2 Sequence characterization and phylogenetic analysis using bioinformatics tools

BLAST analysis of the nucleotide and deduced amino acid sequences revealed that the peptide belonged to hepcidin family. Similarity searches using BLASTn indicated that the nucleotide sequence of *Le*-Hepc showed only 88 % similarity with *Dicentrarchus labrax* (GenBank ID: KJ890400), 87 % similarity with that of *Morone chrysops* (GenBank ID: AF394246) and 83 % similarity with *Pagrus major* (GenBank ID: AY557619) hepcidin precursor nucleotide sequences. The deduced prepropeptide sequence of *L. equulus* showed 78 % similarity with the recombinant bass hepcidin precursor of *M. chrysops* x *M. saxatilis* followed by 77% similarity with that of *D. labrax* and 71 % similarity with *Zanclus cornutus* precursor hepcidin respectively.

SignalP 3.0 analysis revealed the existence of a putative cleavage site for signal peptidase positioned between 24$^{th}$ and 25$^{th}$ amino acid, SSA-VP residue of *Le*-Hepc, producing a 24 amino acid signal peptide (Fig. 2.7a). ScanProsite analysis revealed that the *Le*-Hepc sequence

contains a region which is essentially cysteine rich (residues 67-84). Common motifs identified apart from the cysteine rich region includes one protein kinase C phosphorylation site at $Ser^{55}$-$Ser^{56}$-$Arg^{57}$, one cAMP-CGMP-dependent protein kinase phosphorylation site at $Lys^{59}$-$Arg^{60}$-$His^{61}$-$Ser^{62}$ and three N-myristoylation sites at $Gly^{66}$-$Cys^{67}$-$Arg^{68}$-$Phe^{69}$-$Cys^{70}$-$Cys^{71}$,$Gly^{72}$-$Cys^{73}$-$Cys^{74}$-$Pro^{75}$-$Asn^{76}$-$Met^{77}$ and $Gly^{79}$-$Cys^{80}$-$Gly^{81}$-$Val^{82}$-$Cys^{83}$-$Cys^{84}$. ProP 1.0 predicted the cleavage sites for propeptide convertase positioned between $Arg^{60}$ and $His^{61}$ after the motif RHKR, resulting in a 36 amino acid prodomain and 26-mer mature peptide with eight conserved cysteine residues (Fig. 2.7b). The 26 amino acid mature peptide of *L. equulus* hepcidin will be referred hereafter as *mLe*H. The DAS prediction server also identified the presence of a trans-membrane amino acid sequence (6–19) in the N-terminal region of *Le*-Hepc, encompassing the signal peptide region. *In vivo* aggregation propensity determined using AGGRESCAN predicted the presence of two hot spots in *mLe*H with a calculated value of 0.314 and 0.295 for the sequences (-CRFCCGC-) and (-CGVCCRF) respectively.

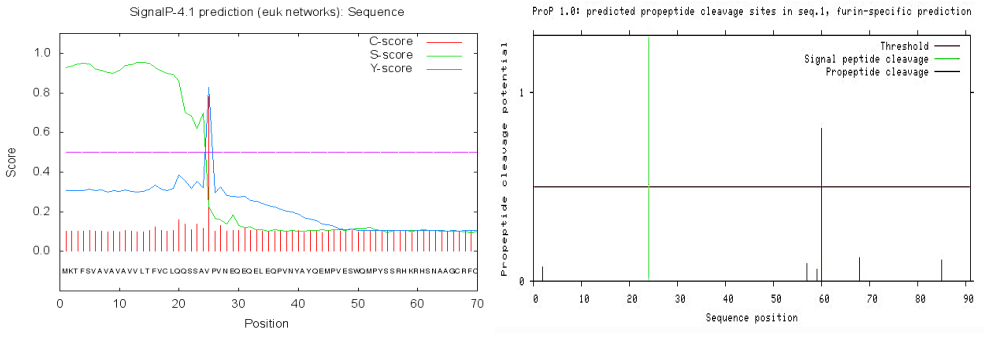


(a) (b)

**Fig. 2.7** (a) Signal peptide analysis and (b) Propeptide analysis of *Le*-Hepc (GenBank ID: **KM034809)** as predicted by the SignalP 4.1 and ProP 1.0 server respectively.

Peptide characterisation as predicted by ProtParam tool disclosed that the *mLe*H has a molecular weight of 2.73 kDa, a net positive charge of +2, theoretical p*I* of 8.23 and a total hydrophobic ratio of 53 %, while the precursor molecule possess no net charge and has a net hydrophobic ratio of only 45 %. *Le*-Hepc was found to be rich in amino acids such as Val (12 %), Cys (10 %), and Ala (8 %) while its mature region contained more Cys (30 %) and Gly (15 %). Amphipathic character of *Le*-Hepc as analysed by ProtScale tool is represented as Kyte-Doolittle plot (Fig. 2.8).

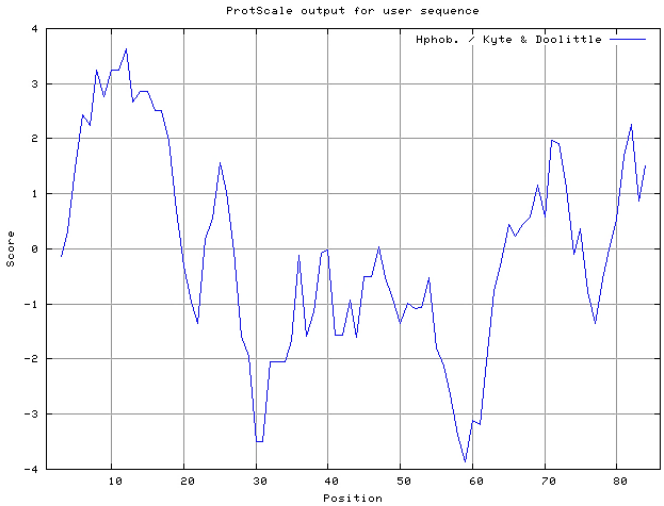


**Fig**. **2.8** Kyte-Doolittle plot showing hydrophobicity of *Le*-Hepc (GenBank ID: **KM034809).** The peaks above the score (0.0) indicate the hydrophobic nature of the predicted peptide.

Kyte-Doolittle plot demonstrated the presence of hydrophobic amino acids concentrated in the first 20 residues and last few residues of the peptide. The cationicity of the mature domain was found to be mainly contributed by histidine and arginine residues, as no lysine residue was found to be present. The estimated half-life of the *mLe*H is predicted to be

about 3.5 h in mammalian reticulocytes and greater than 10 h in *Escherichia coli in vivo*. The instability index of the mature peptide was computed to be 35.07 which classify the peptide as a stable peptide. Moreover, the predicted mRNA structure of *Le*-Hepc had a MFE value of -76.60 kcal/mol and indicated that the RNA is mostly paired with very few nucleotides left unpaired (Fig. 2.9).

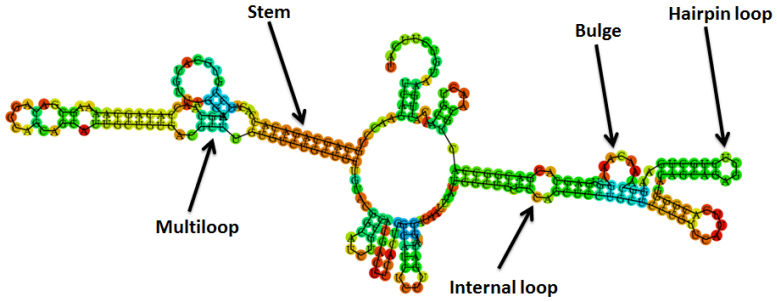


**Fig. 2.9** mRNA structure of *Leiognathus equulus* hepcidin, *Le*-Hepc drawn using RNA fold server. The different regions of mRNA are appropriately marked.

Multiple sequence alignment of *Le*-Hepc with the related pre-propeptide hepcidin sequences retrieved from the GenBank outlined the conserved domains and residues in fish, amphibian, and mammalian hepcidins (Fig. 2.10A). Multiple sequence aligned members showed high similarity in the signal peptide region, though a great variation could be observed in the prodomain (Fig. 2.10B a and b). The 8 cysteine residues that participated in disulphide bond formation were found to be highly conserved in the mature realm of all the representative group members (Fig. 2.10B c). Moreover, the C-terminus (–CCR/KF) of the mature domain showed a high degree of conservation among most of the fish hepcidins.

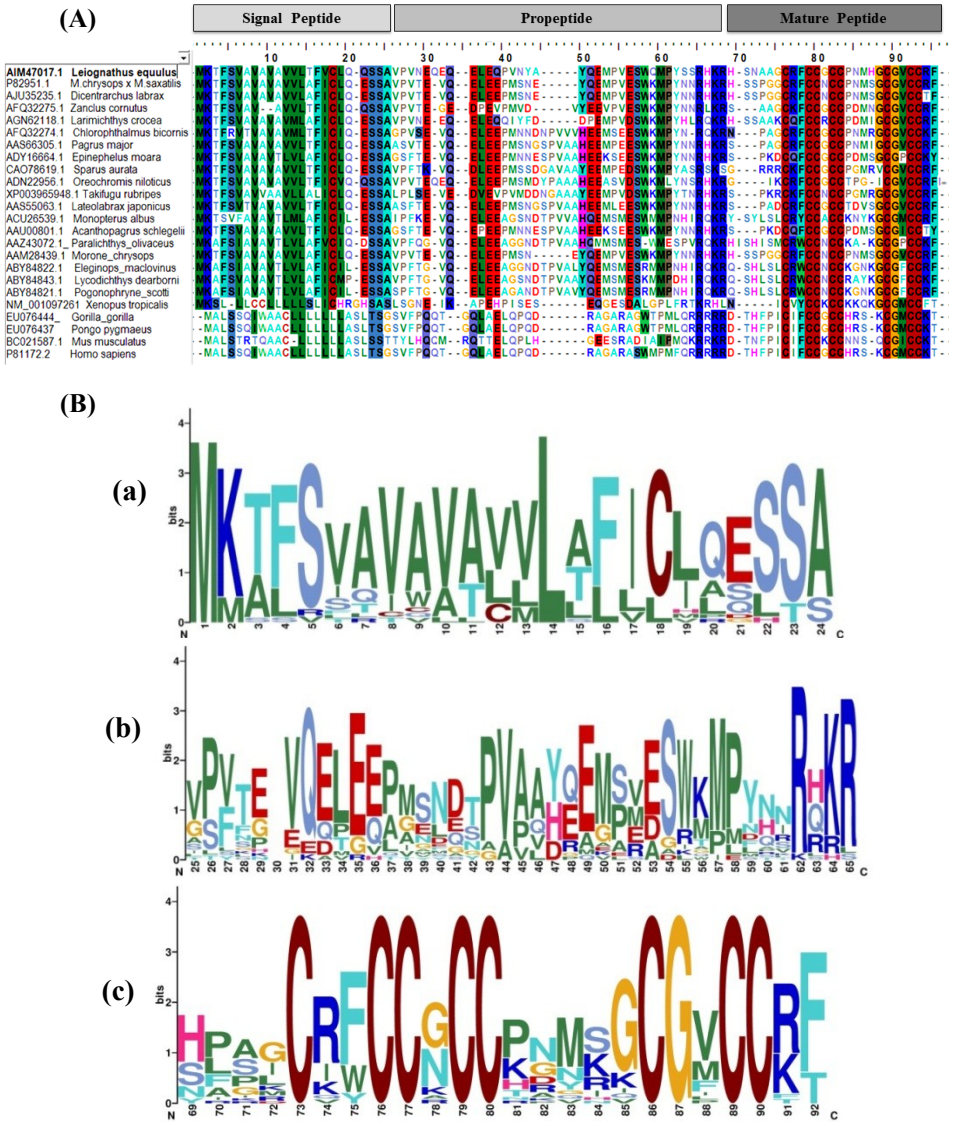


**Fig. 2.10** (A) ClustalW multiple alignment of *Leiognathus equulus* hepcidin, *Le*-Hepc with other reported fish and non-fish vertebrate hepcidins obtained using BioEdit software. The relative positions of signal peptide, propeptide and mature peptide of all the sequences are marked. The identical residues are highlighted with background colours. (B) WebLogo visualization of the consensus motif based on multiple alignments of hepcidins. (a) Sequence logo of the signal peptide region, (b) sequence logo of the pro-peptide region and (c) sequence logo of the mature peptide region. The height of the letters indicates the relative frequency of the letter at that position and the overall height of the stack indicates the sequence conservation in terms of information content in bits.

The phylogenetic tree constructed based on the prepro-hepcidin sequences, revealed the relationship of *Le*-Hepc (GenBank Protein ID: AIM47017) with other vertebrate hepcidins retrieved from GenBank. The unrooted phylogenetic tree (Fig. 2.11) of *Le*-Hepc showed a marked separation between the two largest branches, the mammalian–amphibian group and the fish group. The percentages of replicate trees in which the associated taxa clustered together in the bootstrap test (1000 replicates) are shown next to the branches of the tree. *L. equulus* hepcidin was found to be deeply nested within the fish clade and seen more closely related to *Z. cornutus* hepcidin (GenBank ID: JX13300) and *D. labrax* hepcidin (GenBank ID: KJ890397.1). The two broad evolutionary lineages of hepcidins, HAMP1 and HAMP2, were seen as distinct and separate clades as illustrated in the phylogenetic tree. Antarctic fishes formed a separate subcluster. Phylogenetic analysis reconfirmed the inclusion of *Le*-Hepc in the HAMP2-like group of peptides and its possible role as an antimicrobial peptide rather than an iron regulatory hormone.

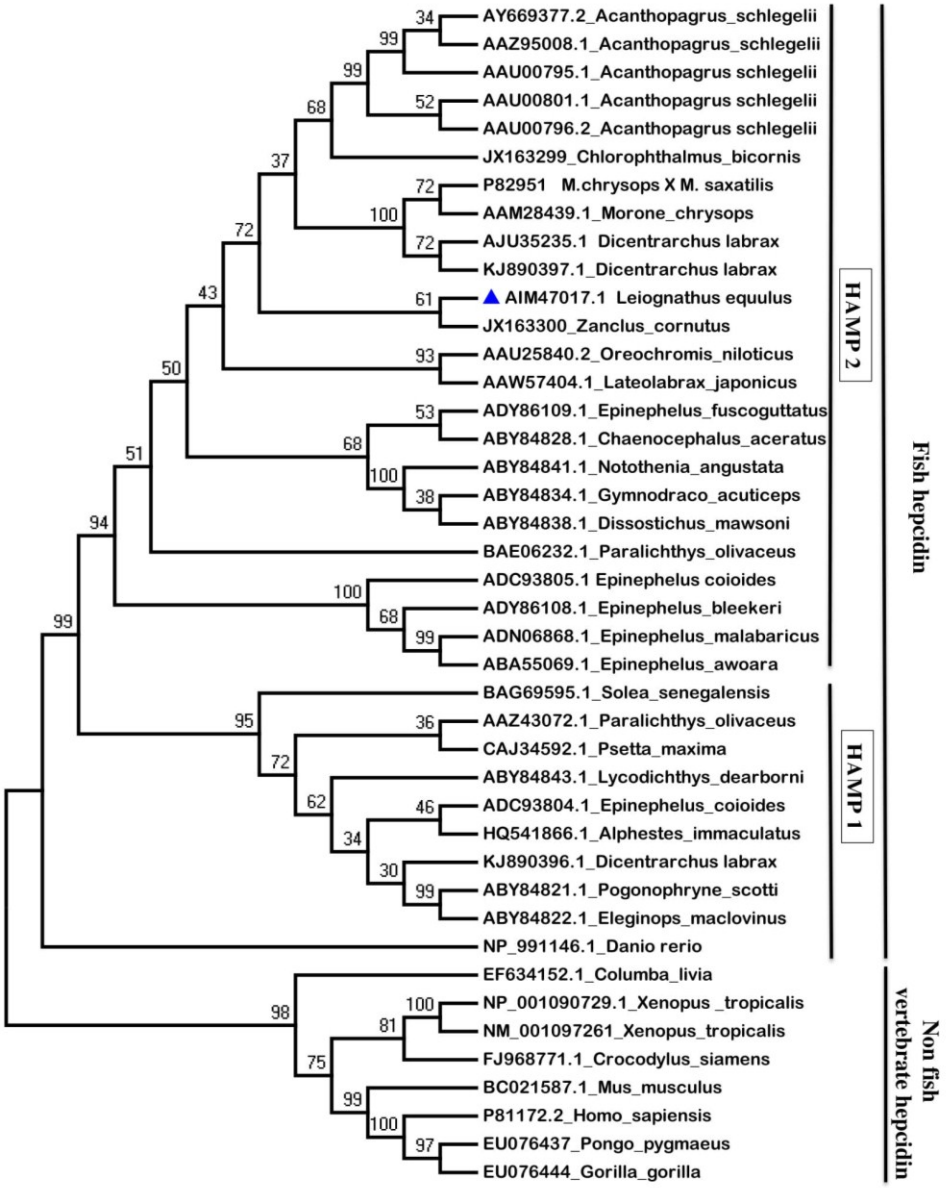


**Fig. 2.11** A bootstrapped Maximum Likelihood tree obtained using MEGA version 6.0.6, illustrating the phylogenetic relationship of *Leiognathus equulus* hepcidin, *Le*-Hepc with prepro-hepcidins of fishes as well as representatives from other vertebrate classes obtained from GenBank. The numbers shown at the branches denote the bootstrap majority consensus values of 1000 replicates.

Secondary structural analysis of *Le*-Hepc indicated an α-helical N-terminal region followed by random coiled regions (Fig. 2.12a). Apparently, signal peptide residues constituted the α-helical regions while the propeptide domain formed the random coiled portion. Among the 26 amino acids (aa) forming *mLe*H, only 21 residues were found to be largely involved in the formation of a stable secondary structural conformation. Secondary structure analysis of *mLe*H (Fig. 2.12b), as predicted by PDBsum, revealed the presence of one β-hairpin-like structure, two β turns and two γ turns. The formation of a β hairpin involved two β strands that are adjacent in their primary structure, but oriented in an antiparallel direction. The amino acids $Arg^{68}$, $Phe^{69}$, and $Cys^{70}$ constituted the β1 sheet while the amino acids $Gly^{81}$, $Val^{82}$, and $Cys^{83}$ framed the β2 sheet. The two β turns present in the mature peptide are of type IV and are constituted by CCGC ($Cys^{70}$- $Cys^{73}$) and the CPNM ($Cys^{74}$-$Met^{77}$) motifs. Also, the two inverse γ turns are formed by the CPN ($Cys^{74}$-$Asn^{76}$) motif and the MHG ($Met^{77}$-$Gly^{79}$) motif. The secondary structure is strengthened by four disulphide bonds in the following patterns, $Cys^{67}$–$Cys^{84}$, $Cys^{70}$–$Cys^{83}$, $Cys^{71}$–$Cys^{80}$, and $Cys^{73}$–$Cys^{74}$. The disulphide bonds in the $Cys^{70}$–$Cys^{83}$ and $Cys^{71}$–$Cys^{80}$ residues are of the right handed hook and short right handed hook types, respectively.

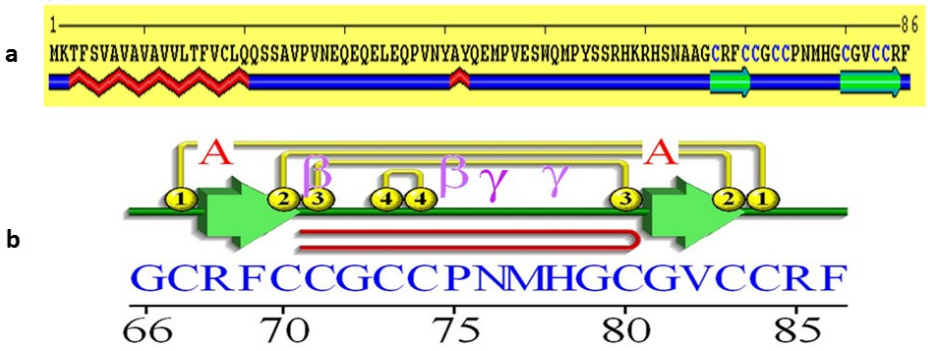


**Fig. 2.12** (a) Secondary structure annotation of *Leiognathus equulus* hepcidin, *Le*-Hepc predicted using POLYVIEW-2D. The α-helix region is shown in zig zag red lines, β-strand is shown in green arrows, and the coil region is shown in blue lines. The conserved cysteine residues are highlighted in blue colour. (b) Secondary structure wiring diagram of the mature peptide of *Le*-Hepc as predicted by PDBsum. The residues or motifs forming the β hairpins, β turns and the γ turns are shown. The cysteine residues forming the four disulphide bonds are also indicated.

The three-dimensional structure of *Le*-Hepc mainly consists of two antiparallel β sheets with intertwining random coiled portions stabilised by four disulphide bonds. It contains both charged residues and hydrophobic moieties that allow strong interactions between the peptides and the membranes. The spatial structure of *Le*-Hepc (Fig. 2.13) was constructed based on homology modelling using the solution structure of hybrid white striped bass hepcidin (PDB ID: 1S6W) as the template. *Le*-Hepc showed 90.5 % structural similarity with hybrid white striped bass hepcidin against a 57.9 % similarity with the NMR structure of human hepcidin 20 (PDB ID: 1m4e) as validated by PDBsum results.

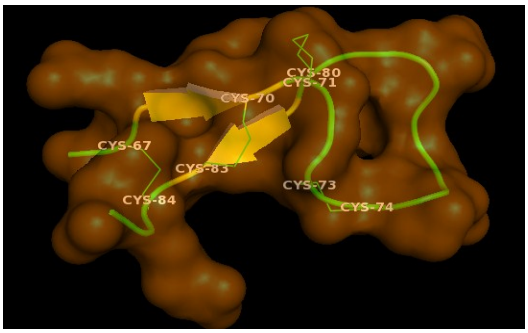


**Fig. 2.13** Spatial structure of *Le*-Hepc constructed by homology modelling using PyMOL software using the PDB ID: 1S6W, obtained from SWISS-MODEL server. The two antiparallel β-pleated structures are seen as yellow coloured ribbons. Cysteine residues that participate in disulphide bonds which stabilize the β -hairpin are highlighted.

The Antimicrobial peptide (APD2) database prediction confirmed the antimicrobial property of *mLe*H. The mature domain net charge (+2) with protein binding potential (Boman index) of 0.99 kcal/mol ensured its antimicrobial property. APD2 analysis indicated the presence of 14 hydrophobic residues on the hydrophobic surface of the mature peptide accounting for a grand average of hydropathicity (GRAVY) of 0.34, emphasising a strong interaction with the membrane of microbes and hence its role as an antimicrobial peptide. Additionally, sequence alignment of *mLe*H with other peptides in the APD2 database exhibited 84 %, 73.07 %, 61.53 %, and 60.7 % similarity with *Acanthopagrus schlegelii* (hepcidin 2), hybrid bass hepcidin (*Morone chrysops* x *M. saxatilis*), *Sparus aurata* hepcidin, and *Oreochromis mossambicus* hepcidin, respectively. The $CAMP_{R3}$ database with its various algorithms indicated that the sequence $His^{61}$-$Arg^{86}$, i.e., the 26-mer mature domain, possessed the highest probability of being an antimicrobial peptide among all the segments of *Le*-Hepc. The support vector machine (SVM) {1}, random

forest classifier (RFC) {0.72}, discriminant analysis classifier (DAC) {1}, and artificial neural classifier (ANN) calculated the probability percentage of the mature peptide (values given in curly brackets) and classified *mLe*H as an antimicrobial peptide.

### 2.3.2 Recombinant production and functional characterization of *mLe*H

Analysis of *Le*-Hepc with various bioinformatics tools predicted the mature peptide of *Le*-Hepc, excluding the signal peptide possessed the biologically active region. Hence the selected region designated as *mLe*H, was subjected to recombinant expression and for analyzing its biological activity.

#### 2.3.2.1 PCR amplification and cloning of the target gene with restriction sites

Selective amplification of the target gene, *mLe*H was performed using restriction primers designed (Table 2.2). Approximately 100 bp target gene amplicon was obtained by PCR amplification using pGEMT-*Le*-Hepc as template (Fig. 2.14). The PCR product was purified and cloned into pGEM®-T Easy cloning vectors and transformed into *E. coli* DH5α competent cells. Colony PCR was performed with vector specific and gene specific primers to confirm the presence of plasmid with the target gene. Approximately 100 bp amplicons (comprising restriction sites) was obtained using gene specific (pET *Le*-Hepc F and R) and 241 bp (100 bp + 141 bp) with vector specific primers (T7 F and SP6 R) respectively (Fig. 2.15). From the positive colonies, plasmids with inserts were extracted and sequencing of the plasmid was done to check the presence of restriction site and orientation of target gene.

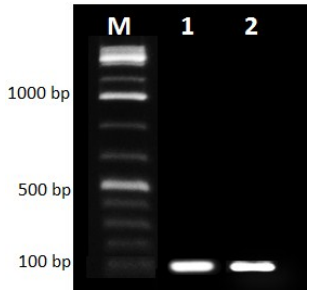


**Fig. 2.14** Agarose gel of PCR amplified mature peptide region of *Le*-Hepc with restriction primers. Lane M: 100 bp ladder, Lane 1-2: PCR amplified product (100 bp).

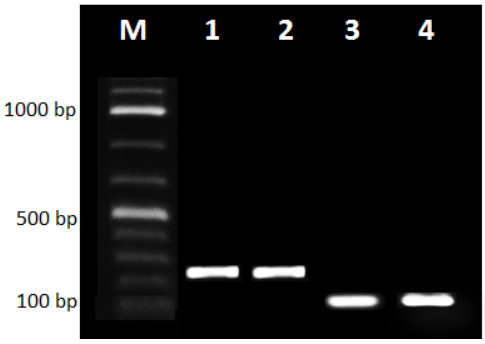


**Fig. 2.15** Agarose gel image of colony PCR. Lane M: 1 kb ladder, Lane 1-2: amplicon (241 bp) of PCR using vector specific primers, Lane 3-4: amplicon (~100 bp) obtained for PCR with insert specific primers.

### 2.3.2.2 Restriction enzyme digestion and cloning of target gene into pET-32a(+) expression vector

Recombinant plasmids after confirmation of the presence and orientation of the restriction sites and the target gene were subjected to restriction digestion using NcoI and HindIII restriction enzymes. Agarose gel analysis of the restriction digested products confirmed the release of inserts. Two distinct bands, one at the bottom of the gel (~100 bp) representing the released insert and other one at the top of the gel, the cut plasmid could be observed from the gel image (Fig. 2.16a). No much

difference in size in the digested recombinant pGEMT plasmid and the control pGEMT plasmid could be observed as only a small fragment is released by restriction digestion. Subsequently, pET-32a(+) expression vector was also digested using the same RE (Fig. 2.16b). Following double digestion, the restriction digested insert and vector were gel eluted using GenJET™ Gel Extraction Kit.

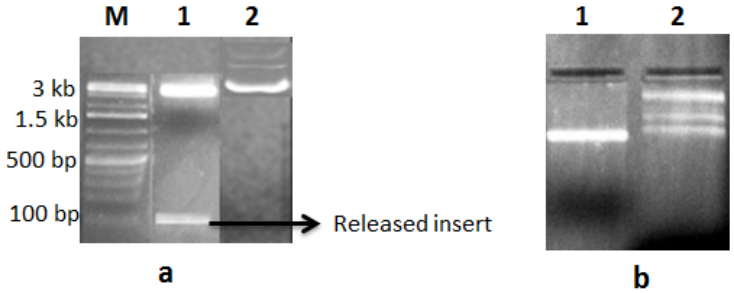


**Fig. 2.16** Agarose gel image of plasmids digested with Nco1 and HindIII restriction enzymes. (a) Lane M: 1kb ladder, Lane 1: Restriction enzyme digested pGEMT-*mLe*H plasmid with released insert, Lane 2: Un-digested pGEMT-*mLe*H plasmid (b) Lane 1: restriction enzyme digested linearized pET-32a(+) vector, Lane 2: Un-digested pET-32a(+) vector

Restriction digested target gene and pET-32a(+) vector were subjected to ligation and transformed to *E. coli* DH5α. Screening for the recombinant clones were done by colony PCR. Amplicons of size 850 bp (100 bp + 750 bp) and 100 bp were obtained for vector specific primers (T7 F and T7 R) and gene specific primers respectively (Fig. 2.17a). Plasmids were extracted from positive clones and sequenced using T7 F and T7 R primers to ensure correct orientation of the expression cassette without any frame shift (Fig. 2.17b). The recombinant vector pET-32a(+)-*mLe*H was transformed to expression host *E. coli* Rosetta-gami$^{TM}$ B (DE3) pLysS and colonies were obtained in LB agar plates with ampicillin and kanamycin.

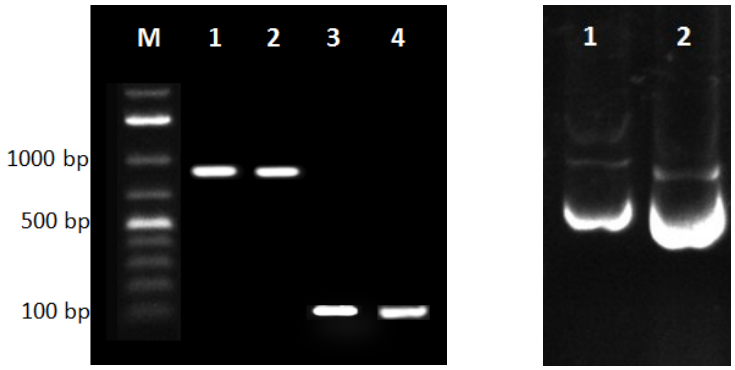


**Fig. 2.17** (a) Agarose gel image of colony PCR of pET-32a(+) vector construct with *mLe*H insert using T7 forward and T7 reverse primers. Lane M: 1 kb DNA marker, Lane 1 and 2: 850 bp amplicons of PCR performed using vector specific primers, Lane 3 and 4: 100 bp PCR amplicons amplified using insert specific primers. (b) Plasmid gel image of the recombinant plasmid and the control pET plasmid. Lane 1: pET-32a(+) plasmid with the *mLe*H insert, Lane 2: pET plasmid without any insert.

### 2.3.2.3 Recombinant expression of *mLe*H as fusion protein

The mature peptide of HAMP2 isoform, *mLe*H from *L. equulus* was successfully produced as a fusion protein containing 6 x His tag and thioredoxin tag. Transformed Rosetta-gami™ B (DE3) pLysS cells were cultured in LB both with preferred antibiotics by providing incubation at 37 °C with orbital shaking at 250 rpm. *E. coli* Rosetta-gami™ (DE3) pLysS cells harboring the recombinant expression plasmid, pET-32a(+)-*mLe*H, expressed the target trxA-6 x His tag-*mLe*H fusion protein following induction with 0.1 mM IPTG. The fusion protein produced in the heterologous expression system appeared as a monomer and was found to be expressed in soluble form in the cytoplasm. Tricine- SDS-PAGE analysis of the proteins expressed in *E. coli* from the pilot scale expression aliquots revealed a prominent band at 22.7 kDa corresponding to the size of recombinant hepcidin (Fig. 2.18). The observed molecular

mass of the fusion protein was in agreement with the calculated molecular mass based on their deduced amino acid sequences. i.e., 2.7 kDa of *mLe*H combined with approximately 20 kDa of the fusion thioredoxin protein. The intensity of expression increased from the time of induction with IPTG to a maximum by 5 h. The expression level was found to be fairly constant thereafter (Fig. 2.18). Also, no basal level expression was observed at the $0^{th}$ h. Hence mass production of *mLe*H was carried out at 37 °C, with shaking at 250 rpm for 5 h post induction. The cells were then harvested and stored at -20 °C.

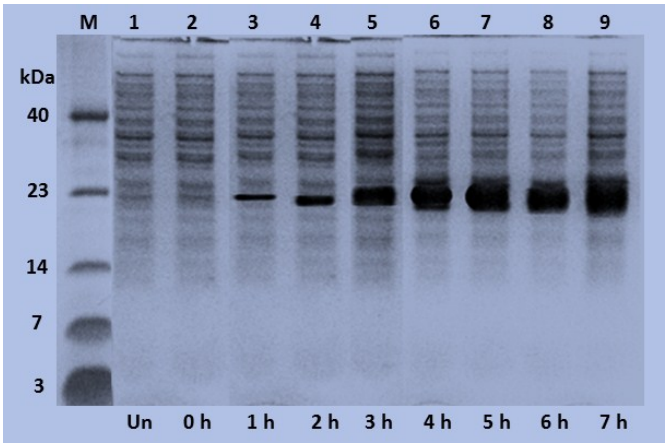


**Fig. 2.18** Tricine SDS-PAGE analysis of recombinant expression of *mLe*H, before and after IPTG induction on a time-course basis. Lane M: Low-range protein ladder, Lane 1: uninduced control (before IPTG induction), Lane 2: recombinant cells at the time of induction; Lane 3-9: IPTG induced cells after 1-7 hours of induction.

Meanwhile, heterologous production of thioredoxin (Trx) with 6x-His-tag (negative control) was also performed in a similar manner. The transformants with empty pET-32a(+) vector with no insert was induced with 0.1 mM IPTG, cultured under the same growth conditions.

A distinct band at 20.4 kDa representing Trx fusion protein was detected as early as 2nd h post induction (Fig. 2.19). Hence mass production of the control protein was carried out in 2 l media and cells were harvested second hour post induction and kept at -20°C.

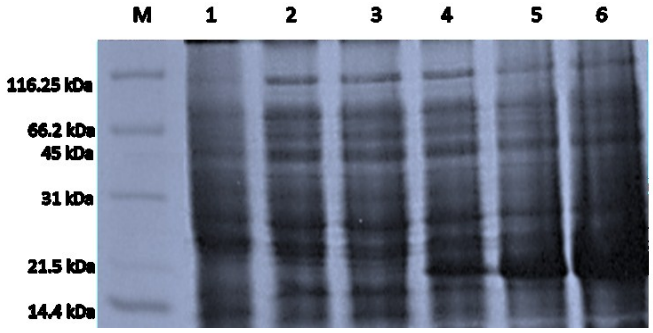


**Fig. 2.19** Tricine SDS-PAGE analysis of recombinant expression of Thioredoxin, Trx, before and after IPTG induction on a time-course basis. Lane M: High-range protein ladder, Lane 1: un-induced control (before IPTG induction), Lane 2-6: IPTG induced cells after 0-4 hours of induction.

### 2.3.2.4 Purification, refolding and quantification of the recombinant protein

The r*mLe*H and rTrx samples were purified by immobilized metal affinity chromatography (IMAC) using Ni-NTA columns. The eluted fractions were analysed by SDS-PAGE (Fig. 2.20a) and the N-terminal His tagged recombinant proteins were detected by Anti-His antibody in the western blot (Fig. 2.20b). Amicon cut off filtration unit was used for concentrating and refolding the purified recombinant proteins from the eluted fraction. Protein concentration of r*mLe*H and rTrx were quantified using Quant-iT™ protein assay kit and the concentration was found to be 2.47mg/ml and 1.42 mg/ml respectively.

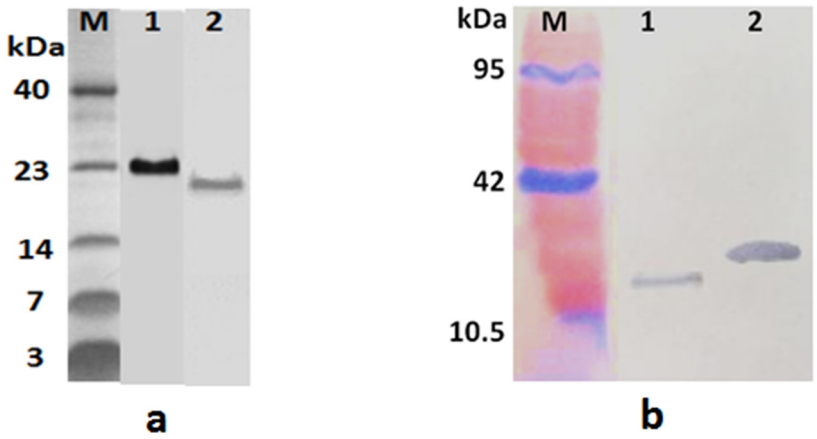


**Fig. 2.20** (a) Tricine SDS-PAGE analysis of Ni-NTA purified proteins. Lane M: Low range weight protein marker, Lane 1: purified recombinant *mLe*H (22.7 kDa), Lane 2: purified recombinant Trx (20.4 kDa). (b) Western blot showing the purified recombinant proteins, Lane M: Mid-range coloured marker, Lane 1: purified rTrx, Lane 2: purified r*mLe*H.

### 2.3.2.5 *In vitro* cytotoxicity and haemolytic activity of the recombinant proteins

Cytotoxicity of r*mLe*H and rTrx control peptide was tested against NCI-H460 cell lines ranging from 0.625 µM to 20 µM by using XTT assay. r*mLe*H and rTrx demonstrated minimal cytotoxic activity at the tested concentration. At higher concentration of r*mLe*H and rTrx tested, the peptides exhibited only 4 % and 2 % growth inhibition and thus found to be non-cytotoxic to the NCI H460 cells. Melittin, a positive control, showed significant cytotoxic activity at the highest peptide concentration tested (20 µM) and exhibited an $IC_{50}$ of 16.6 µM (Fig. 2.21).

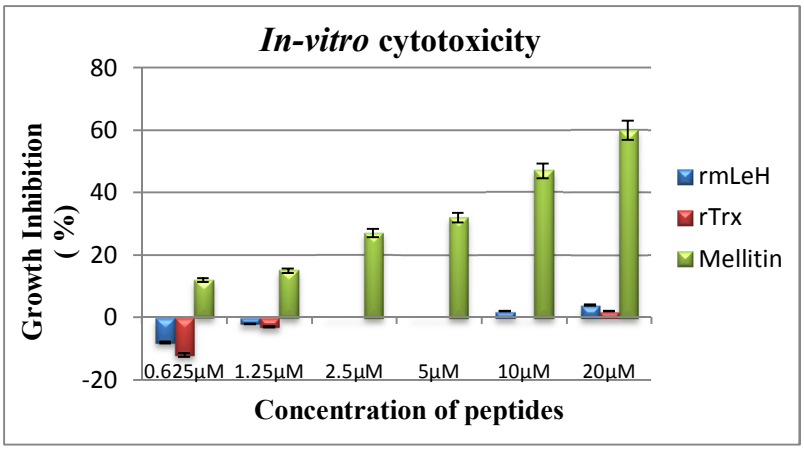


**Fig. 2.21** *In vitro* cytotoxicity of the recombinant peptides r*mLe*H, rTrx and mellitin in NCI-H460 cells at various concentrations.

Cytotoxicity against normal mammalian cells, the human RBCs was used to analyse the haemolytic activity of the recombinant peptides. The recombinant peptides, r*mLe*H and rTrx, demonstrated very weak haemolytic activity indicating that they might be safe to use in the concentrations tested. The highest concentration of r*mLe*H tested (20 µM), lysed only 0.3 % of erythrocytes, compared to the positive control mellitin (Fig. 2.22).

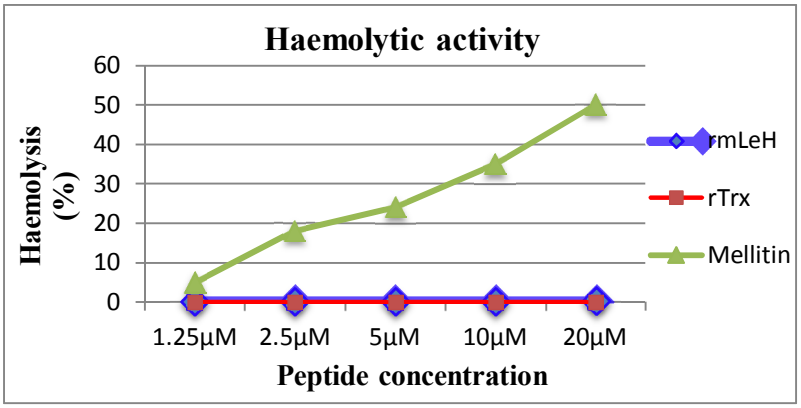


**Fig. 2.22** Haemolytic activity of the recombinant peptides r*mLe*H, rTrx and mellitin in human RBCs at various concentrations

### 2.3.2.6 Antimicrobial activity

Broth microdilution assay was performed to analyse the antimicrobial activity of recombinant *mLe*H, at a concentration ranging from 20 µM to 0.625 µM. Thioredoxin protein, rTrx, expressed from the empty pET-32a (+) vector was maintained as the internal control. Incubation of the bacteria with the control peptide had no apparent effect on bacterial survival suggesting that the observed bactericidal effects were specific to recombinant *mLe*H. The test peptide r*mLe*H exhibited considerable antimicrobial activity towards *Staphylococcus aureus* (99 % growth inhibition; MIC of 5 µM and MBC of 10 µM) and *Escherichia coli* (99.8 % growth inhibition; MIC of 5 µM and MBC of 10 µM), *Aeromonas hydrophila* (99 % growth inhibition; MIC of 10 µM and MBC of 20 µM), and *Edwardsiella tarda* (99 % growth inhibition; MIC of 10 µM and MBC of 10 µM). Though, all the other tested pathogens were found to be sensitive to r*mLe*H, the MIC and MBC values were observed to be >20 µM.

The growth inhibition percentage of r*mLe*H at 20 µM observed for rest of the organisms were *B. cereus* - 71 %, *V. parahaemolyticus* - 73 %, *V. cholera* - 85%, *V. alginolyticus* - 94 %, *V. proteolyticus* - 93 %, *V. vulnificus* - 88%, *P. aeruginosa* - 88 % (Fig. 2.23).

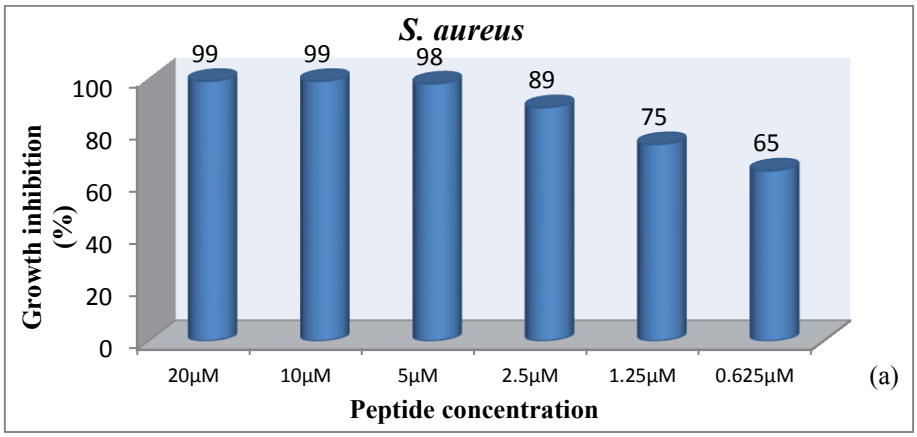


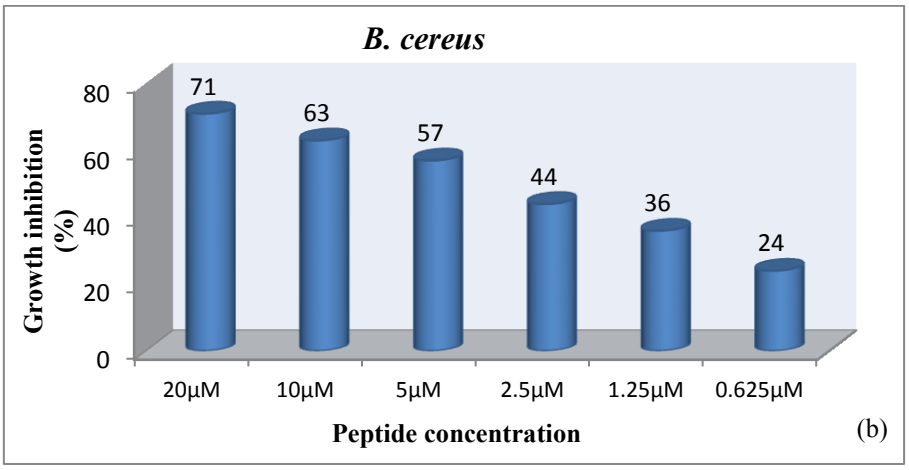


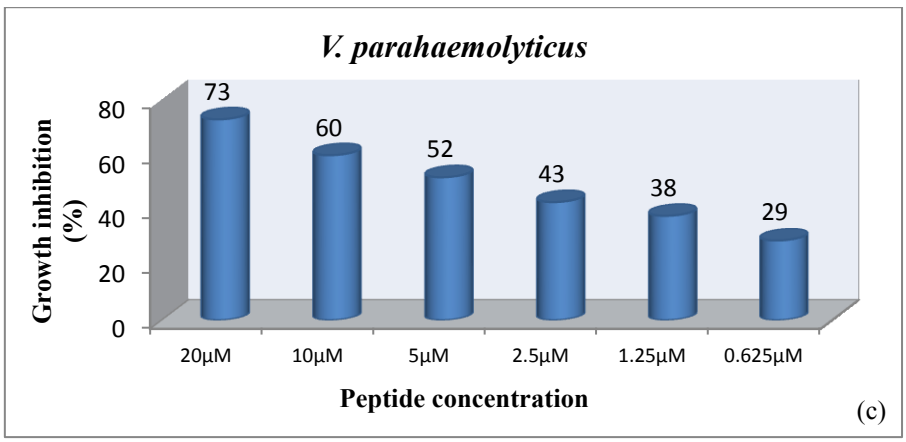


*Fig. 2.23 Continued…*

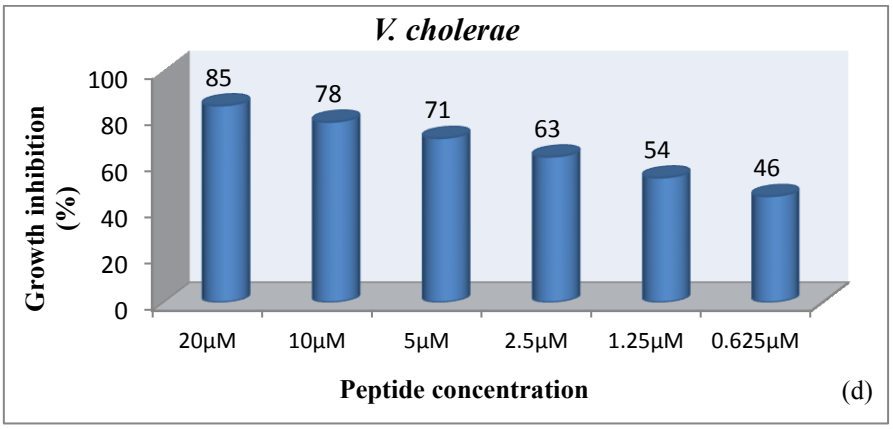


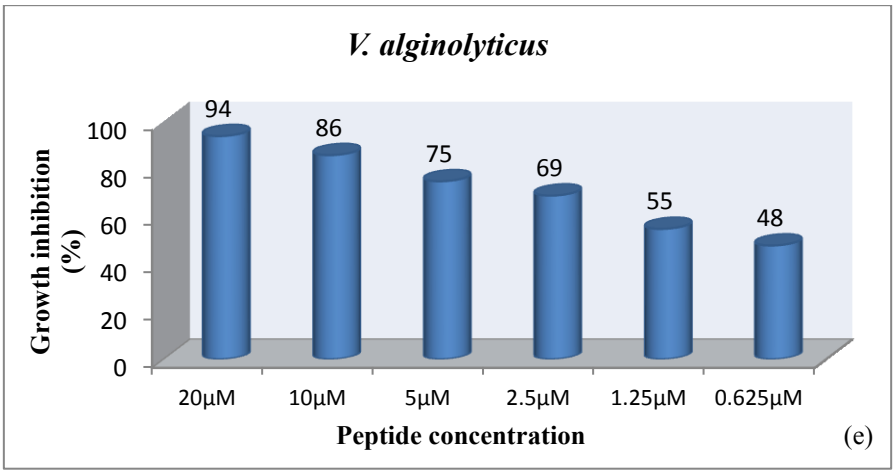


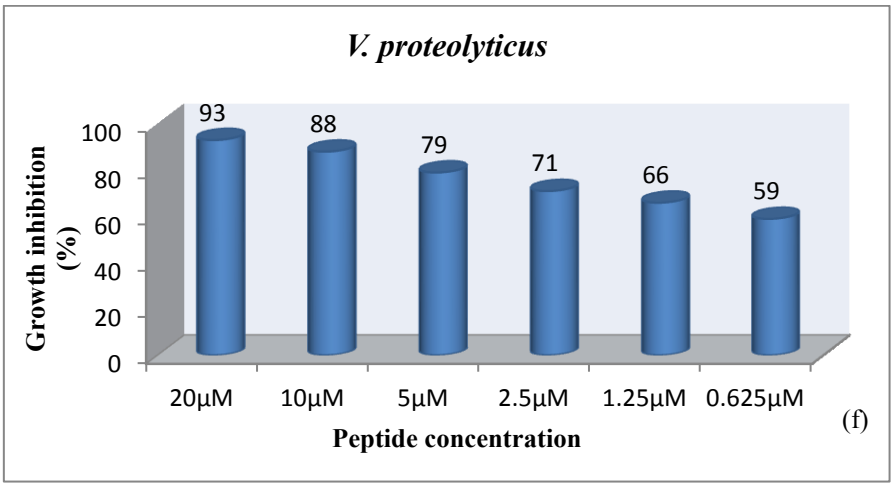


*Fig. 2.23 Continued…*

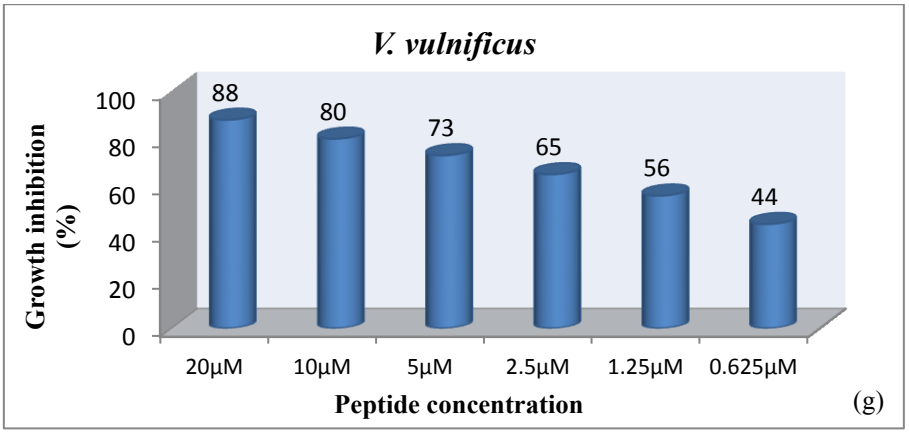


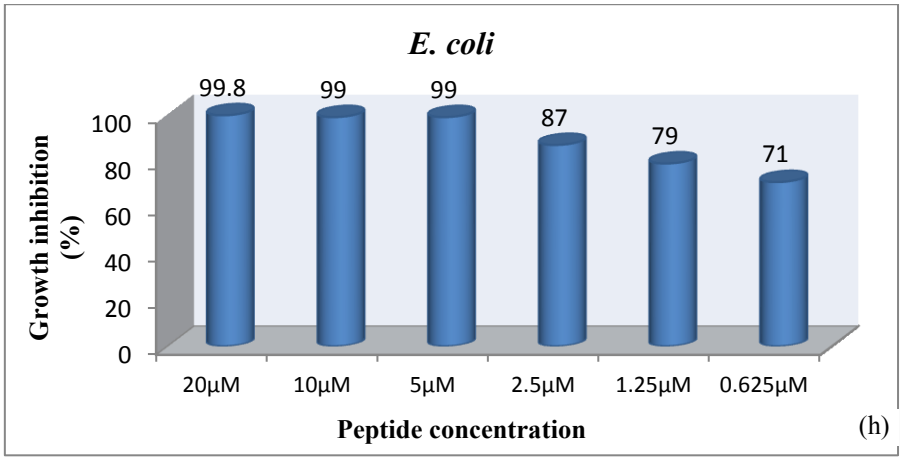


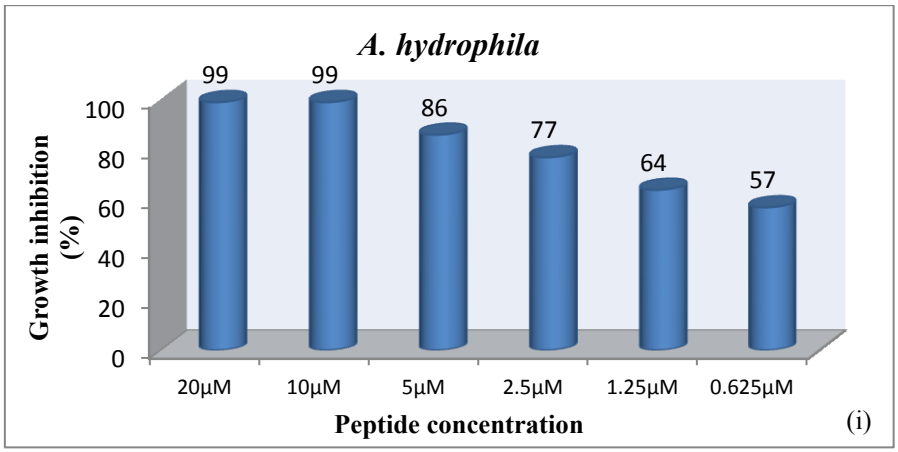


*Fig. 2.23 Continued…*

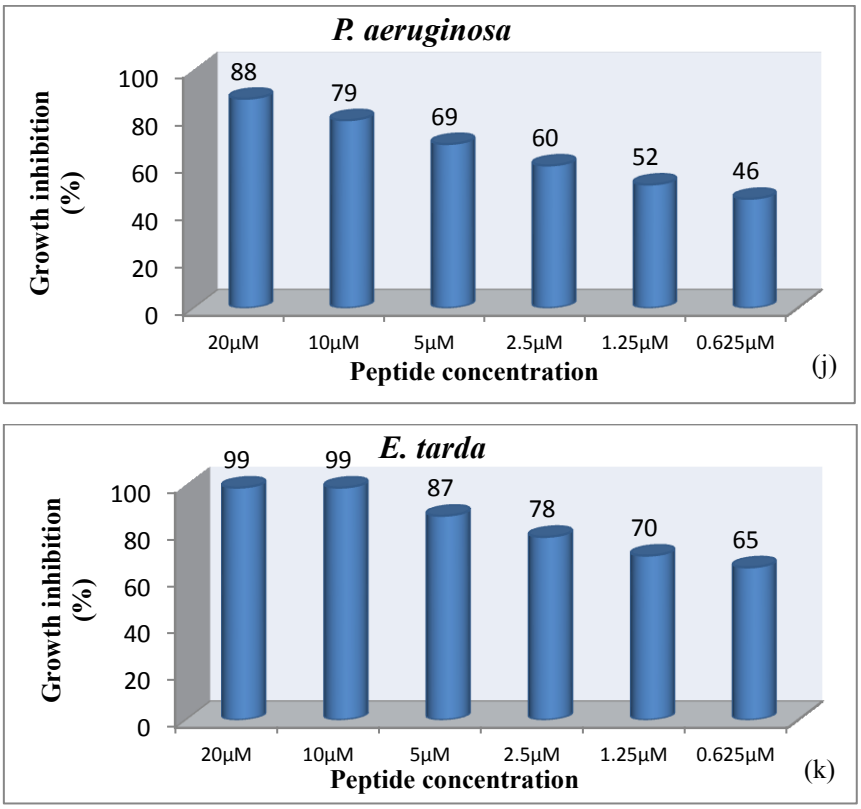


**Fig. 2.23 (a-k)** Antimicrobial activity of r*mLe*H against various bacteria at different concentrations

### 2.3.2.7 PI staining

Fluorescence emission of propidium iodide was detected and used as a dead cell marker for recombinant peptide treated bacteria (*S. aureus, E. coli, Aeromonas hydrophila*, *E. tarda*). The dye cannot penetrate the live and intact cells but can easily enter cells whose membrane has been disrupted and intercalates the DNA, emitting fluorescence with high intensity. Figure 2.24 represents the fluorescence images of susceptible bacteria taken at 100 X magnification. The control live cells exhibit less fluorescence; whereas majority of the cells treated with the peptide appeared red, suggesting, possible mode of action of r*mLe*H causing membrane damage.

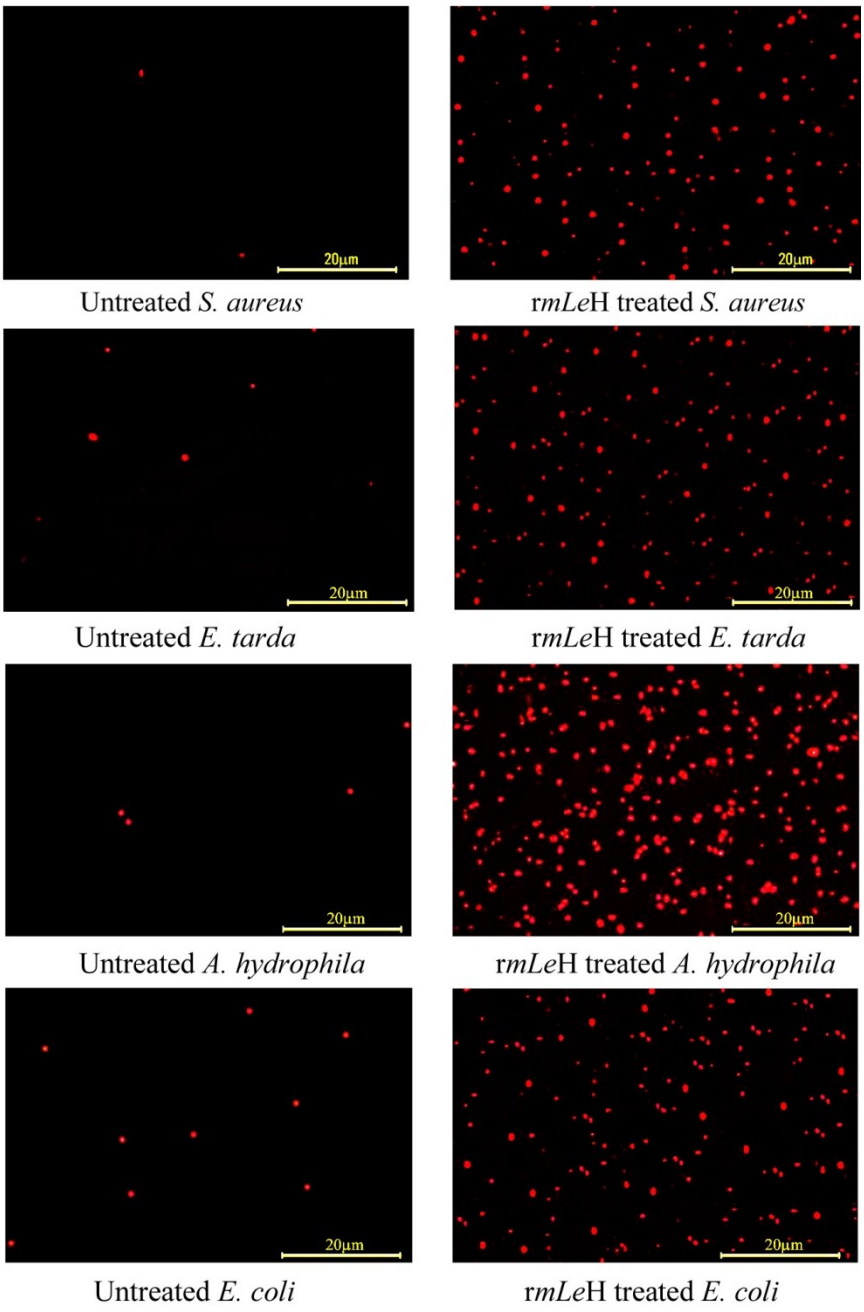


**Fig. 2.24** Fluorescent microscopy images of bacterial cells stained with propidium iodide without peptide treatment and after incubation with r*mLe*H peptide.

### 2.3.2.8 SEM analysis

The effect of r*mLe*H on the morphology of susceptible bacterial cells was analyzed using scanning electron microscopy (SEM).

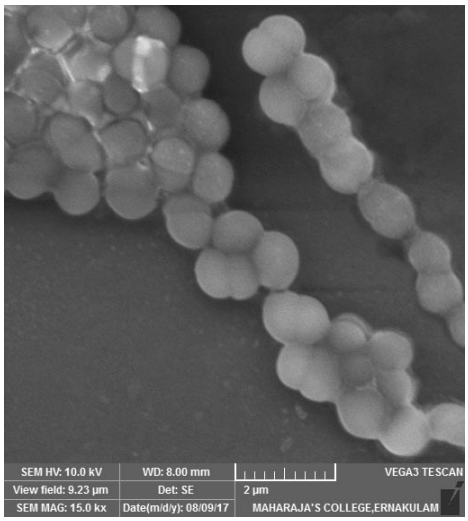


Untreated *S. aureus*

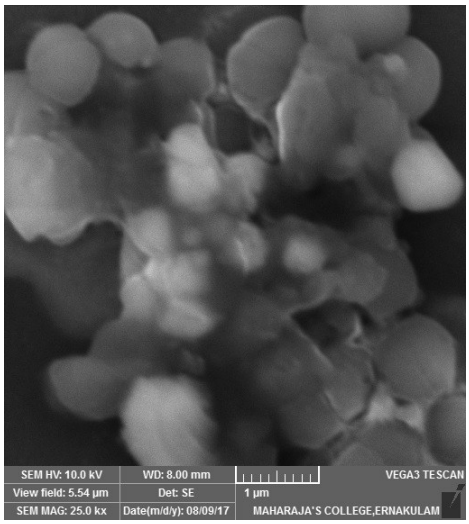


r*mLe*H treated *S. aureus*

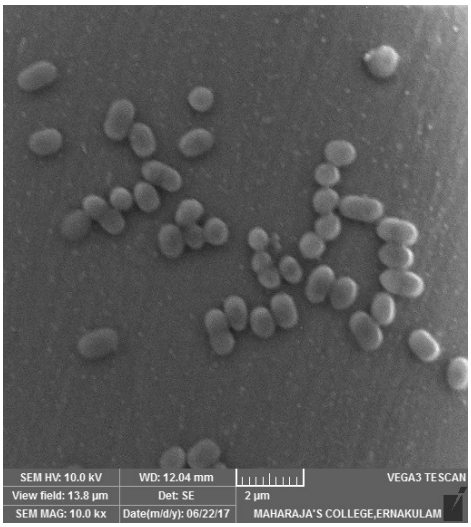


Untreated *E. tarda*

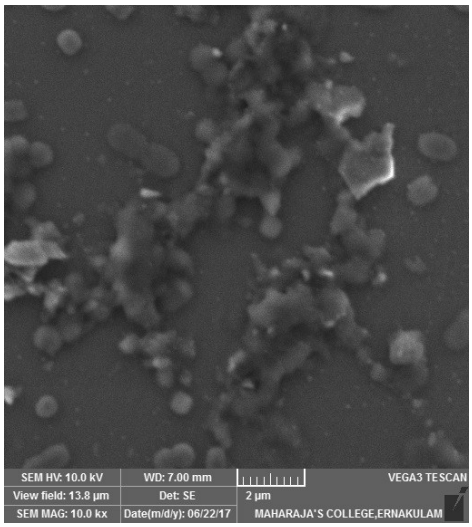


r*mLe*H treated *E. tarda*

**Fig. 2.25** SEM images of representative members of pathogens, control-untreated and r*mLe*H peptide treated pathogens.

Fig. 2.25 shows the topography of control bacteria and bacterial cells treated with the peptide. Morphological changes including membrane bleb formation and complete disruption of cells are evident in r*mLe*H treated bacteria. On the contrary, control untreated cells were smooth with no ruptures or pores. Thus, SEM analysis concluded that the peptide r*mLe*H attacks the cell membrane of the bacteria resulting in pore formation and eventually death confirming the potential antimicrobial activity of the peptide.

## 2.4 Discussion

A growing body of evidence indicates that the fish genome encodes several unique AMP genes that play a role in the innate immunity of the fish, particularly in environments that are rich in microbial pathogens. Hepcidins are comparatively a new addition to the AMP family that plays vital roles in combating infection and maintaining iron homeostasis in vertebrates (from fish to humans). Hepcidins represent a family of cysteine rich peptides that are primarily expressed in the liver of living organisms (Krause et al., 2000; Park et al., 2001; Ganz, 2003). Hepcidins or hepcidin isoforms have not yet been reported from Leiognathideae family and this is the first report from the common pony fish, *Leiognathus equulus*. The present study involves the identification, cloning, molecular and biological characterization of the hepcidin isoform from *Leiognathus equulus*. The characterized pre-propeptide sequence, *Le*-Hepc, isolated and identified from the gill mRNA transcripts shared all the typical characteristics of hepcidin including hepcidin signature motif and showed significant sequence similarity with other reported hepcidin isoforms during homology searches.

It is widely known that the hepcidin family of peptides are generally synthesized as a prepropeptide and the bioactive mature peptide is produced by the proteolytic cleavage of the signal peptide and prodomain from the precursor peptide (Valore and Ganz, 2008). The 261 bp cDNA obtained from the gill mRNA transcripts of *L. equulus* coded for a 86 amino acid peptide, comprised of a more or less conserved 24 aa signal peptide, 36 aa variable pro region followed by a highly conserved 26 aa mature peptide. The length of the signal peptide was found to be consistent with most of the reported fish hepcidins, in contrast to a slightly shorter counterpart observed in *Zanclus cornutus* and *Gadus morhua* which has only a 22 amino acid signal peptide. In conjunction with the above, signal peptide seemed to be enriched with hydrophobic amino acids such as Val (25 %), Ala (16.7 %) and Ser (12.5 %). Cleavage of the signal peptide would result in the formation of a prohepcidin which is exported to the lumen of endoplasmic reticulum. The prohepcidin undergoes a second cleavage by the action of furin and related propeptide convertases like PC5, PC7 and PACE4 (Schranz et al., 2009; Singh et al., 2011) leading to consequential release of the bioactive mature peptide. The hepcidin cleavage site (RX(K/R)R) for propeptide convertase furin (Nakayama, 1997) known to cleave human prohepcidin is conserved in mammals, amphibians and fishes alike (Shi & Camus, 2006) and its presence was also detected in *Le*-Hepc. The propeptide possesses a negative charge and neutralizes the charge of the mature cationic domain protecting the host cell from its toxic effects and also helping in its transport *via,* subcellular compartments (Valore and Ganz, 2008). Unlike other cysteine rich AMPs like defensins, the release of mature peptide

from propeptide of hepcidin is usually fast, indicating the efficiency of hepcidin in immune response (Valore and Ganz, 2008).

The mature peptide of *L. equulus* hepcidin was endowed with a net charge of +2, theoretical molecular weight of 2.7 kDa and a net hydrophobic ratio of 53 %. The $NH_2$-termini of the mature peptides were assigned based on the amino acid sequence of human hepcidin (Krause et al., 2000; Park et al., 2001) and the proximity to the RX(K/R)R motif characteristic of processing sites for the propeptide convertases, while the C-terminus (–CCR/KF) is conserved among most of the fish hepcidins. For the fish HAMP2 sequences, the mature peptide is cationic, but the prepropeptide and propeptide sequences are anionic. However, the predicted p*I* of 5.10, 4.75 and 8.23 for *Le*-Hepc prepropeptide, propeptide and mature peptide respectively were slightly lower than the recorded average p*I* of HAMP2 from other species of fish (Hilton and Lambert, 2008). Moreover the cationic charge of the mature peptide arose from the amino-terminal portion of the mature peptide, same as observed for all the HAMP2 group of hepcidin peptides (Hilton and Lambert, 2008). On the contrary, the calculated *p*I (6.74) of the amino-terminal region of the mature peptide of *Le*-Hepc was a little less than the recorded *p*I of 7.79 reported for most of the fish hepcidins, while the variable loop region of the mature peptide was anionic.

By phylogenetic analysis, two classes of hepcidins (HAMP1 and HAMP2) are proposed. Every fish species has only one copy of the HAMP1 gene which is an orthologue of mammalian sequences; the other multiple copies always fall into the HAMP2 class (Hilton and Lambert,

2008). The functional divergence of duplicated genes occur through three main processes, i.e., neo functionalization, sub functionalization, and sub neo functionalization (Lynch et al., 2001; He and Zhang, 2005; Rastogi and Liberles, 2005). Phylogenetic analysis grouped *Le*-Hepc into the HAMP2 group of peptides owing to the absence of a Q-S/I-H-L/I-S/A-like motif. This N-terminal signature motif (Q-S-H-L-S) represents the mammalian counterpart (D-T-H-E-P) that takes part in the internalization of the ferroportin molecule (Nemeth and Ganz, 2006). Moreover, the present results of the phylogenetic tree are in line with the suggested adaptive evolution probably associated with the host-pathogen interaction in different environments (Padhi and Verghese, 2007; Xu et al., 2008; Xu et al., 2012) due to positive Darwinian selection in HAMP2.

The general structure of fish hepcidin (Huang et al., 2007; Chaturvedi et al., 2014) consists of a β-sheet with four disulphide bridges (formed by eight cysteines) with an unusual vicinal bridge at the hairpin turn. However, sequence analysis of fish hepcidins has shown the presence of hepcidins containing 7, 6 or 4 cysteines (Xu et al., 2008). Various hepcidin variants exist widely in fish more than in mammals and are thought to be associated with adaptive differentiation to the complexity of the aquatic environment (Wang et al., 2009). The eight cysteines involved in one vicinal and three interstrand disulphide bridges in human and bass hepcidin (Lauth et al., 2005) are conserved in the majority of hepcidins, including the *L. equulus* hepcidin. Kemna et al. (2008) speculated that the vicinal disulphide bonds formed at the hairpin turn ($Cys^4$-$Cys^5$) could be the possible critical domain for biological activity of the molecule. Also, it has been demonstrated that the formation of a bond

between these adjacent cysteines may confer high chemical reactivity to this region (Hunter et al., 2002). The formation of a vicinal disulphide bond would create a closed eight-atom loop that may be conformationally mobile and shows the highest degree of sequence diversity between species. In addition, they are often located in the centre of a type VIII β-turn in the peptide backbone (Carugo et al., 2003). Thus the conserved cysteines in hepcidin and the variable loop have structural and functional roles in its spatial conformation (Douglas et al., 2003). Vicinal disulphide bonds share a number of common stereochemical features, including a non-planar peptide bond in the *trans* conformation. The mature peptide of *Le*-Hepc, *mLe*H, is well structured over the majority of its length (residues 7–24). The three-dimensional structure of *Le*-Hepc appeared to be consistent with the crystal structure of bass hepcidin. On comparison of their mature peptide sequences, apart from the total number of amino acids, the replacement of Asn7 and Ser13 in the mature bass hepcidin with Gly12 and His18 in the *Le*-Hepc mature region could only be seen. Taking into account the structural homology with bass mature peptide, it is reasonable to speculate that *mLe*H functions similarly to bass hepcidin and other hepcidins with a proven record of antimicrobial activity. Thus from the above facts, it is obvious that *Le*-Hepc belonged to HAMP2 group of hepcidins, mainly attributed with antimicrobial functions.

Most of the *in vitro* antimicrobial activities of fish and mammalian hepcidins are determined using synthetic mature hepcidin peptides (Yang et al., 2011; Zhou et al., 2011; Cai et al., 2012; Boumaiza et al., 2014; Ke et al., 2015; Alvarez et al., 2016; Liu et al., 2017). Majority of them demonstrated suspiciously low efficacy and in some cases no antibacterial

activity was observed (Huang et al., 2007; Yang et al., 2011). The low level activity may be associated with incorrect folding of the synthetic peptides and or abnormal disulfide bond formation. Proper folding of proteins is highly essential for the proteins to be functional. Also, the recombinant proteins are usually found expressed in *E. coli* as insoluble inclusion bodies. Other caveats that stand as a barrier to recombinant protein production are cytotoxicity to the expression host and sensitivity to proteolytic degradation. These challenges can sometimes be overcome by fusing the target protein to a highly soluble, non-toxic, anionic and proteolytically stable partner protein (Kozlov et al., 2008). In this study, pET-32a(+) was used to express Trx–*mLe*H fusion protein. Thioredoxin is a disulphide reductase that can effectively catalyze disulfide bond and display chaperone-like activity (Stewart et al., 1998; McCoy and Ville, 2001; Xu et al., 2006). Thioredoxin is a most widely used fusion partner that can promote the solubility and correct folding of fusion proteins (Huang et al., 2009). This is particularly important with short cysteine rich target peptides such as *mLe*H that is only 26 residues long (2.7 kDa) and with four disulphide bonds. Moreover, some AMPs fail to get expressed in certain hosts due to codon incompatibility (Qu et al., 2013). Hence, Rosetta-gami$^{TM}$ B (DE3) pLysS strain was selected and used for heterologous expression to overcome rare codon bias and to obtain soluble proper folded disulphide bonded peptide in *E.coli* cytoplasm. In this study, recombinant expression plasmid pET-32a(+)-*mLe*H was constructed and soluble recombinant product was successfully obtained in *E. coli* Rosetta-gami$^{TM}$ B (DE3) pLysS cells. In a similar experiment, recombinant expression of channel catfish hepcidin mature peptide, mCH,

was carried out with pET-32a(+) vector in *E. coli* BL21 (DE3), but the recombinant fusion protein, trxA–mCH was solubly expressed at 25 °C than at 37 °C, using 1mM IPTG (Tao et al., 2014). On the contrary, soluble expression of *mLe*H in the expression host was achieved with relatively low levels of IPTG (0.1 mM) and also at comparatively higher temperature (37 °C). Usually, an IPTG concentration of 0.1 mM to 1M is used for induction of culture (Moon et al., 2007; Srinivasulu et al., 2008; Liang et al., 2013). Higher concentrations of IPTG (1M), would yield low expression cell densities (Schein and Noteborn, 1998; Sorensen and Mortensen, 2005) and the hepcidin would get expressed as inclusion bodies (Zhang et al., 2005). Also, the difference in temperature of induction for soluble expression might be due to different expression host used. Recombinant *mLe*H thus produced was purified, concentrated, refolded, and characterized for antimicrobial, cytotoxic and haemolytic activity.

In general, hepcidins are active against wide range of Gram-positive and Gram-negative bacteria, fungi, parasites and viruses (Wang et al., 2010; Pan et al., 2011; Masso-Silva and Diamond, 2014). Similarly, some recombinant hepcidins expressed in *E. coli* have showed that it could inhibit the growth of some Gram-positive bacteria (*S. aureus, B. subtilis, Micrococcus luteus*) and Gram-negative bacteria (*E. coli, A. hydrophila, A. sobria, Pseudomonas aeruginosa, P. fluorescens*, *Vibrio anguillarum*) (Wallace et al., 2006; Srinivasulu et al., 2008; Cai et al., 2012; Gao et al., 2012; Hao et al., 2012; Qu et al., 2013; Lin et al., 2014; Tao et al., 2014; Janakiraman et al., 2015). In certain cases, removal of the fusion partner by enterokinase digestion was found to be imperative for regaining the

antimicrobial activity of the released mature peptide (Gagliardo et al., 2008; Tao et al., 2014; Wang et al., 2016) and in some cases it was not required (Lin et al., 2014). Antibacterial activity of r*mLe*H was analysed against 11 different pathogenic strains. r*mLe*H exhibited noticeable activity towards *Staphylococcus aureus* and *E. coli* at 5 μM concentration and *Aeromonas hydrophila*, and *Edwardsiella tarda* at 10 μM concentration. The MIC values obtained for r*mLe*H were comparatively low with respect to the recombinant His-tagged mature peptide hepcidin-2 of zebrafish (rHCD). The rHCD inhibited the growth of the *E. coli*, *V. anguillarum*, *S. aureus* and *B. subtilis* with minimum inhibitory concentrations of 18, 15, 13 and 9 μM, respectively (Lin et al., 2014). Moreover, no significant activity was demonstrated against *B. cereus* and the other vibrio strains tested, though varied levels of inhibition could be seen. Incubation of the bacteria with the controls had no apparent effect on bacterial survival suggesting that the observed bactericidal effects were specific to *mLe*H. Among the controls, thioredoxin favoured the growth of bacteria than the PBS control and hence antibacterial assay of *mLe*H was performed with the fusion recombinant protein. Similar experimental strategy used could be found in related reports (Krusong et al., 2012; Arockiaraj et al., 2013; Qu et al., 2013; Lin et al., 2014). Besides, minimum inhibitory concentrations of fish hepcidins vary widely depending on the particular pathogen, the fish species from which it is derived, and the hepcidin isoform itself (Lin et al., 2014; Tao et al., 2014; Zhang et al., 2014). Hence inhibition pattern similar to previous reports could not be expected for a novel uncharacterized hepcidin isoform.

Antimicrobial property of hepcidin has been proven beyond doubt; even though, their exact mode of action is still not clear. Similar to the activity spectrum of various hepcidin isoforms, mode of action of different isoforms vary considerably. LEAP-2 disrupts the physical integrity of bacterial membranes (Townes et al., 2009) and human LEAP-2 binds to the plasmid DNA (Hocquellet et al., 2010). Some hepcidin isoforms like, turbot hepcidin, tilapia hepcidin 1-5 etc. are membrane lytic in nature while certain others like medaka hepcidin (Om-hep1) exhibit an unknown mechanism of action apart from lytic mode (Cai et al., 2012 Zhang et al., 2014). In addition, hepcidin may kill bacteria by a mechanism independent of membrane permeability. Antimicrobial activity of trout hepcidin was shown not to occur through membrane disruption but rather appeared to be through the interaction with the bacterial DNA (Alvarez et al., 2014). SEM analysis further affirmed the antibacterial activity of r*mLe*H. Clear morphological disruption of the bacterial cell as well as membrane blebbing in certain areas could be observed. Similar results were observed for other hepcidins including rHCD (Lin et al., 2014), SmHep1P and SmHep2P (Zhang et al., 2014) and AN-hepc (Chi et al., 2015). In this study, alteration in the surface structure of susceptible bacteria treated with r*mLe*H was probably due to the destructive interactions between the peptide and the cells, which caused damage to the membrane. It is most likely that this membrane destruction is responsible for the bactericidal effect observed with r*mLe*H.

Many AMPs like mellitin are known to be “double-edged swords” because of their capability to destroy both microbial membrane and the blood cell membrane. Thus haemolytic activity of AMPs potentially

limits their clinical applications (Ginsburg and Koren, 2008). Even the highest concentration of r*mLe*H (20 µM) lysed less than 0.5 % erythrocytes suggesting that there was no significant toxicity to haemocytes. Also, r*mLe*H was found to be non-cytotoxic to NCI-H460 cancer cell lines at the tested concentrations. *mLe*H could therefore be used as a potential antimicrobial agent, particularly in aquaculture.

In conclusion, a novel HAMP2 isoform of hepcidin from the common pony fish named, *Le*-Hepc, was cloned and characterized. The peptide *Le*-Hepc encodes for a 24 amino acid (aa) signal peptide coupled to a 36 aa prodomain followed by a 26 aa mature peptide. Recombinant expression of the mature peptide *mLe*H, was done in *E. coli* Rosetta-gami™ B (DE3) pLysS and the purified and refolded peptide was found to be active against both Gram-positive and Gram-negative pathogens. Also the peptide demonstrated non-haemolytic and non-cytotoxic properties at tested concentrations. The antimicrobial activity against environmental as well as clinical isolates displayed in this study is also remarkable and reveals the antibacterial potential of this recombinant peptide. Hence, r*mLe*H is particularly significant as a prospective antimicrobial agent in aquaculture and human medicine.

Chapter 3

# MOLECULAR CHARACTERIZATION, RECOMBINANT PRODUCTION AND FUNCTIONAL ANALYSIS OF HISTONE DERIVED PEPTIDE FROM *MUGIL CEPHALUS*

Contents

3.1 Introduction
3.2 Materials and methods
3.3 Results
3.4 Discussion

## 3.1 Introduction

In eukaryotic cells, the genomic DNA is condensed into a complex nucleoprotein structure named chromatin which balances the compactness of the genome and the accessibility of regulatory proteins to DNA (Li and Fang, 2015). Histones represent the major components of chromatin, playing key roles in DNA replication, transcriptional regulation, and cell growth control (Parseghian and Luhrs, 2006). The basic structures of the nucleosome is formed by an octameric complex constituted by the core histones (H2A, H2B, H3 and H4), while the linker histones (H1) are involved in the generation of the higher-order chromatin structure which seal loops of DNA and maintains the nucleosome structure. Histones are highly abundant in animal cells due to their important structural role and most are highly conserved evolutionarily throughout eukaryotes. In addition

to their structural role, several other functions for histones have also been described including their roles in endotoxin-neutralization (Kim et al., 2002), leucocyte stimulation and apoptotic signal transmission (Konishi et al., 2003; Pedersen et al., 2003), cellular signalling (Parseghian and Luhrs, 2006), innate immunity (Brinkmann and Zychlinsky, 2012) and septic shock (Ginsburg et al., 2017).

Initial investigations on potentials of histones as antimicrobial agents came from Miller et al. (1942) who showed that calf thymus histones and histone-like cationic proteins like protamines inhibited respiration in Gram-positive and Gram-negative bacteria. Later in 1958, Hirsch reported the antimicrobial activities of arginine-rich histones (H3 and H4) against various bacteria under different pH and salt concentrations. Although the antimicrobial properties of histone proteins have long been known, the discovery remained unattended till mid 1990s, as there was no theoretical concept as to how they might interact with bacteria for the host's benefit. Decades later, Hiemstra et al. (1993) demonstrated the antimicrobial activity of three molecules isolated from the lysosomal fraction of murine macrophages and established the identity of those molecules as lysine rich histones H1 and H2B. In 1996, Frohm et al. reported the contribution of histone proteins in the antibacterial activity of wound blister fluid suggesting that histones may have a role in immune defence. Subsequently, a number of histones and their related fragments obtained from various sources in various animals were reported to have antimicrobial properties.

Amidst numerous scientific investigations for novel antimicrobial peptides, Park et al. (1996) described a new peptide from the stomach of Korean frog, *Bufo bufo gargarizans*, which they named as Buforin I. Buforin I turned out to be identical to the first 39 amino acids of histone H2A and was shown to have broad-spectrum antimicrobial activities (Kim et al., 1996; Park et al., 1996). Later in the same year, a more potent antimicrobial peptide, buforin II, the amino acid sequence of which corresponded to residues 16–36 of buforin I, was isolated (Park et al., 1996). In subsequent studies, as part of the innate host defence, the same group designed a series of experiments to decipher the mode of histone H2A processing in the toad stomach. The scientific group observed that in the gastric mucosal cell, histone H2A is synthesized in excess of the amount required for DNA packaging and accumulates within cytoplasmic secretory granules. The biochemical and immunohistochemical analyses also revealed that a fraction of the synthesized histone H2A is acetylated and therefore targeted for translocation to the nucleus, whereas the rest of the unacetylated histone H2A, upon secretion into the gastric lumen is cleaved by pepsin isozymes to yield buforin I (Kim et al., 2000).

A 19-amino acid peptide, Parasin I was isolated from the skin mucus of wounded catfish, *Parasilurus asotus*. Similar to buforin I, Parasin I, was also identified as an N- terminal peptide of histone H2A with broad-spectrum antimicrobial activity (Park et al., 1998). Mechanism of production of parasin I in *Parasilurus asotus* revealed that it is produced from unacetylated histone H2A *via,* specific cleavage by cathepsin D at the Ser19-Arg20 bond of histone H2A (Cho et al., 2002a). Also, cathepsin D was shown to be present in the mucus as an inactive

proenzyme, procathepsin D. Surprisingly, an injury-induced matrix metallo-proteinase 2 was found to cleave procathepsin D to generate the active cathepsin D (Cho et al., 2002b). Moreover, immunoreactive parasin-I was widely detected in the skin mucus of several fish species, indicating its role in the innate host defence of the fish against invading microorganism after injury. In 2003, another histone H2A-derived AMP was isolated from the epithelial mucous layer of Atlantic halibut, *Hippoglossus hippoglossus* L. The peptide was named as hipposin and was identified as an N-terminal acetylated peptide, that corresponds to 1–51 amino acid of histone H2A (Birkemo et al., 2003). Since then, histones have been reported to be present in the skin mucus of several fish taxa, including Salmoniformes, Siluriformes and Pleuronectiformes (Smith & Fernandes, 2009).

Among the core histone proteins, histone H2A has demonstrated to be the most potent antibacterial agent. Fernandes et al. (2002) have reported that the 13.6 kDa, trout H2A protein expressed in the skin epithelium, exhibited antibacterial activity against Gram-positive bacteria at sub-micromolar (<0.4 μM) concentrations within 30 minutes of *in vitro* exposure. However, the histone H2A protein exhibited a weak antifungal activity against the yeast, *Saccharomyces cerevisiae* and did not show any haemolytic activity to trout erythrocytes at antimicrobial concentrations (Fernandes et al., 2002). Sooner or later, reports on the antimicrobial HDAPs isolated from marine invertebrates came pouring in. Histone H2A fragments with antimicrobial activity was reported from the shrimp *Litopenaeus vannamei* (Patat et al., 2004). A 2 kDa fraction of histone H2A, actin and filamin A, exhibiting antimicrobial activity were identified

from coelomocyte extract of the starfish *Asterias rubens* (Maltseva et al., 2004, 2007). Li et al. (2007) was the first to report the presence of a H2A derived antimicrobial peptide from scallop *Chlamys farreri*. The full-length H2A DNA was identified by the techniques of homology cloning and genomic DNA walking. In 2009, De Zoysa and his co-workers identified a 40 amino acid AMP designated as abhisin from the N-terminus histone H2A sequence of the disk abalone, *Haliotis discus*. The peptide exhibited significant antimicrobial activity against *Listeria monocytogenes*, *Vibrio ichthyoenteri* and fungi *Pityrosporum ovale* at 250 µg/ml.

In 2012, a 4.27 kDa, 39 amino acid, histone derived AMP from round whip ray, *Himantura pastinacoides* was identified by Sathyan et al. and named it as himanturin (Sathyan et al., 2012a). Later, the same authors had described a couple of other H2A derived antimicrobial peptides named as molluskin from bivalves and gastropods (*Crassostrea madrasensis, Meretrix casta, Saccostrea cucullata, Ficus gracilis and Bullia vittata*) and sunettin from marine clam (*Sunetta scripta*) (Sathyan et al., 2012b; 2012c). In the subsequent year, employing an *in silico* approach, a 52 amino acid residue termed Harriottin-1, a 40 amino acid Harriottin-2, and a 21 amino acid Harriottin-3 were identified to possess antimicrobial sequence motif from the H2A gene of sicklefin chimaera, *Neoharriotta pinnata* (Sathyan et al., 2013). For the first time, Arockiaraj and his co-workers reported a histone H2A protein from fresh water prawn, *Macrobrachium rosenbergii* which was shown to exhibit antimicrobial activity against the Gram-positive bacteria *Lactococcus lactis* (Arockiaraj et al., 2013). Chen et al. (2015) identified a potent

histone H2A derived peptide, Sphistin, from the mud crab, *Scylla paramamosain.* The peptide exhibited antimicrobial activity against a broad range of pathogens including, Gram-positive bacteria, Gram-negative bacteria and yeasts.

In case of fishes, histone H2A derived antimicrobial peptides have been reported from Amur catfish, *Parasilurus asotus* (Park et al., 1998), Atlantic halibut, *Hippoglossus hippoglossus* (Birkemo et al., 2003), Bengal tongue sole, *Cynoglossus semifasciatus* (Chaithanya et al., 2013) and black fin sea catfish, *Tachysurus jella* (Chaithanya et al., 2013). Antimicrobial histone derived AMPs are not only limited to the N-terminus of the histones as was found for the buforin peptide, but also can be found as fragments of both termini, from histones H1, H2B and H6. Onchorhyncin II from *Oncorhynchus mykiss* (Fernandes et al., 2004), Salmon antimicrobial protein from *Salmo salar* (SAM) (Richards et al., 2001) and flounder histone H1-like protein (fH1LP) from *Paralichthys olivaceous* (Nam et al., 2012) were found as derivatives of histone H1. Synergistic properties of H1 derived peptides with other AMPs have also been reported. Peptides related to histone H1 was isolated from the blood and mucus of coho salmon, *Oncorhynchus kisutch*. Besides having no antimicrobial activity, they synergized the antibacterial activity of lysozyme and the AMP pleurocidin (Patrzykat et al., 2001). In case of H2B HDAPs, a C-terminal histone H2B fragment from the chicken liver, exhibiting activity against Gram-positive and Gram-negative bacteria was isolated along with the antimicrobial histones H2A and H2B.V (Li et al., 2007). In mollusc, a histone H2B fragment from the American oyster, *C. virginica* demonstrated strong activity against the Gram-negative *Vibrio parahaemolyticus* and

*V. vulnificus* (Seo et al., 2010). Moreover, Onchorhyncin III, a cleavage product of the non-histone chromosomal protein H6, displayed potent antimicrobial properties against all tested bacteria with MICs in the micromolar range. In particular, the MIC of *Planococcus citreus* was in the range of 0.06–0.12 μM, values approximately 30-fold lower than those observed for cecropin P1 against the same organism (Fernandes et al., 2003). Relatively less evidence for the antimicrobial activities of histones H3 and H4 could be seen as they remain underexplored. In the meantime, few studies pertaining to H3 core histone HDAPs from skin mucus of hagfish, *Myxine glutinous* (Subramanian et al., 2008), synthetic H3 like peptides (Tsao et al., 2009) were reported to exhibit antibacterial activities. Antimicrobial property also has been reported for histone H4 protein. One of the active factors in human sebocyte secretions was found to be histone H4 (Lee et al., 2009) and histone H4 from *Litopenaeus vannamei* haemocytes was shown to have antibacterial properties (Patat et al., 2004).

*Mugil cephalus*, commonly known as the flathead grey mullet or the striped mullet is a cosmopolitan fish that can be found in tropical, subtropical and temperate rivers. Despite being a coastal species, it often enters estuaries and freshwater environments. Flathead mullet represents both fished and a farmed variety that forms an important aquaculture species particularly in many Asian and Mediterranean countries (Fischer and Bianchi, 1984). On the other hand, in case of *Mugil cephalus*, fish diseases due to bacterial infection, particularly *Pseudomonas* sp. and *Aeromonas* sp., causes severe economic losses to fish farms due to high mortality (Atallah and El-Banna, 2005; Saad et al., 2014; Saad and Atallah, 2014).

Keeping aside the facts, literatures relating to the antimicrobial components present in *Mugil cephalus* are scarce, although a few could be identified. Balasubramanian and Gunasekaran (2015) studied the amino acid and fatty acid profile of the epidermal mucus of *Mugil cephalus* and established the presence of 18 amino acids of which lysine, phenylalanine, glycine and proline were found to be dominant. Later, Balasubramanian et al. (2016) demonstrated the anticancer activities of the mucus extract of *Mugil cephalus* against laryngeal cancer cell lines. In addition, Deivasigamani et al. (2017) evaluated the antimicrobial activity of *Mugil cephalus* muscle tissue extract using disc diffusion technique and characterised the bioactive compounds by FTIR, GC-MS and SDS-PAGE analysis. The elixir demonstrated strong antimicrobial activity against *Proteus mirabilis* and *Staphylococcus aureus* and hypothesized the antibacterial potency of the extract to the proteins or glycoproteins present in the fish. However, studies pertaining to role of histone derived AMPs in the immune defence of *M. cephalus* have not been identified, to the best of our knowledge. Therefore, in the present study, with an aim to identify antimicrobial factors that contribute to the innate immunity of *M. cephalus*, we identified and characterised a H2A derived AMP from the flathead grey mullet and its antimicrobial activity with the recombinant H2A HDAP was studied. Also to elucidate the mode of action against bacterial pathogens, epi-fluorescence microscopy after PI staining and SEM analyses were performed. Finally, the toxicity of the recombinant HDAP against human erythrocytes and human lung cancer cells, NCI-H460 was analysed. Thus, altogether, the present study would provide an insight into the antimicrobial defence mechanism that exists in the flathead grey mullet, *Mugil cephalus.*

## 3.2 Materials and Methods

### 3.2.1 Experimental organism

The experimental organism used in the present study includes the flathead grey mullet, *Mugil cephalus* belonging to the mullet family, Mugilidae. Live and healthy specimens of *Mugil cephalus* were collected from Vypeen area, Kochi. Samples were brought to the laboratory in live condition by providing aeration.

**Fig. 3.1** Experimental organism used for the study, flathead grey mullet, *Mugil cephalus*.

### 3.2.2 Precautions for RNA preparation

Basic precautionary measures were taken while working with RNA as explained in section 2.2.2 of Chapter 2.

### 3.2.3 Processing of the tissue

Live samples of *Mugil cephalus* were washed with DEPC treated water to remove the extraneous dirt and other organic matter. Blood was collected from the lamellar artery near gill region of the fish using 5 mL syringes (RNase free) rinsed in precooled anticoagulant solution (RNase free 10 % sodium citrate, pH 7). The samples were homogenised in TRI™ reagent (Sigma) and stored at $-20^0$ C until processed.

### 3.2.4 RNA Isolation

Total RNA was extracted from the haemocytes of *Mugil cephalus* with TRI reagent following manufacturer's instructions. For details of RNA extraction, refer section 2.2.4 of Chapter 2. RNA pellets obtained were dissolved in 30 µl RNase free water by repeated pipetting with a micropipette at 55 °C for 5 min.

### 3.2.5 Determining Quality and Quantity of Extracted RNA

Quality and quantity of extracted RNA was assessed by a spectrophotometer and agarose gel electrophoresis as specified in section 2.2.5 of Chapter 2.

### 3.2.6 cDNA Synthesis

Single stranded cDNA was synthesized using oligo $(dT)_{20}$ primers by reverse transcription as described previously in section 2.2.6 of Chapter 2.

### 3.2.7 PCR amplification

PCR amplification of Histone Derived Antimicrobial Peptide (HDAP) gene from the cDNA of the fish was carried out using gene specific primers (Birkemo et al., 2003). β-actin was used as an internal control to verify the reverse transcription reaction. The sequences of primers used to amplify β-actin and HDAP genes are given in Table 3.1. Amplification of cDNA using gene specific primers was performed in a 25 µl reaction volume as explained in section 2.2.7 of Chapter 2. The thermal profile used was 95 °C for 2 min followed by 35 cycles of 94 °C for 15 s, 60 °C for 30 s and 72 °C for 30 s and a final extension at 72 °C for 10 min.

### 3.2.8 Agarose Gel Electrophoresis

The amplicons were visualized by electrophoresis in 1.5 % agarose gel. Electrophoresis was performed as described in section 2.2.8 of Chapter 2.

### 3.2.9 Cloning of PCR product

The PCR amplicons obtained were cloned onto the pGEM-T Easy vector employing TA-cloning technique as explained in section 2.2.9 of Chapter 2. Ligated cloning vector was transformed to *E. coli* DH5α competent cells. Presence of the insert DNA in the recombinant clones were confirmed by colony PCR using vector specific primers *viz.*, T7 and SP6 as well as gene specific primers (Table 3.1). Plasmids with the insert were then extracted and purified using GenElute HP plasmid MiniPrep kit (Sigma). Recombinant plasmids were sent for sequencing at SciGenom, Kochi, India.

**Table 3.1** List of primers used in the study.

| Target gene | Sequence (5'-3') | Product size (bp) | Annealing Temp. (°C) |
|---|---|---|---|
| **Histone** | F: atgtccggrmgmggsaarac<br>R: gggatgatgcgmgtcttcttgtt | 250 | 60 |
| **β-actin** | F: gatcatgttcgagaccttcaacac<br>R: cgatggtgatgacctgtccgtc | 400 | 60 |
| **T7** | F: tgtaatacgactcactataggg<br>R: ctagttattgctcagcggtg | 750 | 57 |
| **SP6** | R: gatttaggtgacactatag | _ _ | 57 |

### 3.2.10 Sequence characterization and phylogenetic analysis

Analysis of the nucleotide sequence, amino acid sequence and peptide characterization were performed using various softwares and computer based algorithms as explained in section 2.2.11 of Chapter 2. Relevant histone H2A sequences of fishes as well as representatives from other vertebrate classes were retrieved from GenBank and multialigned using ClustalW. Phylogenetic tree was constructed based on nucleic acid sequences by the neighbour-joining (NJ) method using MEGA version 6. Analysis was carried out with complete deletion of gaps subjected to 1,000 bootstrap repetitions.

### 3.2.11 Selection of active peptide region for recombinant expression

Analysis of the histone precursor peptide of *Mugil cephalus* by PeptideCutter tool of ExPASy identified certain enzyme cleavage sites within the peptide releasing a 52-mer active peptide, *Mc*-His. Thus the putative antimicrobial peptide identified from the histone H2A of *Mugil cephalus*, *Mc*-His, was considered for recombinant expression and further functional characterization. The active *Mc*-His sequence showed a high degree of variation from other fish HDAPs. Physico-chemical properties and phylogenetic analysis of the active peptide have already been studied and included in the previous section 3.2.10.

### 3.2.12 Designing of primers for cloning into expression vector

The restriction primers were specially designed to obtain the active peptide of *Mugil cephalus* histone H2A, *Mc*-His. The restriction primers used to amplify *Mc*-His, contained BamHI (GGATCC) restriction sequence in the forward primer and HindIII (AAGCTT) restriction site in the

reverse primer. Sequence and details of restriction primers designed are given in the Table 3.2. Recombinant expression of *Mc*-His gene was performed using pET-32a(+) expression vector system. For details and features of the expression vector, pET-32a(+), refer section 2.2.13 of Chapter 2.

**Table 3.2** Restriction primers designed for *Mc*-His.

| Target gene | Sequence (5'-3') |
|---|---|
| **pET *Mc*-His F** | 5' TAAGCAGGATCCATGTCCGGGCGAGGGAAAAC 3' |
| **pET *Mc*-His R** | 5' TAAGCAAAGCTTTTATTACAGGTAGACGGGAGC 3' |

* Colour definitions

Nucleotide bases included to ensure enzyme digestion.

Restriction enzyme site: BamHI in forward and HindIII in reverse primer

Target gene sequence

Stop codon

### 3.2.13 PCR amplification

The *Mc*-His active peptide region was selectively amplified using the designed restriction primers mentioned in Table 3.2. pGEMT plasmid with *Mugil cephalus* histone H2A precursor insert was used as the template for the PCR amplification. PCR was carried as explained in section 2.2.15 of Chapter 2.

### 3.2.14 Restriction digestion

Restriction digestion of both the amplicons with restriction site and pET-32a(+) expression vector was carried out in separate reactions by using BamHI and HindIII (FastDigest restriction enzymes, Thermo Fisher Scientific). For restriction digestion 50 µl of PCR product was incubated

with 5 µl of 10X reaction buffer and 0.5 units each of BamHI and HindIII for 1 h at 37° C. The enzymes were subsequently inactivated by elevating the temperature to 65° C for 20 min. The digested products were resolved in 1.2 % agarose gel.

### 3.2.15 Purification of restriction digested insert and expression vector

Restriction enzyme digested insert and pET-32a(+) vector, were gel purified using GenJET™ Gel Extraction Kit (Thermo Fisher Scientific, USA) as explained in section 2.2.17 of Chapter 2.

### 3.2.16 Construction of recombinant expression vector and transformation into *E. coli* DH5α competent cells

Restriction digested *Mc*-His gene and vector was ligated using T4 DNA ligase following manufacturer's instruction. Ligation reaction was carried out as mentioned in section 2.2.18 of Chapter 2. The ligated recombinant construct was then transformed to *E. coli* DH5α competent cells as discussed in section 2.2.9.3 of Chapter 2.

Recombinant colonies were selected on LB/ampicillin (50 µg/ml) plates. Presence of the vector with *Mc*-His gene insert was confirmed by colony PCR using insert specific restriction primers (Table 3.2) and vector specific T7 F and T7 R primers (Table 3.1) as discussed in section 2.2.18 of Chapter 2. Single colony of the positive clone was then propagated in 10 ml LB broth supplemented with ampicillin (50 µg/ml) for plasmid isolation. The cultured cells were incubated at 37 °C with shaking at 250 rpm for 16 hrs.

### 3.2.17 Plasmid extraction and sequencing

Plasmid extraction of pET-*Mc*-His was carried out from the overnight culture of recombinant clone as mentioned in section 2.2.9.5 of Chapter 2. The recombinant plasmids were sequenced by vector specific T7 F and T7 R sequence at SciGenom, Kochi, India. The sequences were analyzed using GeneTool software to ensure that the reading frame of pET32a(+) expression vector and that of the insert gene are in-frame. The sequence was also checked for the presence of stop codon in the insert gene for the proper production of the recombinant protein.

### 3.2.18 Transformation into expression host

The expression construct, pET-*Mc*-His was transformed into the expression host, *E. coli* Rosetta-gami$^{TM}$ B (DE3) pLysS strain by heat shock method. The transformation mixture was then and plated onto LB agar plates, containing the antibiotics ampicillin (50 µg/ml), kanamycin (15 µg/ml), chloramphenicol (34 µg/ml) and tetracycline (12.5 µg/ml). For details, please refer section 2.2.20.2. Positive clones were selected and confirmed by colony PCR with vector specific as well as insert specific restriction primers.

### 3.2.19 Induction and expression of pET-*Mc*-His fusion protein

Cultures (100 ml) of transformed Rosetta-gami$^{TM}$ B (DE3) pLysS cells were grown in LB media containing ampicillin (50 µg/ml) and 15 µg/ml kanamycin. Cells were cultured at 37 °C with orbital shaking at 250 rpm till $OD_{600nm}$ attained 0.6. Expression of *Mc*-His fusion protein was induced by adding IPTG to a final concentration of 0.1mM. Uninduced and also pET-thioredoxin cells were maintained as controls as mentioned in

section 2.2.21. Cells were further incubated at 37 °C for 6 h and aliquots of 2 ml cultures were removed at hourly time intervals. Cell pellet was harvested by centrifugation and stored at -20 °C for SDS-PAGE analysis.

### 3.2.20 SDS-PAGE analysis of the recombinant protein

Time-point samples of transformed cells were analysed by SDS-PAGE to detect the production of recombinant *Mc*-His (r*Mc*-His). r*Mc*-His as a fusion protein was detected as described previously in section 2.2.22 of Chapter 2.

### 3.2.21 Western blotting

SDS-PAGE of recombinant peptide, r*Mc*-His was done as explained in the previous section. Western blotting of r*Mc*-His was performed as described previously in section 2.2.23 of Chapter 2.

### 3.2.22 Scale-up production of r*Mc*-His fusion protein

Recombinant expression of *Mc*-His was done in Rosetta-gami$^{TM}$ B (DE3) pLysS cells. The scale up production of r*Mc*-His was carried out in a 2 litre culture medium as described in section 3.2.19. The culture was induced with 0.1 mM IPTG when $OD_{600nm}$ reached 0.6. The transformed cells were harvested by centrifugation at 12000 x g for 2 min after 5 h induction. The cell pellets were stored at -20 °C for further analysis.

### 3.2.23 Affinity purification of recombinant *Mc*-His

The r*Mc*-His purification was performed in batch mode using nickel-charged agarose affinity chromatography spin column (Qiagen®) as described previously in the section 2.2.25 of Chapter 2. The eluted protein was stored at -20 °C for further analysis.

### 3.2.24 Concentration and re-folding of recombinant *Mc*-His

The recombinant *Mc*-His was concentrated and refolded in refolding buffer using Amicon ultra centrifugal filters with 3 kDa cut-off membranes (Millipore) as defined in the section 2.2.26 of Chapter 2.

### 3.2.25 Quantification of recombinant *Mc*-His

Purified and concentrated r*Mc*-His was quantified with Quant-iT$^{TM}$ protein assay kit using Qubit fluorometer (Invitrogen, UK) as described in section 2.2.27 of Chapter 2.

### 3.2.26 Haemolytic activity of recombinant *Mc*-His

Haemolytic activity of r*Mc*-His was determined against human red blood cells (hRBCs). The haemolysis percentage was calculated and plotted as explained in the section 2.2.28 of Chapter 2.

### 3.2.27 *In vitro* cytotoxicity assay

Cytotoxicity of r*Mc*-His was measured against human cancer cells NCI-H460 using the standard XTT assay. Inhibition percentage of the peptide treated against the control group was recorded and calculated as explained in section 2.2.29 of Chapter 2.

### 3.2.28 Antimicrobial assay

Antimicrobial activity of r*Mc*-His was tested against bacterial pathogens by broth microdilution assay. Microscopic observation of peptide treated pathogens was carried out using epifluorescence microscopy after propidium iodide staining. Moreover, morphological changes of peptide treated bacteria was analysed by scanning electron microscopy (SEM) as described in section 2.2.30 of Chapter 2.

## 3.3 Results

### 3.3.1 Molecular characterization of a histone derived peptide from *Mugil cephalus*

In the present study, a Histone Derived AMP (HDAP), from the haemocytes of *M. cephalus* was identified and characterized.

#### 3.3.1.1 PCR amplification, TA cloning and sequencing

A 243 bp amplicon encoding 81 amino acids was amplified from the cDNA of *M. cephalus via*, RT-PCR (Fig. 3.2). The amplicons were then cloned into pGEM®-T Easy cloning vector and gene insertion was confirmed using vector-specific and gene specific primers by colony PCR (Fig. 3.3a). The recombinant pGEMT plasmids with the insert H2A gene (Fig. 3.3b), isolated from the positive colonies were sequenced and analysed. The nucleotide and deduced amino acid sequences of *M. cephalus* histone H2A has been submitted to the NCBI GenBank under the accession number **MF966482** (Fig. 3.4).

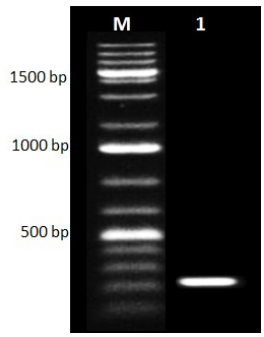


**Fig. 3.2** Agarose gel of PCR amplification of *M. cephalus* HDAP gene. Lane M: 100 bp DNA marker, Lane 1: 243 bp amplicon of *M. cephalus* HDAP gene.

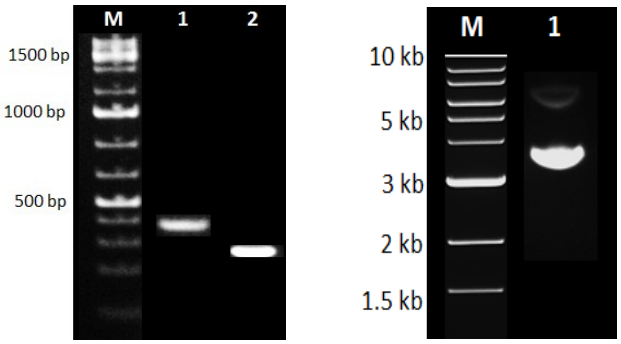


**(a)** **(b)**

**Fig. 3.3** (a) Colony PCR gel image of *M. cephalus* HDAP gene amplicon obtained from the recombinant pGEMT vector. Lane M: 100 bp DNA ladder, Lane 1: 384 bp amplicon obtained with vector specific primers and Lane 2: 243 bp amplicon obtained using gene specific primers (b) Plasmid extracted from positive clones of pGEMT vector with *M. cephalus* HDAP gene insert. Lane M: 1 kb DNA marker, Lane 1: pGEMT plasmid with *M. cephalus* H2A gene insert.

```
atgtccgggcgagggaaaaccggaggcaaagccagagctaaggctaagacccgctcttct
 M  S  G  R  G  K  T  G  G  K  A  R  A  K  A  K  T  R  S  S
cgtgcaggacttcagttcccagtcggccgtgtccacaggctgctgcgtaaaggcaactat
 R  A  G  L  Q  F  P  V  G  R  V  H  R  L  L  R  K  G  N  Y
gccgagcgtgttggagccggcgctcccgtctacctggcggctgtgcttgagtacctgacc
 A  E  R  V  G  A  G  A  P  V  Y  L  A  A  V  L  E  Y  L  T
gctgagatcctggagttggctggaaacgctgcccgtgacaacaagaagacgcgcatcatc
 A  E  I  L  E  L  A  G  N  A  A  R  D  N  K  K  T  R  I  I
cct
 P
```

**Fig. 3.4** Nucleotide sequence (grey colour) and deduced amino acid sequence (yellow and green) of histone H2A gene amplified from *M. cephalus*, (GenBank ID**: MF966482)**. The highlighted region in yellow represents the biologically active peptide region (*Mc*-His).

### 3.3.1.2 Sequence characterization and phylogenetic analysis

BLAST analysis of the nucleotide and deduced amino acid sequences revealed that the peptide belonged to histone H2A family. The nucleotide sequences showed marked difference with other reported histone H2A sequences and shared only 94 % and 90 % identity to *Larimichthys crocea* histone2A mRNA (GenBank ID: XM_019263858.1) and *Lates calcarifer* histone2A mRNA (GenBank ID: XM_018703374.1)

respectively. However, the deduced amino acid sequences of the *M. cephalus* histone H2A shared complete sequence similarity with the predicted histone H2A like peptide of *Oreochromis niloticus*. A high degree of degeneracy of genetic code could be observed when compared with other fish H2A sequences as the nucleotide sequences of the fish exhibited considerable variation among themselves.

SignalP analysis of the deduced *M. cephalus* H2A sequence revealed that it lacked a signal peptide region. However, the DAS prediction server identified the presence of two transmembrane amino acid spanning regions (residues 48–61 and 51–57) in the precursor peptide. ScanProsite analysis disclosed that the deduced amino acid *M. cephalus* histone sequence contains a histone 2A signature region at $Ala^{22}$-$Gly^{23}$-$Leu^{24}$-$Gln^{25}$-$Phe^{26}$-$Pro^{27}$-$Val^{28}$. Other than this gene specific motif, *M. cephalus* histone contains 2 common motifs including one protein kinase C phosphorylation site at $Ser^{19}$-$Ser^{20}$-$Arg^{21}$ and two modified phophoserine residues at $2^{nd}$ and $19^{th}$ position. Furthermore, a DNA binding (residues 30–78) site and two acetylation ($Lys^{6}$ and $Lys^{10}$) sites were also found to be present in the precursor peptide.

The PeptideCutter tool of ExPASy predicted that the 81-mer histone precursor peptide possessed a potential cleavage site at the C-terminal part of $52^{nd}$ residue for proteolytic enzymes chymotrypsin, pepsin, proteinase K, and thermolysin, releasing a 52-mer active peptide, herein denoted as *Mc*-His. ClustalW multiple alignment of *Mc*-His with other previously reported HDAPs revealed that *Mc*-His is highly similar to hipposin, a highly potent antimicrobial peptide reported from the skin mucus of Atlantic Halibut, *Hippoglossus hippoglossus*. Apart from the

initiator methionine, the only difference noted was His[41] in hipposin replaced by Glu[42] in *Mc*-His. Multiple sequence alignment also outlined the conserved domains and dissimilar residues found in teleost fish, scallop and the crustacean class from which each of those selected peptides taken for alignment were reported (Fig. 3.5a)**.**

**(a)**

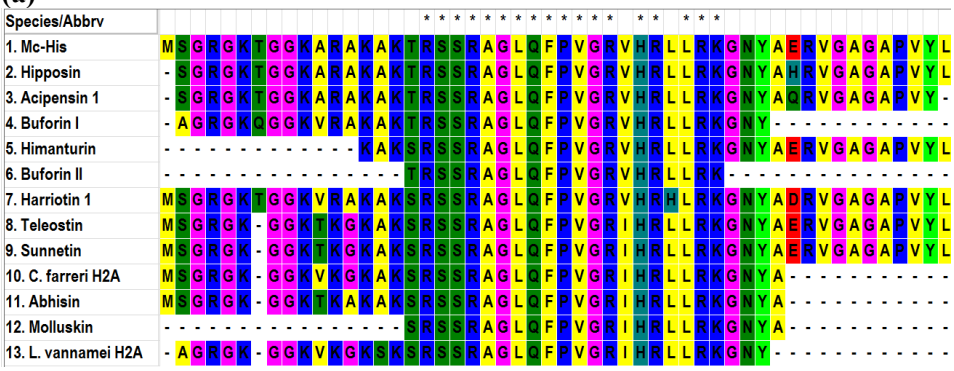


**(b)**

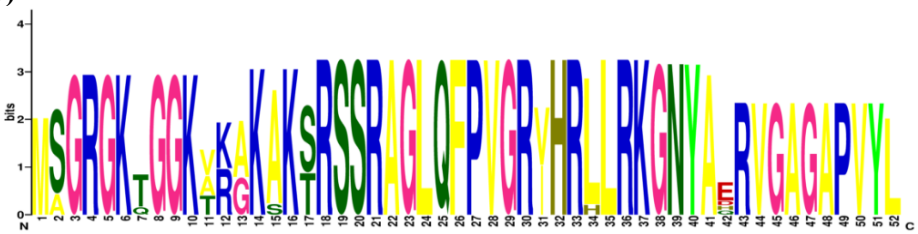


**Fig. 3.5** (a) ClustalW multiple alignment of *Mc*-His with previously reported histone H2A derived AMPs, from fishes, molluscs and crustaceans obtained using MEGA version 6 software. The highly conserved regions are marked with an asterisk. Gaps are inserted to obtain maximum homology (b) WebLogo visualization of the consensus motif based on multiple alignments of HDAPs. The relative heights of the amino acid symbols at each position represent the degree of sequence conservation at each of these positions based on information content in bits.

Peptide characterisation by ProtParam tool of ExPASy disclosed that the precursor peptide possessed a predicted molecular weight of 8.676 kDa, a theoretical p*I* of 11.76, total hydrophobic ratio of 38 % and a net positive

charge of 12. The aforesaid parameters for the active *Mc*-His peptide were found to be 5.52 kDa, 12.01, 32 % and +12 respectively. The dominant amino acids found in *Mc*-His were Gly (17.6 %), followed by Arg (15.7 %), Ala (13.7 %), Lys (9.6 %), Leu and Val contributing to 7.8 %, while its precursor peptide was rich in Ala (16 %), Arg (12.3 %) and Gly (12.3 %) residues. The cationicity of the active peptide was found to be mainly contributed by lysine and arginine residues. *In vivo* aggregation propensity determined using AGGRESCAN identified the presence of a hot spot in the precursor peptide, with a calculated value of 0.44 for the motif ($Val^{50}$-$Leu^{66}$), while no hotspots could be identified for the active peptide. The estimated half- life of the active peptide, *Mc*-His, was found to be around 30 h in mammalian reticulocytes, greater than 20 h in yeast and greater than 10 h in *Escherichia coli in vivo*. The instability index of the active peptide was computed to be 38.71 and classified the peptide to be a stable one.

The secondary structure analysis of *M. cephalus* H2A by POLYVIEW server showed that the peptide contained 58.02 % α-helical region (47 residues) and 41.97 % random coiled regions (34 residues) (Fig. 3.6). However, no β strands or sheets could be observed. The helical and coiled regions of *Mc*-His accounted for 52 % (27 residues) and 48 % (25 residues) respectively. In *Mc*-His, the coiled regions were found to be constituted by $Met^{1}$-$Ala^{13}$ and $Lys^{37}$- $Ala^{48}$ whereas the helical regions were framed by $Lys^{14}$- $Arg^{36}$ and $Val^{49}$- $Leu^{52}$.

**Fig. 3.6** Secondary structure of *Mc*-His precursor peptide predicted using POLYVIEW server. The alpha helical region is shown in zig zag red lines and the coiled region is shown in blue lines.

The helical structure of the peptide was further confirmed with helical wheel modelling of the histone H2A of *Mugil cephalus*. The helical wheel analysis of N-terminal region of the protein (52 residues) i.e., *Mc*-His clearly demonstrated the amphipathic nature of the peptide (Fig. 3.7). Hydrophilic residues such as serine (S), lysine (K), histidine (H), arginine (R), asparagine (N), glutamine (Q) and hydrophobic residues such as methionine (M), valine (V), glycine (G), alanine (A), phenylalanine (F), tyrosine (Y), leucine (L), proline (P) are positioned opposite to each other in the helical wheel. Moreover, analysis of the *Mc*-His sequence using the Kyte-Doolittle plot demonstrated that the hydrophobic amino acids are localized towards the middle (residues 23–27 and residues 30–32) and terminal portion of the peptide (residues 44–52 ) (Fig. 3.8).

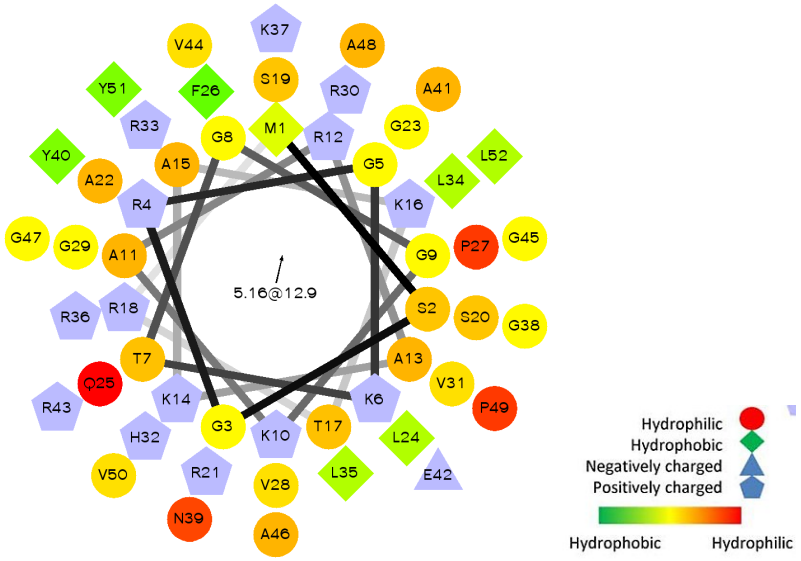


**Fig. 3.7** Helical wheel diagram of *Mc*-His demonstrating its predictive α-helical amphipathic conformation. Helical wheel projects the positional arrangement of amino acids where hydrophobic and hydrophilic residues face opposite facets of the wheel. The values for hydrophobic moment displacement (5.16) and hydrophobic moment angle (12.9) are indicated respectively.

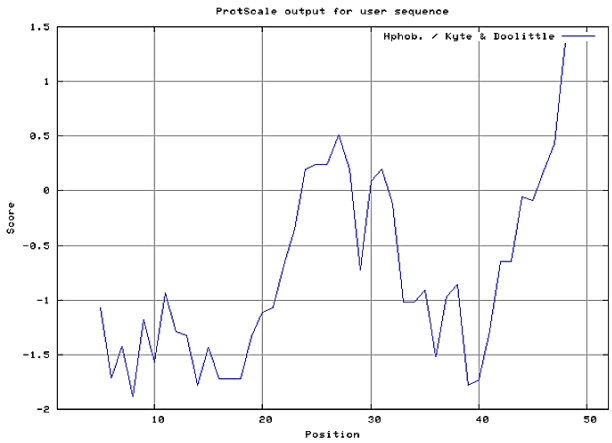


**Fig. 3.8** Kyte-Doolittle plot showing the hydrophobic nature of *Mc*-His**.** The peaks above the score (0.0) indicate the hydrophobic nature of the predicted peptide.

The three dimensional structure of *Mugil cephalus* histone 2A was predicted with the pdb data generated by SWISS-MODEL server employing the software PyMOL by homology modelling using 3av1.1c as the template (Fig. 3.9a).

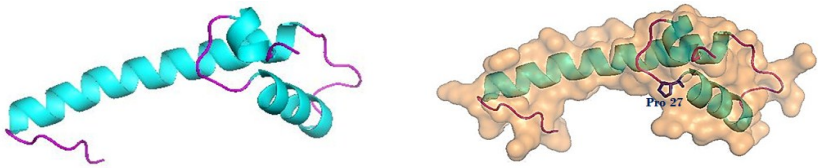


**Fig. 3.9** Predicted 3-dimensional structure of *Mugil cephalus* histone 2A constructed by homology modelling using PyMOL software (PDB ID- 3av1.1c) (b) Spatial structure of *Mugil cephalus* histone 2A with its proline hinge highlighted in blue colour.

The three dimensional structure revealed the existence of 3 α-helices and 4 random coiled regions, the coiled regions extending on either side of the helix (Fig. 3.9b). *Mc*-His exhibited 96.15 % structural similarity with human histone H2A type1 (PDBID- 3av1.1c). The 3-D structure of *Mc*-His consisted of both charged residues and amphipathic moieties which allow strong interaction of peptides with the microbial membranes.

The antimicrobial property of *Mc*-His peptide was predicted by APD2 database combining the helical structural details and its strong cationic nature. The results indicate that *Mc*-His has at least 7 hydrophobic residues on the same hydrophobic surface for interaction with the microbial membranes. Moreover, *Mc*-His net charge of +12 with protein binding potential (Boman index) of 2.38 kcal/mol further ensured its antimicrobial property. Also, sequence alignment of *Mc*-His with other peptides deposited in APD2 database showed 96.15 %, 94.23 % and 69.23 % similarity with Hipposin, Acipensin 1 and Buforin I respectively; all with proven track of antimicrobial activity. The discriminant analysis classifier algorithm (90 %) classified the peptide *Mc*-His as an antimicrobial one. The predicted RNA fold structure of *Mc*-His with minimum free energy (MFE) is given in Fig. 3.10. The MFE of the RNA structure of *Mc*-His was predicted to be -52.40 kcal/mol. The coloured MFE structural analysis showed that there are no blue coloured bases present indicating that most of the nucleotides in the mRNA are paired, which further demonstrates the strong stable nature of *Mc*-His mRNA.

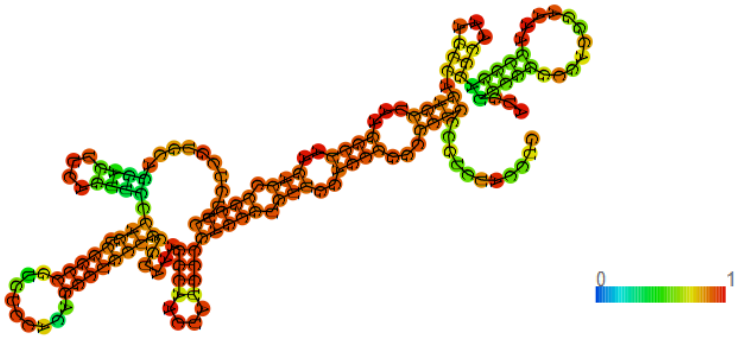


**Fig. 3.10** The mRNA structure of *Mc*-His predicted using RNA fold server. The MFE structure is coloured based on the base-pairing probabilities. Blue coloured bases denote the unpaired ones while red coloured bases denote the paired ones.

Bootstrapped phylogenetic analysis based on the nucleotide sequence of histone H2A reported from invertebrates and vertebrates created a phylogenetic tree wherein the *Mugil cephalus* histone H2A aligned with the fishes and the amphibian group (Fig. 3.11). *Mugil cephalus* H2A was seen more closely related to *Larimichthys crocea* indicating its close resemblance with other teleost fishes.

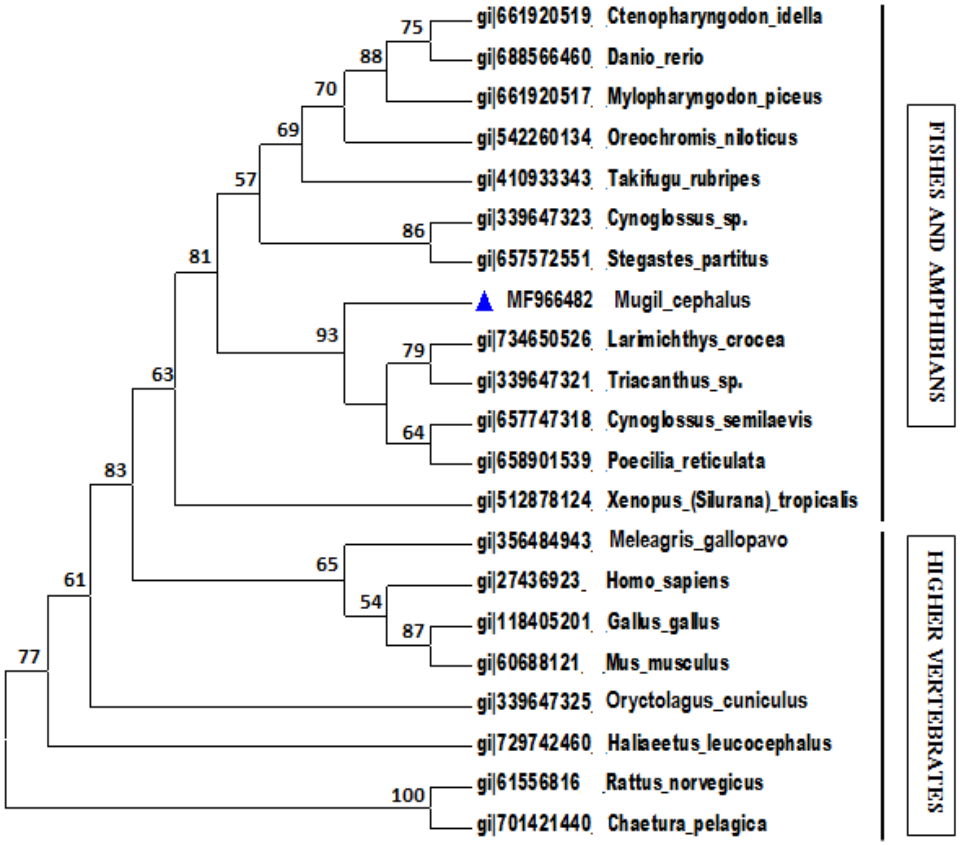


**Fig. 3.11** Consensus neighbour-joining phylogenetic tree of *Mugil cephalus* histone H2A gene (**GenBank ID: MF966482**) with other vertebrates constructed using Mega 6.06. The values at the forks indicate the percentage of times in which this grouping occurred after bootstrapping (1000 replicates).

### 3.3.2 Recombinant production and functional characterization of *Mc*-His

Bioinformatics analysis of the *Mugil cephalus* HDAP predicted that the precursor peptide possessed potential cleavage site for various enzymes at the C- terminal part of 52$^{nd}$ residue suggesting the possibility of formation of a 52-mer active peptide (*Mc*-His) extending from the N-terminus of the peptide. On further analysis, *Mc*-His was endowed with antimicrobial attribute by various algorithms. Thus, the selected region designated as *Mc*-His, was subjected to recombinant expression and for analyzing its biological activity.

#### 3.3.2.1 PCR amplification and cloning of *Mc*-His with restriction sites

Selective PCR amplification of *Mc*-His gene was obtained by specially designed restriction primers (Table 3.2) using recombinant pGEMT plasmids with insert *Mugil cephalus* H2A gene as the template. Approximately 160 bp amplicons including restriction sites were obtained by the PCR reaction (Fig. 3.12a). Purified amplicons were cloned using pGEM®-T Easy cloning vector and transformed to *E. coli* DH5α competent cells. Colony PCR with gene specific (pET *Mc*-His F and R**)** and vector specific primers (T7 F and SP6 R) yielded amplicons of size ~160 bp and ~300 bp (160 bp + 141 bp) respectively (Fig. 3.12b). Plasmids were extracted from the recombinant clones and sequencing of the plasmid was done to check the presence of restriction site (Fig. 3.12c).

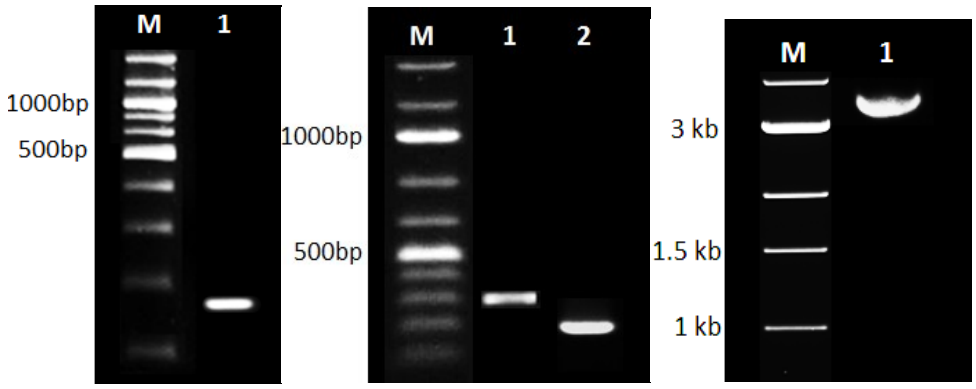


**Fig. 3.12** (a) Agarose gel of selective amplification of *Mc*-His region with restriction primers, Lane M: 100 bp ladder; Lane 1: PCR amplified product (~ 160 bp) ; (b) Colony PCR gel image of amplicons obtained with pGEMT-*Mc*-His plasmid using vector and gene specific primers, Lane M: 100 bp ladder; Lane 1: ~300 bp amplicon obtained with vector specific primers and Lane 2: ~160 bp amplicon obtained with insert specific primers; (c) Recombinant pGEMT plasmids with *Mc*-His restriction primer amplified gene.

### 3.3.2.2 Restriction enzyme digestion and cloning into pET-32a(+) expression vector

pGEMT plasmids containing the *Mc*-His restriction primer amplified gene and the expression vector pET-32a(+) were double digested using BamHI and HindIII restriction enzymes (Fig. 3.13). Insert release and vector digestion were confirmed by AGE. The released insert of size ~150 bp and the linearized vector is shown (Fig. 3.13a and b). Followed by RE digestion, the insert and vector were gel eluted using GenJET™ Gel Extraction Kit (Thermo Scientific, USA).

**(a)** **(b)**

**Fig. 3.13** (a) Agarose gel image of pGEMT plasmid containing *Mc*-His restriction primer amplified gene digested with BamHI and HindIII enzymes. Lane M: 100 bp ladder, Lane 1: Undigested pGEMT-*Mc*-His plasmid, Lane 2: Released insert (~150 bp) from the pGEMT-*Mc*-His plasmid (b) Agarose gel image of pET-32a(+) vector restricted digested with BamHI and HindIII enzymes. Lane 1: Linearised pET vector after digestion, Lane 2: Uncut pET vector.

The purified gel eluted vector and insert were ligated and transformed into the cloning host *E. coli* DH5α. Colony PCR using vector specific primers (T7 F and T7 R) and gene specific primers yielded amplicons of size 900 bp (~150 bp + 750 bp) and 150 bp respectively (Fig. 3.14a). Recombinant pET plasmids with *Mc*-His gene insert were isolated from the positive clones (Fig. 3.14b). Sequenced plasmids with *Mc*-His in frame expression cassette and pET-32a (+) without insert were transformed to expression host Rosetta-gami$^{TM}$ B (DE3) pLysS. Recombinant colonies were obtained in LB agar plates with ampicillin and kanamycin.

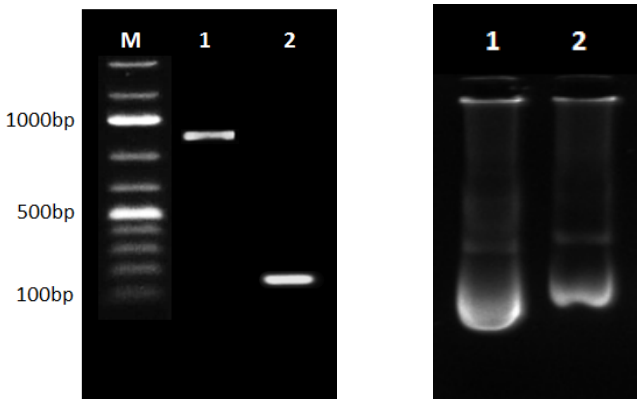


**Fig. 3.14** (a) Colony PCR gel image of amplicons obtained with pET-*Mc*-His plasmid using vector and gene specific primers. Lane M: 100 bp ladder; Lane 1: ~900 bp amplicons obtained using vector specific primers, Lane 2: ~150 bp amplicons obtained using vector specific primers. (b) Plasmid gel image of the recombinant pET-32a (+)-*Mc*-His and the empty pET plasmid. Lane 1: control pET vector, Lane 2: pET plasmid with *Mc*-His insert.

### 3.3.2.3 Recombinant expression of *Mc*-His as fusion protein

The *Mc*-His was successfully produced as a fusion protein containing N-terminal His tag, S tag and thioredoxin tag in the expression host. Rosetta-gami$^{TM}$ B pLysS *E. coli* strains that contained the recombinant *Mc*-His expression plasmid was cultured under conditions as described in section 3.2.19. After 1$^{st}$ h of 0.1 mM IPTG induction, the cells were centrifuged and the pellet was treated with the sample buffer. Initial SDS-PAGE analyses of the total bacterial extracts of induced bacteria were compared at various time points with the uninduced sample. The induced lysates clearly demonstrated the presence of a band at around 25.5 kDa which was consistent with the expected molecular weight of r*Mc*-His protein (5.52 kDa of *Mc*- His + ~ 20 kDa of Trx protein) (Fig. 3.15). Also the SDS–PAGE gel indicated that r*Mc*-His fusion protein was expressed

as a monomer, in a soluble form in the cytoplasm of the expression host (bacteria). The intensity of expression increased from the time of induction, reaching to a plateau within 4 h, and found to be consistent thereafter (Fig. 3.15). Also, no basal level expression was noticed at the time of induction. Hence recombinant mass production of *Mc*-His was done at 37 °C, with orbital shaking at 250 rpm for 4 h post induction. The cells were then harvested and stored at -20 °C.

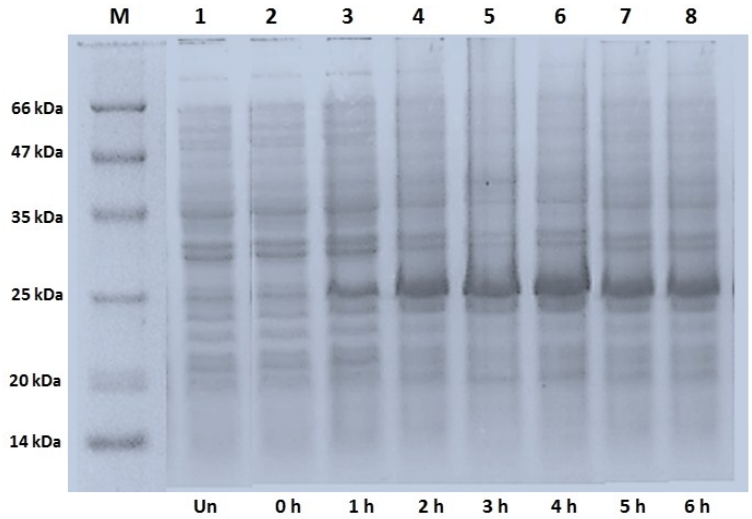


**Fig. 3.15** Tricine SDS-PAGE analysis of recombinant expression of *Mc*-His, before and after IPTG induction on a time-course basis. Lane M: Mid-range protein ladder, Lane 1: uninduced control (before IPTG induction), Lane 2: recombinant cells at the time of induction, Lane 3-8: IPTG induced cells from 1-6 h post induction.

### 3.3.2.4 Purification, refolding and quantification of the recombinant protein

The recombinant protein from the soluble fractions was purified on a Ni-NTA agarose column as described in section 3.2.23. Protein purified from the pellet of recombinant bacteria was analyzed using Tricine-SDS-PAGE and a band at around 25.5 kDa corresponding to the size of

recombinant *Mc*-His was observed (Fig. 3.16a). SDS-PAGE profiles of various protein fractions clearly demonstrated an efficient purification of r*Mc*-His in the eluted fraction. Furthermore, western-blot resulted in a strong immunoreactive band at a position comparable to its expected size (Fig. 3.16b). Eluted fractions were concentrated using Amicon cut off filtration system and refolded in the refolding buffer. The purified and refolded r*Mc*-His was quantified using Quant-iT$^{TM}$ protein assay kit and the concentration was found to be 2.13 mg/ml (83.53µM).

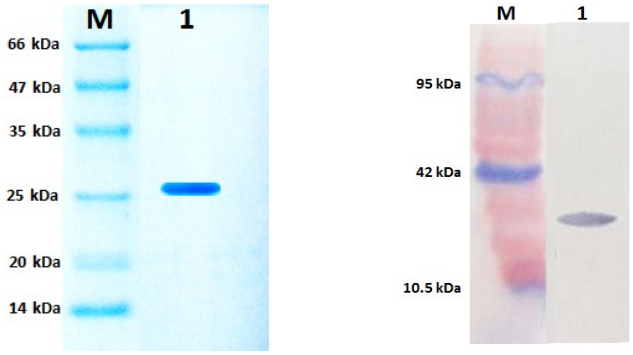


(a) (b)

**Fig. 3.16** (a) Tricine SDS-PAGE analysis of Ni-NTA purified r*Mc*-His. Lane M: Mid-range protein marker, Lane 1: purified r*Mc*-His (25.5 kDa) (b) Western blot of purified r*Mc*-His. Lane M: mid-range coloured marker, Lane 1: purified r*Mc*-His.

### 3.3.2.5 *In vitro* cytotoxicity and haemolytic activity of r*Mc-His*

To examine the cytotoxic effects of recombinant *Mc*-His, NCI-H460 cell lines were exposed to different concentrations (0.625 µM - 20 µM) of the recombinant protein and cell viability was determined by the XTT assay. The cytotoxic peptide, mellitin was used as the positive control and rTrx as the negative control. The highest tested concentration of r*Mc*-His exhibited only 3 % growth inhibition and thus found to be non-cytotoxic to the NCI-H460 cell lines (Fig. 3.17).

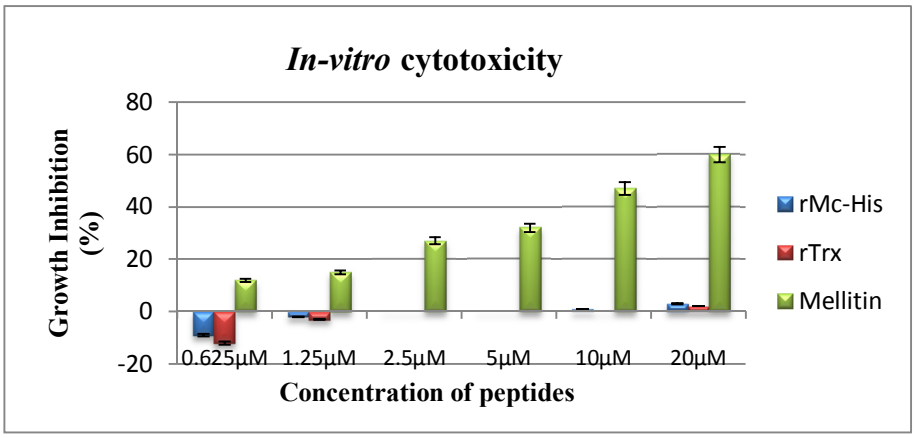


**Fig. 3.17** *In vitro* cytotoxicity of the recombinant peptides r*Mc*-His, rTrx and mellitin in NCI-H460 cells at various concentrations.

Haemolytic activity of r*Mc*-His was tested against human RBCs and the results demonstrated that the recombinant peptide is non-haemolytic. Even at the highest tested concentration of 20 µM r*Mc*-His displayed only 0.2 % haemolysis (Fig. 3.18). Whereas, mellitin and rTrx (thioredoxin) exhibited 50 % and zero percent haemolysis respectively.

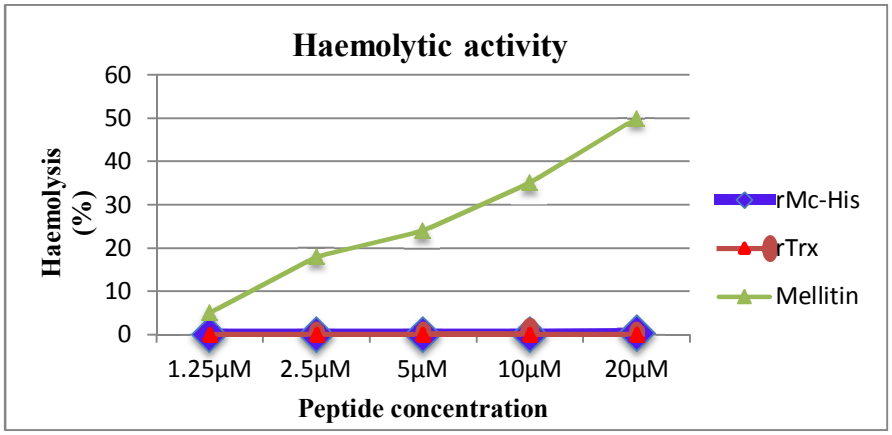


**Fig. 3.18** Haemolytic activity of the recombinant peptides r*Mc*-His, rTrx against human erythrocytes. Five different concentrations have been tested, starting from 20 µM with successive dilutions. Melittin was used for comparison as a classical haemolytic peptide.

### 3.3.2.6 Antimicrobial activity

Antimicrobial activity of r*Mc*-His and rTrx was analysed using broth microdilution assay from a concentration of 20 µM to 0.625 µM. The control peptide rTrx did not exhibit any activity against the tested pathogens. Moreover, the growth of rTrx treated bacteria was almost the same as that of the untreated control. The recombinant peptide, *Mc*-His exhibited significant activity against Gram-negative pathogens, *E. tarda* (MIC and MBC of 5 µM), *V. alginolyticus* and *V. proteolyticus* (MIC and MBC of 20 µM). Other tested pathogens were also found to be sensitive to r*Mc*-His by varied levels of inhibition, but the MIC and MBC values were found to be >20 µM. At the highest tested concentration of 20 µM, the peptide was found to inhibit the growth of pathogens namely, *S. aureus* (77 %), *B. cereus* (86 %), *V. parahaemolyticus* (92 %), *V. cholera* (95 %), *V. alginolyticus* (99 %), *V. proteolyticus* (99 %), *V. vulnificus* (92 %), *E. coli* (90 %), *A. hydrophila* (83 %), *P. aeruginosa* (89 %) and *E. tarda* (99 %) (Fig 3.19 (a-k)).

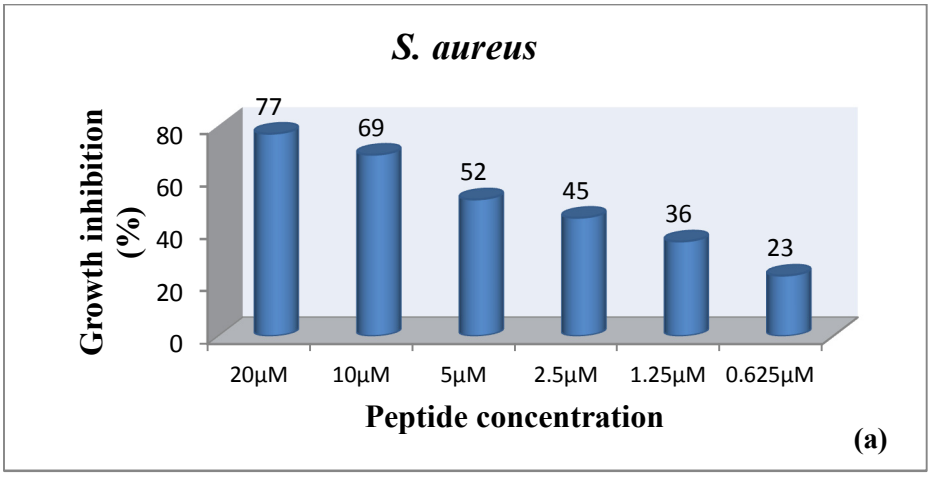


*Fig. 3.19 Continued…*

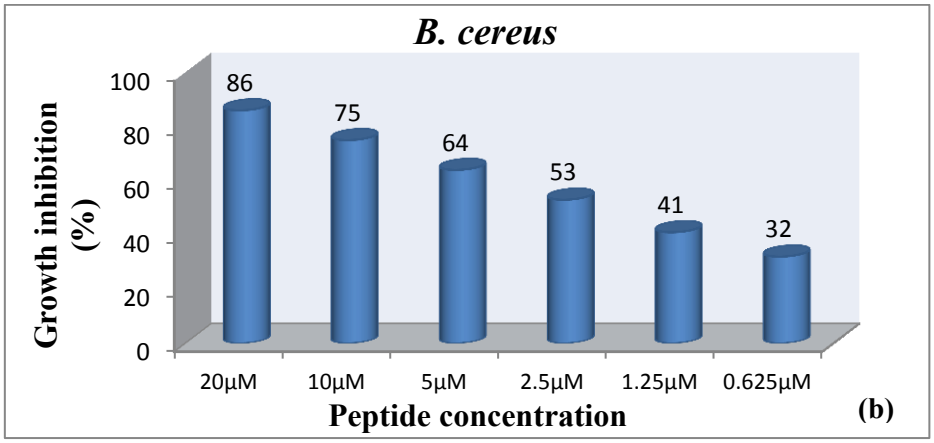


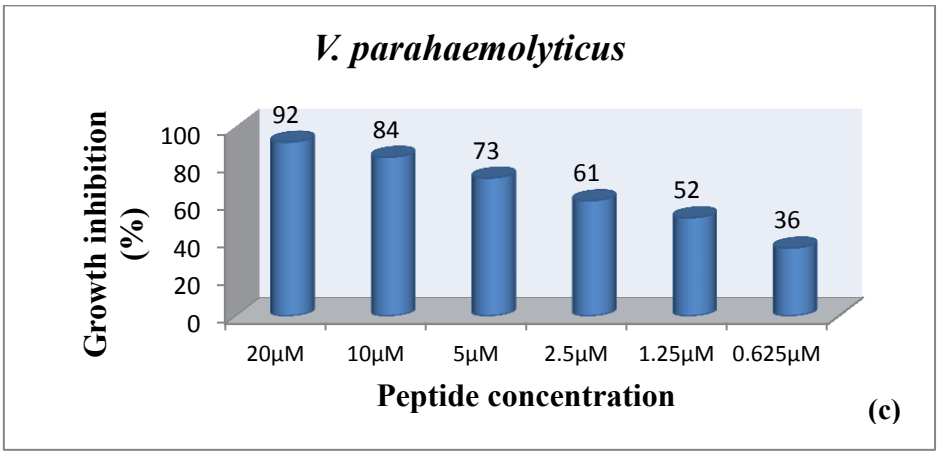


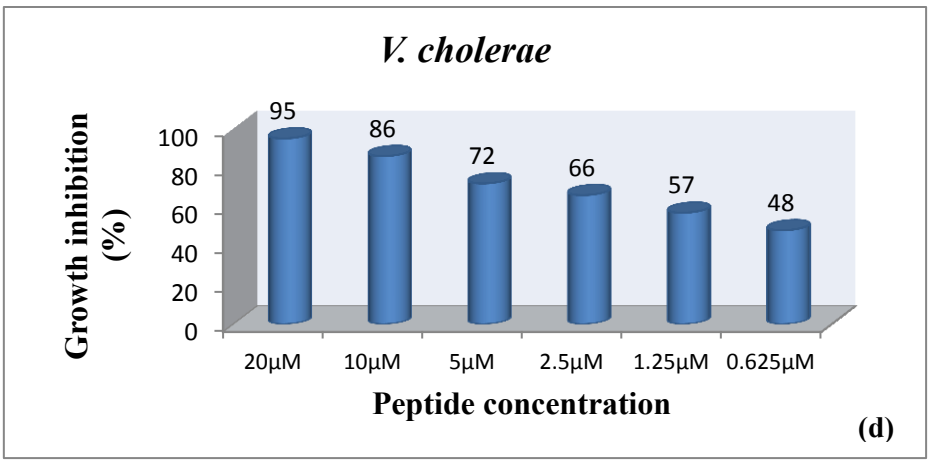


*Fig. 3.19 Continued…*

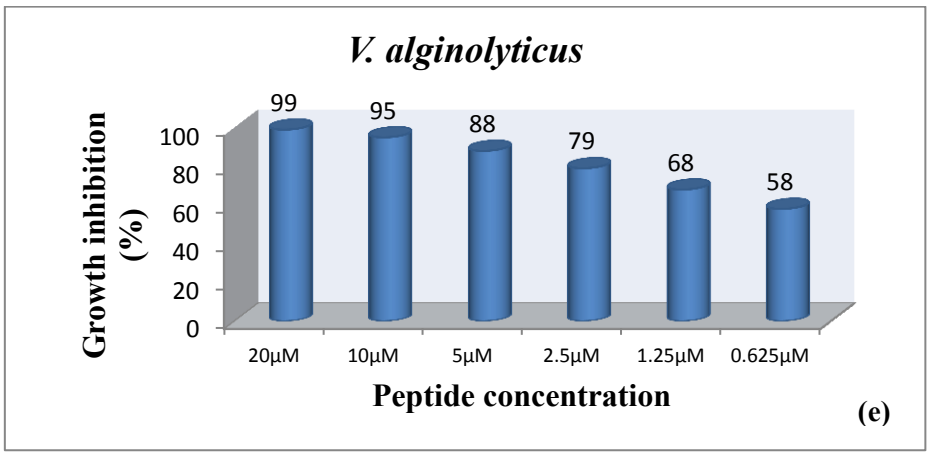


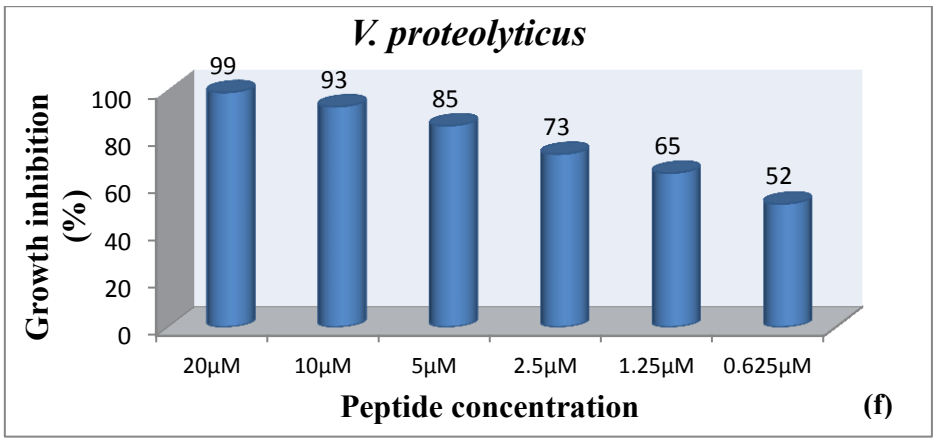


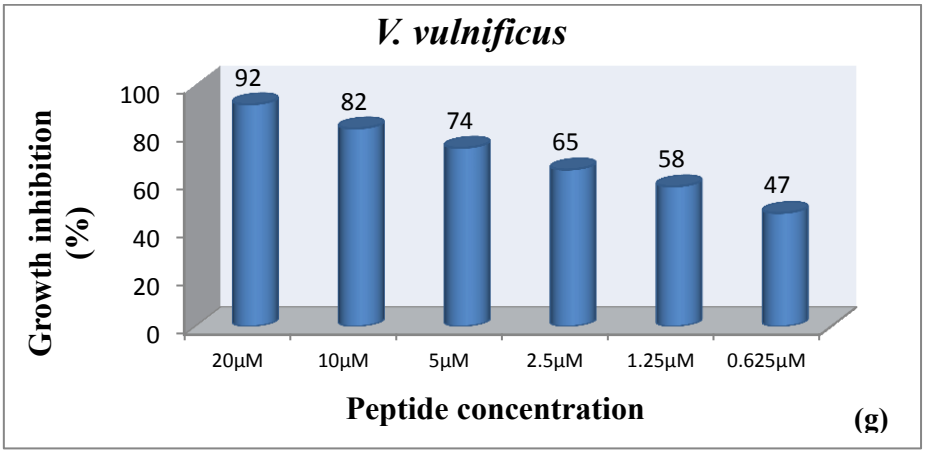


*Fig. 3.19 Continued…*

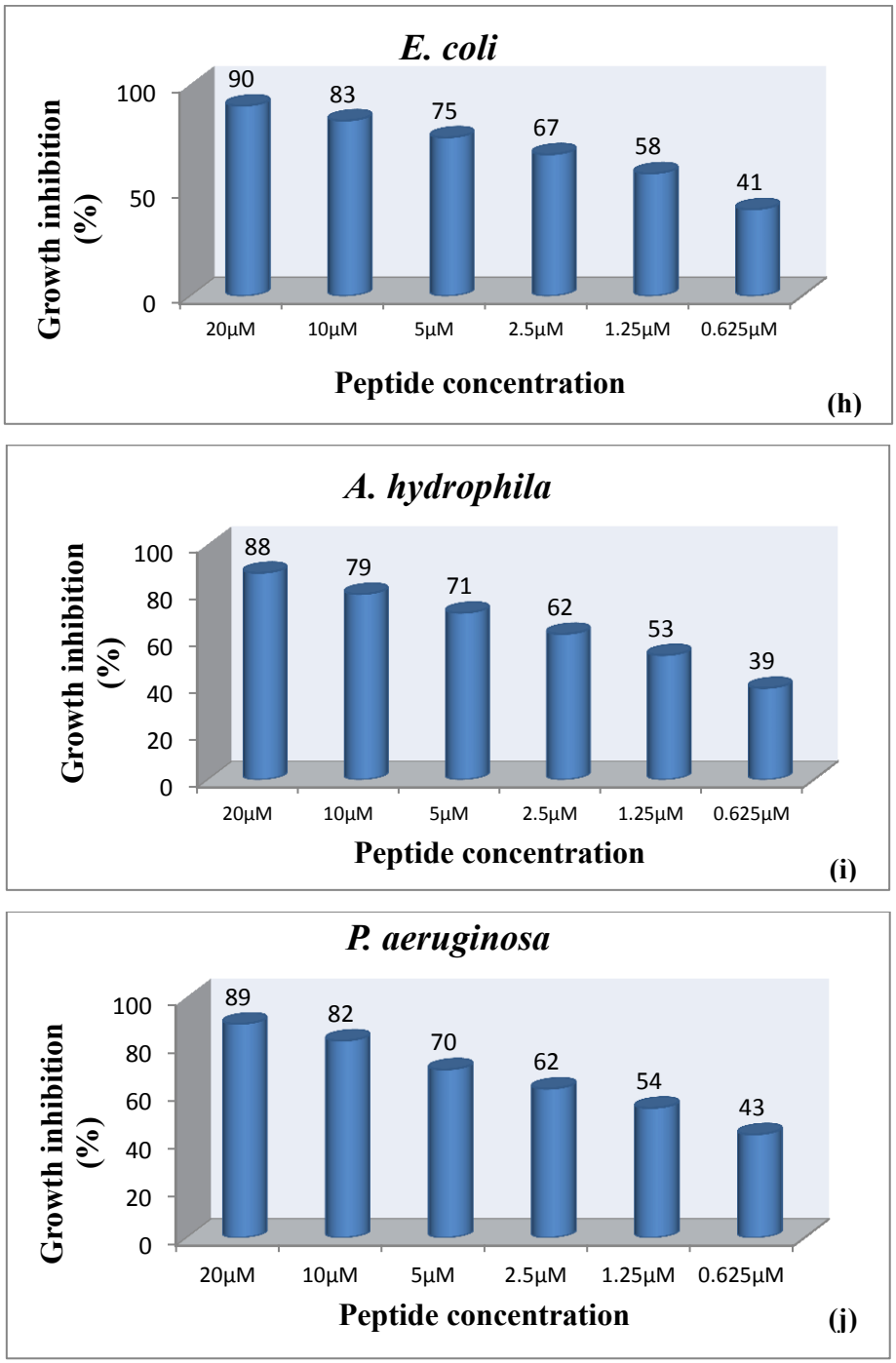


*Fig. 3.19 Continued…*

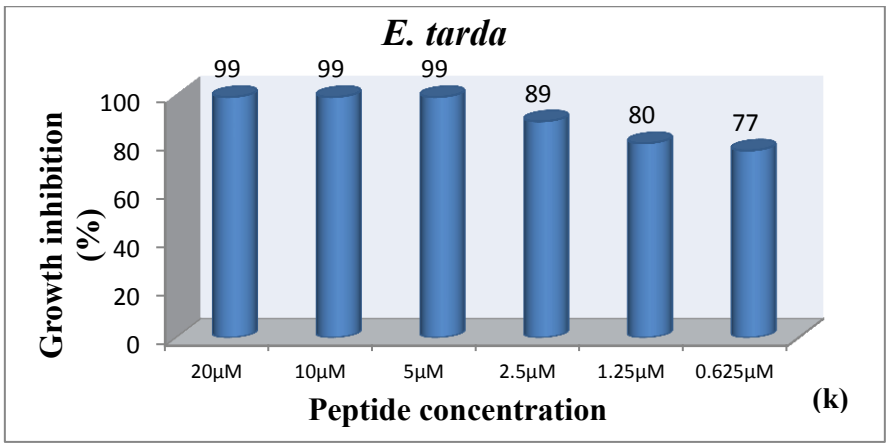


**Fig. 3.19** (a-k) Antimicrobial activity of r*Mc*-His against various bacteria at different concentrations.

### 3.3.2.7 PI staining

Bacteria found susceptible to r*Mc*-His (*E. tarda, V. proteolyticus* and *V. alginolyticus*) were subjected to PI staining after treatment with the peptide and most of the bacteria were stained red (Fig. 3.20). The PI staining results suggests the possible mode of action of r*Mc*-His by membrane pore formation.

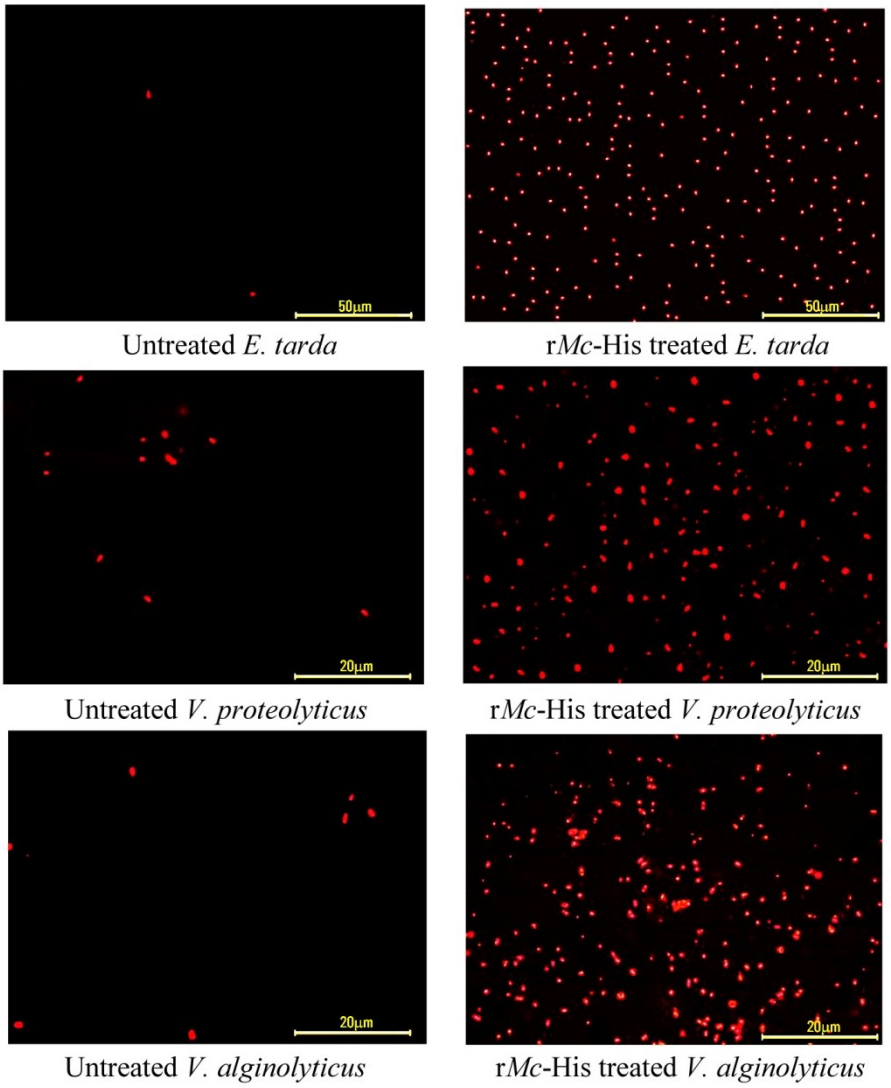


**Fig. 3.20** Propidium iodide stained image of untreated control bacterial cells and recombinant r*Mc*-His treated cells taken using epifluorescence microscope.

### 3.3.2.8 SEM analysis

Scanning electron microscopy was used to observe the effect of r*Mc*-His on the morphology of peptide treated bacteria. It was found that r*Mc*-His caused damage to the cells of *E. tarda, V. proteolyticus* and

*V. alginolyticus*. Compared to the untreated control, cytoplasmic leakage of cell contents and severe damage to the cell membrane are evident from Fig. 3.21. A significant amount of cellular debris was also observed in samples treated with r*Mc*-His.

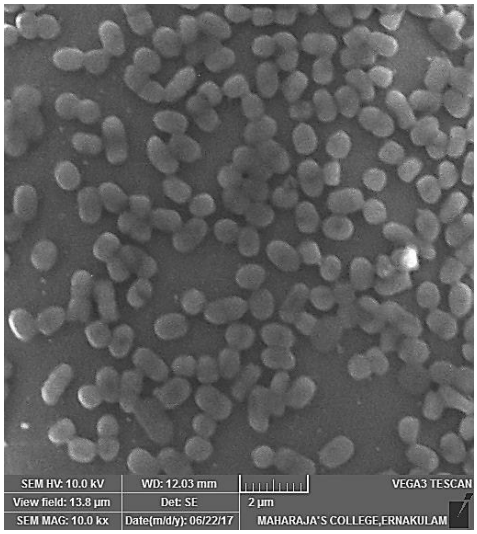


Untreated *E. tarda*

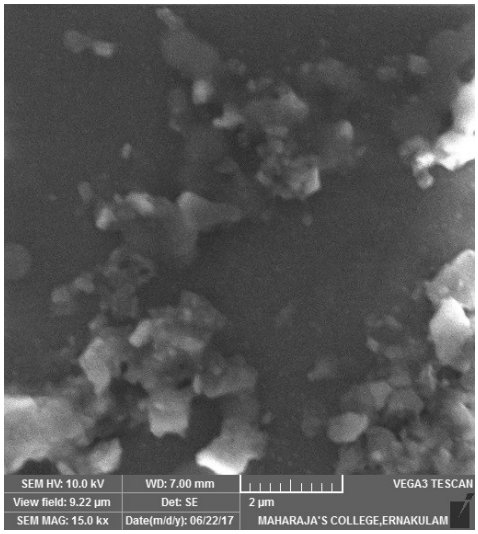


r*Mc*-His treated *E. tarda*

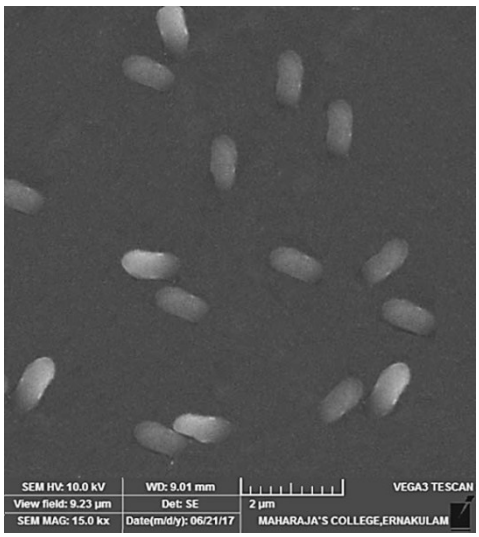


Untreated *V. proteolyticus*

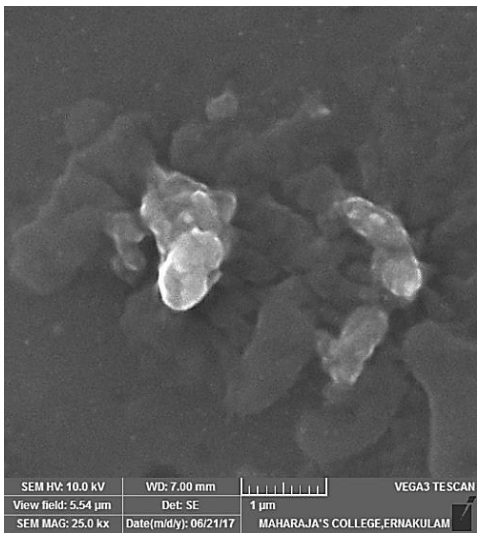


r*Mc*-His treated *V. proteolyticus*

*Fig. 3.21 Continued…*

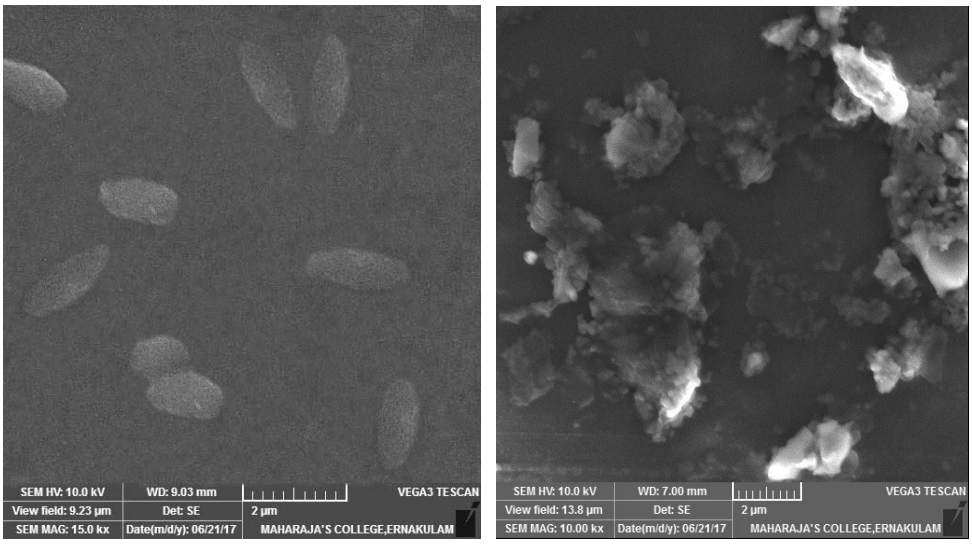


Untreated *V. alginolyticus* r*Mc*-His treated *V. alginolyticus*

**Fig. 3.21** SEM images of r*Mc*-His treated *E. tarda*, *V. proteolyticus*, and *V. alginolyticus* showing a clear rough surface and collapsed membrane architecture in contrast to the respective control bacterial cells.

## 3.4 Discussion

Histones are primarily known as an integral part of chromatin structure in the nucleosome and also for their involvement in nuclear regulation. Subsequently, histones and their polypeptide fragments have been reported to be involved in the host immune response, by acting as antimicrobial peptides (AMPs) (Parseghian and Luhrs, 2006). From then, a number of histone derived antimicrobial peptides (HDAP) have been identified from both vertebrates and invertebrates. In the present study, a partial histone H2A gene was identified and characterized for the first time in flathead grey mullet, *Mugil cephalus*. This histone gene cloned from the haemocytes of *M. cephalus,* possessed typical histone signature domain and shared only 94 % nucleic acid identity to *Larimichthys crocea* histone H2A gene. According to the phylogenetic tree and

BLASTp result, the *M. cephalus* histone belonged to H2A superfamily, of which most of the amino acid sequences are remarkably conserved in comparison with the other known H2A counterparts. Such conservation of amino acid sequences could be seen throughout the members of the order Teleostei due to lower rate of evolution of histone H2A genes (Thatcher and Gorovsky, 1994).

Presence of histone like proteins (HLPs) and fragmented histone derivatives (HDPs) mostly in the skin, gill and spleen have been well documented for certain fishes. These include HLPs of channel catfish (Robinette et al., 1998), hybrid striped bass (Noga et al., 2001), rainbow trout (Noga et al., 2002; Fernandes et al., 2004) and HDPs of Amur catfish (Park et al., 1998), coho salmon (Patrzykat et al., 2001), rainbow trout (Fernandes et al., 2002, 2003), Atlantic halibut (Birkemo et al., 2003), and Atlantic salmon (Luders et al., 2005). On the other hand, the mechanisms with which these peptides are formed are reported only for a few species. The production of parasin by cathepsin D, buforin I by endopeptidase pepsin from the N terminus of histone H2A and buforin II from buforin I by endoproteinase lys-C cleavage have been hypothesized and proved (Kim et al., 2000; Cho et al., 2002a, 2002b). Since little is known about the way these peptides gets cleaved from their precursors, PeptideCutter tool was employed to analyse the activity of proteolytic enzymes on the 81 amino acid histone H2A sequence that may result in the formation of the active peptide. Possible potential cleavage sites for enzymes pepsin, chymotrypsin, thermolysin and proteinase K at the C-terminal of 52$^{nd}$ residue would release an active peptide, which was denoted as *Mc*-His.

Several studies on histone activation to form antimicrobial fragments *in vivo* have demonstrated that they are stimulated either by injury/infection as in the case of production of parasin I by matrix metalloprotease activated cathepsin D upon the epidermal injury of *Parasilurus asotus* (Cho et al., 2002a; Cho et al., 2002b) or by neutrophil extracellular traps (NETs) (Brinkmann et al. 2004; Palic et al. 2007a). Recently, NETs, a novel antimicrobial mechanism comprising of H2A-H2B-DNA complexes and elastases, were identified in human and fish neutrophils that form extracellular fibres to trap and kill microbes (Brinkmann and Zychlinsky, 2007; Guimaraes-Costa et al., 2009). These fibers are mostly covered in histones, which bring them into contact with bacteria more effectively, facilitating their antimicrobial activities. This phenomenon of NETs production has also been described in some fish species such as the fathead minnow (Palic et al., 2007a), zebrafish (Palic et al., 2007b), goldfish (Katzenback and Belosevic, 2009), carp (Pijanowski et al., 2013) and teleost fish tongue sole (Wen et al., 2017). However, exact mechanism of histone activation in flat head grey mullet remains unclear and needs further investigation.

The antimicrobial properties of histones are determined based on the number of cationic residues and amphipathic secondary structure. Further, this property of histones appears to be connected to their role of damaging pathogenic microbes and not to their capacity of arranging stable pores (Fernandes et al., 2002). The secondary structural analysis of *Mc*-His showed that it contained more α-helical regions (52 %) than coiled regions (48 %). Boman (2003) and Papagianni (2003) as well as Koo and co-workers (2008) have earlier stated that peptide possessing

antimicrobial property will have more number of alpha-helix regions. Interestingly, there were no cysteine residues noticed in *Mc*-His, which clearly indicated that it is an α-helical AMP without any cysteine residue. The Kyte-Doolitle plot clearly demonstrated the localisation of hydrophobic residues towards the centre and middle segments of *Mc*-His indicating its functionality in partitioning the lipid bilayer or membrane. Moreover, *Mc*-His is largely cationic (+12) owing to the presence of lysine (9.6 %) and arginine residues (15.7 %), which is important for an AMP for the initial electrostatic interactions to bind with anionic components of bacterial membranes as suggested by Boman (2003) and Tagai et al. (2011). In addition to this, the presence of DNA binding sites correlates with the high amount of lysine at the N-terminal site of histone H2A suggesting its possible role in DNA binding (Balicki et al., 2002). Moreover, the AMP prediction results clearly showed that *Mc*-His can have antimicrobial property as its sequence have significant similarity with the earlier reported AMPs such as hipposin (Birkemo et al., 2003) and buforin I (Park et al., 1996). All these AMPs share several characteristic features including net positive charge, molecular mass, hydrophobic and membrane-active molecules with multiple arginine and lysine residues (Park et al., 1996; Birkemo et al., 2003; Vassilevski et al., 2008; Zhou et al., 2011).

Multiple sequence alignment of *Mc*-His with other known H2A HDAPs disclosed that it is much similar to the 51-mer HDAP hipposin. *Mc*-His has a net charge of +12 as against a +13 charge of hipposin. Hipposin is among the most potent antimicrobial peptides discovered to date (Birkemo et al., 2003). It has a broad spectrum activity against several Gram-positive and Gram-negative bacteria, and the activity could be detected down

to a concentration of 1.6 µg/ml (Birkemo et al., 2003). Moreover, hipposin is an AMP devoid of any acidic amino acids. The reduced cationicity of *Mc*-His is mainly because of replacement of His by Glu, which would reduce the cytotoxic activity of the *Mc*-His and make it more specific to anionic bacterial membranes (Khandelia and Kaznessis, 2006).

The 3D structure predicted by SWISS-MODEL program, viewed through PyMol, indicated the presence of a proline hinge region, in *Mc*-His (Fig. 3.9b), which is a major structural component of histone AMPs and is responsible for cell penetration (Park et al., 1996). The spatial structure also displayed a larger positive electrostatic surface to interact with the bacterial membranes. Furthermore the helical wheel analysis clearly indicates that *Mc*-His is a linear α-helical molecule, having polar and non-polar residues oriented along the long axis of the amphipathic helix. The result of the helical wheel analysis of *Mc*-His is consistent with the earlier reports (Park et al., 1998; Richards et al., 2001; Li et al., 2007; De Zoysa et al., 2009; Sathyan et al., 2013). The predicted RNA structure of *Mc*-His along with its MFE value clearly indicated that the mRNA of *Mc*-His is highly stable. According to Xiong and Waterman (1997), the MFE value of mRNA depends on AU/GC pairing. The paired base pairs receive negative value and unpaired base pairs receive positive value. In this study, *Mc*-His mRNA received -52.40 kcal/mol, hence it is possible to suggest that many nucleotide base pairs of *Mc*-His are paired and a very few nucleotides in the mRNA are left unpaired thus indicating the stable nature of *Mc*-His mRNA molecule.

The NJ phylogenetic tree based on the nucleic acid sequences of histone H2A reported from wide range of vertebrates indicate a common

ancestral origin for the histones and their adaptive divergence to the present positions. Considering the similar topology of major histone H2A phylogeny to the eukaryotic phylogeny, histone H2A could be used as a molecular marker for classification of the higher hierarchy (Thatcher and Gorovsky, 1994; Lee and Lee, 2003). The histone H2A sequence of *M. cephalus* aligned with the clade formed by the fishes and the amphibians. Grouping of fishes together with amphibians as a clade indicate a slow pace of evolution from fishes to amphibians and a similar evolutionary line for these groups.

Most of the antimicrobial studies of HLPs and HDAPs are carried out with synthetic or natural forms (Li et al., 2007; De Zoysa et al., 2009). Researches pertaining to recombinant expression of H2A genes are scarce. Hence recombinant expression of *Mc*-His protein was performed in an attempt to study the antimicrobial activity with the recombinant protein. Moreover, due to the natural destructive character towards microorganisms and relative sensitivity to proteolytic degradation, AMPs are often produced by fusing peptides to a fusion partner protein in the heterologous hosts. This strategy shielded the bacterial cells from the toxic effects of the peptide thereby increasing their expression levels in the hosts (Lee et al., 1998; Rao et al., 2005; Kim et al., 2006; Zhong et al., 2006; Yadav et al., 2016). In a study performed by Lee et al. (2002) buforin II was expressed as a fusion protein in tandem repeats to increase the production yield. Additionally, this multimeric expression was subsequently proved to improve *via*, stabilization of the long transcripts with a DEAD-box protein or by carrying out recombinant protein expression in an oxidizing environment using *trx*B mutant *E. coli* as the host cells. In another study carried out by Kim et al. (2008), F4, a truncated fragment of the *E. coli* PurF protein was used as a

fusion partner for histonin, a synthetic analogue of buforin II. It was observed that F4 reinforces the formation of inclusion bodies and thus prevents the proteolytic degradation of the expressed recombinant histonin. So far, heterologous expression of H2A genes have been carried out in *E. coli* (Luger et al., 1997; Lee et al., 2002; Tanaka et al., 2004; Kim et al., 2008; Arockiaraj et al., 2013) and *Pichia pastoris* (Li et al., 2007). High level expression of histone genes of lower order animals does not necessitate adaptation of codon usage, despite the presence of several codons with low usage in *E. coli* (Tanaka et al., 2004). Also, the rationale behind selecting only the buforin I like region for expression rather than the full histone H2A gene comes from the observation that use of histone H2A as such might pose some drawbacks to be used as an antimicrobial agent in cells due of its large size and extra functional regions involved in nucleus targeting. Nevertheless, buforin I like region fulfils almost all common structural motifs of an antimicrobial peptide more completely than histone H2A itself in its amphipathicity and composition of positively charged amino acids. As a result, in this study, recombinant expression of only the bioactive peptide *Mc*-His was carried out. Recombinant expression of *Mc*-His was achieved with pET-32a(+) vector in Rosetta-gami$^{TM}$ B (DE3) pLysS *E. coli* cells for the proper production of protein in the cytoplasm and to facilitate purification with N-terminal His tag. Recombinant *Mc*-His was successfully expressed in the cytosol of the host, at 37 $^{0}$C using 0.1mM IPTG.

In general, histones from biological samples, synthetic histones or recombinant histones show antimicrobial activity *in vitro* against various Gram-positive and Gram-negative pathogens (Birkemo et al., 2003; Nam et al., 2012). Antibacterial activity of r*Mc*-His protein was analysed

against 11 different pathogens. rTrx produced using parent vector pET-32a(+) in *E. coli* Rosetta-gami$^{TM}$ B (DE3) pLysS was used as the negative control in the functional assays as done previously in the case of other recombinant AMPs, *viz*., hepcidins (Lin et al., 2014), anti-lipopolysaccharide factors (Sun et al., 2015) and crustins (Liu et al., 2016; Sruthy et al., 2017). In the present study, recombinant *Mc*-His exhibited strong antimicrobial activity against Gram-negative pathogens, *E. tarda*, *V. alginolyticus* and *V. proteolyticus*; important pathogens in aquaculture. Li and co-workers (2007) described that the recombinant scallop histone H2A-derived AMP demonstrated 2.5 times more antibacterial activity against Gram-positive bacteria than that observed against Gram-negative bacteria. Similarly, recombinant H2A proteins or peptides such as *Macrobrachium rosenbergii* H2A (Arockiaraj et al., 2013) and *Scylla paramamosain* H2A (Chen et al., 2015) exhibited a much better activity towards Gram-positive bacteria. Comparatively lesser degree of activity was observed for r*Mc*-His against the tested Gram-positive bacteria. This possible discrepancy in action may be due to the overall difference in the peptide characteristics, amphipathicity, hydrophobicity and the charge (Malmsten et al., 2007; Pasupuleti et al., 2012). Moreover, r*Mc*-His significantly reduced the growth of the bacteria in a manner that depended on the dose of the protein. Additionally, no remarkable difference in the antibacterial activity against Gram-positive bacteria than Gram-negative bacteria was observed for parasin I and hipposin (Park et al., 1998; Birkemo et al., 2003). In contrast, incubation of the bacteria with the control peptide rTrx had no apparent effect on bacteria, suggesting that the observed bactericidal effects were specific to r*Mc*-His. Importantly, r*Mc*-His was

also found to be non-lytic for human erythrocytes and non-cytotoxic to NCI-H460 cancer cell lines at the concentrations tested. Hence, this antimicrobial peptide could exert its biological effects more specific to bacteria without damaging the host tissues. All these characteristics indicated that the *Mc*-His, like other N-terminal fragment of histone H2A, was a potential AMP in flat head grey mullet.

Based on the sequence and structure analysis, it was found that *Mc*-His was a cationic antimicrobial peptide which forms an amphipathic α-helical structure. AMP's mode of action is still a matter of debate, yet membrane disruption and subsequent bioenergetic collapse of the cell being the most convincing mode of action for AMPs (Yount et al., 2006). Previous studies reveal that antimicrobial mechanism of histone derived AMPs involve not only targeting the membranes but also secondary effects such as interactions with nucleic acids (Koo et al., 2008; Sathyan et al., 2012a; Fischer, 2013; Bustillo et al., 2014). Since *Mc*-His shared striking similarity with 51-mer hipposin identified from Atlantic halibut, *Hippoglossus hippoglossus*, both in its sequence and structure, it was intriguing to know whether *Mc*-His act in a similar way to hipposin. Bustillo et al. in 2014 have proved that hipposin kills bacteria by inducing membrane permeabilization, and this membrane permeabilization is promoted by the presence of the N-terminal parasin domain. The entire hipposin sequence incorporates sequences of parasin and buforin II. These peptides operate *via,* different antimicrobial mechanisms as parasin causes membrane permeabilization while buforin II translocate into bacteria and interact with the intracellular nucleic acids. Portions of hipposin lacking the parasin sequence do not cause membrane permeabilization and

function more similar to buforin II by entering cells without causing significant membrane disruption. As expected, mechanism of antibacterial action of *Mc*-His was also found to occur through membrane permeabilization. The results of the cAMP algorithm calculator as well as AGGRESCAN and transmembrane prediction results were concurrent with this finding. Electron microscopy analysis of r*Mc*-His treated bacteria, paired with PI uptake results further affirmed the membrane-breaking effects of r*Mc*-His. Similar type of morphological effects were also previously reported by Richards et al. (2001) in H1-SAM treated *E. coli*, by De Zoysa et al. (2009) in H2A-Abhisin treated *P. ovale* and by Chen et al. (2015) in H2A-Sphistin treated *S. aureus, E.coli* and *P. pastoris*.

In conclusion, a 52-amino acid AMP designated as *Mc*-His from the N-terminus of *M. cephalus* histone H2A sequence was identified and characterised. *Mc*-His clearly displayed all characteristic features of AMP including net positive charges and higher hydrophobic residues similar to vertebrate and invertebrate histone H2A derived AMPs. *Mc*-His forms an amphipathic α-helical structure with no cysteine residue. Recombinant expression of *Mc*-His was performed in *E. coli* Rosetta-gami$^{TM}$ B (DE3) pLysS. The recombinant *Mc*-His exhibited strong bactericidal activity against tested Gram-negative bacteria and less cytotoxicity towards hRBCs. The antimicrobial mechanism of *Mc*-His was likely due to membrane permeabilisation. *Mc*-His therefore could be considered as a potent therapeutic agent for use in aquaculture taking into account its potent antimicrobial activity and less cytotoxicity.

Chapter 4

# MOLECULAR CHARACTERIZATION AND FUNCTIONAL ANALYSIS OF HISTONE H2A DERIVED SYNTHETIC PEPTIDE OF *ETROPLUS MACULATUS*

Contents

4.1 Introduction
4.2 Materials and methods
4.3 Results
4.4 Discussion

## 4.1 Introduction

The vertebrate immune system encompasses numerous distinctive and interdependent components having its own inherent protective value. The teleost skin in particular, is unique and histologically diverse. The surface of fish gill, skin and gastrointestinal tract with mucus acts as a thin physical barrier between the external environment and the internal milieu that are vulnerable to microbial attack (Iger and Abraham, 1990; Shephard, 1994). The skin mucus has robust mechanisms that can entrap and immobilize bacteria and viruses before they can gain access to the epithelial surfaces, and remove them with the water current (Mayer, 2003). It is well known that the aquatic environment is microbe laden. Therefore, the epidermal mucus layer of fish is enriched with several antimicrobial agents that provide the first line of defence against invading

pathogens preventing the stable colonisation of infectious microbes (Shephard, 1994). These include certain non-specific humoral innate immune components like antimicrobial peptides (AMPs). AMPs are generally small peptides (< 50 amino acids) containing a positive charge and an amphipathic structure. They symbolise molecules that are retained by organisms throughout the course of evolution as a part of defence mechanism against the microbial enemies. Antimicrobial property of epidermal mucus against various infectious pathogens has been demonstrated in several fish species (Ellis, 2001; Nagashima et al., 2003; Chinchar et al., 2004; Kuppulakshmi et al., 2008; Wei et al., 2010; Su, 2011). Over the past two decades, many investigators have attempted to isolate AMPs and the genes encoding their precursors from the skin extracts or secretions of various animals. Among the major families of fish AMPs, histone derived AMPs (HDAPs) and pleurocidins form the two main groups that are reported from the fish mucus (Birkemo et al., 2003; Douglas et al., 2003).

Traditionally, histone proteins are known to be involved in the packaging of DNA, essentially serving to wind up the long DNA strands in a spool-like manner. The role of histones in chromatin structure formation, nuclear targeting, and the regulation of gene expression have been well identified. It is assumed that the antimicrobial property of histones have evolved as an ancient innate defence component against pathogenic organisms that may have been co-opted from its structural role as components of the chromatin structure of eukaryotic organisms (Kawasaki and Iwamuro, 2008; Smith et al., 2010). These conspicuous proteins of chromatin are encoded by multigene families that occur in

clusters (Marzluff et al., 2002; Albig et al., 2003), allowing differential expression of selected genes for histones subtypes (Alami et al., 2003). There are several types of histones of which H2A, H2B, H3 and H4 are the core histones that form the nucleosome, and H1 and H5 are the linker histones. The AMPs rich in proline, tryptophan, arginine, lysine, or histidine, are indeed mimics of nuclear cationic histones that are able to interact with negatively charged microbial membrane to disrupt the bilayer curvature, beyond a threshold concentration of membrane bound peptide (Ginsburg et al., 2017). In fact, these cationic agents can be considered as evolutionarily ancient weapons against microbial infections. They also play a vital role in innate immunity of the host and characterize themselves as agents for specific uses because of their natural antimicrobial properties and a low propensity for the development of bacterial resistance.

Their role in host defence is revealed by the upregulation of various histone genes in response to pathogenic challenge in vertebrates and invertebrates. In most cases, this upregulation was found to be linked with the antimicrobial activity of histones seen associated with the host. A significant upregulation of linker histone-like protein (H1M) was observed when zebrafish skin was exposed to bacterium *Citrobacter freundi* (Lu et al., 2012). Also, rhesus macaque monkey kidney epithelial cells exposed to monkey pox virus, showed a steep upregulation of histone genes (Alkhalil et al., 2010). These patterns of differential expression of histones in response to immune challenge support its possible role in innate immunity. Besides, histones also play a role in the immune system when the organisms are exposed to abiotic stress or pollution (Robinette and Noga, 2001). Histones genes were found to be

upregulated in rapidly growing oyster larvae (Meyer and Manahan, 2010) and in oyster adults and larvae in response to many different environmental stressors (Chapman et al., 2011; Zhang et al., 2012). Also a similar kind of histone gene upregulation was found in mussels maintained along a copper pollution gradient (Dondero et al., 2006). Moreover, further studies showed that the expression of several histone-derived AMP genes were induced under conditions of stress in specific tissues of different fish species (Robinette et al., 1998; Terova et al., 2011).

Histones could have multiple mechanisms of action in both vertebrates and invertebrates. The modus operandi of histones in immunity appears to involve mechanisms that facilitate direct contact of concentrated histones with pathogens, such as the release of extracellular traps (ETs) as shown in many vertebrates and a few invertebrates (Brinkman et al., 2004; Brinkman and Zychlinsky 2007; Altincicek et al., 2008; Ng et al., 2013). Extracellular traps are a part of innate immune response first described in vertebrate neutrophils. In the course of neutrophil cell death, by a process named as NETosis, the intracellular organelle membranes disintegrate leading to the formation of a complex, composed of nuclear and cytoplasmic components (Fuchs et al., 2007; Metzler et al., 2011; Mesa and Vasquez, 2013). The extracellular complex, function through the release of granular proteins (such as elastase and myeloperoxidase) and chromatin (DNA and histones) forming extracellular fibres that trap and kill both Gram-negative and Gram-positive bacteria, yeast, and parasites (Brinkmann et al., 2004; Urban et al., 2006; Brinkmann and Zychlinsky, 2007; Guimaraes-Costa et al., 2009; Urban et al., 2009; Brinkmann and Zychlinsky, 2012;

Saffarzadeh et al., 2012). Formation of extracellular traps has also been reported in a few invertebrate species, including the greater wax moth *Galleria mellonella* (Altincicek et al., 2008), marine crabs (Smith et al., 2010), and the Pacific white shrimp (Ng et al., 2013). Another potential role of histones in immunity has recently been described in the fruit fly, *Drosophila melanogaster* and the nematode, *Caenorhabditis elegans.* Histones bound to fat storage organelles, the lipid droplets, in the cytosol of cells are released upon immunological stimulii, killing bacteria (Anand et al., 2012). In case of invertebrate model nematode, *Caenorhabditis elegans*, a variant of linker histone H1 (HIS-24) interacts with heterochromatin protein-1 regulating the transcription of many immune-related genes (Studencka et al., 2012).

Histones and histone-derived fragments are alkaline peptides rich in lysine or arginine residues, possessing broad-spectrum antimicrobial activity. Histones from shrimp (Patat et al., 2004), fish (Robinette et al., 1998; Richards et al., 2001; Fernandes et al., 2002; Bergsson et al., 2005; Noga et al., 2011), frog (Kawasaki et al., 2003), chicken (Silphaduang et al., 2006; Li et al., 2007) and mammals (Hiemstra et al., 1993; Rose et al., 1998; Kim et al., 2002; Howell et al., 2003; Jacobsen et al., 2005) have been identified as antimicrobial agents. Among the five groups of nuclear proteins, H1, H2A and H2B constitute the lysine-rich histones and H3 and H4 form the arginine-rich histones. Schmidt et al. (2010) have demonstrated that increasing the arginine composition of these peptides enhances their activity regardless of their mechanism. Further, these results provide support for the general strategy of enhancing the membrane activity of AMPs through increased arginine content.

Histones account for a large proportion of the antibacterial activity of skin exudates from amphibians (Park et al., 1996) and teleost fish (Park et al., 1998; Robinette et al., 1998; Patrzykat et al., 2001; Richards et al., 2001). The activity spectrum is not only limited to bacteria but also displayed against several protozoan fish pathogens, including water molds (*Saprolegnia* sp.) and the dinoflagellate, *Amyloodinium ocellatum* (Noga et al., 2011). Histone derived peptides with antimicrobial activity are derived from the proteolytic digestion of intact histones. In addition to intact histones, histone-derived AMPs with potent antimicrobial activity also have been isolated. Toad H2A fragments, buforins I and II, which have high degrees of structural similarity to histone H2A, were isolated from the stomach extract of the Korean frog *Bufo bufo gargarizans* (Park et al., 1996). Hipposin I and parasin I are also fragmented histone H2A peptides isolated from the skin mucus secretions of Atlantic halibut and channel catfish, respectively (Park et al., 1998; Birkemo et al., 2001). In addition, an N-terminal histone H1 peptide fragment with broad-spectrum antimicrobial properties was found in the skin mucus of the Atlantic salmon (*Salmo salar*) (Luders et al., 2005). Similarly, oncorhyncin II, a 69- amino acid C-terminal fragment of histone H1, was isolated from rainbow trout, *Oncorhynchus mykiss* skin secretions (Fernandes et al., 2004). The epithelial surface of fish is constantly at the risk of abrasion and sloughing, hence damage to the cells from similar minor injuries might permit histones and other intracellular antibacterial proteins to become exposed to potential invaders from the surrounding water. Histones as well as their fragments, in combination with other molecules released into the haemocytes, would then be able to exert

their antimicrobial and LPS-binding activities against extracellular pathogens. Moreover, based on their ability to bind DNA and LPS, histones may also be present on the surface of haemocytes, serving as receptors for Pathogen Associated Molecular Patterns (PAMPs). Thus, AMPs such as histones provide a powerful defence system that can protect the mucosal surfaces from infection and signal host cells to change their behaviour in response to external injury. The development of antibiotic resistance by bacterial pathogens provides an impetus for further attempts to search for new antimicrobial agents which combat infections and overcome the problems of resistance with no side effects.

*Etroplus maculatus* popularly known as the Orange chromide, is one among the three Cichlid species that is well known for its parenting behaviour. The species is euryhaline and mostly inhabits brackish estuaries, coastal lagoons and the lower reaches of rivers and is a native of South India and Sri Lanka. *E. maculatus* is a small sized fish in the genus with long spinous anal fin and black spots in the body. The members of the species are normally found to co-occur with the Green chromide (*E. suratensis*). The species is usually utilized for consumption in many parts of its range and also finds good market demand as an ornamental fish. Hence, better understanding of the immune parameters of *E. maculatus* may definitely help to improve its health and survival in artificial environment. There are relatively no reports of AMPs identified from the Orange chromide, *E. maculatus*. The present study deals with the molecular characterisation of histone derived AMPs from *E. maculatus* and its functional characterization using the synthetic peptide corresponding to the buforin II sequence.

## 4.2 Materials and Methods

### 4.2.1 Experimental organism

Experimental organism used in the present study is Orange chromide, *Etroplus maculatus* belonging to the order Perciformes, family Cichlidae and subfamily Etroplinae. Live and healthy specimens of *E. maculatus* were collected from Cochin estuary, Kerala. Samples were brought to the laboratory in live condition by providing aeration.

**Fig. 4.1** Experimental organism used for the study Orange chromide, *Etroplus maculatus*.

### 4.2.2 Precautions for RNA preparation

Tissue collection for total RNA isolation and the sample processing were done with necessary cautionary measures. Basic precautions taken during and before RNA isolation have been explained in section 2.2.2 of Chapter 2.

### 4.2.3 Processing of the tissue

Live samples of the specimen were washed with DEPC treated water to remove the extraneous dirt and other glutinous organic matter.

Blood was collected from the lamellar artery near gill region of the fish using 5 mL syringes (RNase free) rinsed in precooled anticoagulant solution (RNase free 10 % sodium citrate, pH 7). The tissue samples were taken after the fish was killed humanely.

Tissue samples such as gills, liver, kidney, muscle, intestine and kidney were dissected out and transferred to TRI™ reagent (Sigma). The samples were homogenised in TRI™ reagent and stored at -20° C until processed.

### 4.2.4 Total RNA isolation

The total RNA was isolated from *E. maculatus* haemocytes using TRI reagent (Sigma) as per manufacturer's instructions, as explained in section 2.2.5 of Chapter 2. The RNA pellet thus obtained was dissolved by adding 30 µl of DEPC treated RNase free water. Finally, for complete dissolution of RNA, the pellet was incubated at 55 °C for 5 min.

### 4.2.5 Quality assessment and quantification of RNA

Quality of total RNA was analysed by agarose gel electrophoresis and quantified using UV-Vis spectroscopy as described in section 2.2.5 of Chapter 2.

### 4.2.6 cDNA synthesis

Single stranded cDNA was synthesised from total RNA by reverse transcription using specific oligo d($T_{20}$) primers as explained previously in section 2.2.6 of Chapter 2.

### 4.2.7 PCR amplification

The reverse transcription reaction was confirmed with a PCR with house-keeping gene, β-actin primers using cDNA as the template. Confirmation of the PCR with the control gene was followed by PCR amplification of Histone Derived Antimicrobial Peptide (HDAP) gene from the cDNA of *E. maculatus* using gene specific primers (Table 4.2) (Birkemo et al., 2003). The PCR conditions employed were as follows: 95 °C for 2 min, 35 cycles of 94 °C for 15 s, 60 °C for 30 s and 72 °C for 30 s. The final extension was carried out at 72 °C for 10 min.

**Table 4.1** Primer sequence and details of primer used in the present chapter.

| Target gene | Sequence (5'-3') | Product size (bp) | Annealing Temp. (°C) |
|---|---|---|---|
| **Histone** | F: atgtccggrmgmggsaarac | 250 | 60 |
| | R: gggatgatgcgmgtcttcttgtt | | |
| **β-actin** | F: gatcatgttcgagaccttcaacac | 400 | 60 |
| | R: cgatggtgatgacctgtccgtc | | |
| **T7** | F: tgtaatacgactcactataggg | _ _ | 57 |
| **SP6** | R: gatttaggtgacactatag | _ _ | 57 |

### 4.2.8 Agarose gel electrophoresis

The PCR products obtained were analysed in 1.5 % agarose gel. Electrophoresis was performed as described in section 2.2.8 of Chapter 2.

### 4.2.9 TA cloning of amplicons and sequencing

The PCR amplicons obtained were cloned onto the pGEM-T Easy cloning vector as described in section 2.2.9 of Chapter 2. The recombinant

plasmids were isolated and sequenced as described in the section 2.2.9.5 and 2.2.10 of Chapter 2.

### 4.2.10 Sequence characterization and phylogenetic analysis

The nucleotide sequence obtained and the deduced amino acid sequence were analysed by various biological computational tools as described in section 2.2.11 of Chapter 2. Phylogenetic analysis was done with nucleotide sequences of selected Histone H2A genes retrieved from GenBank. The phylogenetic tree was constructed using the neighbour-joining method, and the topological stability of the neighbor-joining (NJ) trees was tested using bootstrap resampling (with 1000 replicates).

### 4.2.11 Peptide synthesis

Based on multiple sequence alignment of *E. maculatus* HDAP with other reported potent HDAPs and sequence conservation in most species, sequence showing homology with Buforin II was selected to investigate the biological activity of the peptide. Physicochemical characteristics of the synthetic peptide were also studied using various computational tools as explained in the section 2.2.11. The peptide was synthesized as a linear peptide with end modifications (N-terminal acetylation and C-terminal amidation). Chemical synthesis of peptide with FITC labelling was carried out at M/s Zhejiang Ontores Biotechnologies Co., Ltd China by solid phase procedure of Fmoc (*N*-(9-fluorenyl) methoxycarbonyl) chemistry with >95 % final purity.

### 4.2.12 Mass spectrometry analysis of the synthetic peptide

Verification of the molecular mass and quality of the synthetic peptide was done by mass spectrometry at M/s Zhejiang Ontores Biotechnologies Co., Ltd, China. The MS analysis was performed with a Thermo Finnigan LCQ Duo mass spectrometer equipped with an electrospray source and Xcaliber software. Synthetic peptide was reconstituted in 50 % 0.1 % acetonitrile (v/v) and 50 % 0.1 % trifluoracetate (v/v) and analyzed using Electrospray Ionization (ESI) probe. The nebulizer gas flow was maintained at 1.5 l/min. Ions were detected and analyzed in the positive mode on the basis of their m/z ratio.

### 4.2.13 Purity determination of synthetic peptide using HPLC

The purity of the synthetic peptide was determined using analytical reverse-phase HPLC at Zhejiang Ontores Biotechnologies Co., Ltd, China. Synthetic peptide was dissolved in 50 µl of 0.1 % trifluoroacetic acid (TFA) in water and 10 µl of the sample was injected to the Welchrom $C_{18}$ column of dimensions 4.6 mm × 250 mm. Solvent system comprised of Solvent A (0.1 % TFA in 100 % $H_2O$) and Solvent B (0.1 % TFA in 100 % acetonitrile). Purification was performed with a linear gradient of 0.1% (v/v) TFA/acetonitrile, increasing from 25 % to 45 % in 20 min. Flow rate was adjusted and maintained at 1 ml/min throughout the purification and eluents were monitored by UV absorbance at 220 nm.

### 4.2.14 Haemolytic activity

Haemolytic activity of the synthetic peptide was analysed using human RBCs. Haemolytic activity of the peptide was tested for eight different concentrations, ranging from 400 µM to 3.125 µM and the activity was expressed as percentage haemolysis, calculated as described in the section 2.2.28 of Chapter 2.

### 4.2.15 Antimicrobial activity

Antimicrobial activity of the synthetic peptide was determined by broth microdilution assay against eleven different bacterial strains. Minimum Inhibitory Concentration (MIC) of the synthetic peptide was analysed from six dilutions of the peptide ranging from 50 µM to 1.625 µM. Further, bactericidal activity of the peptide was confirmed by plating the pathogens after 12 h incubation with the peptide. To know the mechanism of action of the peptide, microscopic observation of peptide treated pathogens were done using PI staining by Epi-fluorescence Microscopy and by SEM as described in section 2.2.30.3 and 2.2.30.4 of Chapter 2. The protocol employed for all the aforementioned experiments are explained in the section 2.2.30 of Chapter 2.

### 4.2.16 DNA binding assay

The DNA binding activity of the synthetic peptide was examined by a gel retardation assay with slight modifications as described by Park et al. (1998). Briefly, 50 ng of pUC-18 plasmid DNA was incubated with increasing concentrations of peptide with a peptide to DNA ratio of 0:1,

2.5:1, 5:1, 10:1, 20:1 and 50:1 in 20 µl of binding buffer (5 % glycerol, 10 mM Tris–HCl (pH 8.0), 1 mM EDTA, 1 mM DTT, 20 mM KCl and 50 µg/ml BSA) for 1h at room temperature. The DNA bands were then analyzed in a 1.5 % agarose gel stained with ethidium bromide and visualized under UV light.

### 4.2.17 Anticancer activity

#### 4.2.17.1 *In vitro* cytotoxicity assay

Human non-small cell lung carcinoma cell lines, NCI-H460 and human laryngeal carcinoma derived human epithelial type 2 cell lines, HEp-2 purchased from NCCS, Pune were used for the *in vitro* toxicity studies. The cells were maintained in DMEM/F-12 supplemented with 10 % fetal bovine serum (FBS), penicillin and streptomycin in a humidified atmosphere containing 5 % $CO_2$ at 37 °C.

Cell viability was determined using XTT assay for both the cell lines as described earlier in the section 2.2.29 of Chapter 2. Cells were treated with eight different concentrations of synthetic peptide (ranging from 200 µM to 1.625 µM). The experiments were performed in triplicate. The results are expressed as a percentage of inhibition rates for the viable cells. Synthetic mellitin with FITC tag was used as the positive control. $IC_{50}$ values of the synthetic peptide for each cell line were evaluated individually. $IC_{50}$ value was calculated by probit analysis using SPSS 21.0 software.

#### 4.2.17.2 Gene expression analysis using real-time reverse-transcription polymerase chain reaction (RT-PCR)

To analyse the anticancer activity of the synthetic peptide, NCI-H460 and HEp2 cell lines incubated in DMEM supplemented with 10 % FBS and antibiotics (1 % penicillin-streptomycin) were treated with 25 µM and 100 µM of the peptide for 24 h. Cells incubated without peptide was treated as the control. Total RNA was isolated from cells of both treated and untreated group using TRI reagent (Sigma) according to manufacturer's recommendations as explained in section 2.2.4 of Chapter 2. Amplification of actin mRNA was performed to confirm the steady state level of expression of a house keeping gene and to provide an internal control for the real time gene expression analyses.

Single stranded cDNA was synthesised from 0.5 µg total RNA as described in the section 2.2.6 of Chapter 2. Amplification of GAPDH was performed to confirm the steady-state level of expression of a housekeeping gene and to provide an internal control for the gene expression analysis (Table 4.2). A real-time PCR was used to determine the effect of peptide on cell function by analysing the gene expression pattern of twenty three different genes namely Bcl-2, Bax, Caspase-3, Caspase-9, Cathepsin-G, Calpain-5, Rb1, p-53, Akt1, MAPK-1, JNK, IL-1β, IL-2, IL-6, IL-10, IL-12, IFN-β, IFN-γ, TNF-α, viperin, MX1, ISG15 and IFITM3 in NCI-H460 and HEp2 cell lines following treatment with and without the peptide. Specific primer pairs were used for the selected genes listed above, while primer pair of GAPDH was used for the

reference gene. The nucleotide sequences of the primers used are listed in (Table 4.2).

The relative quantification of the genes in the treated and the untreated group were detected by Quantitative Real time PCR (qRT-PCR) using SYBR® Green PCR master mix (ABI, USA) and the StepOnePlus real-time PCR system (Applied Biosystems). The qRT-PCR was performed in 10 µl reaction volume, containing 3 µl diluted 0.5 µg of cDNA, 5 µl SYBR mix, 0.4 µl of each primer (10 pmol/µl), and 1.2 µl PCR-grade water. The cycling conditions applied were 50 °C for 2 min and 95 °C for 10 min, followed by 40 cycles at 95 °C for 15 s and 60 °C for 1 min. The threshold cycle number ($C_T$) was calculated with ABI software. The expression levels of the transcripts at each context were determined by the $\Delta\Delta C_T$ method (Livak and Schmittgen, 2001) with GAPDH as the reference gene amplified from the same samples. $\Delta C_T$ is expressed as the difference in the threshold cycles of mRNA for selected genes relative to those of GAPDH mRNA; i.e., $\Delta C_T = C_T$ (target gene) - $C_T$ (GAPDH). Relative expression levels of the target genes were determined by the following formula $\Delta\Delta C_T = \Delta C_T$ (treated) - $\Delta C_T$ (control). The real-time RT-PCR was performed in triplicate for each experimental group. Normalized fold difference in gene expression pattern is presented graphically to compare the level of transcription.

**Table 4.2** List of primers of the various genes used for real time qPCR analysis

| Sl. No. | Primer Name | Sequence (5'-3') |
|---|---|---|
| 1 | GAPDH – F | CGGAGTCAACGGATTTGGTC |
| | GAPDH – R | AGCCTTCTCCATGGTCGTGA |
| 2 | Bcl2 – F | ACCTGCACACCTGGATCCA |
| | Bcl2 – R | AGAGACAGCCAGGAGAAATCAAA |
| 3 | Bax – F | AAGCTGAGCGAGTGTCTCCGGCG |
| | Bax – R | CAGATGCCGGTTCAGGTACTCAGTC |
| 4 | Caspase 3 – F | ATACCAGTGGAGGCCGACTTC |
| | Caspase 3 – R | CAAAGCGACTGGATGAACCA |
| 5 | Caspase 9 – F | TGTCCTACTCTACTTTCCCAGGTTTT |
| | Caspase 9 – R | GTGAGCCCACTGCTCAAAGAT |
| 6 | Cathepsin G – F | TCAAGTTTCCTGCCCTGGAT |
| | Cathepsin G – R | CCTGTGTCCCCGAGAAGAAG |
| 7 | Calpain 5 – F | CAGGTCCTCTCAGAGGCAGATAC |
| | Calpain 5 – R | ACCTCTCCAGGGACCTTAACG |
| 8 | Rb1 – F | GAACATCGAATCATGGAATCCCT |
| | Rb1 – R | AGAGGACAAGCAGATTCAAGGTGAT |
| 9 | p-53 – F | GGGTTAGTTTACAATCAGCCACATT |
| | p-53 – R | GGGCCTTGAAGTTAGAGAAAATTCA |
| 10 | Akt 1 – F | GCACAAACGAGGGGAGTACAT |
| | Akt 1 – R | CCTCACGTTGGTCCACATC |
| 11 | MAPK – F | CAATGGCGGTGTGGTGTTC |
| | MAPK – R | AGCTCCCTTATGATCTGGTTCC |
| 12 | JNK – F | TGGACTTGGAGGAGAGAACCA |
| | JNK – R | CGACGATGATGATGGATGCT |
| 13 | IL-1β – F | GCAGCCATGGCAGAAGTACCTGA |
| | IL-1β – R | CCAGAGGGCAGAGGTCCAGGTC |
| 14 | IL-2 – F | CTGCTGGATTTACAGATGATTTGA |
| | IL-2 – R | TGGCCTTCTTGGGCATGT |
| 15 | IL-6 – F | CCTGACCCAACCACAAATGC |
| | IL-6 – R | CCTTAAAGCTGCGCAGAATGA |
| 16 | IL-10 – F | CTGGGTTGCCAAGCCTTGT |
| | IL-10 – R | AGTTCACATGCGCCTTGATG |
| 17 | IL-12 – F | CCTGGACCACCTCAGTTTGG |
| | IL-12 – R | ACGGCCCTCAGCAGGTT |
| 18 | IFN-β – F | CTCCTGTTGTGCTTCTCCACT |
| | IFN-β – R | GGCAGTATTCAAGCCTCCCA |
| 19 | IFN-γ – F | CTTTAAAGATGACCAGAGCATCCA |
| | IFN-γ – R | ATCTCGTTTCTTTTTGTTGCTATTGA |
| 20 | TNF-α – F | CCCAGGGACCTCTCTCTAATC |
| | TNF-α – R | ATGGCTACAGGCTTGTCACT |
| 21 | Viperin – F | CGTGAGCATCGTGAGCAATG |
| | Viperin – R | GCTGTCACAGGAGATAGCGA |
| 22 | Mx1 – F | CCAGCTGCTGCATCCCACCC |
| | Mx1 – R | AGGGGCGCACCTTCTCCTCA |
| 23 | ISG15 – F | TGGCGGGCAACGAATT |
| | ISG15 – R | GGGTGATCTGCGCCTTCA |
| 24 | IFITM3 – F | TCCCACGTACTCCAACTTCCA |
| | IFITM3 – R | AGCACCAGAAACACGTGCACT |

## 4.3 Results

In the present study, a histone H2A derived AMP was identified and characterized from the haemocytes of *E. maculatus*.

### 4.3.1 PCR amplification and TA cloning and sequencing

A 243 bp amplicon encoding 81 amino acids was amplified from the cDNA of *E. maculatus via,* RT-PCR (Fig. 4.2). The PCR products were then cloned into pGEM®-T Easy cloning vector and the gene insertion was confirmed using vector-specific and gene specific histone primers by colony PCR. Approximately 384 bp and 243 bp amplicons were obtained with vector and gene specific primers respectively (Fig. 4.3a). The recombinant pGEMT plasmids with the insert H2A gene of *E. maculatus* (Fig. 4.3b), isolated from the positive colonies were sequenced and analysed. The nucleotide and deduced amino acid sequences of *E. maculatus* histone H2A have been submitted to the NCBI GenBank under the accession number **MF966483** (Fig. 4.4).

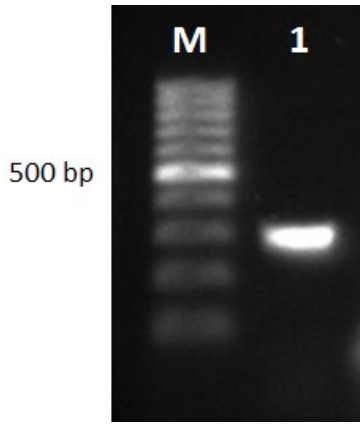


**Fig. 4.2** Agarose gel electrophoretogram of PCR amplification of *E. maculatus* H2A gene. Lane M: 100 bp DNA marker, Lane 1: 243 bp amplicon of *E. maculatus* HDAP gene.

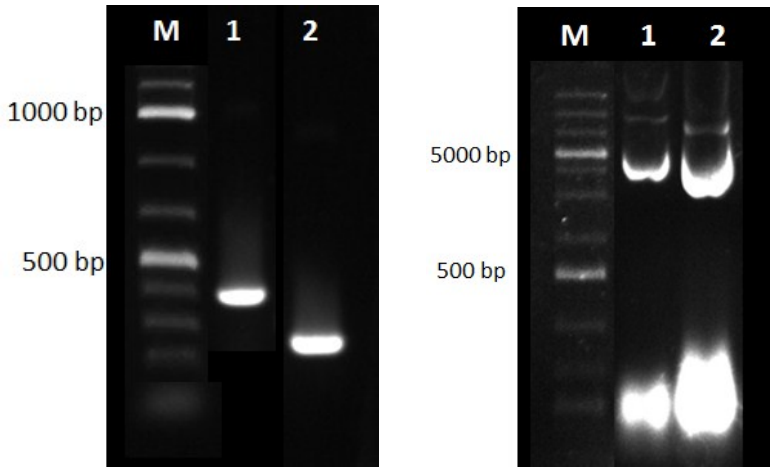


**Fig. 4.3** (a) Colony PCR gel image of gene amplicons obtained from the recombinant pGEMT vector. Lane M: 100 bp DNA ladder, Lane 1: 384 bp amplicon obtained with vector specific primers and Lane 2: 243 bp amplicon obtained using gene specific primers (b) Plasmid extracted from the recombinant clones of pGEMT vector with *E. maculatus* HDAP gene. Lane M: 1 kb DNA marker, Lane 1: pGEMT plasmid with *E. maculatus* H2A gene insert, Lane 2: control pGEMT vector without any insert.

```
atgtccgggcgcggcaagaccggaggcaaagccagagcaaaggctaagactcgctcatcc
 M  S  G  R  G  K  T  G  G  K  A  R  A  K  A  K  T  R  S  S
cgtgccgggcttcagttccccgtgggtcgtgtccacaggctgctgcgcaaaggaaactat
 R  A  G  L  Q  F  P  V  G  R  V  H  R  L  L  R  K  G  N  Y
gcggagcgtgtgggagccggcgcccccgtttacctggcagctgtgctcgagtacctgacc
 A  E  R  V  G  A  G  A  P  V  Y  L  A  A  V  L  E  Y  L  T
gctgagatcctggagttggctggaaacgctgcccgtgacaacaagaagacgcgcatcatc
 A  E  I  L  E  L  A  G  N  A  A  R  D  N  K  K  T  R  I  I
cct
 P
```

**Fig. 4.4** Nucleotide and deduced amino acid sequence of the HDAP from the haemocyte mRNA transcripts of *E. maculatus* (GenBank ID: **MF966483**). The nucleotide sequences are showed in green colour and the amino acid sequences are highlighted in both yellow and grey colour. The region highlighted in yellow represents the biologically active peptide region of *E. maculatus* HDAP, *Em*-His1, and the underlined area corresponds to *Em*-His2, the sequence similar to buforin II.

### 4.3.2 *In silico* sequence analysis and characterization

Homology searches using BLAST analysis of the nucleotide and deduced amino acid sequences revealed that the peptide belonged to the vertebrate histone H2A family. BLASTn analysis of the *E. maculatus* histone H2A sequence showed only 96 % similarity with *Oreochromis niloticus* histone H2A mRNA (GenBank ID: XM 019363284), 88 % similarity with *Poecilia mexicana* histone H2A mRNA (GenBank ID: XM 014972148) and 87 % similarity with *Takifugu rubripes* histone H2A mRNA (GenBank ID: XM 003980002). Though the nucleotide sequences exhibited marked differences, the deduced amino acid sequence of *E. maculatus* H2A was found to be similar with the predicted histone H2A like peptides reported from other fishes.

The PeptideCutter tool of ExPASy predicted that the 81-mer histone precursor peptide of *E. maculatus* H2A possessed potential cleavage sites for proteolytic enzymes chymotrypsin, pepsin, proteinase K, and thermolysin at position 52 from the N-terminus of the precursor peptide and for enzymes proteinase-K (between 16 and 17 residue) and trypsin (between 37 and 38 residue) releasing a 52-mer and 21-mer active peptide herein denoted as *Em*-His1 and *Em*-His2 respectively. Regions representing *Em*-His1 and *Em*-His2 are depicted in Fig. 4.4. Since *Em*-His1 shared complete sequence identity with that of *Mugil cephalus* H2A derived peptide, *Mc*-His, and as its molecular characterisation has been dealt in detail in Chapter 3, only peptide characterisation of *Em*-His2 would be discussed further.

Sequence analysis of *Em*-His2 was done using ProtParam tool of ExPASy and APD3 and found to have a predicted molecular weight of 2.435 kDa, net charge of +6 and a theoretical isoelectric point (*p*I) of 12.60 respectively. The dominant amino acids found in *Em*-His2 were Arg (23.8 %) and Leu (14.3 %). Other residues such as Val, Ser, and Gly contributing to 9.5 % each, and Lys, Ala, Pro, Phe, and Thr each contributing to 4.8 % could also be seen. Cationicity of *Em*-His2 was primarily due to the presence of six positive amino acid residues *viz*., Arg (5 Nos) and Lys (1 No.). *In vivo* aggregation propensity determined using AGGRESCAN identified no hotspots of aggregation in *Em*-His2. The estimated half- life of *Em*-His2 was found to be around 7.2 h in mammalian reticulocytes, greater than 20 h in yeast and greater than 10 h in *E. coli in vivo*. The instability index of the active peptide, *Em*-His2 was computed to be 84.20, categorizing the peptide to be a highly unstable one.

The ClustalW multiple sequence alignment (MSA) based on the deduced amino acid sequences of *Em*-His2 with histone H2A family members of vertebrates and invertebrates is represented in (Fig. 4.5a). The results revealed that, even though the length of the amino acids varied from species to species, many conserved residues were observed among the sequences (Fig. 4.5b). *Em*-His2 exhibited exact sequence identity with that of Buforin II. However, the nucleic acids coding for the amino acid sequence were found to be different as evidenced by the MSA of their nucleic acids (Fig. 4.6).

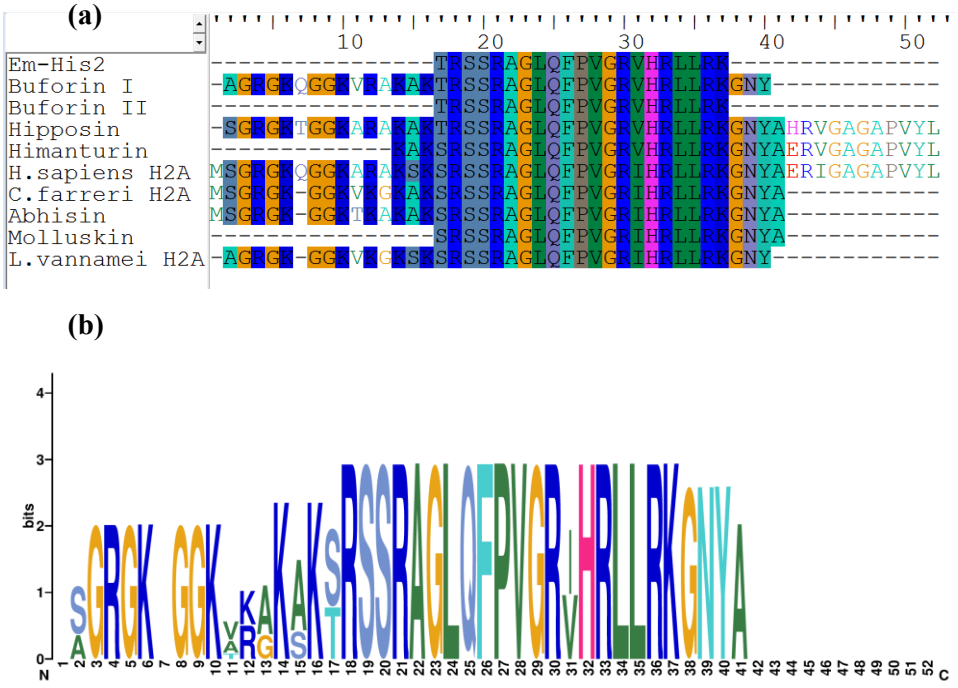


**Fig. 4.5** (a) Multiple sequence alignment of *Em*-His2 (*Etroplus maculatus*) with Buforin I and II (*Bufo bufo gargarizans)*, Hipposin (*Hippoglossus hippoglossus*), Human H2A (*Homo sapiens*) Litopenaeus AMP (*Litopenaeus vannamei*), Scallop AMP (*Chlamys farreri*), Abhisin (*Haliotis discus*), Molluskin (*Crassostrea madrasensis*, *Saccostrea cucullata*, *Meretrix casta*, *Ficus gracilis*, *Bullia vittata*) and Himanturin (*Himantura pastinacoides*) created using BioEdit software (b) The sequence consensus of the ClustalW alignment, obtained with WebLogo is shown in the lower panel.

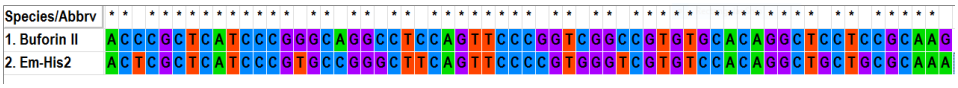


**Fig. 4.6** ClustalW nucleotide sequence alignment of *Em*-His2 with Buforin II. The MSA of both the sequences illustrate a remarkable sequence variation.

The secondary structure analysis of *Em*-His2 by POLYVIEW server showed that the peptide contains 71.43 % α-helical region (15 residues)

and 28.57 % random coiled regions (6 residues) (Fig. 4.7). The coiled regions were found to be constituted by $Thr^{1}$ and $Gly^{7}$- $Pro^{11}$ whereas $Arg^{2}$- $Ala^{6}$ and $Val^{12}$- $Lys^{21}$ encased the helical regions. No β strands or sheets have been noticed in the secondary structure of *Em*-His2.

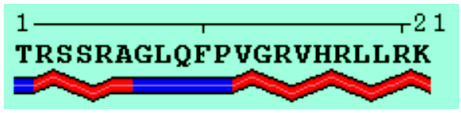


**Fig. 4.7** Secondary structure depiction of *Em*-His2 by POLYVIEW programme. The coiled regions are represented with blue lines and the α-helical regions as zig-zag lines in red.

The *α*-helical structure of *Em*-His2 was further sustained by its three dimensional structure representation. The 3-D structure of *Em*-His2 was constructed based on homology modelling using the crystal structure of human nucleosome core particle (PDB ID: 2cv5) as the template (Fig. 4.8a). The *Em*-His2 sequence shared 95 % sequence identity with the template. The representation clearly revealed the presence of a N-terminal random coiled portion followed by an extended helix region and a regular C-terminal helical region. The perfect amphipathic nature of the peptide was delineated by the helical wheel analysis of *Em*-His2 where the hydrophobic residues and hydrophilic residues faced opposite to each other in the helical wheel (Fig. 4.9). The Kyte-Doolittle plot of *Em*-His2 (Fig. 4.10) further confirmed the amphipathic structure of the peptide with substantial occurrence of hydrophobic amino acids concentrated in the centre of the peptide.

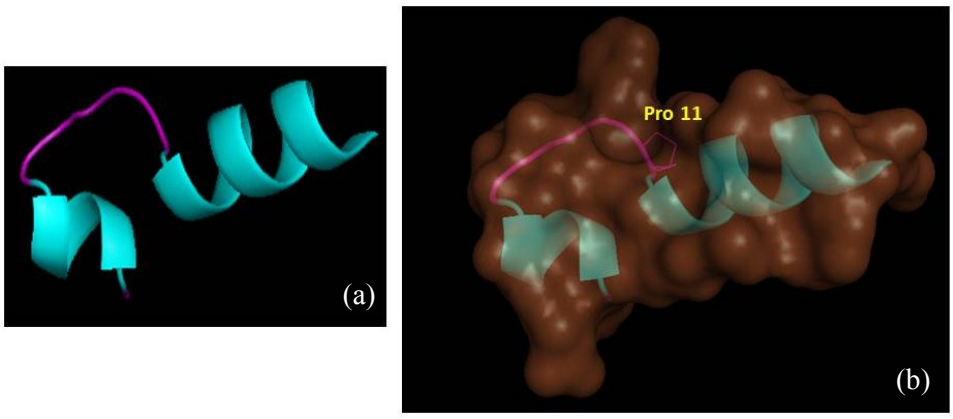


**Fig. 4.8** (a) Predicted 3-dimentional structural arrangement of *Em*-His2 generated using PyMol software using PDB ID: 2cv5 as the template; (b) Spatial structure representation of *Em*-His2. The proline hinge which confers structural flexibility to the peptide is also marked.

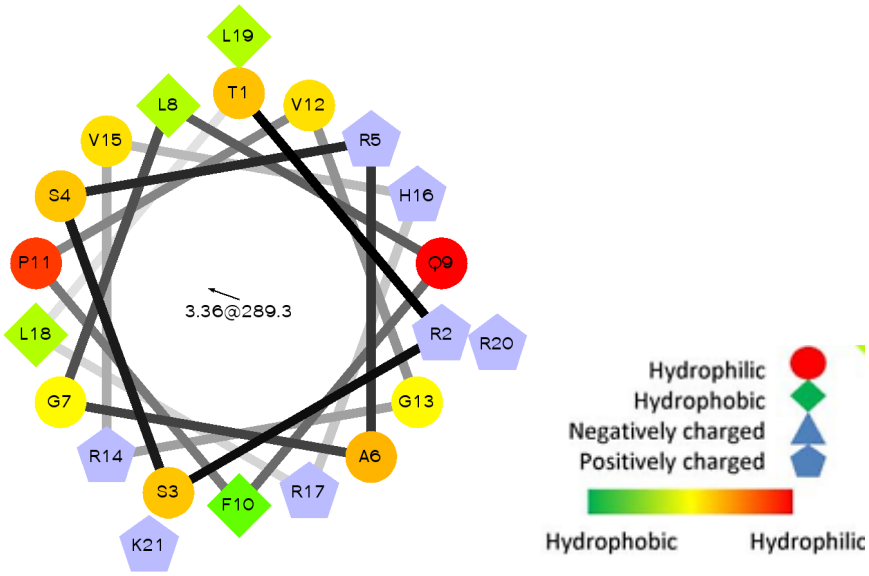


**Fig. 4.9** Helical wheel representation of *Em*-His2. The helical wheel projection demonstrates the clustering of the hydrophobic residues into one side and the cationic residues into the other side of the wheel, indicating the strong amphipathic character of the peptide.

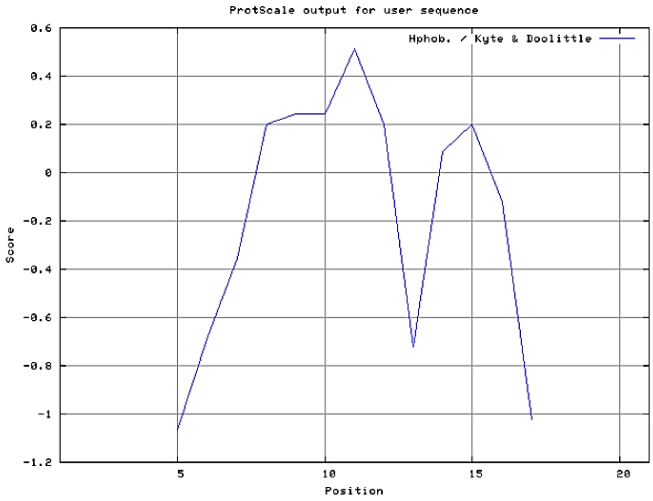


**Fig. 4.10** Kyte-Doolittle plot showing hydrophobicity of *Em*-His2. The peaks above the score (0.0) indicate the hydrophobic nature of *Em*-His2 peptide.

APD predicted the antimicrobial activity of *Em*-His2 with a protein binding potential (boman index) of 3.34 kcal/mol and a total hydrophobicity of 33 %. The predicted RNA fold structure of *Em*-His2 with minimum free energy (MFE) is depicted with double stranded stem as well as looped regions (Fig. 4.11). The predicted RNA structure had an MFE of -17.01 kcal/mol. Additionally, absence of any blue residue indicated the paired nature of *Em*-His2 mRNA.

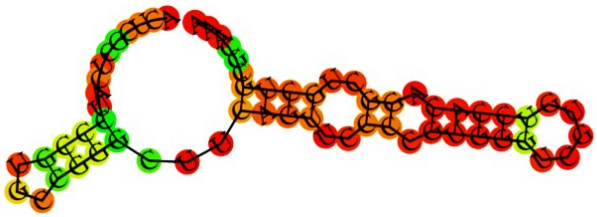

**Fig. 4.11** Predicted mRNA secondary structure of *E. maculatus* histone derived peptide, *Em*-His2 with minimum free energy.

The NJ phylogenetic tree constructed based on the nucleotide sequence of histone H2A of *E. maculatus* formed two separate clades one of higher vertebrates and the other of fishes and frogs, although significant overlap between the two clades could be observed. The *E. maculatus* H2A grouped within the fishes and the amphibian cluster (Fig. 4.12). Based on the phylogenetic analysis, *E. maculatus* H2A was found clustered in the subclade formed by *Poecilia reticulata*, *Takifugu rubripes*, *Oreochromis niloticus*, *Danio rerio*, *Ctenopharyngodon idella* and *Mylopharyngodon piceus*, but was seen more closely related to its ortholog from *Poecilia reticulata*.

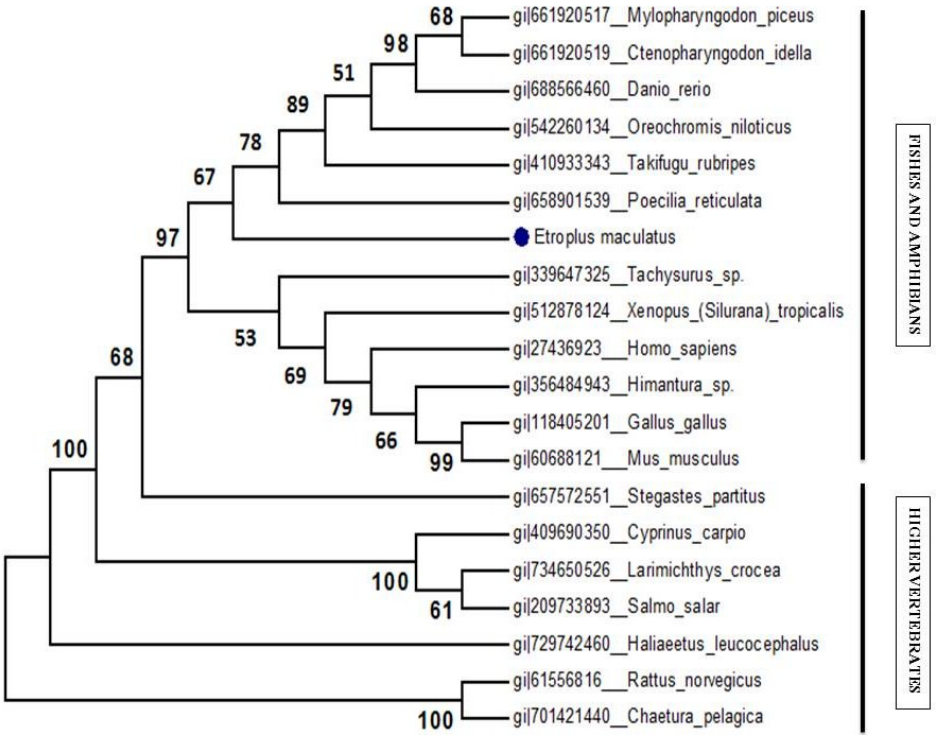


**Fig. 4.12** A bootstrapped neighbor-joining tree obtained using MEGA 6 illustrating the evolutionary relationship between the *E. maculatus* H2A (GenBank ID: **MF966483)** with other members of the vertebrate family.

### 4.3.3 Peptide synthesis and functional characterization of *Em*-His2

This study represents the first report of a histone H2A derived peptide from *E. maculatus.* As a proof of principle, a 21 amino acid length region of the peptide (TRSSRAGLQFPVGRVHRLLRK) sharing similarity to buforin II (histone derived AMP), identified by multiple sequence alignment and homology conservation across various species, was selected for solid phase peptide synthesis. *Em*-His2 is a cationic peptide with a net charge of +6 with a predicted mass 2.435 kDa and *p*I of 12.6. The *Em*-His2 peptide was synthesised as a linear peptide with FITC labelling. The N-terminal residue of *Em*-His2 synthetic peptide was blocked by acetylation, and the C-terminal residue was amidated to increase the peptide stability.

### 4.3.4 Molecular mass determination and purity check of synthetic *Em*-His2

Verification of molecular weight of synthetic peptide *Em*-His2 was done by electrospray ionization mass spectroscopy (ESI-MS). The ESI mass spectrum of *Em*-His2 peptide is shown in Fig. 4.13. The MS data were acquired over an m/z range, 400 to 1700 at a scan time of 5 s. ESI-MS of the purified peptide yielded a major peak with an average isotopic mass of 2865.28 Da. The most abundant ion in the spectrum was observed at a mass to charge ratio of 717.6. This m/z coincides with *Em*-His2 ionized to +4 (rounded off MW = 2865.28 Da + 4H+ = 2869.28). Thus the mass to charge ratio is 2869.28/4 = 717.32. The other relatively abundant ion present in the spectrum was seen at m/z of 956.3 ionized to +3 (rounded off MW = 2865.28 Da + 3H+ = 2868.28) and thus the m/z is 2868.28/3=956.09.

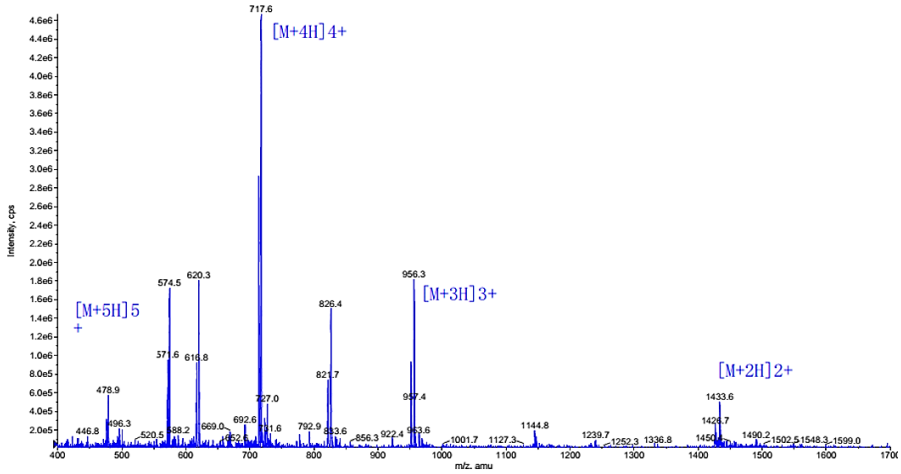


**Fig. 4.13** Electrospray ionization mass spectrum (ESI-MS) of *Em*-His2 shown as a function of abundance over the mass to charge ratio (m/z).

Purity of the synthesised peptide was tested by RP-HPLC. The HPLC chromatogram obtained for synthetic *Em*-His2 is shown in Fig. 4.14. Synthetic *Em*-His2 peptide was purified to about 95 % homogeneity as evidenced by the percent area of the main peak observed at a retention time of 14.234 min as seen in Fig. 4.14.

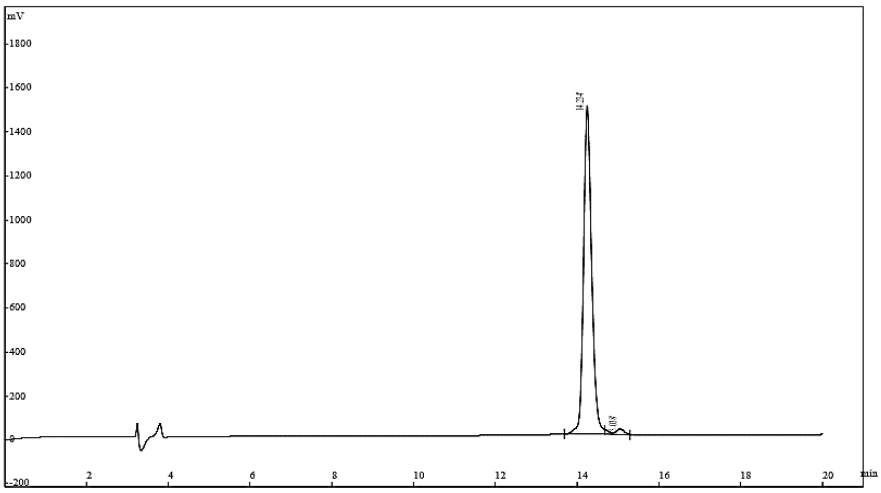


**Fig. 4.14** HPLC chromatogram of synthetic *Em*-His2.

### 4.3.5 Haemolytic activity

Haemolytic activity of synthetic *Em*-His2 peptide was tested against human RBCs at different concentrations. *Em*-His2 exhibited no haemolytic activity against human erythrocytes at concentrations below 100 µM although at higher concentrations it displayed a weak dose-dependent haemolytic activity compared to that of melittin (Fig. 4.15). As shown in Fig. 4.15 only about 14 % of RBCs were lysed even after treatment with 400 µM of *Em*-His2 peptide.

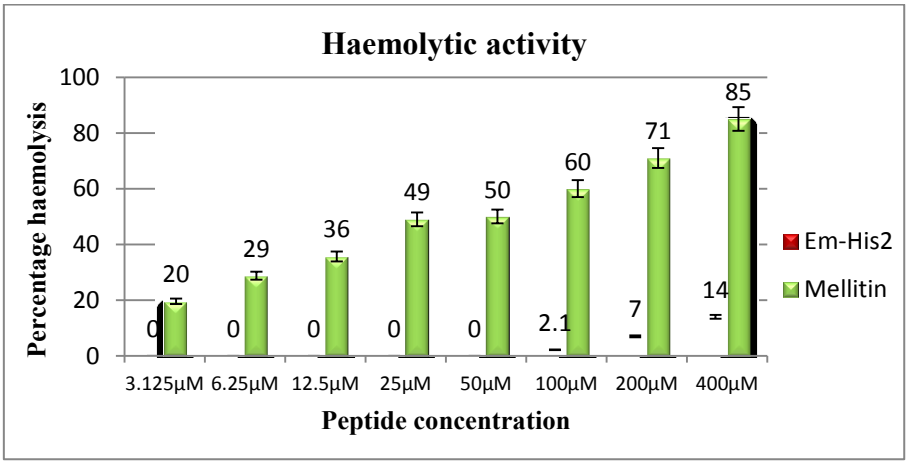


**Fig. 4.15** Haemolytic activity of synthetic *Em*-His2 and mellitin against human RBCs at various concentrations.

### 4.3.6 Antimicrobial activity

Broth microdilution assay was used to determine the antibacterial potency of synthetic *Em*-His2. The antibacterial activity of synthetic *Em*-His2 against all tested bacteria at different concentrations is shown in Fig. 4.16 (a-k). Synthetic *Em*-His2 exhibited strong antibacterial activity against Gram-negative pathogens *P. aeruginosa, E. coli* and *V. parahaemolyticus* with an MIC and MBC of 25 µM each. Although for

*E. tarda* and *V. alginolyticus,* the MIC was found to be 50 µM, their MBC values were found to be greater than the highest tested concentration. Other tested bacteria were found to be sensitive towards *Em*-His2 at varied inhibitory levels. At the highest tested concentration of 50 µM, *Em*-His2 was found to inhibit the proliferation of pathogens namely, *S. aureus* (97 %), *B. cereus* by (96 %), *V. parahaemolyticus* (99 %), *V. cholera* (94 %), *V. alginolyticus* (99 %), *V. proteolyticus* (68 %), *V. vulnificus* (90 %), *E. coli* (99 %), *A. hydrophila* (79 %), *P. aeruginosa* (99 %) and *E. tarda* (99 %).

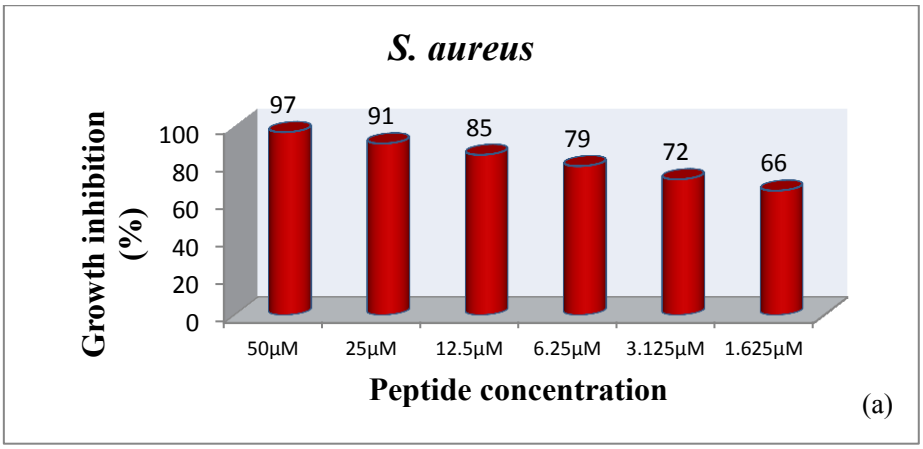


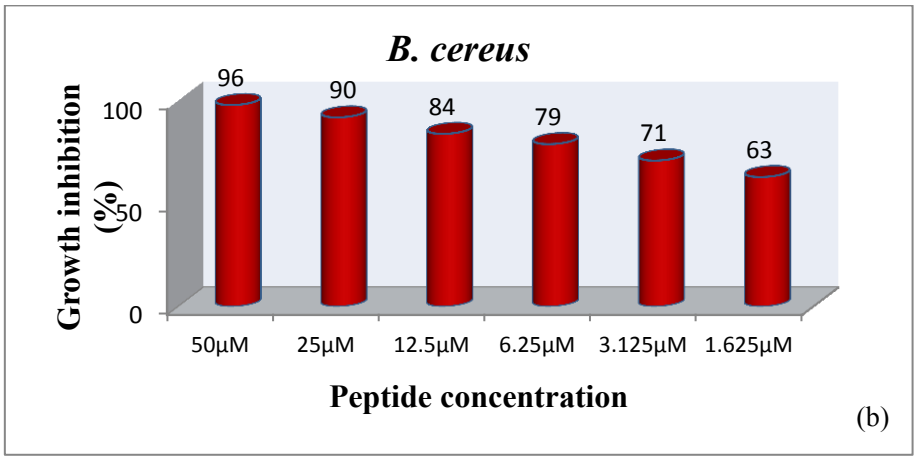


*Fig. 4.16 Continued…*

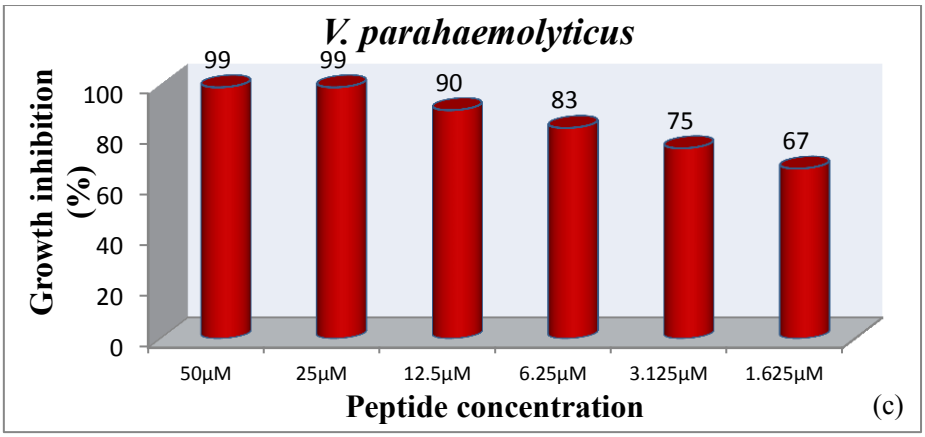


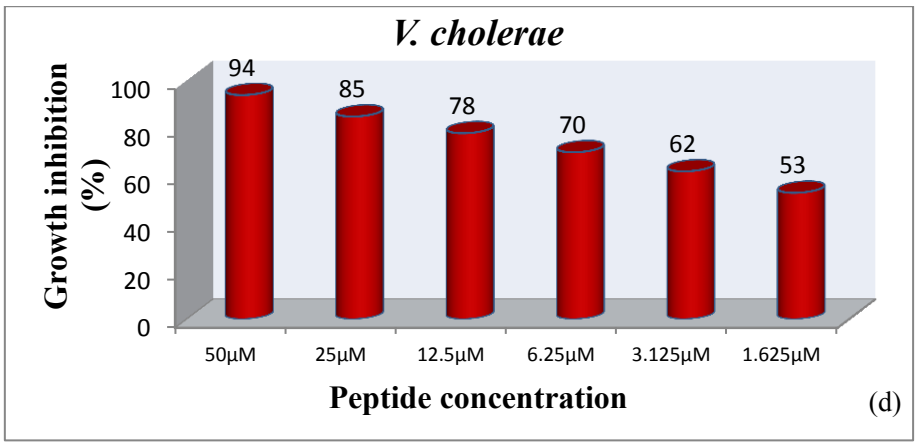


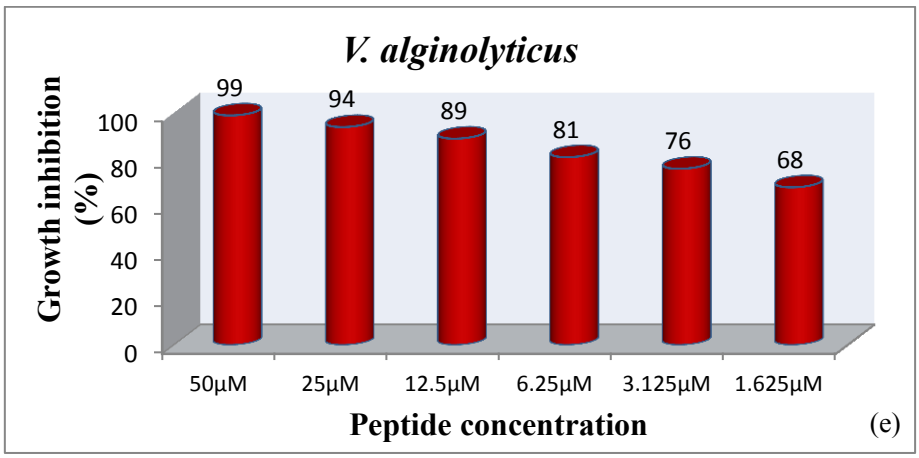


*Fig. 4.16 Continued…*

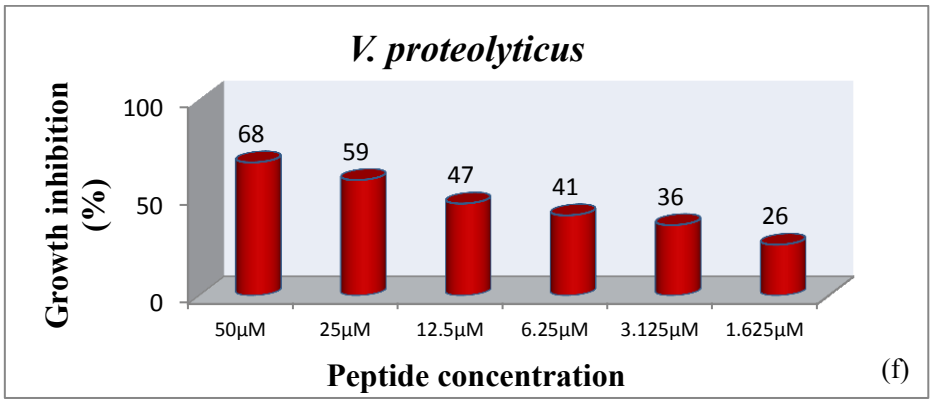


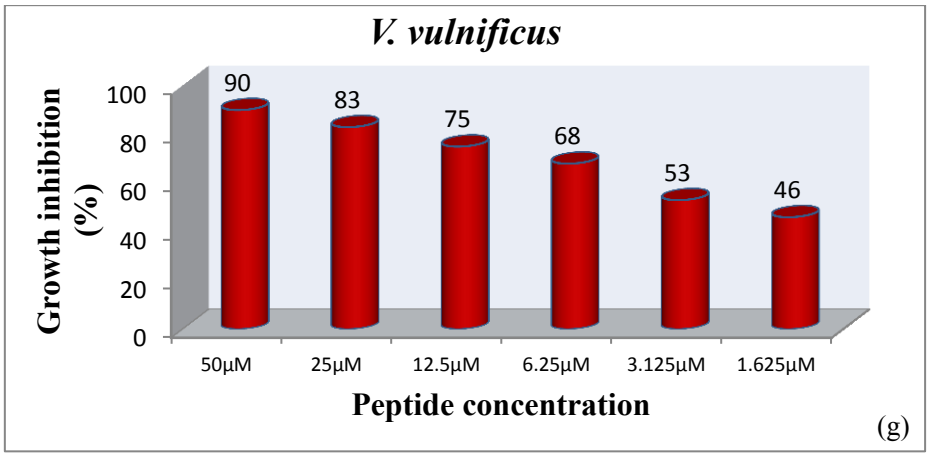


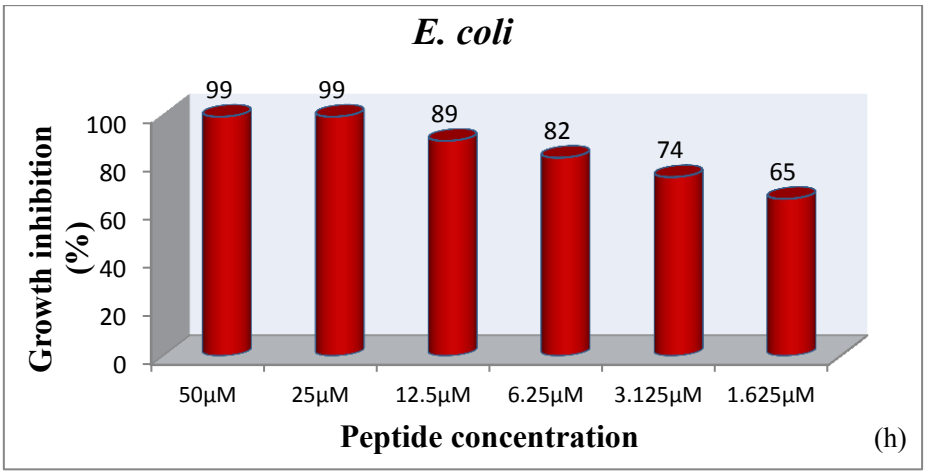


*Fig. 4.16 Continued…*

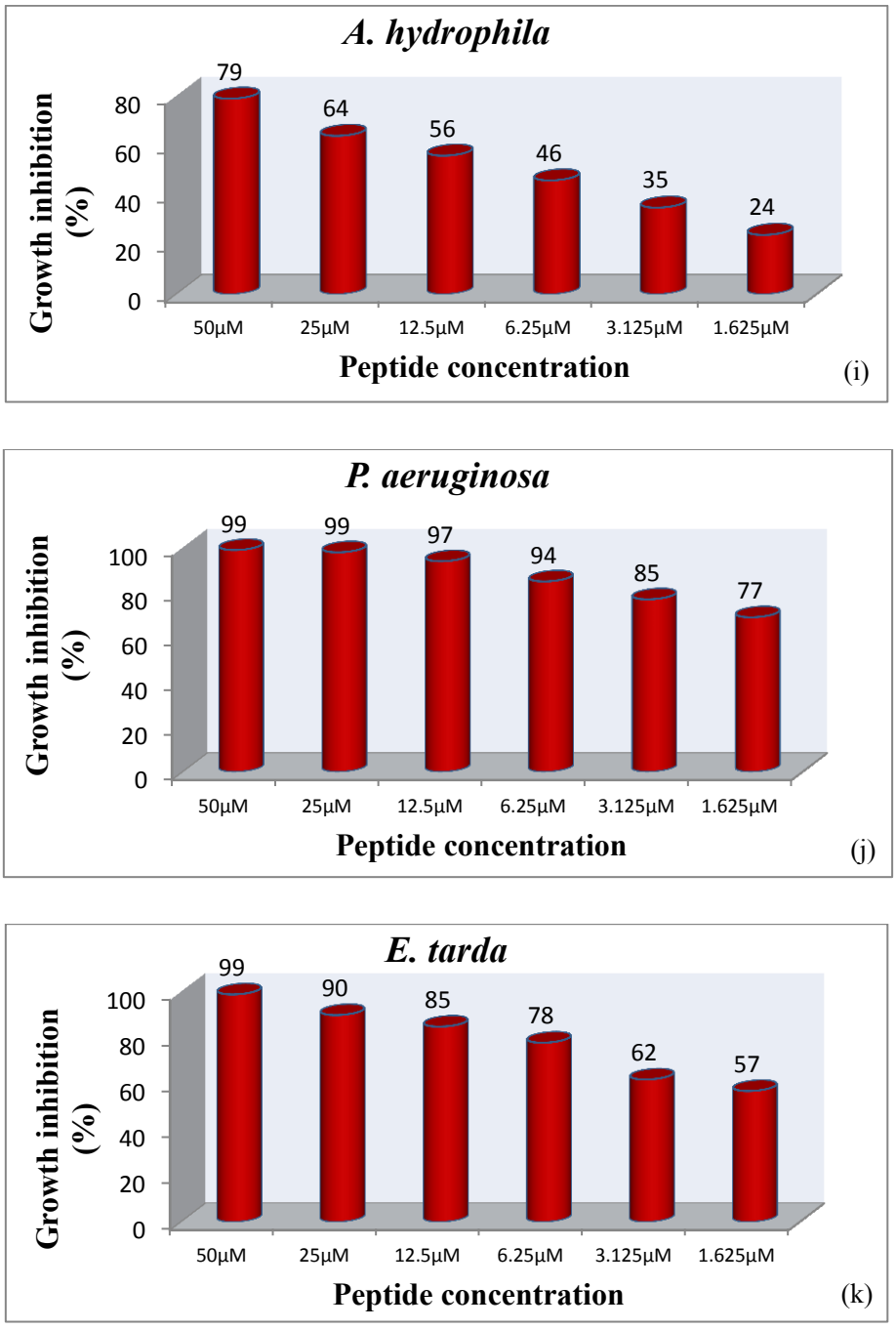


**Fig. 4.16** (a-k) Antimicrobial activity of synthetic *Em*-His2 against various bacteria at different concentrations.

### 4.3.7 PI staining

Propidium iodide staining was done for synthetic *Em*-His2 peptide treated bacteria to assess the killing efficiency in terms of the live/dead bacterial cells (Fig. 4.17). Cells that internalized the peptide into the cytoplasm were detected as green through the FITC filter due to presence of FITC tag in the peptide. Meanwhile, the percentage of membrane damaged dead bacterial cells, seen as red, was comparatively less in the PI stained image of *Em*-His2 treated bacteria. Thus the mode of action of peptide was assumed to be different from the usual membrane pore forming way of action of AMPs.

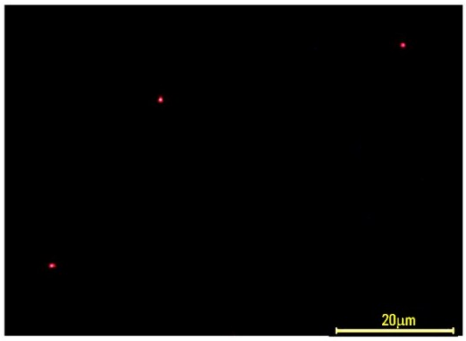


Untreated *V. parahaemolyticus*

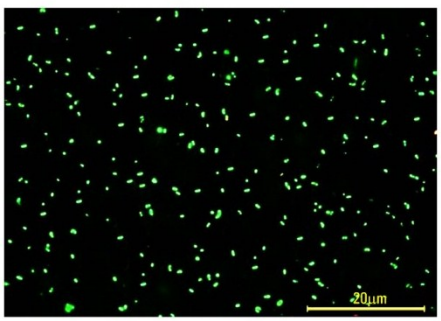


*Em*-His2 treated *V. parahaemolyticus* (FITC filter)

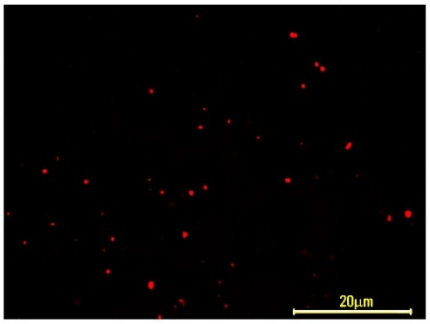


*Em*-His2 treated *V. parahaemolyticus* (PI filter)

*Figure 4.17 Continued….*

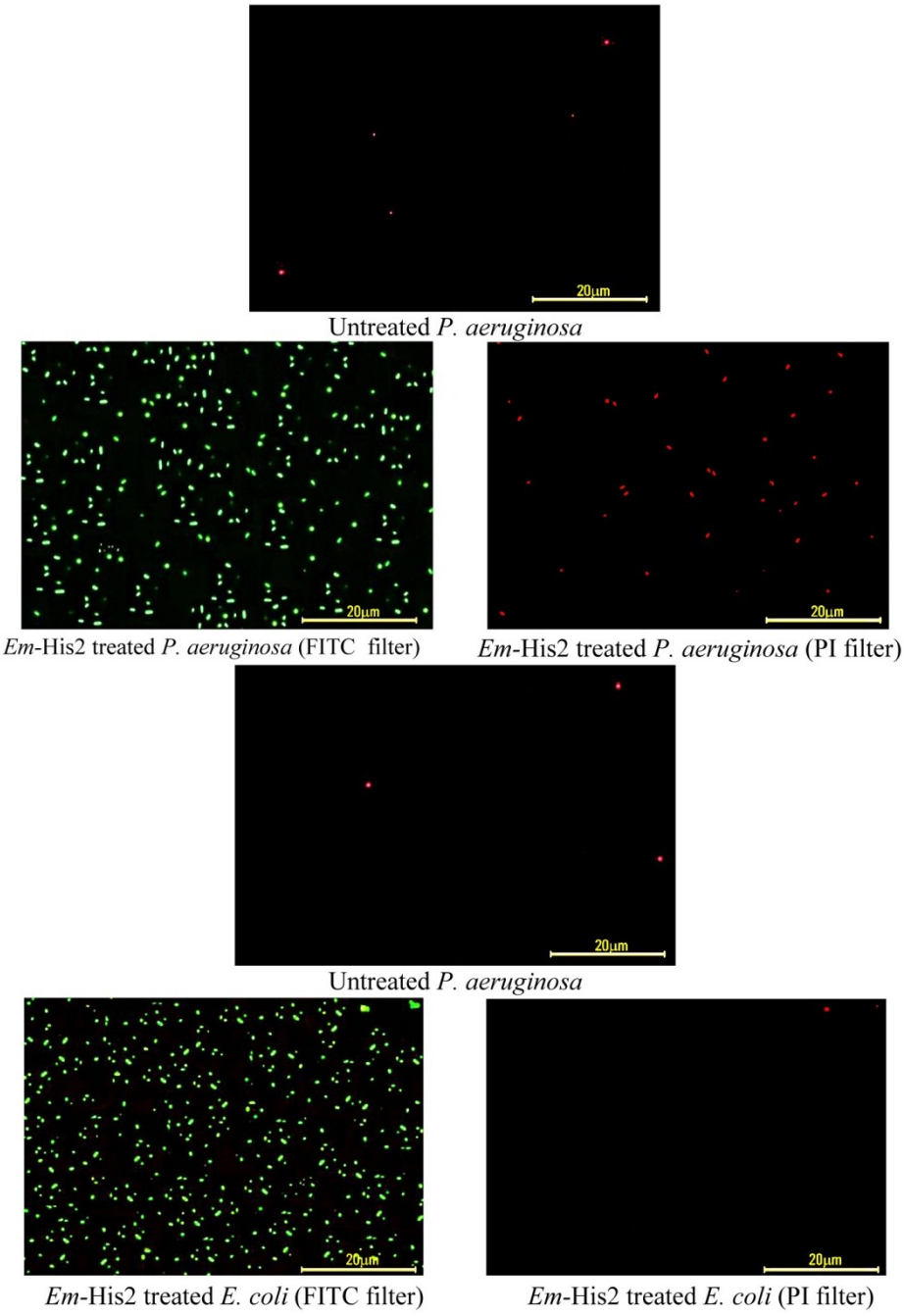


**Fig. 4.17** PI stained image of untreated control pathogens and synthetic *Em*-His2 treated pathogens under FITC filter and PI filter.

### 4.3.8 SEM analysis

Morphological alterations of *Em*-His2 treated bacteria were visualized by scanning electron microscopy (SEM) (Fig. 4.18). SEM imaging of cells incubated with synthetic *Em*-His2 peptide revealed that the general cell morphology remained unchanged, even though the cells appeared little smaller.

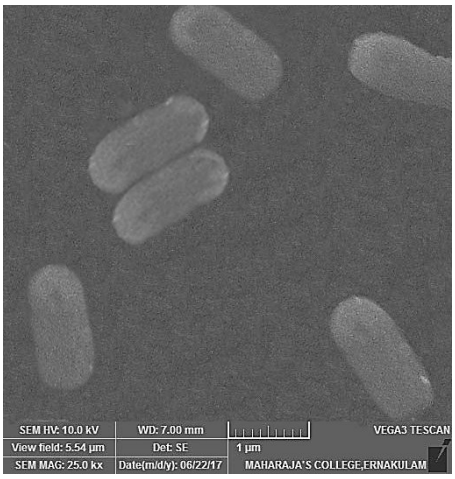


Untreated *E. coli*

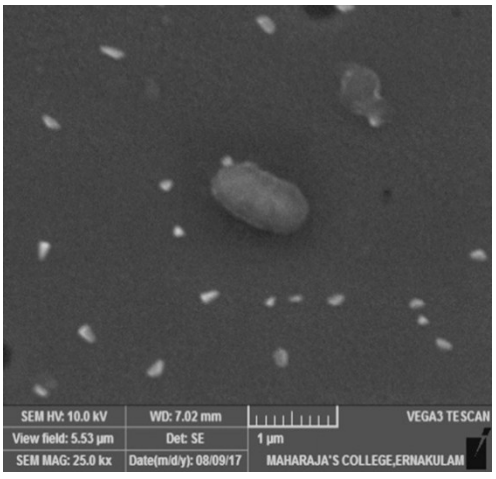


*Em*-His2 treated *E. coli*

Untreated *V. parahaemolyticus*

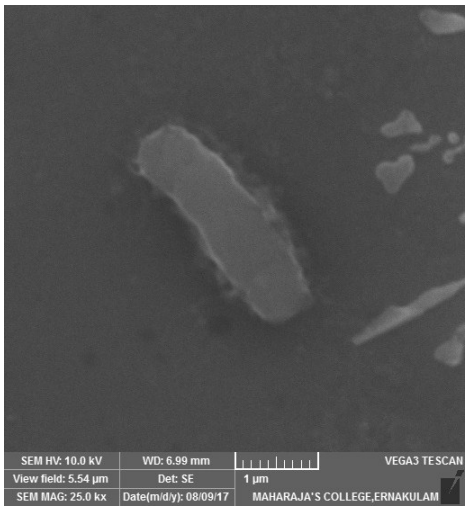


*Em*-His2 treated *V. parahaemolyticus*

*Figure 4.18 Continued….*

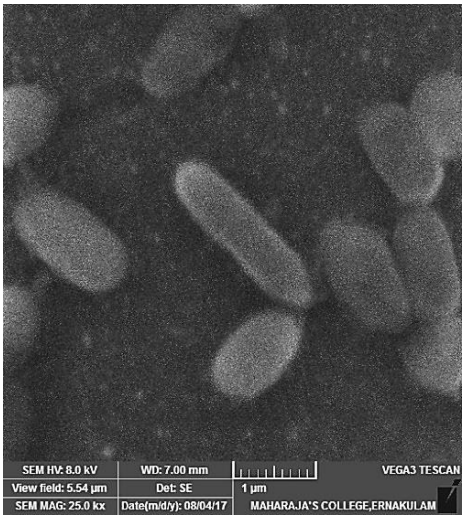


Untreated *P. aeruginosa*

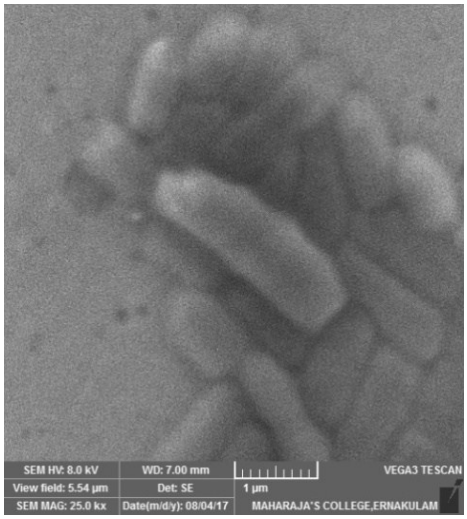


*Em*-His2 treated *P. aeruginosa*

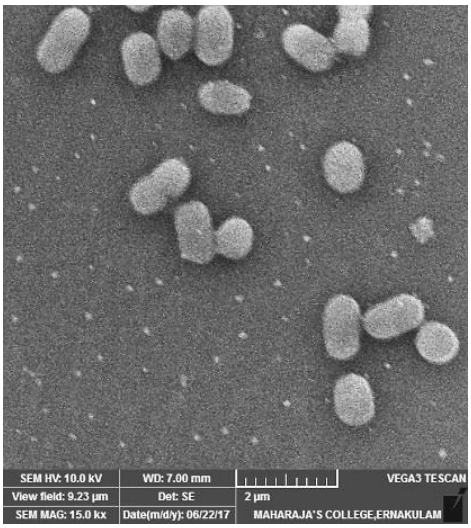


Untreated *E. tarda*

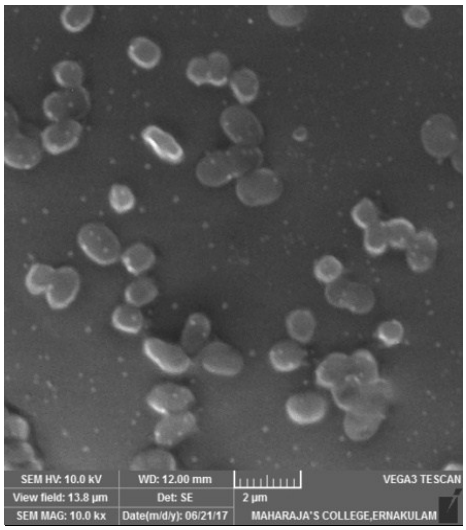


*Em*-His2 treated *E. tarda*

**Fig. 4.18** SEM image of untreated control pathogens and synthetic peptide, *Em*-His2 treated pathogens. The overall cell morphology appeared normal without apparent cellular debris, in the *Em*-His2 treated group.

### 4.3.9 DNA Binding assay

In order to explore any intracellular targeting mechanisms exist for *Em*-His2, the DNA binding affinity of *Em*-His2 was tested by electophoretic mobility shift assay (gel retardation assay). Gel retardation of the pUC-18 plasmid was analysed by treating the vector with different concentrations of peptide (200 µM – 1.625 µM). It was noted that *Em*-His2 effectively retards the electrophoretic mobility of pUC-18 plasmid from a concentration of 25 µM to 200 µM (Fig. 4.19). The bound DNA could be seen restricted in the gel well due to its reduced electrophoretic mobility.

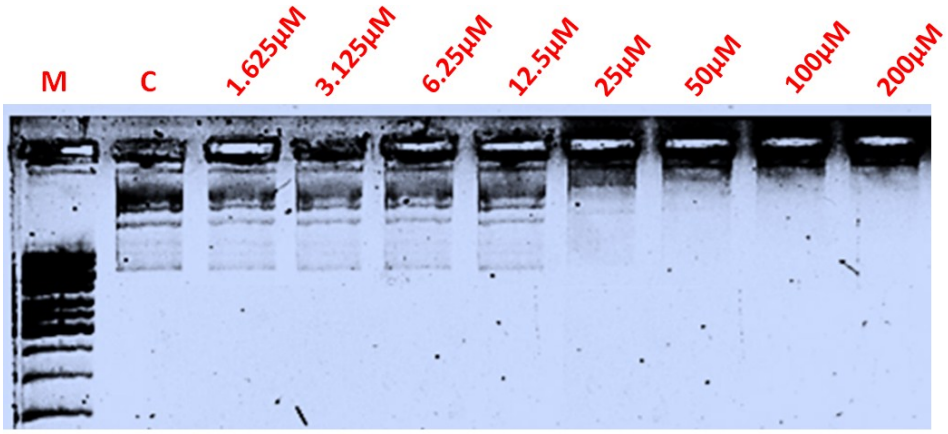


**Fig. 4.19** Agarose gel image of the DNA binding assay of synthetic *Em*-His2. Lane M: 1 kb ladder, Lane 1: Control pUC-18 plasmid, Lane 2-9: 1.625 µM to 200 µM concentration of peptide with 50 ng of pUC-18 vector.

### 4.3.10 *In vitro* cytotoxicity assay

Cytotoxicity of synthetic *Em*-His2 peptide was analysed from 1.625 µM to 200 µM in NCI-H460 and HEp-2 cell lines by XTT assay. The result of the cytotoxicity assay of *Em*-His2 and mellitin are represented in Fig. 4.20a and Fig. 4.20b respectively. *Em*-His2 at 200 µM, exhibited potent cytotoxic activity against NCI-H460 and comparatively less

cytotoxicity towards HEp-2 cell lines with growth inhibition percentage of 50 and 38 respectively. The $IC_{50}$ value of *Em*-His2 against NCI-H460 cells was estimated to be 200± 39.88 µM and 260.16 ± 38.72 µM for HEp-2 cells. Also, the cytotoxic activity of *Em*-His2 against NCI-H460 and HEp-2 cell lines was found to be concentration dependent.

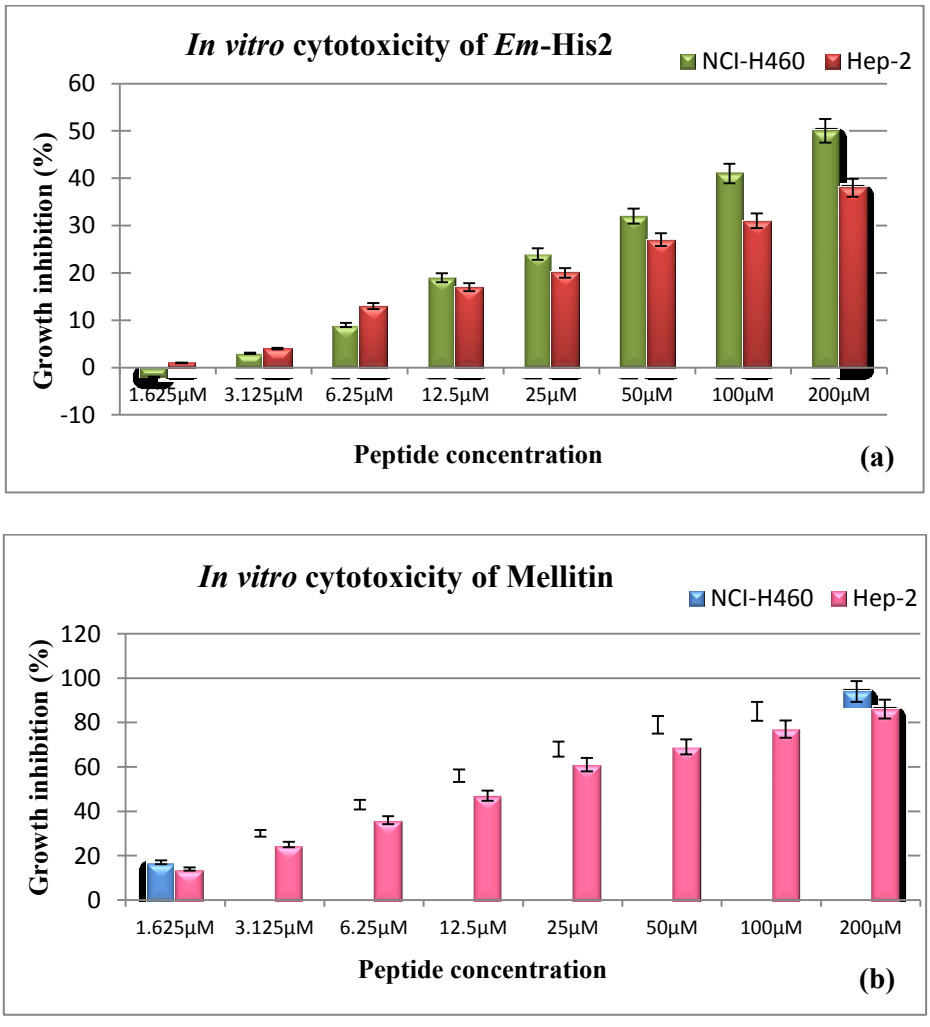


**Fig. 4.20** *In vitro* cytotoxicity of (a) the synthetic peptide, *Em*-His2 and (b) mellitin against NCI-H460 and Hep-2 cells at various concentrations.

### 4.3.11 Anticancer activity

#### 4.3.11.1 Relative gene expression analysis of cancer related genes in *Em*-His2 treated NCI-H460 cell line

To analyse the dose response cytotoxic activity of *Em*-His2 against NCI-H460 cell lines, 25 μM and 100 μM of peptide was treated with the cells and the *in vitro* gene expression levels of cancer related genes was analyzed by qRT-PCR. Quantitative PCR analysis showed that most of the cancer associated genes were observed to be up-regulated in response to *Em*-His2 treatment. Relative expression of Caspase 3, Caspase 9, Bax, p53, NFkB and Rb-1 were found to be high than Bcl-2, Cox-2 and ikBα. Enhanced up-regulation of Cathepsin-G and Calpain-5 could also be noticed after *Em*-His2 treatment. Among the interferon induced immune genes, upregulated expression of MX1F could only be noticed; while the rest of the genes were found downregulated compared to the control untreated group. Enhanced production of various cytokine related immune genes were found, especially TNF-α, IFN-b, IFN-c, IL-6 and IL-12. While, IL-10 was found to differentially express in response to the two different dose of *Em*-His2 (25 μM and 100 μM). *Em*-His2 treatment also enhanced the expression of cell cycle associated genes such as MAPK-1 and JNK (Fig. 4.21).

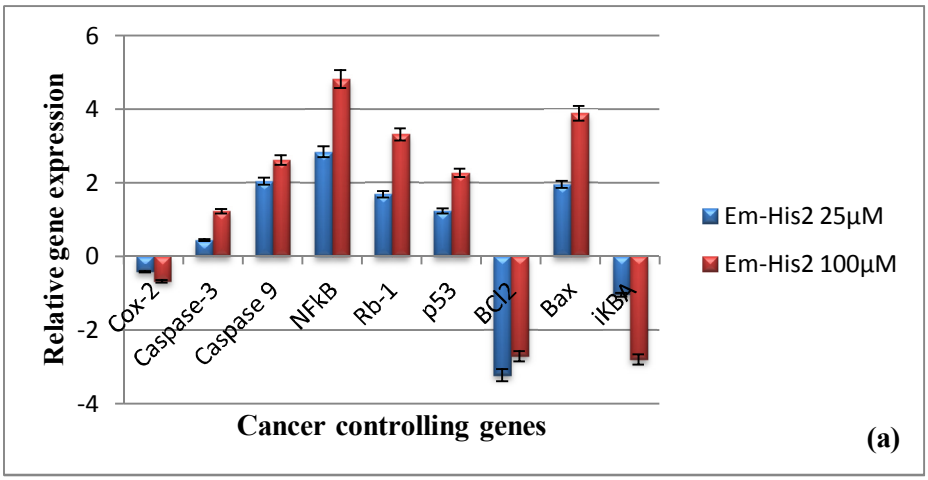


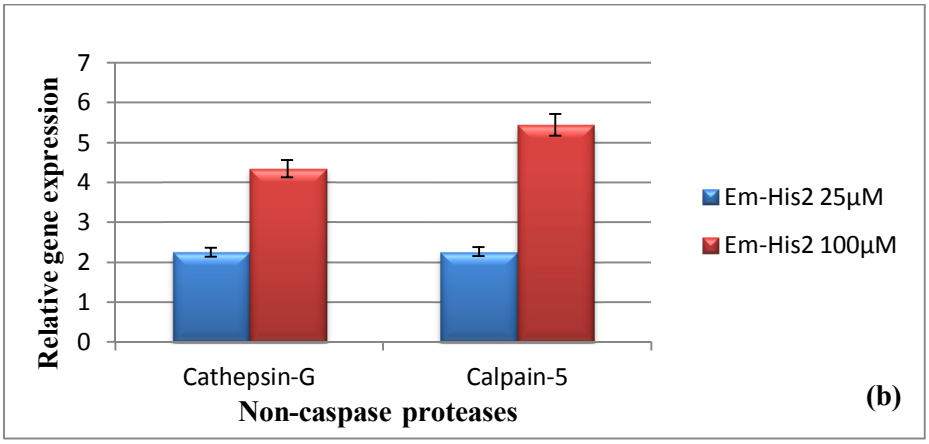


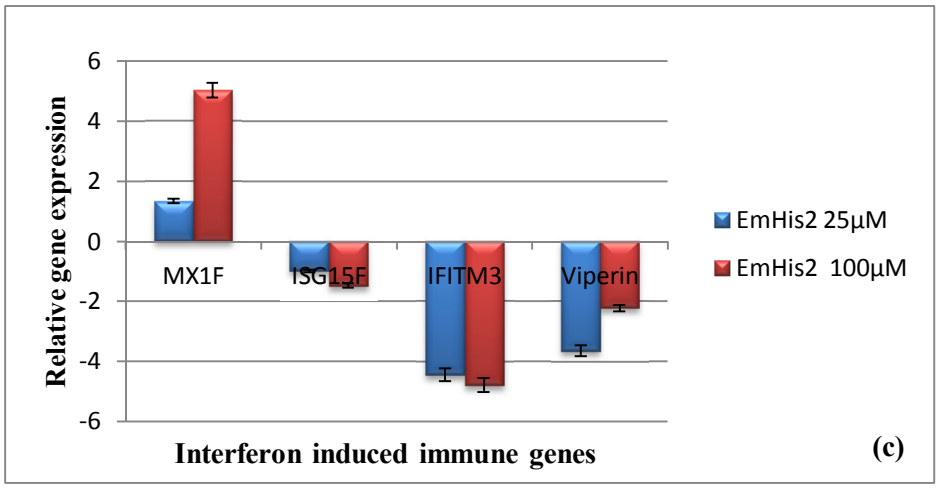


*Fig. 4.21 Continued…*

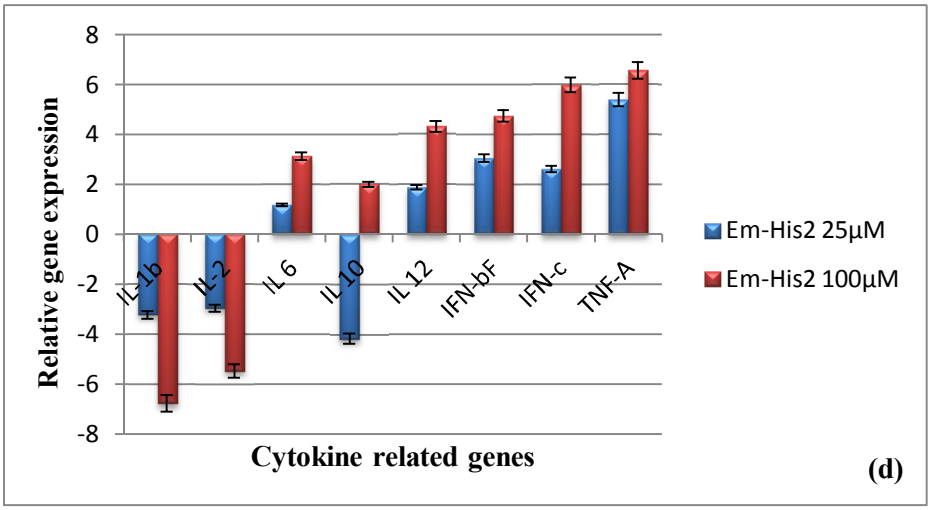


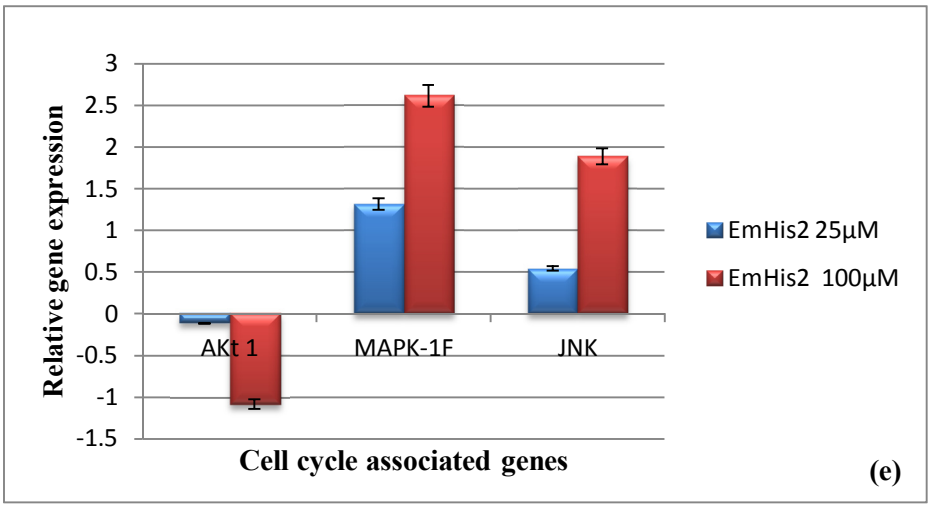


**Fig. 4.21** **(a-e)** Relative gene expression levels of different cancer related genes using quantitative real-time PCR in *Em*-His2 peptide treated NCI-H460 cell lines.

#### 4.3.11.2 Relative gene expression analysis of cancer related genes in *Em*-His2 treated HEp-2 cell line

Relative gene expression profile of various cancer related genes in HEp-2 cells treated with 25 µM and 100 µM of *Em*-His2 was analyzed by qRT-PCR and the results are given in Fig. 4.22. RT-PCR analysis demonstrated a marked upregulation of various cancer related genes analysed such as Bax, Caspase-3, Caspase-9, NFkB, Rb1 and p-53. The prominent cancer genes that showed downregulation were Cox-2, Bcl-2 and ikBα. Expression of both the non-caspase proteases analysed, Cathepsin-G and Calpain-5, were found upregulated. The various cytokine related genes displayed differential expression in response to *Em*-His2 treatment. Enhanced expression of various interleukins such as IL-1β, IL-6 and IL-10 could be noticed, while IL-2 and IL-12 were found to be downregulated. An up-regulated expression of other cytokine related genes such as IFN-β, IFN-γ and TNF-α could also be noticed after *Em*-His2 treatment in Hep-2 cells. Remarkable up-regulation of JNK and MAPK-1 could be noticed among the cell cycle associated genes. *Em*-His2 treatment also elevated the expression of interferon induced immune genes especially the viperin and ISG15 with respect to the control group.

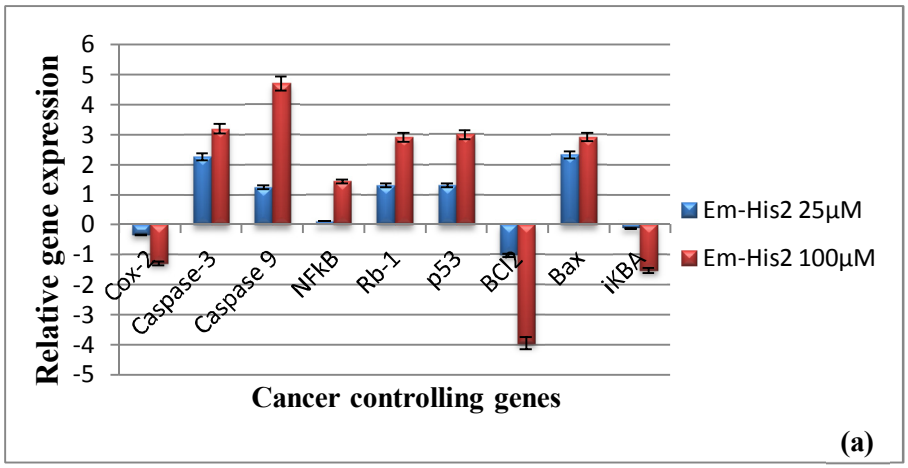


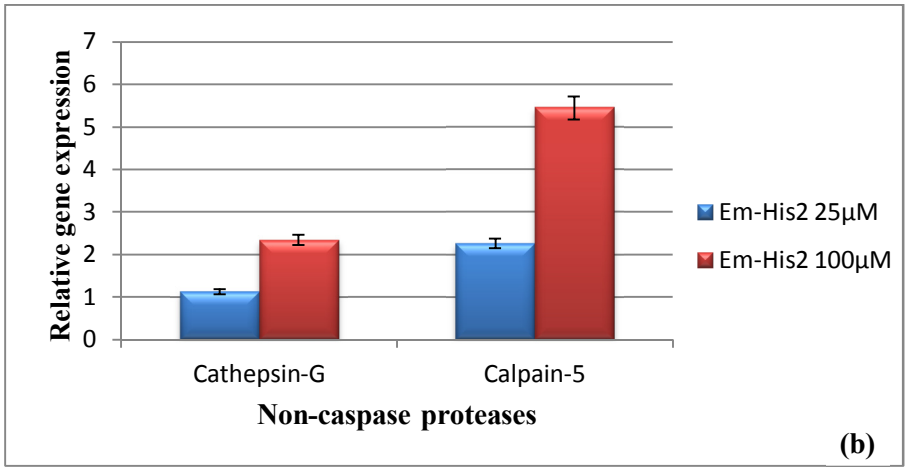


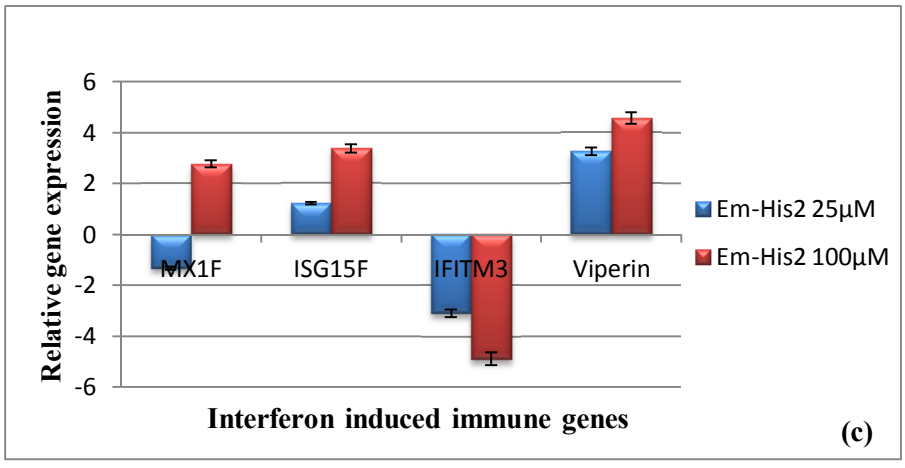


*Fig. 4.22 Continued…*

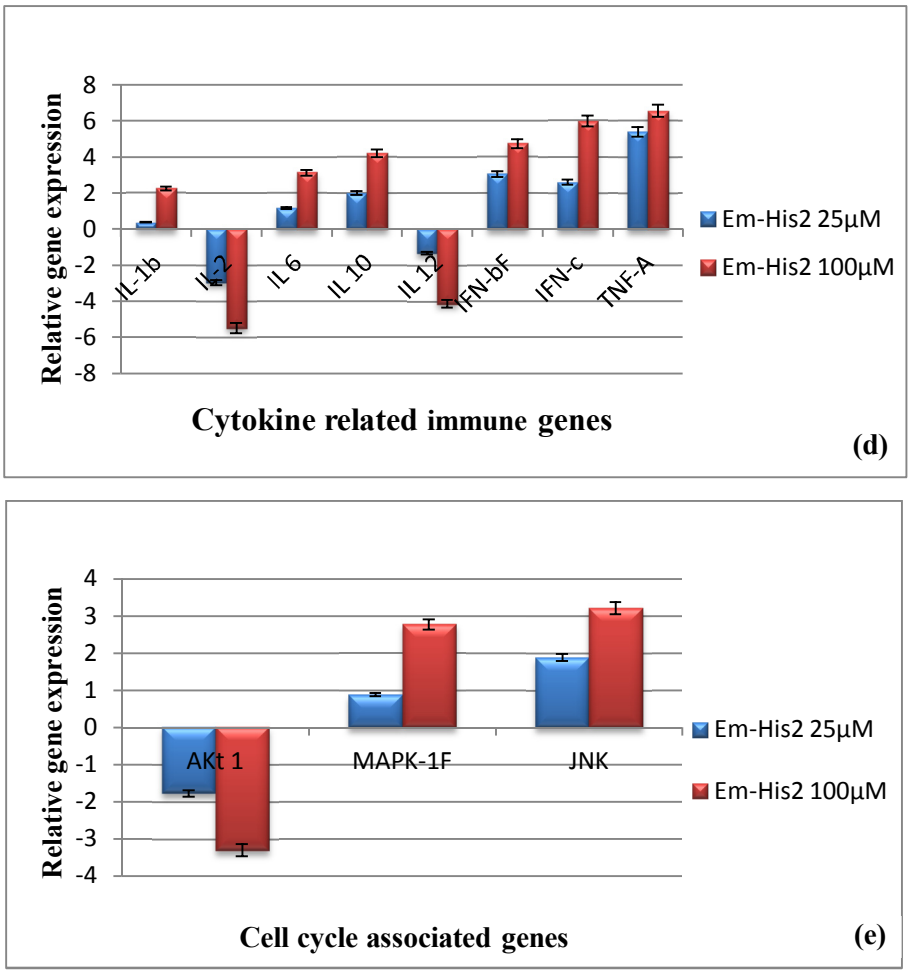


**Fig. 4.22** **(a-e)** Quantitative gene expression levels of different cancer related genes using RT-PCR in *Em*-His2 peptide treated HEp-2 cell lines.

## 4.4 Discussion

Antimicrobial peptides function as multi-faceted peptides in the innate immune system of the host whose fundamental biological role has been proposed to be focused on the elimination of pathogenic microorganisms (Diamond et al., 2009). Fragments of histone H2A protein are reported to play a vital role in the host defence mechanisms

against infection as AMPs, in addition to their role in nucleus as elements of chromatin structure in eukaryotes (Patrzykat et al., 2001). In the present study, two histone H2A-derived antimicrobial peptides from the haemocytes of *Etroplus maculatus* have been identified and designated as *Em*-His1 and *Em*-His2. Till date, there is hardly any study regarding the host defence peptides or the physiological process involved in the immune system of the Orange chromide, *E. maculatus*. The histone gene characterised in the current study which was cloned from the haemocytes of *E. maculatus,* possessed the characteristic histone signature domain at $Ala^{22}$-$Gly^{23}$-$Leu^{24}$-$Gln^{25}$-$Phe^{26}$-$Pro^{27}$-$Val^{28}$. Among the putative domains observed, lysine and arginine play major roles, with the former often getting acetylated ($Lys^{6}$ and $Lys^{10}$) (Doenecke and Gallwitz, 1982) and later shown to be involved in pH-dependent antimicrobial activity and DNA-binding ($Arg^{30}$, $Arg^{33}$, $Arg^{36}$, $Arg^{43}$) (Ebralidse et al., 1988; Kacprzyk et al., 2007).

It is widely known that the antimicrobial histone derived peptides are formed by proteolytic processing of either the N-terminal or C-terminal portions of histones. Therefore, the action of various proteolytic enzymes on the histone H2A of *E. maculatus* was studied using PeptideCutter tool of ExPASy. The analysis established potential cleavage sites for chymotrypsin/pepsin/proteinase-K/thermolysin and proteinase-K/trypsin that would result in the formation of 52 amino acid, *Em*-His1 and 21 amino acid, *Em*-His2. Apparently, the *Em*-His1 sequence appears to serve as a precursor molecule for *Em*-His2. However, the clear mechanism of histone activation in *E. maculatus* needs further investigation. Since the sequence of *Em*-His1 matched with the

characterised *Mc*-His sequence (discussed in Chapter 3) and considering this sequence similarity, analysis based on *Em*-His2 alone was studied additionally.

Histone derived peptides have been described from various organisms with almost the same amino acid sequence or differing in a single amino acid, as the sequences are homologous to different histone peptide fragments (Masso-Silva and Diamond, 2014). Homology searches using BLASTp revealed the similarity of *Em*-His2 to known representative histone–H2A members, in particular to Buforin II. Nevertheless, the two HDAPs exhibited a great degree of variation in their nucleotide sequences and this variability at the nucleotide level seems to be as the result of a larger amount of non-synonymous variation, which affects to some extent, the structural domain comprising the histone fold (Gonzalez-Romero et al., 2008). At the same time they shared similarity in the conserved characteristic motifs with other vertebrates and invertebrate HDAPs. Such conservation of sequences arise due to the slow pace of evolution of histone H2A genes (Thatcher and Gorovsky, 1994).

Multiple sequence alignment of *Em*-His2 with other reported HDAP counterparts revealed the existence of conserved residues as well as outlined the differences between vertebrates and invertebrate HDAPs. Altogether, the ClustalW protein alignment results indicate that the histones might be widely conserved and prevail as an original component of innate immunity in both vertebrates and invertebrates. While noting the differences, in *Em*-His2, presence of Threonine instead of Serine at the N-terminus region could be noticed when compared to other HDAPs from

vertebrates (except for the human H2A peptide). Additionally, replacement of Valine in the C-terminal of *Em*-His2 with Isoleucine could also be noted in a similar line for all other invertebrate HDAPs. In the phylogenetic tree, significant overlap was observed in the histone H2A nucleotide sequences of "amphibians and fishes" and "birds and mammals" from which it could be inferred that histone proteins remain relatively unchanged throughout the course of evolution. Histone genes evolve very slowly and therefore, evolutionary analyses of histones should be informative with regard to the phylogenetic relationships of distantly related organisms (Thatcher and Gorovsky, 2004).

It has been reported that the electrostatic interaction between the positively charged amino acids and the negatively charged moieties on the bacterial membrane plays vital roles in the initial antimicrobial interactions of AMPs (Matsuzaki et al., 1997a; Xie et al., 2014). *Em*-His2 was predicted to be a cationic antimicrobial peptide, with a net charge of +6. The cationic characteristic of the peptide made it possible to exert its antimicrobial function *via,* electrostatic attraction. These cationic residues 'snorkel' towards the interface of lipid bilayer, while phenylalanine residues of the peptide played dominant roles in the peptide-membrane interactions (Jafari et al., 2017). Furthermore, the spatial structure indicated that *Em*-His2 displayed a larger positive electrostatic surface. Meanwhile, Huang et al. (2014) explained in their study with D- and L- diastereomeric peptides, that peptide helicity plays a critical role on the antimicrobial activity of α-helical antimicrobial peptides. *Em*-His2 is a 21 amino acid cationic peptide having a net positive charge of +6, molecular weight of 2.435 kDa, *p*I of 12.60 and hydrophobicity of 33 %. Moreover,

*Em*-His2 exhibited a linear amphipathic nature due to the absence of cysteine residue. Ward et al. (2009) observed that the amphipathicity of the α-helices cause a net positive charge to accumulate at the point so that they can interact with negatively charged phosphate groups on DNA. The findings of KD-plot and the helical wheel analysis of *Em*-His2 are in total agreement with the amphipathic character of the peptide. The amphipathic nature coupled with perfect α-helical structure demonstrates the strong antimicrobial nature of *Em*-His2 as with known histone H2A derived AMPs (Park et al., 1998; Sathyan et al., 2012a). Furthermore, the antimicrobial property of *Em*-His2 was analyzed using APD3. The database predicted *Em*-His2 to be an antimicrobial peptide since it formed alpha helices and had a significant number of residues on the same hydrophobic surface which allowed the peptide to interact with microbial membranes.

In 2011, Sperstad and his co-workers have stated that identification and characterization of the new AMPs in marine organisms have become imperative in order to find new alternatives to the existence of bacterial resistance towards conventional antibiotics. Particularly, the antimicrobial mode of action of α-helical cationic peptides have been intensively studied and reported (Dathe and Wieprecht, 1999; Giangaspero et al., 2001; Nguyen et al.,2011; Lee et al., 2015). The antimicrobial effects of these peptides have been suggested to occur *via*, three main general mechanisms: (1) cell surface binding (2) permeabilization of the membrane and (3) indirect secondary effects such as DNA/RNA/protein binding, altering the composition of membranes, interference with essential cellular components etc.

To understand the antimicrobial potential of *Em*-His2, its activity spectrum was determined using a synthetic peptide, whose sequence was selected based on the framework of conserved sequence identified by multiple sequence alignment of peptides. The peptide was synthesized as a linear peptide with end modifications and an FITC-tag. According to the study conducted by Lee et al. (2008), FITC labelling showed no apparent effect on the cytotoxicity of buforin IIb when compared with the unlabelled peptide. Several studies have reported the antimicrobial activities of histone H2A derived antimicrobial peptides against both Gram-positive and Gram-negative bacteria and fungi (Richards et al., 2001; Patat et al., 2004; Li et al., 2007; Kawasaki and Iwamuro, 2008; De Zoysa et al., 2009; Shamova et al., 2014). The antimicrobial activity demonstrated by synthetic *Em*-His2 was in accordance with the earlier reports by Park et al. (1996 and 1998), Birkemo et al. (2003) and De Zoysa et al. (2009). Synthetic *Em*-His2 was found to be active against both Gram-positive and Gram-negative bacteria with strong antimicrobial activities exhibited against *P. aeruginosa, E. coli* and *V. parahaemolyticus* (MIC and MBC (25 μM)). However, the MIC and MBC values observed for *Em*-His2 was comparatively high with respect to Buforin II (MIC, 1-4 μM) (Park et al., 2000). This disparity in activity between both the peptides would have resulted from the end modifications of *Em*-His2 which have resulted in a slight dip in the overall charge of the peptide.

The synthetic peptide, *Em*-His2 was designed based on buforin II sequence; it was unclear whether *Em*-His2 imbued the characteristic buforin II like mode of action. The mechanism of action of buforin II is particularly noteworthy because it employs a relatively uncommon

mechanism wherein it kills bacteria through interacting with the DNA by crossing the bacterial membrane without causing cell lysis (Park et al., 1998). Earlier studies with certain α-helical antimicrobial peptides showed that they form transient holes when the local concentration of the peptides reaches a threshold level, as evidenced by their ion-channel activities (Ludtke et al., 1996; Matsuzaki et al., 1997a). As a result of these toroidal holes, histone H2A reaches the cytosol or the nucleus, where it could exert its antimicrobial action by inhibiting cellular functions (Shai, 1999; Ebran et al., 1999). Later in 2000, Kobayashi and his co-workers showed that Buforin II can enter lipid vesicles and its membrane translocation was due to toroidal pore formation. The mechanism of action of *Em*-His2 was analysed by incubating the bacteria with the FITC labelled peptide followed by PI uptake. As expected, the number of cells emitting green fluorescence (FITC filter) was more in contrast to the cells emitting red fluorescence when observed through the PI filter. Green fluorescence from *Em*-His2 treated bacteria was due to the containment of FITC labelled peptide in the cytosol of the bacterial cells. In contrast, the lower red fluorescence observed was not due to the presence of live bacteria, but could be attributed to the nature of toroidal pores. These pores being transient in nature rapidly disassemble, blocking the entry of PI, which could permeate only in membrane compromised cells. The epifluorescence microscopy results of FITC labelled *Em*-His2 treated bacteria were on par with the translocation studies carried out by DesHDAP1(Pavia et al., 2012), HipB (BF2 F10W) (Bustillo et al., 2014) and Buforin II (Cutrona et al., 2015).

To further substantiate the mechanism of action of *Em*-His2, DNA binding activity and SEM analysis of peptide treated bacteria was

performed. The synthetic peptide *Em*-His2 displayed marked DNA binding activities from 25 μM, which matched the MIC observed for *P. aeruginosa, E. coli* and *V. parahaemolyticus*. Therefore, DNA binding affinity of *Em*-His2 correlated linearly with their antimicrobial potency. DNA binding studies of buforin II and buforin III variants have shown that the property is critical to the bactericidal mechanism of those peptides (Uyterhoeven et al., 2008; Pavia et al., 2012; Jang et al., 2012). The findings of DNA binding studies of *Em*-His2 were in accordance with the above reports. Moreover, the SEM analysis results suggested that the antimicrobial mode of action of *Em*-His2 could be *via*, DNA interaction as no significant morphological change could be noticed for the peptide treated bacteria.

The toxicity of AMPs against eukaryotic cells is the key obstacle for their clinical application. Most of the HDAPs such as Buforin IIb, Sphistin and Acipensins are found to be non-cytotoxic to normal eukaryotic cells (Lee et al., 2008; Chen et al., 2015; Shamova et al., 2015). Much like the reported HDAPs, *Em*-His2 was also found to be non-cytotoxic towards mammalian erythrocytes *via*, a haemolytic assay. It could be the hydrophobic moieties of *Em*-His2 that determine the balance between both peptide antibacterial activity and cytotoxic activity (Saint Jean et al., 2017). Also, *Em*-His2 displayed anticancer activity against cancer cell lines including lung cancer (NCI-H460) cells and the pharyngeal cancer (HEp-2) cells. Display of non-toxic behaviour of the peptide against mammalian cells (hRBCs) and potential toxicity towards the cancer cell lines indicates its prospective value for clinical trials.

Recently, cationic antimicrobial peptides have become the focus of research mainly due to their ability to kill a variety of microorganisms and tumour cells (Hye et al., 2011; Wu et al., 2014; Hancock et al., 2016). Only few studies have discussed the antitumor/anticancer potential of histone H2A derived peptides (Birkemo et al., 2003; Patat et al., 2004; Bergsson et al., 2005; Lee et al., 2008; Jang et al., 2011; Lim et al., 2013). Similar findings have been described for other cationic AMPs such as magainin 10 (Cruciani et al., 1991), cecropin (Moore et al., 1994), LL-37 (Henzler-Wildman et al., 2003) and melittin (Gajski and Garaj-Vrhovac, 2013). In particular, anticancer mechanism of buforin IIb have been studied in detail by Lee et al. (2008) against 60 human cancer cell lines and found that it selectively targets cancer cells through interaction with the cell-surface gangliosides, phosphatidylserine and heparin sulfate. Buforin IIb then traverses cancer cell membranes without damaging the cells and induces the activation of caspase-9 and caspase-3 following cytochrome-c release, leading to mitochondria-dependent apoptosis.

*Em*-His2 displayed potential cytotoxicity towards NCI-H460 and HEp-2 cells; hence its anticancer mechanism with respect to the expression of various cancer related genes was analysed using qRT-PCR. In the present study, *Em*-His2, similar to Buforin IIb, has shown to cause an upregulation of both Caspase-3 and Caspase-9 in both the cell lines. Caspase family of proteins are vital players in the initiation and execution of apoptosis. Caspase-9 as an initiator caspases is primarily responsible for the initiation of the apoptotic pathway and caspase-3 function as effector caspase which is responsible for the actual cleavage of cellular components during apoptosis (Li et al., 1997; Srinivasula et al., 1998). Specifically, levels of

Caspase-9 were found to get increased following *Em*-His2 treatment than Caspase-3. Thus, apparently, *Em*-His2 could lead to an intrinsic apoptotic pathway in both the analysed cancer cells, by cytochrome-*c* leakage which can then bind to apoptotic protease activating factor-1 forming the apoptosome, activating caspase-9 and later cleaving caspase-3.

Most tumour cells resist apoptosis due to deregulation of pro- and anti-apoptotic proteins (Leung and Wang, 1999). Particularly, ratio of Bax to Bcl-2 determines the susceptibility of cells to death signals (Bali et al., 2015). Here, an enhanced expression of pro-apoptotic protein, Bax along with down-regulation of anti-apoptotic protein Bcl2 was observed in both cell lines upon *Em*-His2 exposure indicating its potential to control expression of apoptosis related genes. Moreover, mRNA levels of p53 and Rb1, both of which are tumour suppressor genes were found to be up-regulated in both the cancer cells. Similar kinds of upregulation of p53 have been noticed for many linker histones which are released in a p53-dependent manner (Konishi et al., 2003). Upregulated mRNA transcripts of non-caspase proteases, Cathepsin-G and Calpain-5 could also be noticed in both cell lines indicating apoptotic death of cancer cells. Thus together with other caspases, these non-caspase proteases aid in the apoptosis process in these cell lines.

Cytokines enable the rapid progression of immune signalling in a multifaceted and efficient manner by direct stimulation of immune effector cells and stromal cells at the tumour site (Lee and Margolin, 2011). It also mediates the enhancement of tumour cell recognition by cytotoxic effector cells. In the present study, only interleukin (IL) IL-6 was seen upregulated in both the cell line. Similarly, an up-regulation of interferons (IFN) such as

IFN-β and IFN-γ and also tumour necrosis factor (TNF) TNF-α has been noticed. However, the other cytokines analysed were found to be differentially expressed in both the cell lines, with IL-12 seen upregulated in NCI-H460 and IL-1β, IL-10 upregulated in HEp-2 cell line. The results indicate the pleiotropic and overlapping function of cytokines during infection or inflammation. The upregulation of proinflammatory cytokines in HEp-2 cell line was comparable to the results observed for tilapia hepcidin (TH 1-5) treated HT1080 cell lines (Chang et al., 2011). Consequently, the anticancer activity of *Em*-His2 could also be ascribed to its ability to induce the production of proinflammatory cytokines such as TNF-α. c-Jun N-terminal protein kinase (JNK) and p38 mitogen-activated protein kinase-1 (MAPK-1) form the sub family members of MAPK superfamily, which function in a cell context-specific and cell type-specific manner to integrate signals that affect various cell processes such as proliferation, differentiation, survival and migration (Roux and Blenis, 2004). While, AKT1, a serine/threonine-protein kinase is an important intermediate of the AKT kinase signalling pathway, involved in the regulation of cell proliferation, survival, growth and angiogenesis (Kumar et al., 2013). It acts as an anti-apoptotic protein by preventing the release of cytochrome-c from the mitochondria and by phosphorylating and inactivating the pro-apoptotic factors BAD and procaspase-9 (Wang et al., 2004). While analysing the mRNA levels of the cell cycle associated genes, MAPK super family members, MAPK1 and JNK, showed a marked upregulation in contrast with the AKT1 gene in both the cell lines, enhancing the anticancer activity of the *Em*-His2 peptide. Relative gene expression of IFN-inducible proteins, such as GTPase Mx1

(myxovirus resistance 1), ISG15 (IFN-stimulated protein-15 kDa), Viperin (virus inhibitory protein, endoplasmic reticulum-associated, interferon-inducible) and IFITM3 (IFN-induced transmembrane protein) were found to be differentially expressed in both cell lines as a result of *Em*-His2 treatment. Interestingly, in NCI-H460 cells, only significant up levels of Mx1 gene could be noticed while genes for all the other IFN-inducible proteins were seen downregulated. In contrast, in HEp-2 cell line, notable increase in IFITM3 gene expression could only be marked from the other IFN-inducible proteins analysed. Thus the current observations of anticancer screening of *Em*-His2 peptide in NCI-H460 and HEp-2 cells revealed the peptides immunomodulatory activity besides its anticancer activity. However, further studies are needed to evaluate its exact mode of action against cancer cells.

To sum up, a putative histone derived peptide, *Em*-His2 was identified from *E. maculatus* and its antibacterial and anticancer potential determined with the synthetic peptide. The synthetic peptide, *Em*-His2 exhibited robust antimicrobial activity against *P. aeruginosa, E. coli* and *V. parahaemolyticus.* The peptide was found to kill microbes *via,* membrane translocation and subsequent interactions with DNA. The peptide also displayed non-toxicity towards human erythrocytes. The anticancer activity of *Em*-His2 was seen effected by the upregulation of apoptosis related genes and tumour suppression genes in NCI-H460 and HEp-2 cell lines. Thus, *Em*-His2 stands as a contender, providing opportunities to develop new drugs for chemotherapeutic use.

Chapter 5

# MOLECULAR CHARACTERIZATION AND FUNCTIONAL ANALYSIS OF HISTONE H2A DERIVED SYNTHETIC PEPTIDE OF *HIMANTURA PASTINACOIDES*

Contents

5.1 Introduction
5.2 Materials and methods
5.3 Results
5.4 Discussion

## 5.1 Introduction

Histones are known as principal protein components of chromatin and their function has been studied mainly in connection with DNA stabilization and regulation of gene expression. However, a growing collection of evidence suggests that histones are present not only within but also outside the nucleus and these "extra nuclear" histones have various physiological roles, particularly in innate defence mechanisms, by acting as AMPs (Parseghian and Luhrs, 2006). The linker histone, H1 was detected in the extracts of the liver, intestine and stomach of Atlantic salmon, *Salmo salar*, which showed anti-*E. coli* activities similar to magainin 2 (Richards et al., 2001). Moreover, proteins related to histone H1 were found in the gill, skin and spleen extracts of rainbow trout, *Oncorhynchus mykiss* and sunshine bass, *Morone saxatilis* that showed

anti-infective properties against the parasitic dinoflagellate, *Amyloodinium ocellatum*, which causes one of the most serious diseases in warm water marine aquaculture (Noga et al., 2001).

Histones demonstrate strong antimicrobial character not only as complete molecule but also through fragments at both the N and C-termini. In spite of the extensive research, exact mechanism of action of histones and histone fragments is still under discussion and their selectivity towards specific targets is not fully understood. Owing to their highly cationic nature, Stromstedt and his co-workers (2010) suggested that the antimicrobial properties of HDAPs could be mediated through the electrostatic attraction of AMPs to the negatively charged membranes resulting in the destabilization and subsequent pore formation of planar lipid bilayer leading to the death of the organism (Stromstedt et al., 2010). However, the histone H2A isolated from trout mucus did not induce ion channels in membranes, but rather caused direct disintegration or micellization of the cell membrane, suggesting the disruption of cell membrane through the 'carpet' mechanism' (Ebran et al., 1999; Fernandes et al., 2002). Nonetheless, parasin, an HDAP, derived from histone H2A of catfish, *Parasilurus asotus*, exerted its antimicrobial action by forming barrel staves lined with α-helical peptides leading to pore formation and cell lysis (Zhao et al., 2015). Also, hipposin, a H2A derived peptide from Atlantic halibut has been found to be extremely damaging to the cell membrane (Fischer, 2013). Moreover, further research revealed that the N-terminal portion of hipposin and parasin is highly essential for the membrane permeabilizing property (Koo et al., 2008; Fischer, 2013). In contrast, buforin II, HDAP from Asian toad, display drastic different mode

of action. Buforin II translocate into the cytosol without causing much membrane impairment, where it could exert its antimicrobial action by interacting with DNA and activating intracellular cascades leading to the death of the organism (Park et al., 1998; Uyterhoeven et al., 2008; Cho et al., 2009). With reference to the other core histones, Tagai and his colleagues in 2011 demonstrated that the lysine rich histone, H2B penetrated the membrane of *E. coli* JCM549 (*Omp*T- outer membrane protease T gene expressing strain), while the arginine rich histones, H3 and H4 remained on the cell surface and disrupted the cell membrane structure with bleb formation (Tagai et al., 2011).

Other fascinating properties of histones include their lipopolysaccharide (LPS) binding ability and capability to act as pattern recognition receptors. Histones H2A and H2B in humans, show dose-dependent inhibition of the endotoxin activity of LPS by binding and blocking the core and lipid A moieties of LPS (Augusto et al., 2003). Moreover, the LPS binding site was shown to be located in the C-terminal region of histones. Binding of histones to LPS released from Gram-negative bacteria may also block the production of cytokines such as tumor necrosis factor-alpha (TNF-α) that leads to fatalities from toxic shock in humans (Kim et al., 2002). Similarly, histones have proved the ability to bind to viral proteins like the Human Immunodeficiency Virus (HIV) envelope glycoprotein gp120 and its receptor CD4 (Mamikonyan et al., 2008). Potential role of histones as pattern recognition receptors (PRRs) was materialized through the identification and characterization of a histone-like protein in the membranes of non-specific cytotoxic cells (NCAMP-1) of catfish that recognizes bacterial DNA, oligodeoxynucleotides, and

polyguanosine motifs (Connor et al., 2009). Subsequently, this protein was demonstrated to possess antimicrobial activity. Thus, these antimicrobial histones and the fragments that act as physiological barriers of cells, expend their activities in various ways including bacterial cell membrane permeabilization, penetration into the membrane followed by binding to bacterial DNA or RNA, binding to bacterial lipopolysaccharide in the membrane, neutralizing the toxicity of bacterial LPS, and entrapping pathogens as a component of neutrophil extracellular traps (NETs) (Park et al., 1998; Fernandes et al., 2002; Kim et al., 2002; Brinkmann et al., 2004).

Histones and histone-derived peptides could be used as potentially useful targets in the development of novel drugs for the prevention and treatment of infectious diseases in the aquaculture industry (Nikapitiya et al., 2013). Furthermore, to accentuate its use as novel drugs, anticancer activities of HDAPs also have been reported. However, the knowledge on anticancer HDAPs is limited to the small number of antimicrobial peptides which has been studied. Buforin IIb, displayed selective cytotoxicity against 62 cancer cell lines by specifically targeting cancer cells through interaction with cell surface gangliosides (Lee et al., 2008). It is a synthetic analog of buforin II that contains a proline hinge in the middle and an α-helical sequence at the C-terminus (3xRLLR) (Park et al., 2000). They traversed cancer cell membranes without damaging them and accumulated primarily in the nuclei. Moreover, *in vivo* analysis revealed that buforin IIb displayed significant tumor suppression activity in mice with tumor xenograft. The remarkable selectivity of buforin IIb for cancer cells results largely from the inability of the peptide to

penetrate normal cell membranes (Lee et al., 2008). Besides, another reported H2A-HDAP from the disk abalone, abhisin, exhibited potent antimicrobial and anticancer activity similar to that of buforin IIb (De Zoysa et al., 2009).

The prospective value of AMPs for clinical purposes includes their use as sole antimicrobial agents, synergistic agents to existing antibiotics and immunostimulatory agents (Gordon et al., 2005). Buforins display many of the desirable features of a novel antibiotic, including low MIC values against pathogens (Giacometti et al., 2000, 2001). Buforin II, by virtue of its amphiphaticity and relative composition of positively charged amino acids, houses a domain that resembles the conserved AMP structural motif more closely than does the corresponding domain of histone H2A (Cho et al., 2009). Sathyan et al. (2012a) identified and characterized a novel histone H2A derived antimicrobial peptide, Himanturin (39 amino acids) from *Himantura pastinacoides*. Hence, in the present study, a region of himanturin homologous to buforin II, was selected and synthesized. Structural and functional characterization of the synthetic peptide was carried to find out the antimicrobial and anticancer property of the molecule besides the structural properties.

## 5.2 Materials and Methods

### 5.2.1 Peptide used for the study

Himanturin (GenBank ID: **HQ720150**), a histone (H2A) derived antimicrobial peptide (HDAP) identified and characterized from the Round whip ray*, Himantura pastinacoides* by Sathyan et al. (2012) was used for the design of the peptide. The Buforin II like region of the

Himanturin was selected for the synthesis of the peptide and was named as *Hp*-His. The source organism, *H. pastinacoides* belongs to Super Class: Pisces; Class: Chondrichthyes; Sub-class: Elasmobranchii; and Family: Dasyatidae.

**Fig. 5.1** Primary structure of the synthetic peptide, *Hp*-His.

The peptide was synthesized at M/s Zhejiang Ontores Biotechnologies Co., Ltd China, as a linear peptide with end modifications and with a FITC label. The product was synthesised using the solid-phase synthesis method using fluoren-90-ylmethoxycarbony (F-moc)-polypeptide active ester chemistry with >95 % final purity. The peptide N-terminus was blocked by acetylation and the C-terminus amidated to increase peptide stability. The synthetic peptide was supplied as lyophilized powder and was solubilized in nuclease and protease free water and stored at -20 °C for further analysis.

### 5.2.2 *In silico* analysis of the properties of the synthetic peptide *Hp*-His

*In silico* analysis of properties of the synthetic peptide *Hp*-His was done by various biological computational tools as described in section 2.2.11 of Chapter 2.

### 5.2.3 HPLC purity determination of synthetic peptide

The synthetic peptides were purified by RP-HPLC and the collected fractions were analyzed again by analytical RP-HPLC as described in

section 4.2.13 of Chapter 4. In short, analytical separation was achieved in a RP-Welchrom C18 column (4.6 × 250 mm). The peptides were purified using a linear TFA/acetonitrile gradient that was eluted at 1mL/min where buffer A was 0.1 % TFA in water and buffer B was 0.1 % TFA in 100 % acetonitrile. The peptides were detected by their absorbance at 220 nm.

### 5.2.4 Mass spectrometry analysis of the synthetic peptide

Mass spectra analysis was performed with a Thermo Finnigan LCQ Duo mass spectrometer as explained in section 4.2.12 of Chapter 4.

### 5.2.5 Haemolytic activity of the synthetic peptide

The ability of synthetic peptide to lyse human erythrocytes was assessed to analyze their toxicity to eukaryotic cells. Erythrocytes were incubated with two fold dilutions of peptide ranging from 400 μM to 3.125 μM. Haemolytic activity was recorded as percentage haemolysis calculated as described in the section 2.2.28 of Chapter 2.

### 5.2.6 Antimicrobial activity

Antimicrobial activity of the synthetic peptide was analysed by broth microdilution assay to determine the MIC and the bactericidal assay to determine the MBC. In order to determine the MIC, six dilutions (50 μM to 1.625 μM concentrations) of the synthetic peptide were tested against eleven different bacterial strains. For details refer section 2.2.30 of Chapter 2. To study the mechanism of interaction of the peptide with pathogens epi-fluorescence microscopic observation of the peptide treated pathogens was performed by PI staining as mentioned in section 2.2.30.3 of

Chapter 2. Further, confirmation of the effect of peptide on bacterial morphology was carried by SEM as described in section 2.2.30.4 of Chapter 2.

### 5.2.7 DNA binding assay

DNA binding activity of the synthetic peptide was performed as mentioned in the section 4.2.16 of Chapter 4.

### 5.2.8 Anticancer activity

#### 5.2.8.1 *In vitro* cytotoxicity assay

Cytotoxicity of the synthetic peptide was determined against NCI-H460 and HEp2 cell lines procured from NCCS, Pune. Cells were treated with different concentrations of the synthetic peptide and incubated for another 24 h. Cell viability was measured at the end of treatment by XTT assay as described earlier in section 2.2.29 of Chapter 2. All the experiments were carried out in triplicates. Results are expressed as percentage inhibition of viable cells. Synthetic mellitin with FITC label was used for comparison. The $IC_{50}$ values were calculated as explained in section 4.2.17.1 of Chapter 4.

#### 5.2.8.2 Relative gene expression analysis using real-time reverse-transcription polymerase chain reaction (RT-PCR)

In order to analyse the anticancer activity of synthetic peptide, NCI-H460 cell lines and HEp2 cells were incubated in DMEM supplemented with 10 % FBS with different concentration of synthetic peptide for 24 h. Cells without peptide treatment were used as the control. After incubation with the peptide, cells were suspended in TRI reagent (Sigma) for RNA isolation as explained in section 2.2.4 of Chapter 2.

Relative gene expression analysis of cancer controlling genes and related immune genes were analysed by qRT-PCR as explained in section 4.2.17.2 of Chapter 4. Relative transcript expression levels were calculated as fold differences relative to the control using the $\Delta\Delta C_T$ method.

## 5.3 Results

In the present study, structural and functional characterization of a synthetic 21 amino acid peptide based on the sequence of a histone H2A derived AMP from *Himantura pastinacoides* was performed.

### 5.3.1 *In silico* analysis of the histone based synthetic peptide *Hp*-His

The DAS prediction server could not detect any transmembrane sequence within *Hp*-His. ScanProsite analysis revealed that the deduced *Hp*-His sequence contains a histone signature region (residues 6-12). Peptide characterisation as analysed by ProtParam tool disclosed that *Hp*-His has a predicted molecular weight of 2.42 kDa, a net positive charge of +6, theoretical *p*I of 12.6 and a total hydrophobic ratio of 33%. The 21 amino acid *Hp*-His was found to be rich in arginine (23 %), Leucine (14%), Serine (14%), Glycine (9.5 %) and Valine (9.5%) as reported in all other histone H2A derived AMPs. Cationicity of *Hp*-His was primarily identified due to the presence of six positive amino acid residues (Arg (5 Nos) +Lys (1 No.)). Polar amino acids + GLY constituted 57.14 % while nonpolar residues represented 42.86 % of the total weight of *Hp*-His. The estimated half- life of *Hp*-His was found to be around 1.9 hrs in mammalian reticulocytes, ≥20hrs in yeast and greater than 10 hrs in *Escherichia coli* in vivo. The instability index of *Hp*-His was computed to be 93.37 and this classifies the peptide to be a highly unstable one.

The ClustalW multiple sequence alignment with representatives members of histone H2A derived AMPs revealed that *Hp*-His is similar to Buforin II except for the N terminal amino acid Threonine which is replaced by Serine in *Hp*-His (Fig. 5.2).

**(a)**

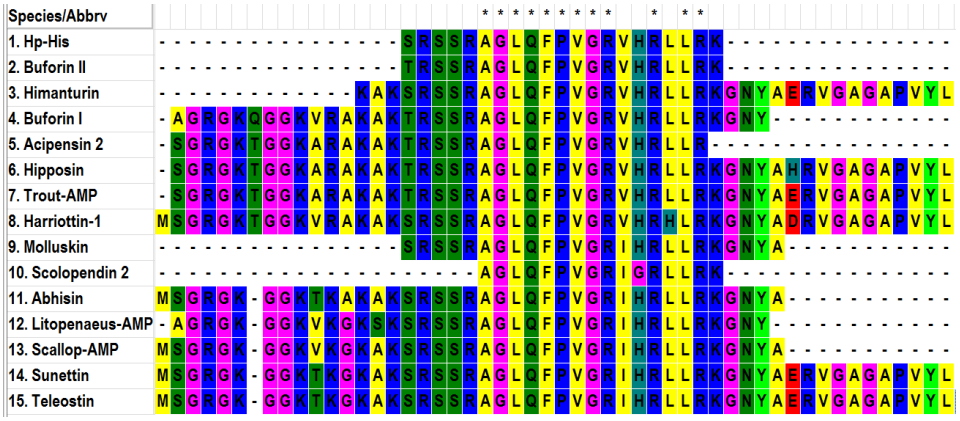


**(b)**

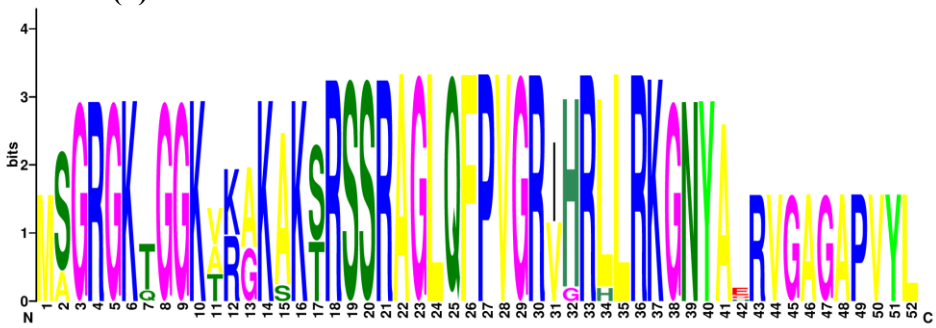


**Fig. 5.2** (a) Multiple sequence alignment of the amino acid sequence of *Hp*-His with different histone H2A derived peptides reported from various vertebrates and invertebrates. Identities are shaded dark with the same colour and the consensus residues are indicated with an asterisk. (b) WebLogo graphical representation of the sequence similarity and the consensus pattern within the multiple aligned sequence members.

Helical wheel projection of *Hp*-His with Hydrophobic Moment (HM) displacement of 3.36 and HM angle of 289.5 is represented in Fig. 5.3. Helical wheel analysis depicted the amphipathic nature of *Hp*-His with hydrophobic and hydrophilic residues placed on opposite sides of the wheel. Hydrophobic residues such as Alanine (A), Leucine (L), Phenylalanine (F), Valine (V) and hydrophilic residues such as serine (S), lysine (K), histidine (H), arginine (R), glutamine (Q) were found to occupy opposite positions in the helical wheel. Furthermore, APD3 analysis indicated the presence of 5 residues on the hydrophobic surface of *Hp*-His accounting for GRAVY of -0.643. In addition, hydrophobicity analysis of *Hp*-His by Kyte-Doolittle plot confirmed the abundance of hydrophobic amino acids, concentrated towards the centre of the peptide (Fig. 5.4)

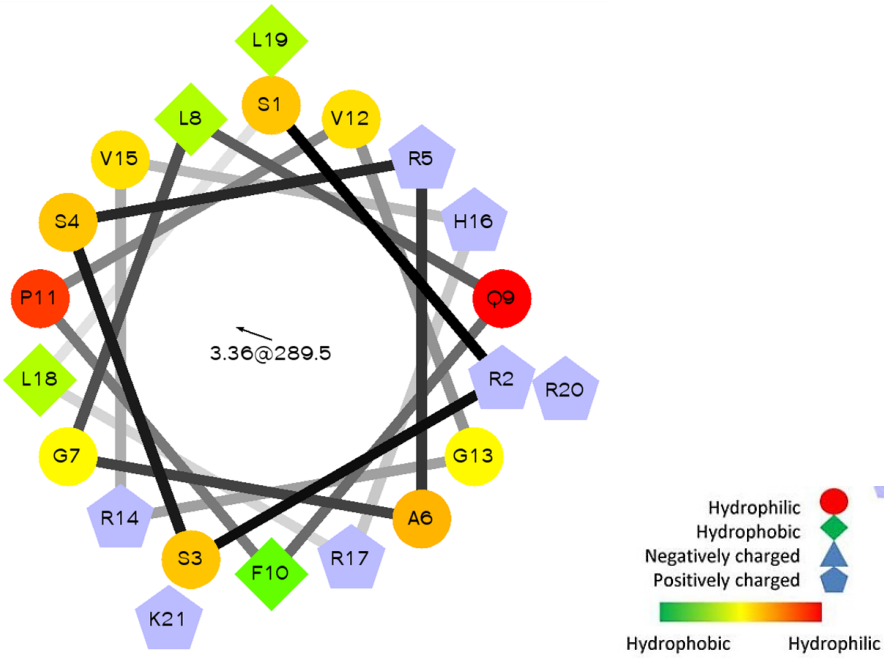


**Fig. 5.3** The helical wheel diagram demonstrating the probable amphipathic α-helical conformation of *Hp*-His.

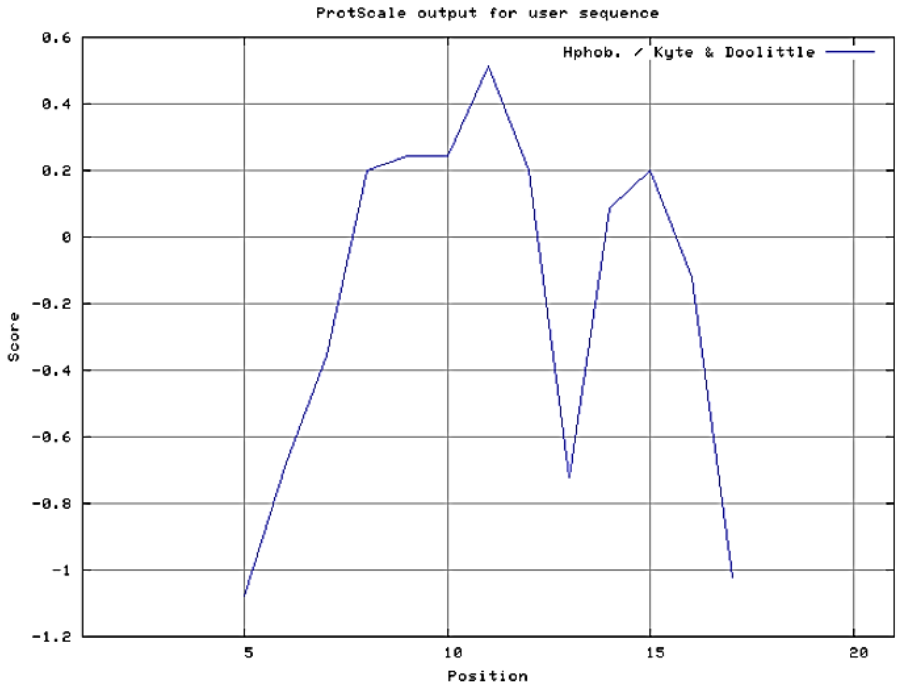


**Fig. 5.4** Schematic representation of the Kyte-Doolittle plot showing the hydrophobic nature of the predicted peptide of *H. pastinacoides, Hp*-His. The hydrophobic moieties clustered in the central region of the peptide are indicated by the peaks above the value (0.0).

Secondary structural elements prediction using POLYVIEW server demonstrated the presence of two α-helical regions in *Hp*-His (Fig. 5.5). The analysis results showed that *Hp*-His peptide contains 71.43 % α-helical region (15 amino acid residues) and 28.57 % coiled regions (6 amino acid residues). No β-sheet region has been noticed in the secondary structure of *Hp*-His. In *Hp*-His, $Arg^{2}$ to $Ala^{6}$ and $Val^{12}$ to $Lys^{21}$ constituted the α-helical regions while, $Ser^{1}$ and $Gly^{7}$ to $Pro^{11}$ formed the coiled regions.

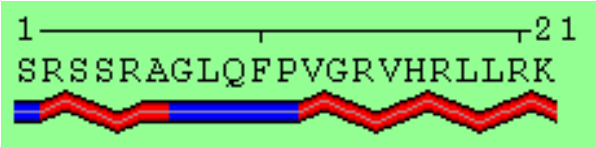


**Fig. 5.5** Secondary structure of *Hp*-His, predicted using POLYVIEW server. The α-helix regions are shown in red zig-zag lines and the coiled regions are shown in blue lines.

Predicted spatial 3D structure of *Hp*-His by homology modelling using crystal structure of native histone H2A (PDB ID: 2aro.1E) by SWISSMODEL server is given in Fig. 5.6b. The model depicted the occurrence of coil-helix-coil domain followed by another helix region (Fig. 5.6a).

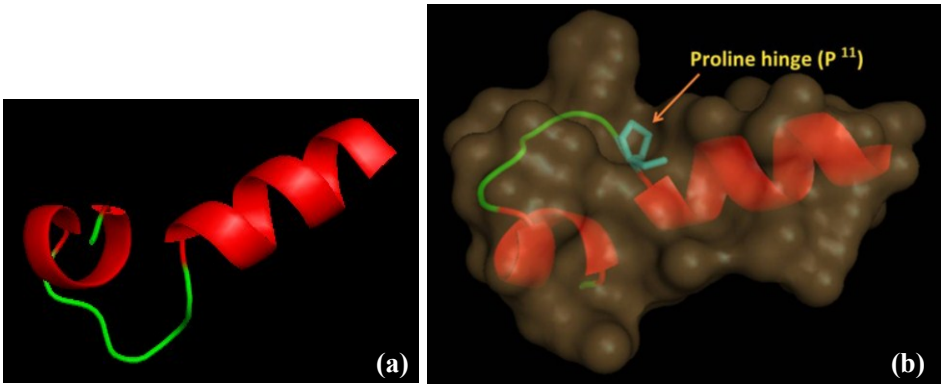


**Fig. 5.6** (a) A ribbon view of the 3D structure of *Hp*-His based on homology modelling using the PDB ID: 2aro.1E, generated by SWISSMODEL server. (b) The spatial structure of *Hp*-His showing the conformationally important proline residue as a cyan stick.

The apparent antimicrobial activity of *Hp*-His was predicted by APD3 with a protein-binding potential (boman index) and wimley-white whole-residue hydrophobicity of 3.38 kcal/mol and 4.15 kcal/mol respectively. Additionally, sequence alignment of *Hp*-His with other peptides in the APD3 database exhibited 95.23 % similarity with Buforin II followed by

66.66 % and 55.55 % similarity with Scolopendin 2 and Acipensin 2 respectively. The CAMPR3 database with its several algorithms such as support vector machine {0.684}, random forest classifier {0.614}, discriminant analysis classifier {0.865} and artificial neural classifier calculated the AMP probability percentage of *Hp*-His. The values of the calculated probability are given in curly brackets.

### 5.3.2 Purification and molecular mass determination of synthetic *Hp*-His

The RP-HPLC chromatogram obtained for synthetic *Hp*-His is shown in Fig. 5.7. HPLC enabled more than 95 % purification of *Hp*-His, as marked by the main peak at retention time 11.481 min in Fig. 5.7.

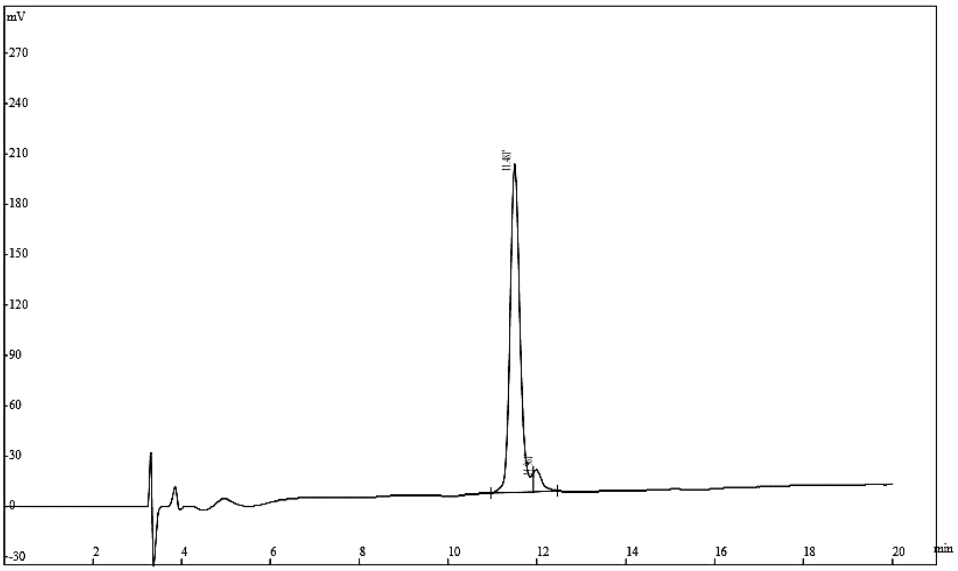


**Fig. 5.7** Chromatographic profile of synthetic peptide, *Hp*-His (RP-HPLC, Welchrom C18, 4.6×250 mm, flow rate: 1.0 ml/min). The chromatogram shows a major peak at retention time of 11.481 min.

The molecular weight of the synthetic peptide *Hp*-His (2851.25 Da) was confirmed by ESI mass spectroscopy. The ESI mass spectrum of *Hp*-His is shown in Fig. 5.8. The mass spectrum illustrates the mass to charge ratio (m/z) from 300 to 1500 of all the ionized particles present in the sample. The most abundant ion seen in the spectrum is at a mass to charge ratio of 571.4. This m/z matches with the *Hp*-His ionized to +5 (rounded off MW = 2851.25 Da + 5H+ = 2856.25). As a result, the mass to charge ratio is 2856.25/5 = 571.25. The other relatively abundant ions recognised in the spectrum were m/z of 476.4 ionized to +6 (round off MW = 2851.25 Da + 6H+ = 2857.25) and m/z of 713.7 ionized to +4 (round off MW = 2851.25 Da + 4H+ = 2855.25), resulting in a mass to charge ratio of 476.21 and 713.81 respectively. Thus, the spectra reveal the molecular mass of the peptide to be 2.8 kDa or 2851.25 Da, which coincides with the theoretical calculated mass of *Hp*-His .

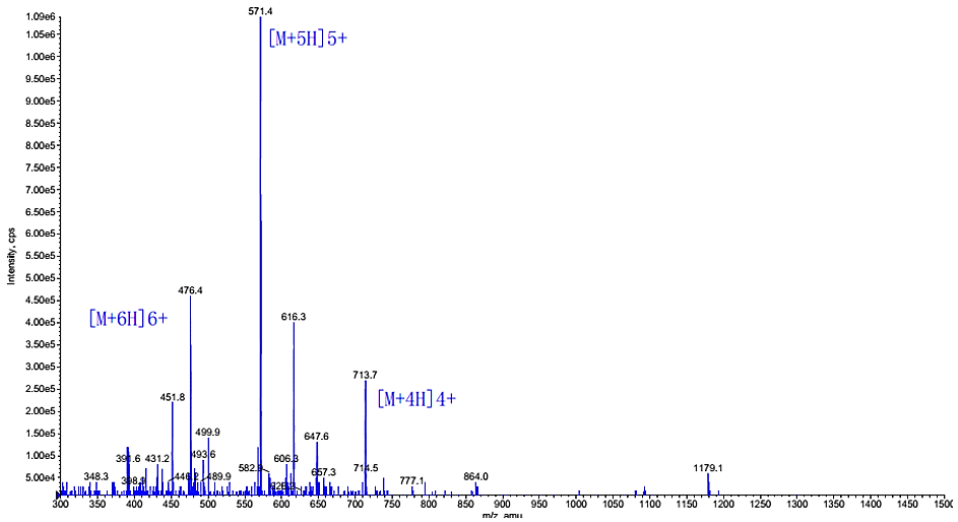


**Fig. 5.8** ESI Mass Spectrum of synthetic *Hp*-His. The most abundant ions in the spectrum is seen at m/z of 571.4 [M+5H]5+ followed by 476.4 [M+6H]6+.

### 5.3.3 Haemolytic activity

Different concentrations (400 µM to 3.125 µM) of synthetic peptide *Hp*-His was tested for haemolytic activity towards human RBCs. Results indicate insignificant haemolysis of about 9 % even at highest tested concentration of *Hp*-His . The reference peptide mellitin, yielded about 71 % and 85 % haemolysis activity at 200 µM and 400 µM. Thus the *Hp*-His peptide exhibited little haemolytic effect at the tested concentrations (Fig. 5.9).

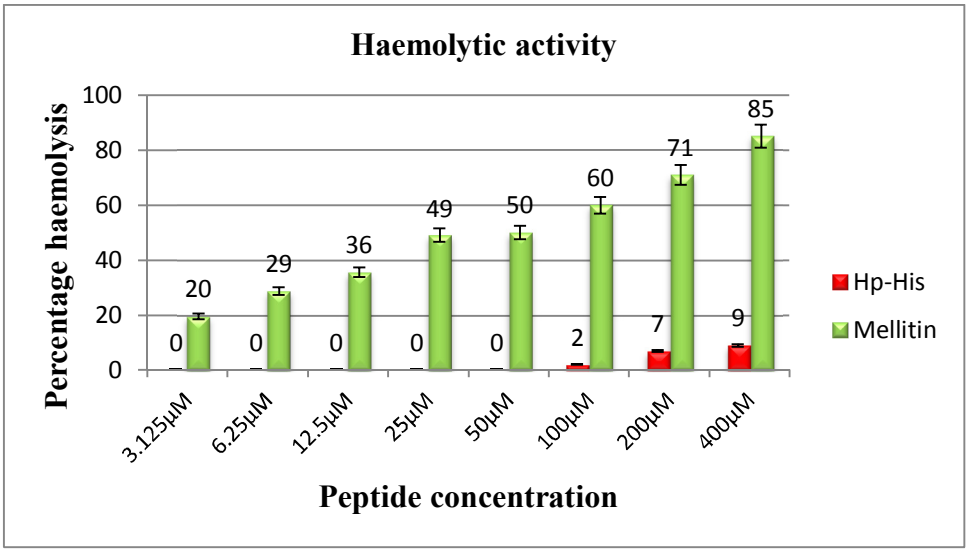


**Fig. 5.9** Haemolytic activity of the synthetic *Hp*-His and mellitin against human RBCs at various concentrations.

### 5.3.4 Antimicrobial activity

To determine whether the synthetic *Hp*-His was biologically functional, the antimicrobial activity of *Hp*-His was determined against a series of microorganisms by both, broth microdilution assay and bactericidal assay. Different concentrations ranging from 1.625 µM to 50 µM of

*Hp*-His was assayed to analyse the inhibitory effect of *Hp*-His on the microbes. Synthetic peptide, *Hp*-His exhibited a stronger antibacterial activity against the major fish pathogens *V. vulnificus* and *V. alginolyticus* with MIC and MBC of 25 µM each. Furthermore, the peptide also displayed significant activity against other Gram-negative pathogens such as *E. tarda, A. hydrophila* and *E. coli* with MIC values at 50 µM. However, the MBC values for those microbes were demonstrated to be greater than the highest tested concentration. Other tested pathogens were also found to be sensitive to synthetic *Hp*-His, but the MIC and MBC values were found to be >50 µM. The antibacterial activity of *Hp*-His against all the tested bacteria is shown in Fig. 5.10 (a-k). At the highest tested concentration of 50 µM, the percentage inhibition obtained for each of the tested bacteria were 79 % for *S. aureus*, 67 % for *B. cereus*, 99 % for *E.coli, 91* % for *V. cholera*, 99 % for *V. alginolyticus*, 87 % for *V. proteolyticus*, *99* % for *V. vulnificus, 87* % for *V. parahaemolyticus, 99* % for *A. hydrophila, 89* % for *P. aeruginosa* and 99 % for *E. tarda*.

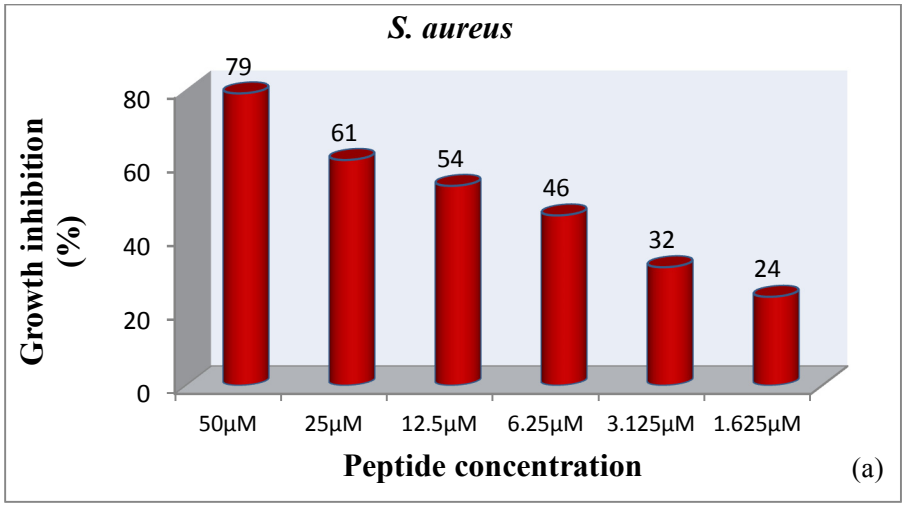


*Fig. 5.10 Continued…*

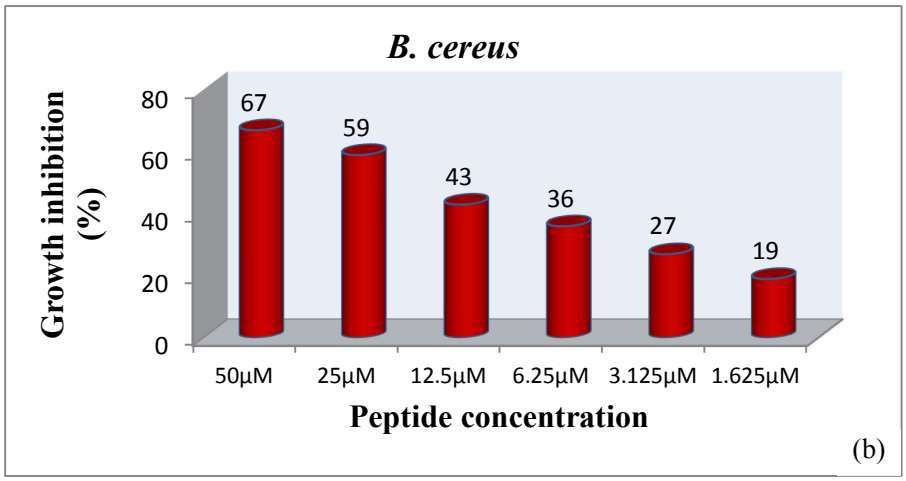


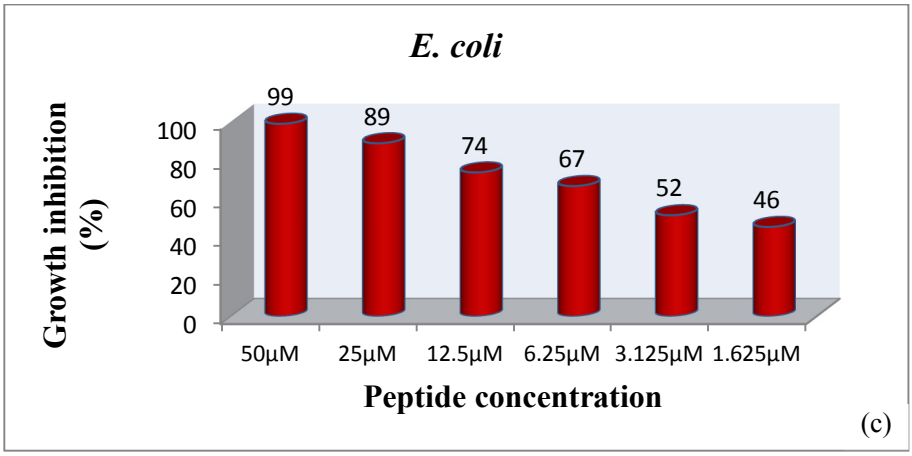


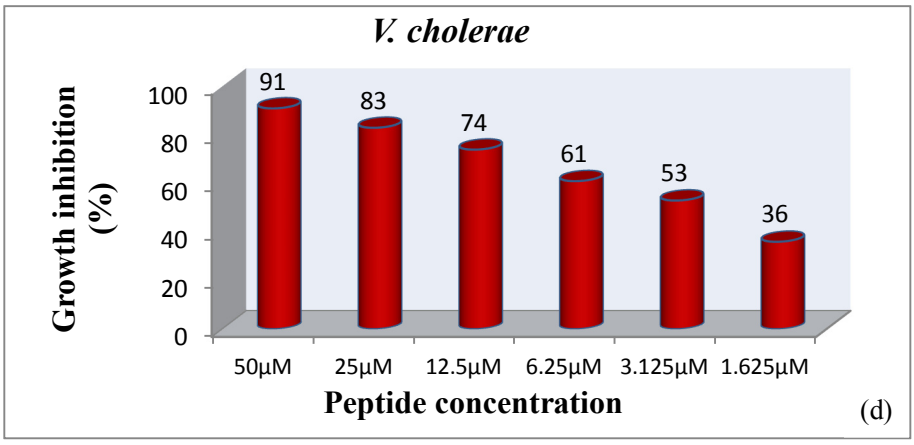


*Fig. 5.10 Continued…*

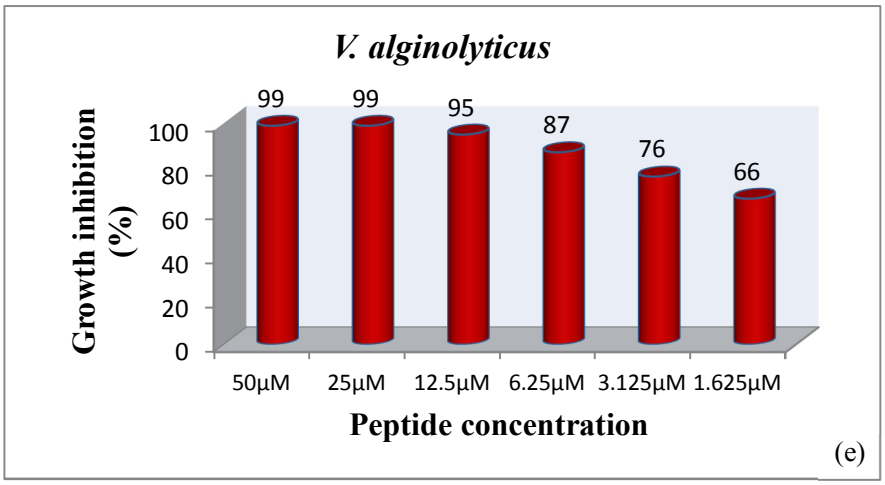


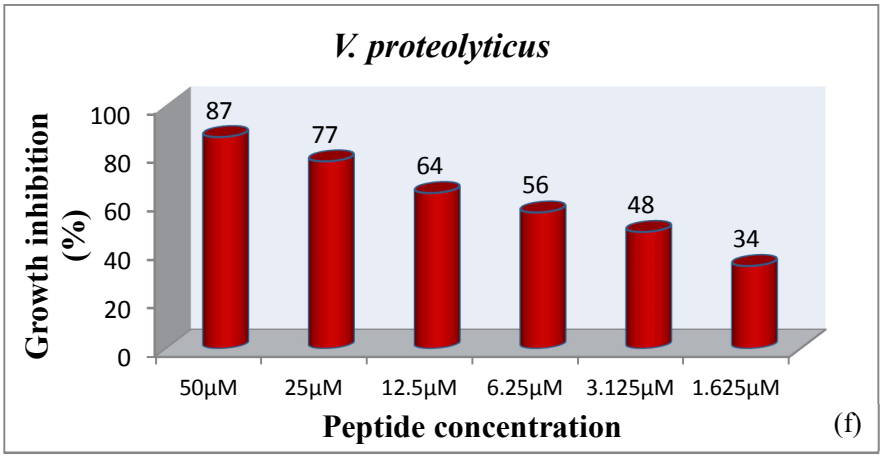


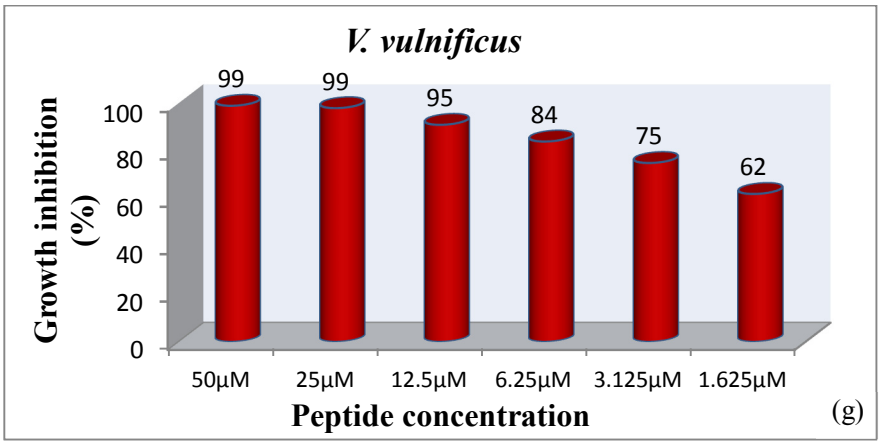


*Fig. 5.10 Continued…*

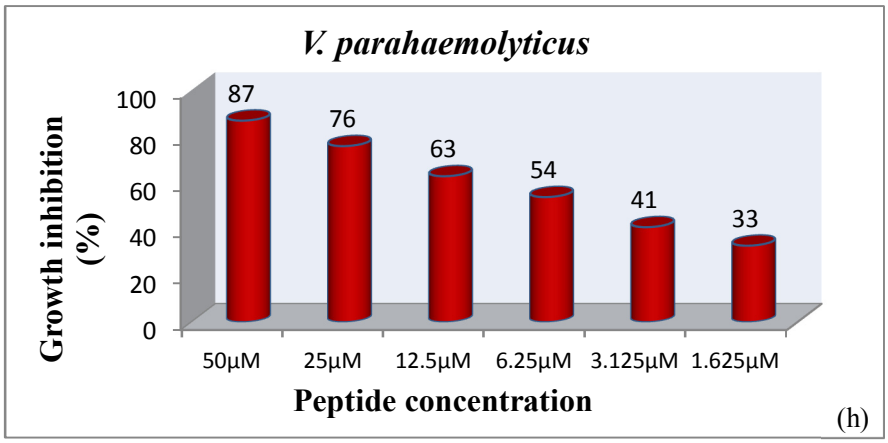


(h)

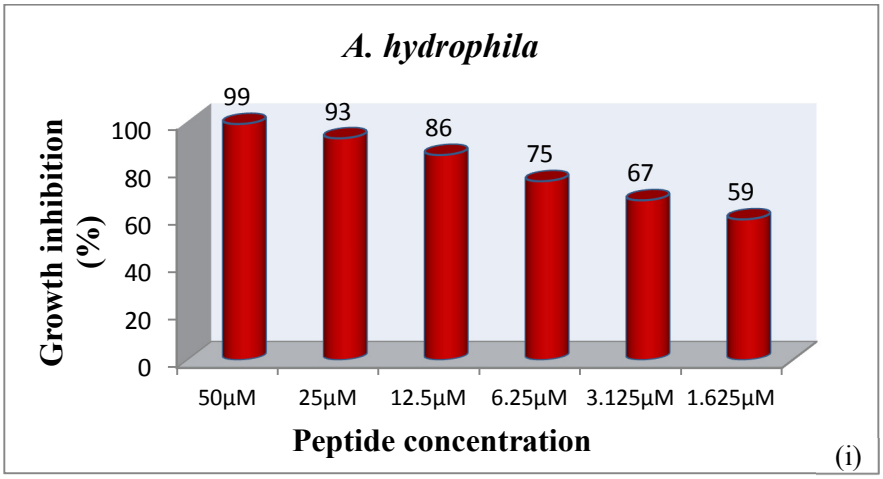


(i)

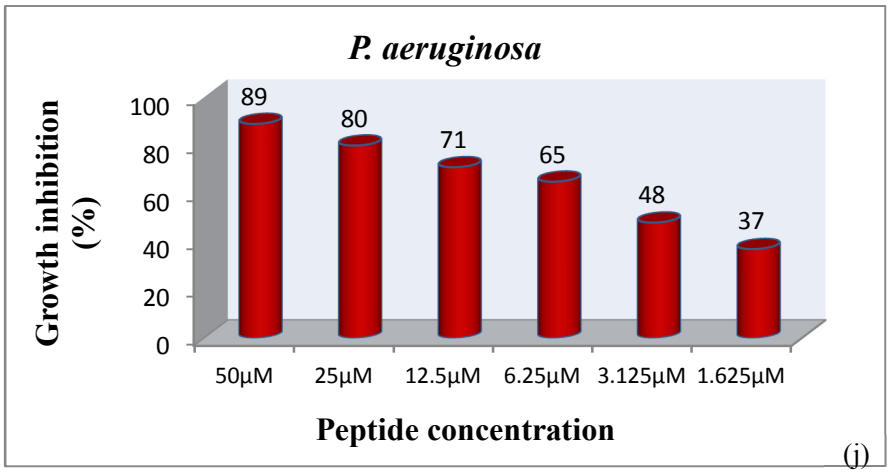


(j)

*Fig. 5.10 Continued…*

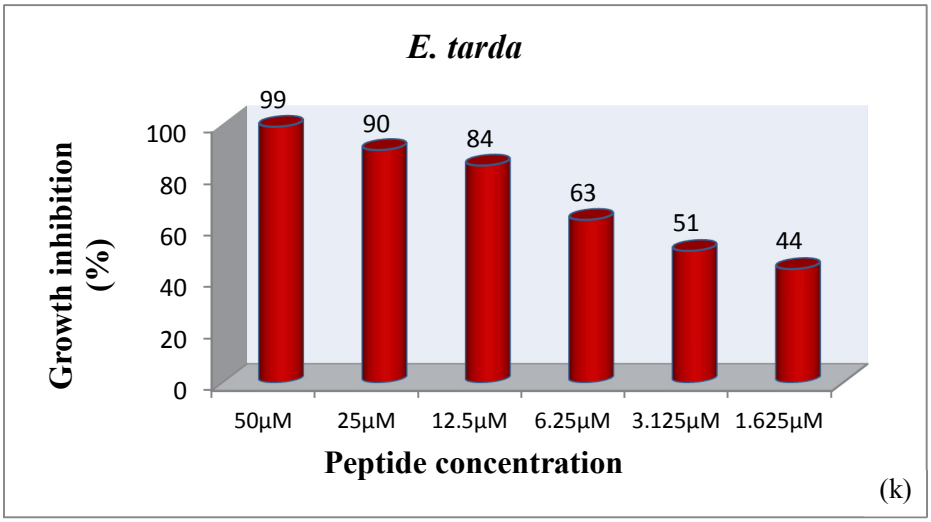


**Fig. 5.10** (a-k) Antimicrobial activity of synthetic *Hp*-His peptide against the bacterial pathogens at various concentrations.

### 5.3.5 PI staining

Intercalation of PI with bacterial DNA in dead cells resulted in the visualization of those cells as red under Epifluorescence Microscope. Since the peptide is marked with a FITC tag, bacterial cells could also be observed as green through the FITC filter. Images were taken with two different filters for PI and FITC on the same microscopic field of Epifluorescence Microscope. Except for *E. tarda*, almost all cells which emitted the green fluorescence also emittted the red fluorescence in the images taken from the same field indicating the lethal effect of *Hp*-His peptide on bacterial cells. Thus the mode of action of *Hp*-His was believed to be mainly due to membrane pore formation.

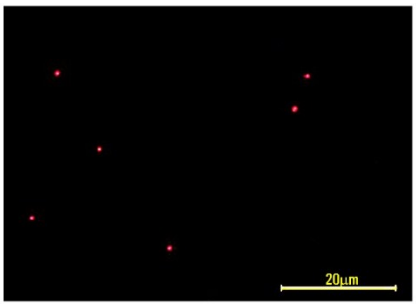


Untreated *V. vulnificus*

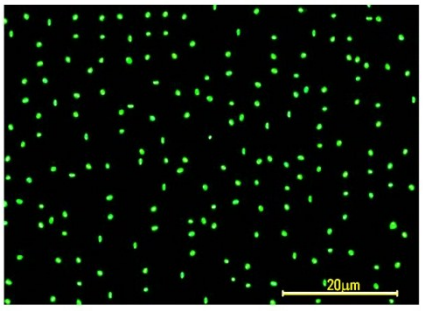


*Hp*-His treated *V. vulnificus* (FITC filter)

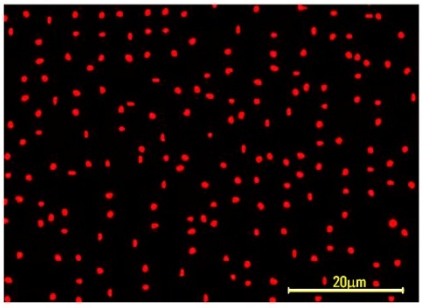


*Hp*-His treated *V. vulnificus* (PI filter)

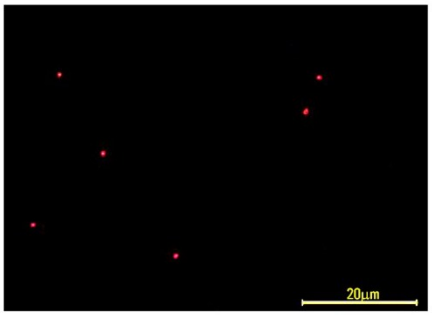


Untreated *V. alginolyticus*

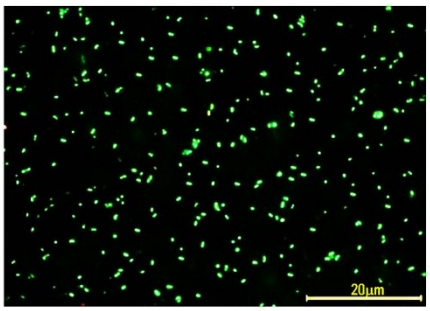


*Hp*-His treated *V. alginolyticus* (FITC filter)

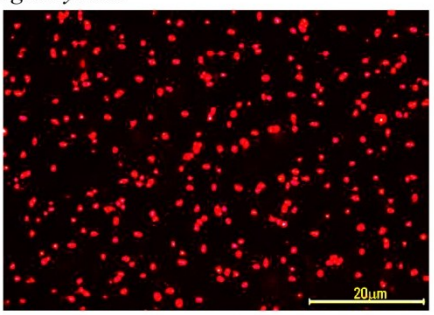


*Hp*-His treated *V. alginolyticus* (PI filter)

*Fig. 5.11 Continued…*

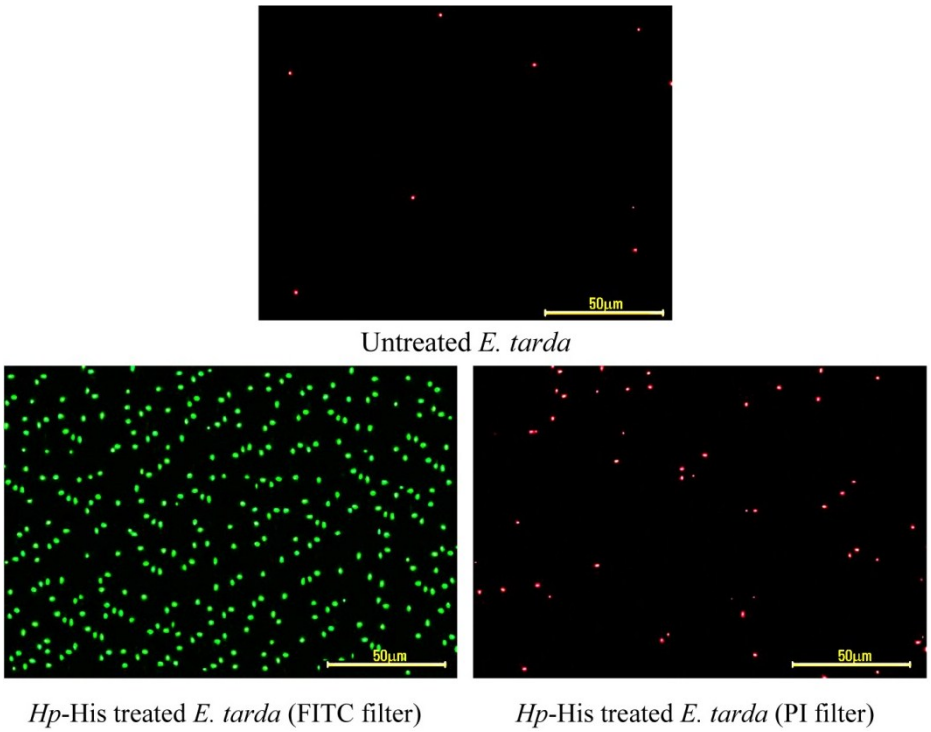


**Fig. 5.11** PI stained images of untreated control bacterial cells and synthetic *Hp*-His treated *V. vulnificus*, *V. alginolyticus* and *E. tarda* cells taken under FITC filter and PI filter.

### 5.3.6 SEM analysis

To further investigate and confirm the mechanism of action in bacterial cells, *Hp*-His treated bacteria were analysed using scanning electron microscopy (SEM) and morphological changes observed were noted. Representative SEM images of the cells treated with the peptide and the control cells are given in Fig. 5.12. Untreated cells were seen to have an intact cell membrane with regular morphology. In contrast, the cells that have been treated with *Hp*-His displayed visibly disrupted membranes and leakage of cytoplasmic contents, except *E. tarda*, which indicated the membranolytic activity of the peptide.

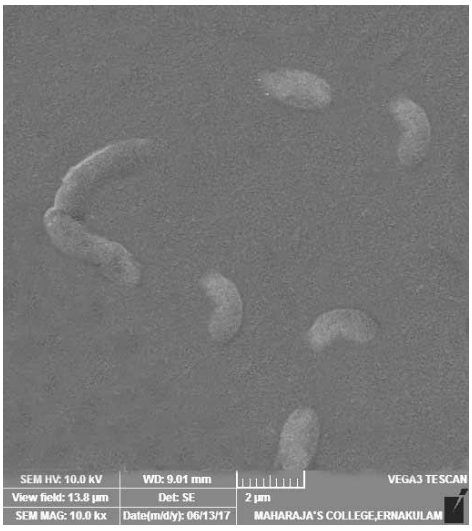


Untreated *V. vulnificus*

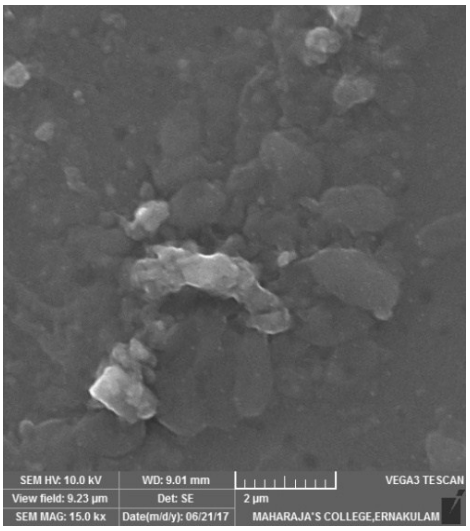


*Hp*-His treated *V. vulnificus*

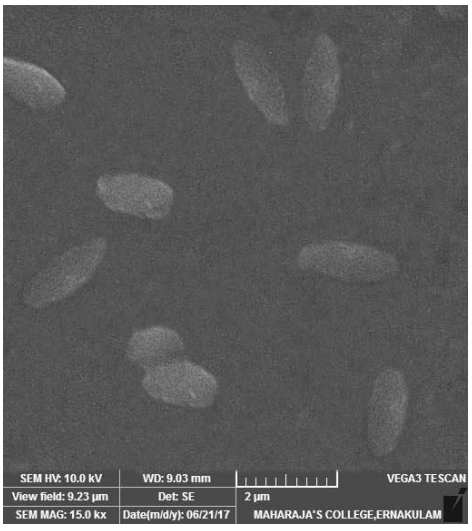


Untreated *V. alginolyticus*

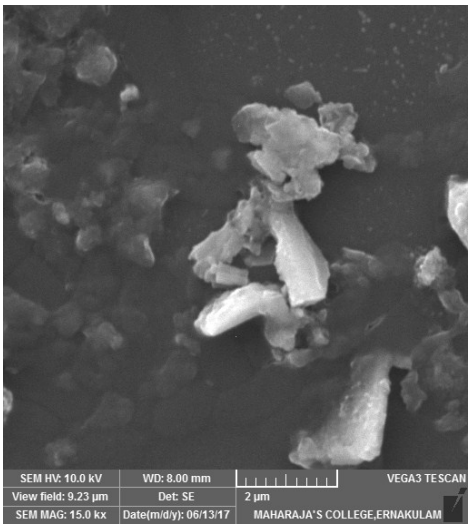


*Hp*-His treated *V. alginolyticus*

*Fig. 5.12 Continued…*

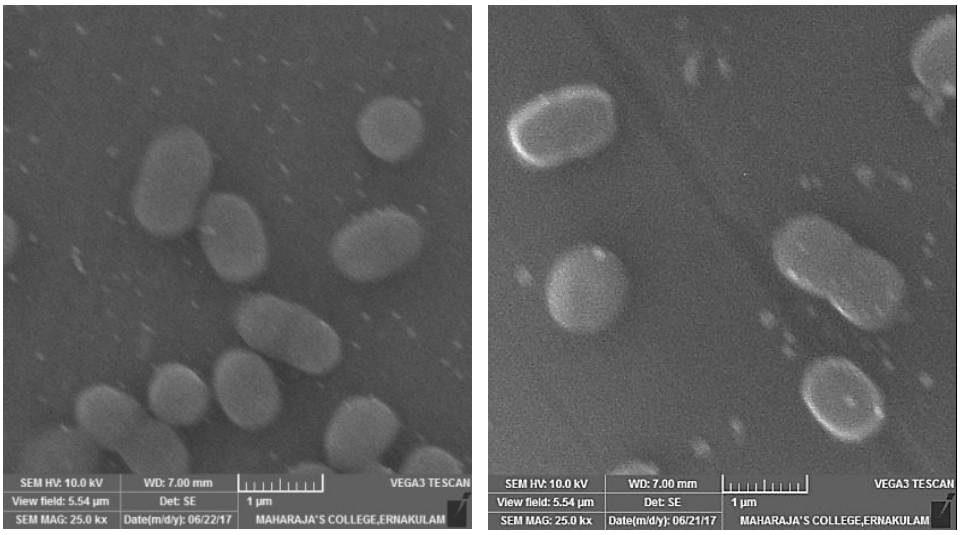


Untreated *E. tarda* *Hp*-His treated *E. tarda*

**Fig. 5.12** Effects of synthetic peptide, *Hp*-His treatment on bacterial cell membranes observed using scanning electron microscopy. Untreated cells show a normal smooth surface, while cells treated with *Hp*-His reveal a disrupted cell membrane, except for *E. tarda*.

### 5.3.7 DNA Binding assay

*Hp*-His peptide was tested for its DNA binding activity to verify the option of peptide targeting the bacterial DNA. DNA binding ability of synthetic *Hp*-His was tested with 50 ng of pUC-18 plasmid from a concentration of 200 µM – 1.625 µM. *Hp*-His was shown to effectively retard the electrophoretic mobility of pUC-18 plasmid from a concentration of 25 µM to 200 µM (Fig. 5.13). The retarded plasmid when treated with the peptide could be clearly seen from the agarose gel image depicting the DNA binding activity of *Hp*-His. In contrast, the electrophoretic mobility of the untreated plasmid control remains unaffected. Also, the DNA binding ability of *Hp*-His was found to be concentration dependent. The ability of synthetic *Hp*-His to bind the DNA

indicates its additional mode of action which involves cytoplasmic targets such as DNA.

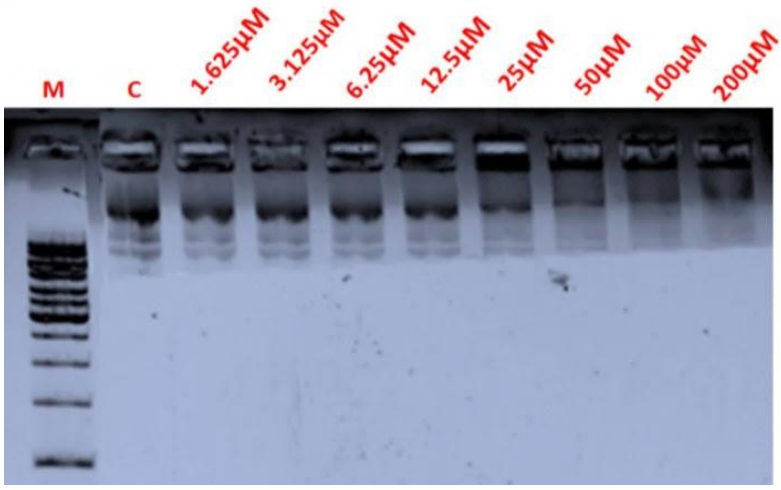


**Fig. 5.13** Agarose gel image of the DNA binding assay of synthetic *Hp*-His. Lane M: 1 kb ladder, Lane 1: control plasmid, Lane 2-9: 1.625 µM to 200 µM concentration of peptide with 50 ng of pUC-18 vector.

### 5.3.8 *In vitro* cytotoxicity assay

Cell viability of *Hp*-His treated NCI-H460 and HEp-2 cell lines were tested from 200 µM to 1.625 µM by XTT assay. The *in vitro* cytotoxic activity displayed by *Hp*-His peptide against NCI-H460 and HEp2 cell lines is represented in Fig. 5.14a. At the highest tested concentration of 200 µM, the peptide was found to be cytotoxic to both cell lines; with an observed growth inhibition of 62 % for NCI-H460 cell line and 49 % for HEp-2 cell line. The cytotoxic activity of mellitin is also represented in Fig. 5.14b, for comparison. The $IC_{50}$ value of *Hp*-His against NCI-H460 cells was estimated to be 114.124 ± 44.276 µM and for HEp-2 cells 206.697 ± 49.212 µM.

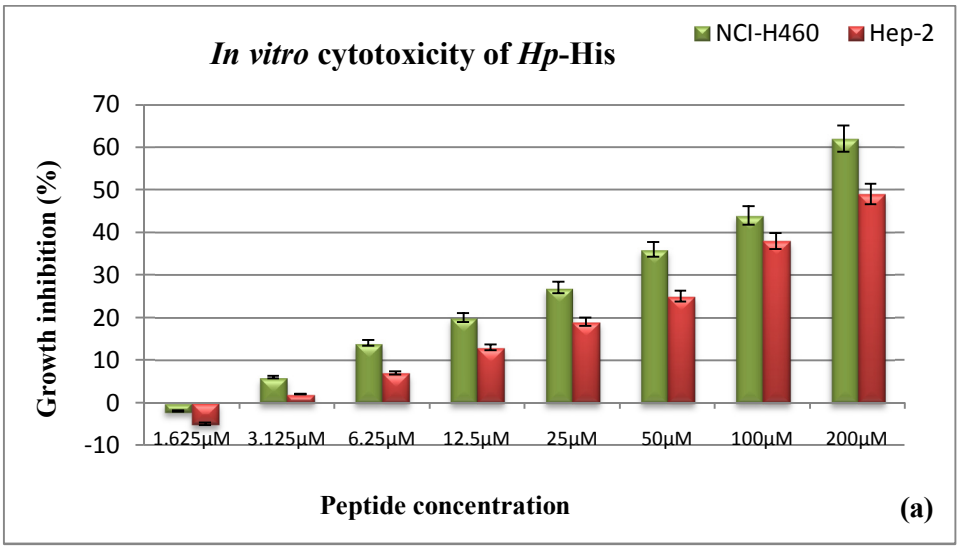


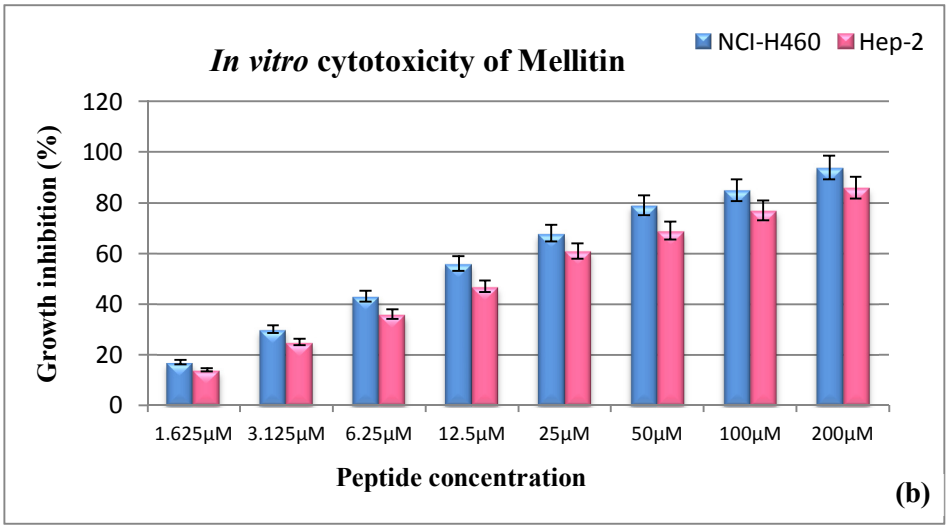


**Fig. 5.14** *In vitro* cytotoxicity of (a) synthetic *Hp*-His and (b) mellitin in HEp2 and NCI-H460 cells at various tested concentrations.

### 5.3.9 Anticancer activity

#### 5.3.9.1 Gene expression profile of cancer related genes in *Hp*-His treated NCI-H460 cancer cells

*In vitro* anticancer activity was analysed against NCI-H460, non-small cell lung cancer cell lines with two different dosages of *Hp*-His synthetic peptide *viz*., 25 µM and 50 µM. Relative gene expression of *Hp*-His treated NCI-H460 cell lines was studied using real-time PCR (RT-PCR). The genes analysed were found to be differentially expressed at the tested concentrations with respect to the untreated control (Fig. 5.15). In response to 25 µM and 50 µM *Hp*-His, upregulation of Caspase-3, Caspase-9, p53 and Bax could be noticed. On the other hand, expression levels of Bcl2, and iKbα were found to be downregulated. Significant up-regulation of non-caspase proteases such as Calpain-5 and Cathepsin-G could be observed in NCI-H460 cells co-treated with the peptide. Moreover, some of the genes such as MAPK-1F, JNK (cell cycle associated genes) and interferon related immune genes like MX1F were also significantly induced in response to synthetic peptide *Hp*-His treatment. Altogether, the synthetic peptide *Hp*-His could exhibit significant anticancer activity against NCI-H460 cells.

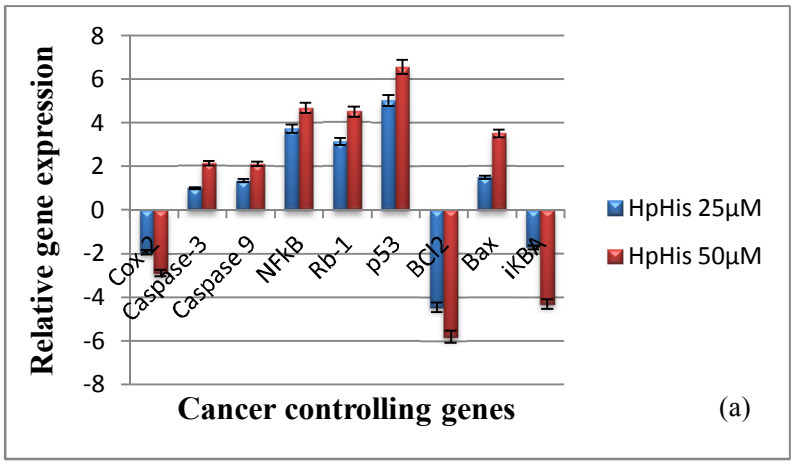


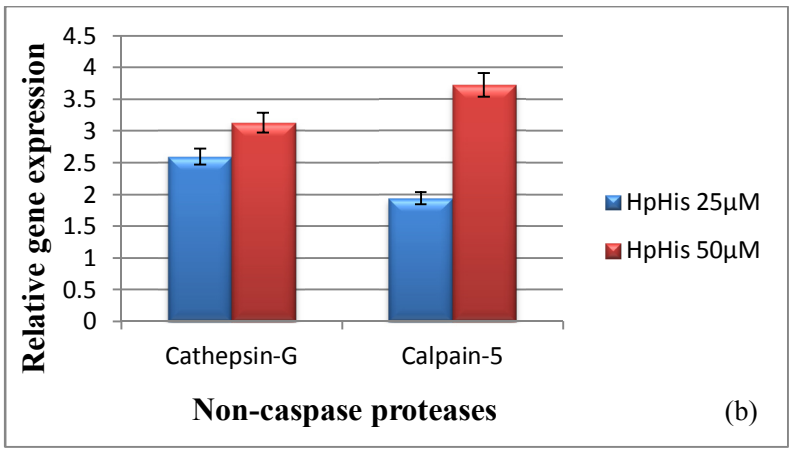


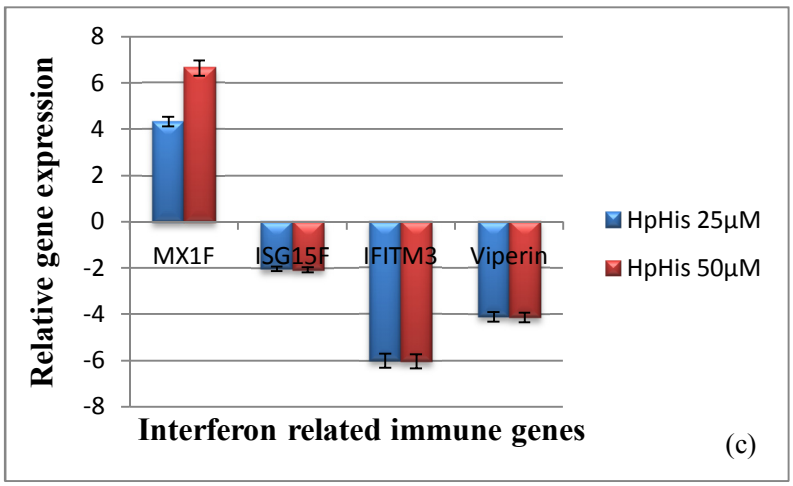


*Fig. 5.15 Continued…*

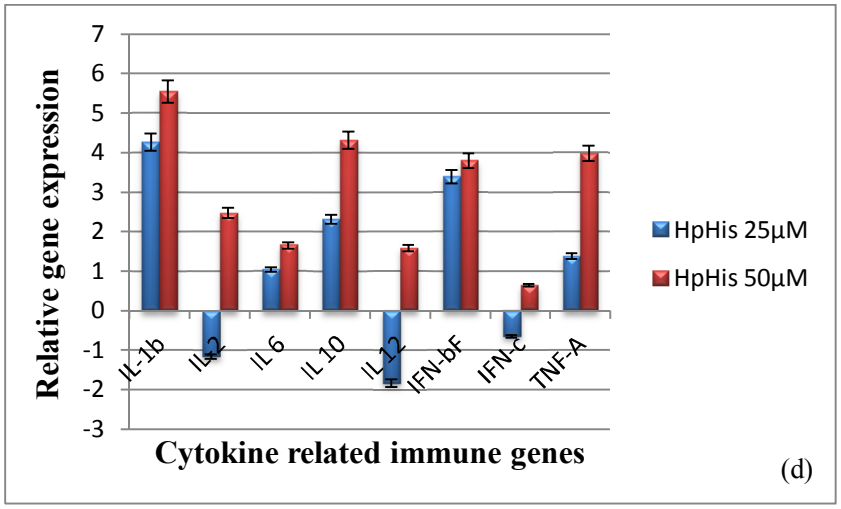


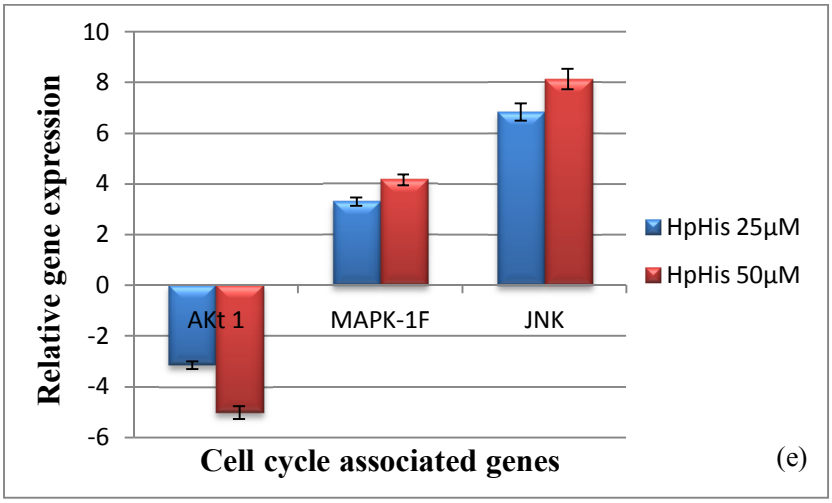


**Fig. 5.15** (a-e) Gene expression pattern of different cancer related genes using real time PCR in *Hp*-His peptide treated NCI-H460 cell lines.

#### 5.3.9.2 Gene expression profile of cancer related genes in *Hp*-His treated HEp-2 pharyngeal cancer cells

Two different concentrations of *Hp*-His, 25 µM and 50 µM were screened for its *in vitro* anticancer activity in HEp-2 cell lines and the relative expression of different cancer controlling genes were analysed by qPCR (Fig. 5.16). Significant upregulation of the major cancer regulating genes such as Cox-2, Caspase-3, Caspase-9, NFkB, Rb-1, p53, and Bax could be detected. Also, down-regulation of cancer controlling Bcl2 and iKBA were also noticed following *Hp*-His treatment. The gene expression levels of non-caspase proteases *viz.*, Cathepsin-G, Calpain-5 were found to be higher. Expression of all the cytokines related genes were observed to be greater, than in the untreated group (control). Moreover, their level of expression was examined to be proportional to the concentration of *Hp*-His, except IL-2, IL-6 and IL-12. Enhanced expression of cell cycle associated genes like the MAPK and JNK were also identified in *Hp*-His co-treated HEp-2 cells. Thus the synthetic peptide, *Hp*-His had demonstrated to exhibit significant anticancer activity against the HEp-2 cell lines.

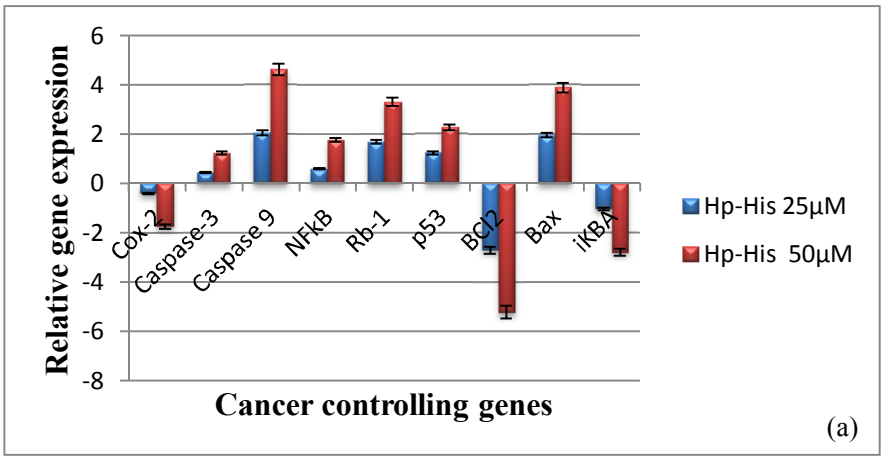


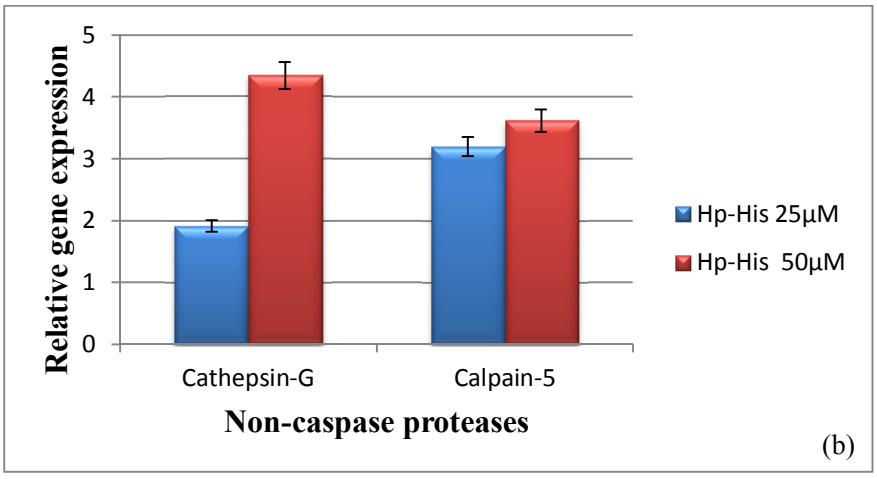


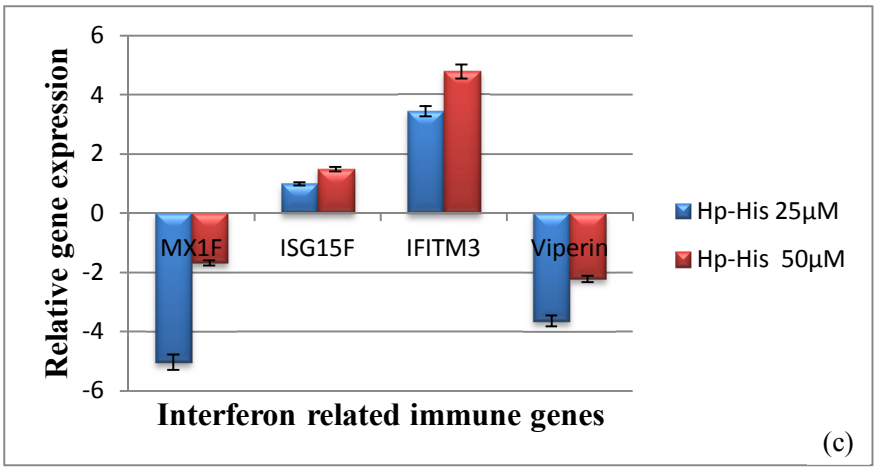


*Fig. 5.16 Continued…*

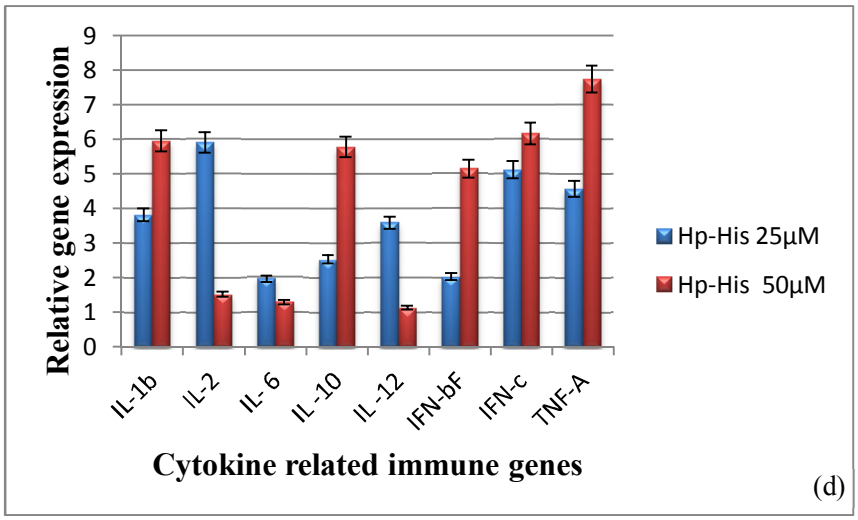


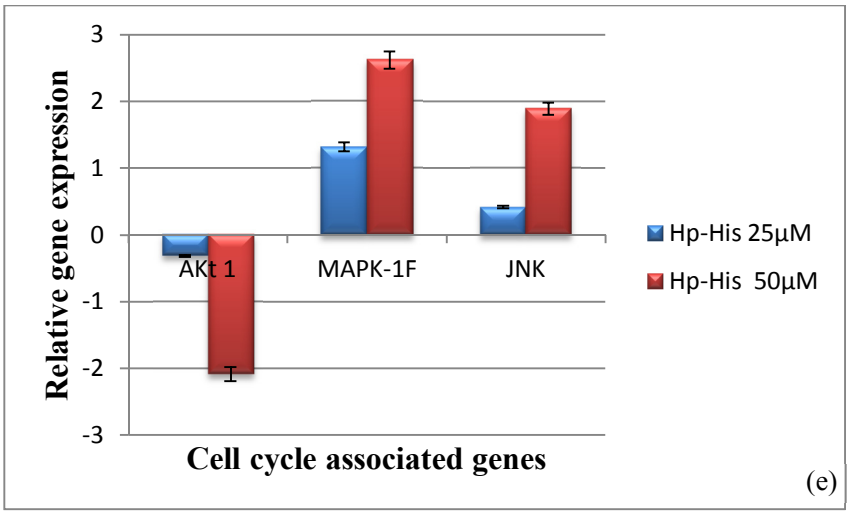


**Fig. 5.16** (a-e) Relative gene expression profile of different cancer related genes in synthetic *Hp*-His peptide treated NCI-H460 cell lines.

## 5.4 Discussion

AMPs are considered to be vital effector molecules of humoral components in fish innate immune system by involving in rapid and non-specific exclusion of pathogenic microorganisms. Most of the AMPs

are derived from precursor molecules encoded by dedicated genes, but some are the result of proteolysis of larger proteins with other functions (Papareddy et al., 2010). Histones constitute the major protein component of chromatin and are known to function in nuclear targeting and regulation of gene expression (Balicki et al., 2002). Histone H2A represent one of the core histones which, together with histones H2B, H3 and H4, forms the nucleosome and has therefore been classically associated with DNA packaging (Dong et al., 1991). Histone derived antimicrobial peptides are identified as a family of cationic helical peptides which are derived from their histone precursors by the action of proteolytic enzymes. As a matter of fact, studies pertaining to AMPs derived from precursor peptides with known function would help to better understand the new mechanisms of immune response in the host defence of both vertebrates and invertebrates (Bulet et al., 2004; Nijnik and Hancock, 2009). In the present study, a histone derived AMP from Himanturin (Sathyan et al., 2012a) designated as *Hp*-His, have been identified and characterized. The antimicrobial and anticancer activities were also studied with the synthetic peptide.

It is well known that, fish and amphibian histone H2A derived peptides have been isolated from skin secretions after undergoing proteolytic cleavage by proteases (pepsin isozymes (Ca and Cb) and cathepsin D) released from the unkeratinized skin epidermis. In addition, immunohistochemical analysis also revealed that unacetylated histone H2A acted as a precursor for both parasin I and buforin I (Kim et al., 2000; Cho et al., 2002a). To explore this idea of action of proteolytic enzymes, Himanturin was analysed by the PeptideCutter tool and

revealed the presence of cleavage sites for trypsin, which would give rise to 21-mer active *Hp*-His. Homology search using BLASTn disclosed that *Hp*-His belongs to the Histone H2A family. Regarding the amino acid sequence, the *Hp*-His H2A was almost identical to other known H2A counterparts.

ClustalW multiple alignment defined the conserved residues among the H2A sequences of both vertebrates and invertebrates. The highest sequence identity over 95 % was observed with Buforin II. To mention the difference between the two, the N-terminal hydrohilic threonine of Buforin II is replaced by a more hydrophilic serine residue in *Hp*-His. The findings of the above data and the characteristic similarities of *Hp*-His with other AMPs add weight to evidence that vertebrate and invertebrate H2A-derived AMPs originate from a common ancestral gene.

*Hp*-His is a 21 amino acid cationic peptide having a net positive charge of +6, molecular weight of 2.42 kDa, *p*I of 12.6 and hydrophobicity of 33 %. Moreover, the cationicity of *Hp*-His was found to be contributed largely by the arginine residues, which is an essential characteristic of an AMP (Boman 2003; Nam et al., 2012). Malmsten et al. (2007), Svensson et al. (2010) and Pasupuleti et al. (2012) observed that the net charge beyond a certain limit may not increase the antimicrobial activity owing to the strong interactions between the peptide and phospholipid head groups, which further prevents structuring and translocation of the peptide into the deeper layers of membranes. However, several studies reported that increasing the hydrophobicity to some extent increases the antimicrobial activity of the peptide (Zelezetsky and Tossi, 2006; Chen et

al., 2007; Pasupuleti et al., 2009). Secondary structural analysis of *Hp*-His was in accordance with the findings of Boman (2003) and Papagianni (2003) with more number of α-helices in the structure. Nevertheless, the net charge, helical propensity and hydrophobicity of AMPs vary from species to species leading to the diversity in the AMPs activity.

It is a well-established fact that the ability of antimicrobial peptides to interact with and insert into negatively charged cytoplasmic membranes of microbial cells are ascribed to the presence of spatially segregated hydrophobic and cationic domains (Zasloff, 2002). Also, the amphipathicity of the peptide is usually segregated along the axis of the α-helix such that during the initial lipid interactions the peptide lie parallel to the membrane with the charged side facing outward towards the head groups and the hydrophobic side embedded into the acyl tail core (Haney et al., 2009). Thus, this uneven distribution of hydrophobic and charged moieties contributes to the amphipathic nature of the peptide which has a profound effect on peptide disruption of natural bio-membranes (Yeaman and Yount, 2003; Teixeira et al., 2012). Also, this cationic/hydrophobic balance was shown to be an important factor in influencing both the antimicrobial and haemolytic activity of the peptide (Kuroda et al., 2009; Kuroda and Caputo, 2013; Takahashi et al., 2017). Besides, the helical wheel projection of *Hp*-His clearly indicated that it adopts an amphipathic structure with patches of hydrophobic and hydrophilic residues clustered opposite to each other. Therefore, as an amphipathic α-helical antimicrobial peptide, *Hp*-His could attach to the bacterial cell by assembling their axes parallel to the membrane plane. The positioning of the hydrophobic residues in *Hp*-His were in line with the previous reports (Tossi et al.,

2000; Arockiaraj et al., 2013; Chaithanya et al., 2013; Chaurasia et al., 2015; Chen et al., 2015). Moreover, the findings of the KD plot supported the amphipathic character of *Hp*-His, demonstrating the role of hydrophobic residues in the partitioning of the phospholipid bilayers.

Studies on structure-activity relationship of AMPs have always produced new insights into unique molecular mechanism of antimicrobial action. Structural analysis of *Hp*-His revealed the presence of a proline hinge between the two helices, similar to Buforin II. The structure of Buforin II was elucidated by Yi et al. (1996) using NMR spectroscopy and restrained molecular dynamics. Yi and colleagues observed that Buforin II adopts a helix-hinge-helix structure in 50 % trifluoroethanol, with a N-terminal extended α-helix constituted by $Arg^{5}$–$Phe^{10}$ and a C-terminal α-helix represented by $Val^{12}$ - $Lys^{21}$. Both the terminal helices are separated by a proline residue ($Pro^{11}$) which acted as a hinge providing more flexibility to the amphipathic structure of Buforin II (Kobayashi et al., 2000). Park et al. (2000) disclosed the positional importance of this proline residue in its function. The proline residue was observed to be the key structural factor for the cell-penetrating property of buforin II. Spatial conformational studies of *Hp*-His also exhibited the same structural features indicating its ability to form a flexible random structure, much like Buforin II. Furthermore, APD3 proposed the antimicrobial property of *Hp*-His, as it showed significant similarity with the other reported AMPs in the database including a histone derived peptide, Buforin II from Asian toad, *Bufo gargarizans* (Park et al., 1996), a cationic AMP, Scolopendin 2 from Chinese red-headed centipede, *Scolopendra subspinipes mutilans* (Lee et al., 2015), a histone

derived peptide, Acipensin 2, from Russian sturgeon, *Acipenser gueldenstaedtii* (Shamova et al., 2014) and Buforin I from Asian toad, *Bufo gargarizans* (Park et al., 1996).

It was intriguing to ponder whether the peptide that would be formed from Himanturin by specific enzymatic cleavage would function separately in a mutually independent manner with dissimilar modes of action. The mechanisms of action of histone H2A derived AMPs described in the literature are slightly different. The main mode of action of buforin II is associated with its ability to penetrate into bacterial cells without causing significant damage to their cell membranes and to interact with nucleic acids, leading to inhibition of vital processes and to their death (Park et al., 1998; Cho et al., 2009; Elmore, 2012). However, another peptide, parasin, exerts its action by damaging the bacterial membranes (Koo et al., 2008; Zhao et al., 2015). A synthetic analogue of hipposin was also demonstrated to have a membrane permeability mode of action against *E. coli* (Bustillo et al., 2014).

Antimicrobial activity of histone H2A derived AMPs have been studied by several researchers (Park et al., 2000, Giacometti et al., 2000 Park et al., 2001; Birkemo et al., 2003; Fernandes et al., 2004; Li et al., 2007; Koo et al., 2008; Bustillo, 2013). Here, in this study, antimicrobial activity of *Hp*-His was carried out with a synthetic peptide with end modifications and FITC labelling. The incorporation of D-amino acids or modification of terminal regions of peptides by acetylation or amidation, in earlier studies have shown to improve their stability by preventing them from proteolytic degradation (McPhee et al., 2005; John et al., 2008;

Stromstedt et al., 2009). Thus the modifications generate a closer mimic of the native peptide increasing its biological activity. The results summarized in Fig. 5.10 for *Hp*-His, indicate a stronger inhibition of growth for *V. vulnificus* and *V. alginolyticus* with MIC of 25 µM. Pathogens like *E. tarda, A. hydrophila* and *E. coli* were found to be inhibited at 50 µM concentration of the peptide.

Microbicidal action of *Hp*-His was demonstrated by plating the peptide treated bacteria onto LB agar plates and the MBC was found to be 25 µM for *V. vulnificus* and *V. alginolyticus.* Additionally, the lethal effect of *Hp*-His against the bacterial pathogens was confirmed by epifluorescence microscopy with the FITC labelled *Hp*-His treated bacteria. In this study, *Hp*-His could induce the influx of PI into all the susceptible pathogens with cells emitting both red and green fluorescence, except for *E. tarda*. This observation suggests a membrane permeabilizing mode of action for these cells. However, for *E. tarda* membrane translocation mode of action was inferred as evidenced by lower red fluorescence and higher green fluorescence observed from the same field. Besides, SEM result directly presented evidence for the induced morphological changes for *V. vulnificus, V. alginolyticus*, *E. coli* and *A. hydrophila.* In contrast, little morphological change could be noticed for *E. tarda.* All the observed SEM results were in in accordance with the results of the PI uptake assays. Moreover, reports of peptides with such dual mode of action against different bacteria have been previously established in the case of other AMPs such as Bactenecins (Podda et al., 2006), Acipensins (Shamova et al., 2014) and SpHyastatin (Shan et al., 2016). However, the current study does not preclude *Hp*-His from

having yet other unidentified target and will be considered as a subject for future research.

To further understand the mode of action of *Hp*-His, gel retardation assay was performed with pUC-18 plasmid using different concentrations of the peptide. DNA binding activities of *Hp*-His could be detected down to the concentration of 25 μM. Uyterhoeven et al. (2008) analysed the nucleic acid binding properties of buforin II using molecular modelling and a fluorescent intercalator displacement assay and demonstrated the role of specific side chains ($R^2$ and $R^{20}$) of buforin II in forming stronger interactions with DNA than the nonspecific electrostatic ones. Recently, Sim et al. (2016) in his experiment with different combinations of DNA sequences discovered that the binding was mostly due to interactions between the peptide and phosphate backbone of nucleic acids, providing an explanation for the lack of sequence specificity observed experimentally. Thus, buforin II was shown to have high affinity for the DNA, and its antimicrobial activity has been found to be dependent upon this binding ability (Uyterhoeven et al., 2008). Since *Hp*-His shows striking similarity to buforin II it is expected to bind to the DNA by a mechanism similar to that of buforin II.

One of the most desired properties of AMPs is its low or no toxicity to eukaryotic cells. The cytotoxicity studies of various concentration of the peptide against human red blood cells showed that *Hp*-His exhibits only a minimal level of damage to mammalian RBC. Thus, *Hp*-His was found to be almost nontoxic to human RBCs at concentration found to cause killing effects in pathogenic bacteria. At the same time, the synthetic

*Hp*-His peptide exhibited significant cytotoxicity against the cancer cell lines, NCI-H460 and HEp-2. The results of cytotoxicity analysis were in line with the HDAP, abhisin which exhibited potent toxicity towards leukemia cancer cells (THP-1) but not towards normal fibroblast Vero cells (De Zoysa et al., 2009).

Taken together, these *in vitro* data indicates synthetic *Hp*-His modest antimicrobial properties along with its anticancer property. Recently, anticancer peptides with cancer selective toxicity have received fair attention as alternative chemotherapeutic agents due to their low intrinsic cytotoxicity, decreased likelihood of resistance development and synergic effects in combination therapy (Papo and Shai, 2005; Hoskin and Ramamoorthy, 2008; Gaspar et al., 2013). Although many AMPs have been reported to inhibit function in tumor cells, the mode of action on cancer cells of only a few peptides have been deciphered (Wang et al., 2008). Previous studies revealed that the synthetic and purified N-terminal region of histone H2A derived AMPs exhibited antimicrobial as well as anticancer activity (Park et al., 1998; Bergsson et al., 2005; De Zoysa et al., 2009; Chen et al., 2015). Buforin IIb, a synthetic analog of buforin II, has been found to exert significant cytotoxic effects towards cancer cells than normal eukaryotic cells (Lee et al., 2008). It also displayed powerful cytotoxic activity when injected into solid tumors in p53-deficient mice (Cho et al., 2009). The selective cancer toxicity observed in buforin IIb is mainly attributed to the differences in membrane composition of both cancerous and non-cancerous cells. Normal mammalian cell membranes are composed largely of neutrally charged phospholipids (Hoskin and Ramamoorthy, 2008), while cancer cell membranes are more negatively charged owing to

richness of anionic molecules such as phosphatidylserine (Utsugi et al., 1991; Dobrzynska et al., 2005), O-glycosylated mucins (Burdick et al., 1997), heparin sulfates (Kleeff et al., 1998) and sialilated gangliosides (Lee et al., 2008). AMPs due to their cationic nature combine with a net negative membrane potential and aids to disrupt negatively charged membranes of cancer cells *via,* electrostatic interactions (Schweizer, 2009). Other peptides that seem to target cancer cells on the basis of charge rather than cell growth are MPI- 1(Zhang et al., 2010), Gomesin (Rodrigues et al., 2008), tilapia hepcidin TH2-3 (Chen et al., 2009a), Pardaxin (Hsu et al., 2011), SVS-1 (Gaspar et al., 2012; Sinthuvanich et al., 2012) and Mellitin (Zarrinnahad et al., 2017).

To investigate the anticancer mechanism of *Hp*-His, gene expression analysis in both NCI-H460 and HEp-2 cell lines was done by using qRT-PCR. Relative gene expression levels of cancer related genes were analysed and found a marked increase in the mRNA levels of initiator caspase-9 and effector caspase-3 in both the cell lines. Mitochondria dependent mode of apoptosis induction is largely observed in the anticancer activity of most of the AMPs. Similar findings have been described for AMPs such as RGD-tachyplesin (Chen et al., 2001), DP1 (Mai et al., 2001) and buforin IIb (Lee et al., 2008). Moreover, the expression levels of both these caspases were found to be concentration dependent in both the cell lines (Kaufmann and Earnshaw, 2000).

Initiation and execution of apoptosis are also regulated by the Bcl-2 family of proteins which function by regulation of cytochrome-*c* release from the mitochondria *via,* alteration of mitochondrial membrane

permeability (Cory and Adams, 2002). Bcl-2 is an anti-apoptotic and Bax is a pro-apoptotic protein under the Bcl-2 family (Cory and Adams, 2005; Dewson and Kluck, 2010). The expression of both Bcl-2 and Bax is regulated by the p53 tumor suppressor gene (Miyashita, 1994). In the present study, levels of Bax and p53 were found to be upregulated in NCI-H460 and HEp-2 cells, following *Hp*-His treatment while Bcl-2 levels in both cells lines were lower. Similar kind of up-regulation of p53 mRNA was observed for epinecidin-1 treated U-937 leukaemia cell lines (Chen et al., 2009b). Also, the other tumor suppressor gene analysed in this study, Rb1, which aid in the regulation of cell growth and division was found to be up-regulated upon *Hp*-His exposure. These results taken together indicate the activation of apoptosis by *Hp*-His through intrinsic apoptotic pathway which involves the release of cytochrome-c from mitochondria.

Involvement of non-caspase proteases in the execution of apoptosis have long been described (Johnson, 2000). Cathepsin mediated activation of pro-apoptotic Bcl-2 family member Bid triggered the mitochondrial pathway to apoptosis (Droga-Mazovec et al., 2008). Elevated expression levels of non-caspase proteases, Cathepsin-G and Calpain-5 were observed in both the cell lines proposing its involvement in the breakdown of cellular components leading to the stimulation of apoptosis. Higher levels of up-regulation of these genes were exhibited in *Hp*-His treated HEp-2 cell line. On analysing the relative mRNA levels of cytokine genes in NCI-H460 cells, upregulation of the following interleukins (IL-1β, IL-10, IL-6), interferon IFN-β and tumor necrosis factor (TNF-α) have been detected. While, all the analysed cytokines were found to be induced in response to *Hp*-His treatment in HEp-2 cell line, similar kinds of

upregulation of cytokine genes were seen in HeLa cell lines treated with pardaxin peptide (Hsu et al., 2011). Thus, an increased expression of IL-6 and TNF-α projects the antitumor activities of *Hp*-His, through the production of first order cytokines like TNFs and IFNs. These data correlated well with the potency of the peptide to increase the level of mRNA expression of IFITM3 gene in HEp-2 cell line, as a parallel increase in the related interferons could be noticed. The other interferon induced immune genes examined such as Mx1, ISG15 and Viperin were found to be differentially expressed in both the cancer cells. The upregulation and downregulation of these immune genes indicate their pleiotropic functions during immune responses and inflammatory reactions.

The influence of *Hp*-His treatment on cell cycle associated gene expressions was evaluated by examining the expressions of various genes that regulate cellular processes. *Hp*-His also was seen to elicit an anticancer effect by downregulating the expression levels of AKT and upregulating the mRNA transcripts for MAPK-1 and JNK in human epithelial and lung cancer cell lines. MAPK-1 and JNK, thus could function as pro-apoptotic kinases that result in the phosphorylation of the substrates involved in various signalling pathways that lead to the enhancement of anticancer effect of *Hp*-His in both the cell lines. A similar pattern for c-JNK gene was observed for tilapia hepcidin (TH2-3) exposed human fibrosarcoma cells (Chen et al., 2009a). AKT on the other hand, function by inactivating critical transcription factors which mediate the expression of genes vital for apoptosis. Among the tested cell lines, higher levels of downregulation were observed for NCI-H460 than HEp-2

cell line. Therefore, *Hp*-His could also induce apoptosis *via,* downregulation of AKT.

Peptides that are able to induce apoptosis in tumor cells are increasingly seen as prime candidates for the development of anticancer therapeutics. In this study, *Hp*-His demonstrated strong anticancer activity against human epithelial and lung cancer cell lines, more probably by eliciting the intrinsic apoptotic pathway. The anticancer activities exhibited by *Hp*-His were on par with the other reported anticancer HDAPs such as buforin IIb. However, its precise mechanism of anticancer activity warrants further research in different cancer cell lines. In conclusion, a 21 amino acid histone H2A derived AMP from *H. pastinacoides*, demonstrated remarkable antimicrobial activity against Gram-negative pathogens, *V. vulnificus*, *V. alginolyticus, E. tarda, A. hydrophila* and *V. parahaemolyticus.* The peptide was found to exhibit a dual mode of action against the selected pathogens. It also demonstrated low toxicity to human erythrocytes. Broad spectrum antimicrobial activity, anticancer potential and low toxicity to human erythrocytes endorse it as a potential therapeutic agent for application in aquaculture and cancer therapy.

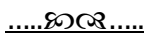

# Chapter 6

# SUMMARY AND CONCLUSION

The worldwide indiscriminate overuse of antibiotics has led to high rates of microbial resistance posing new challenges to human as well as animal health. The search of novel molecules with antimicrobial activity that could overcome this resistance phenomenon has become a priority. In this scenario, naturally-occurring, cationic antimicrobial peptides (AMPs) have attracted the attention of scientists as suitable scaffolds for the development of alternatives to conventional antibiotics. Marine organisms comprise roughly one-half of the total global biodiversity and they have been extensively studied in the last few decades for potential sources of novel bioactive natural products. Marine resources provide an abundant chemical space to be explored in peptide-based drug discovery as marine animals live in a very competitive, and aggressive surrounding compared to the terrestrial environment. Among evolutionary peptides, marine AMPs are considered as a new hope since they are stable against enzymes and various thermal conditions. Antimicrobial peptides derived from fishes extend as a promising candidate not only by being able to able to act directly as antimicrobial agents but also effect by being important regulators of the host innate immune system.

The present study was aimed to bioprospect novel AMPs from marine fishes using genomics approach. Molecular and phylogenetic analyses of AMPs identified in this study were carried out by bioinformatics tools. Functional characterization was accomplished using recombinant and synthetic peptides. In addition, they were screened for their bioactive potentials including antimicrobial and anticancer activity. Cytotoxic activities of the peptides were also tested by haemolytic assay and cell line toxicity assay.

## Salient findings

- In the present study, marine fishes were screened for novel AMP genes using gene based approach. Altogether, 3 AMPs, belonging to the families of hepcidins and histone derived peptides could be identified and characterized. Molecular and phylogenetic characterization of the AMPs were also carried out *in silico*.
- A novel HAMP2 isoform of hepcidin was identified from the gill mRNA transcripts of common pony fish, *Leiognathus equulus*, and was named as *Le*-Hepc (GenBank ID: **KM034809**). The 86 amino acid, *Le*-Hepc was constituted by a 24 amino acid signal peptide, 36 amino acid prodomain and a 26 amino acid mature peptide (*mLe*H).

- Histone H2A derived AMPs, named as *Mc*-His (GenBank ID: **MF966482**) from flathead grey mullet, *Mugil cephalus*, and *Em*-His1 and *Em*-His2 (GenBank ID: **MF966482**) from Orange chromide, *Etroplus maculatus*, were identified and are the first reports from the respective fishes.

- Based on the already reported histone derived peptide sequence from round whipray, *Himantura pastinacoides,* an AMP (named as *Hp*-His) was designed for chemical synthesis.

- The AMPs, *mLe*H and *Mc*-His were produced by recombinant method using pET-32a(+) vector and host *E. coli* Rosetta-gami$^{TM}$ B (DE3) pLysS, for functional characterization of the peptides.

- Two AMPs, *Em*-His2 and *Hp*-His were synthesized as linear peptides with end modifications and FITC labelling, at M/s Zhejiang Ontores Biotechnologies Co., Ltd China by solid phase synthesis using Fmoc chemistry with >95 % final purity. Region homologous to a highly potent AMP, Buforin II was used as the reference peptide for the design and synthesis of the two peptides.

- Functional characterization of the two recombinant peptides and the two synthetic peptides were performed by antibacterial and anticancer assays.

- The recombinant mature peptide hepcidin of *L. equulus*, r*mLe*H exhibited remarkable activity towards *Staphylococcus aureus*

and *Escherichia coli* at 5 μM concentration and *Aeromonas hydrophila*, and *Edwardsiella tarda* at 10 μM concentration. The r*mLe*H was found to be a membranolytic peptide resulting in membrane blebbing and pore formation as evidenced by Scanning Electron Micrographs (SEM).

- The r*mLe*H was found to be non-cytotoxic and non-haemolytic at the tested concentrations (1.25 μM – 20 μM).
- The recombinant peptide, *Mc*-His exhibited significant activity against Gram-negative pathogens i.e., *E. tarda* (MIC and MBC of 5 μM), *Vibrio alginolyticus* and *V. proteolyticus* (MIC and MBC of 20 μM) mainly by inducing membrane destabilization and permeabilization.
- The peptide, r*Mc*-His was found to be non-haemolytic and non-cytotoxic at the tested concentrations (1.25 μM – 20 μM).
- Synthetic *Em*-His2 demonstrated strong antibacterial activity against *Pseudomonas aeruginosa, E. coli* and *V. parahaemolyticus* (MIC and MBC of 25 μM). SEM analysis revealed that the overall cell morphology remained unchanged without any cellular debris.
- DNA binding studies of *Em*-His2 displayed marked DNA binding from 25 μM- 200 μM. The antimicrobial mechanism was likely *via,* membrane translocation and DNA interaction as

no significant morphological change could be noticed for the peptide treated bacteria.

- Synthetic *Em*-His2 was found to be cytotoxic to cancer cell lines (NCI-H460 and HEp-2) and demonstrated low haemolytic activity against human erythrocytes.

- Synthetic *Hp*-His displayed significant antibacterial activities against *V. vulnificus*, *V. alginolyticus* (MIC and MBC of 25 μM) and *E. tarda, A. hydrophila* and *E. coli* (MIC- 50μM, MBC - >50 μM). The peptide exhibited dual mode of antimicrobial action; mainly by membrane disruption for *V. vulnificus, V. alginolyticus*, *E. coli* and *A. hydrophila* and membrane translocation for *E. tarda*.

- The peptide, *Hp*-His was found to be DNA binding (from 25 μM to 200 μM), non-haemolytic against hRBCs and cytotoxic to NCI-H460 and HEp-2 cell lines.

- Anticancer activity of synthetic peptides *Em*-His2 and *Hp*-His against NCI-H460 and HEp-2 cancer cells were analyzed by gene expression analysis *in vitro* using qRT-PCR.

- Gene expression studies disclosed that both the cancer associated genes and immune related genes were differentially expressed in response to *Em*-His2 and *Hp*-His peptide treatment.

- The anticancer activity of *Em*-His2 was seen effected mainly by the upregulation of apoptosis related genes and tumor suppression genes in NCI-H460 and HEp-2 cell lines.
- *Hp*-His demonstrated strong anticancer activity against human epithelial and lung cancer cell lines more probably by eliciting the intrinsic apoptotic pathway and *via,* immune modulation by regulation of cytokine related genes.

Fishes represent the largest vertebrate group in comparison with other flora and fauna and have earned deep consideration as a potential source of bioactive compounds. They have been ignored largely as a potential source of antimicrobial peptides and only a limited number of sequences have been reported from fishes. Elucidating the mechanisms of action of fish AMPs would advocate the use of peptides as antimicrobials and anticancer agents. Moreover, the comparative analysis of the structure of the nucleotides or peptides with that of other phyla contributes to our knowledge of the evolutionary relationships of innate host defense system and phylogeny of vertebrates. Findings of the present study have demonstrated that these AMPs have potent activity against fish pathogens and specific activity against cancer cells. Thus largely the future work need to be focused on understanding the role of these peptides in host defense and the mode of action against microbes and tumor tissues. In context of the ever increasing trend of antibiotic resistance in microbes, there is vast

scope for the development of these peptides and their derivatives as potential therapeutics in aquaculture and human medicine.

# References


[1] Acosta, J., Montero, V., Carpio, Y., Velázquez, J., Garay, H.E., Reyes, O., Cabrales, A., Masforrol, Y., Morales, A. & Estrada, M.P. (2013). Cloning and functional characterization of three novel antimicrobial peptides from tilapia (*Oreochromis niloticus*). *Aquaculture*, *372*, 9-18.

[2] Alami, R., Fan, Y., Pack, S., Sonbuchner, T.M., Besse, A., Lin, Q., Greally, J.M., Skoultchi, A.I. & Bouhassira, E.E. (2003). Mammalian linker-histone subtypes differentially affect gene expression *in vivo*. *Proceedings of the National Academy of Sciences*, *100*, 5920-5925.

[3] Alberola, J., Rodriguez, A., Francino, O., Roura, X., Rivas, L. & Andreu, D. (2004). Safety and efficacy of antimicrobial peptides against naturally acquired leishmaniasis. *Antimicrobial Agents and Chemotherapy*, *48*, 641-643.

[4] Albig, W., Warthorst, U., Drabent, B., Prats, E., Cornudella, L. & Doenecke, D. (2003). *Mytilus edulis* core histone genes are organized in two clusters devoid of linker histone genes. *Journal of Molecular Evolution*, *56*, 597-606.

[5] Alkhalil, A., Hammamieh, R., Hardick, J., Ichou, M.A., Jett, M. & Ibrahim, S. (2010). Gene expression profiling of monkeypox virus-infected cells reveals novel interfaces for host-virus interactions. *Virology Journal*, *7*, 173.

[6] Altincicek, B., Stötzel, S., Wygrecka, M., Preissner, K.T. & Vilcinskas, A. (2008). Host-derived extracellular nucleic acids enhance innate immune responses, induce coagulation, and prolong survival upon infection in insects. *The Journal of Immunology*, *181*, 2705-2712.

[7] Alvarez, C. A., Guzmán, F., Cárdenas, C., Marshall, S. H. & Mercado, L. (2014). Antimicrobial activity of trout hepcidin. *Fish & Shellfish Immunology*, *41*, 93-101.

[8] Alvarez, C.A., Acosta, F., Montero, D., Guzmán, F., Torres, E., Vega, B. & Mercado, L. (2016). Synthetic hepcidin from fish: Uptake and protection against *Vibrio anguillarum* in sea bass (*Dicentrarchus labrax*). *Fish & Shellfish Immunology*, *55*, 662-670.

[9] Anand, P., Cermelli, S., Li, Z., Kassan, A., Bosch, M., Sigua, R., Huang, L., Ouellette, A.J., Pol, A., Welte, M.A. & Gross, S.P. (2012). A novel role for lipid droplets in the organismal antibacterial response. *eLife*, *1*.

[10] Aoki, T., Hikima, J.I., Minagawa, S. & Hirono, I. (2002). The lysozyme gene in fish. *Fisheries Science*, *68*, 1219-1220.

[11] Arnold, K., Bordoli, L., Kopp, J. & Schwede, T. (2006). The SWISS-MODEL workspace: a web-based environment for protein structure homology modelling. *Bioinformatics*, *22*, 195-201.

[12] Arockiaraj, J., Gnanam, A.J., Kumaresan, V., Palanisamy, R., Bhatt, P., Thirumalai, M.K., Roy, A., Pasupuleti, M. & Kasi, M. (2013). An unconventional antimicrobial protein histone from freshwater prawn *Macrobrachium rosenbergii*: Analysis of immune properties. *Fish & Shellfish Immunology*, *35*, 1511-1522.

[13] Atallah, S.T. & El-Banna, S.A. (2005). Effect of fish diseases on economic and productive efficiency of fish farms under Egyptian conditions. In *4th International Scientific Conference,* Monsoura University, *87*,104.

[14] Augusto, L.A., Decottignies, P., Synguelakis, M., Nicaise, M., Le Maréchal, P. & Chaby, R. (2003). Histones: a novel class of lipopolysaccharide-binding molecules. *Biochemistry*, *42*, 3929-3938.

[15] Bae, J.S., Shim, S.H., Hwang, S.D., Park, M.A., Jee, B.Y., An, C.M., Kim, Y.O., Kim, J.W. & Park, C.I. (2014). Expression analysis and biological activity of moronecidin from rock bream, *Oplegnathus fasciatus*. *Fish & Shellfish Immunology*, *40*, 345-353.

[16] Bahar, A.A. & Ren, D. (2013). Antimicrobial peptides. *Pharmaceuticals*, *6*, 1543-1575.

[17] Baker, M.A., Maloy, W.L., Zasloff, M. & Jacob, L.S. (1993). Anticancer efficacy of Magainin2 and analogue peptides. *Cancer Research*, *53*, 3052-3057.

[18] Balasubramanian, S. & Gunasekaran, G. (2015). Fatty acids and amino acids composition in skin epidermal mucus of selected fresh water fish *Mugil cephalus*. *World Journal of Pharmacy and Pharmaceutical Sciences*, *4*, 1275-1287.

[19] Balasubramanian, S., Revathi, A. & Gunasekaran, G. (2016). Studies on anticancer, haemolytic activity and chemical composition of crude epidermal mucus of fish *Mugil cephalus. International Journal of Fisheries and Aquatic Studies, 4,*438-443.

[20] Bali, E.B., Açık, L., Elçi, P., Sarper, M., Avcu, F. & Vural, M. (2015). In vitro anti-oxidant, cytotoxic and pro-apoptotic effects of *Achillea teretifolia* wild extracts on human prostate cancer cell lines. *Pharmacognosy Magazine*, *11*, 308.

[21] Balicki, D., Putnam, C.D., Scaria, P.V. & Beutler, E. (2002). Structure and function correlation in histone H2A peptide-mediated gene transfer. *Proceedings of the National Academy of Sciences*, *99*, 7467-7471.

[22] Bao, B., Peatman, E., Li, P., He, C. & Liu, Z. (2005). Catfish hepcidin gene is expressed in a wide range of tissues and exhibits tissue-specific upregulation after bacterial infection. *Developmental & Comparative Immunology*, *29*, 939-950.

[23] Barnes, A.C., Trewin, B., Snape, N., Kvennefors, E.C.E. & Baiano, J.C. (2011). Two hepcidin-like antimicrobial peptides in Barramundi *Lates calcarifer* exhibit differing tissue tropism and are induced in response to lipopolysaccharide. *Fish & Shellfish Immunology*, *31*, 350-357.

[24] Bastian, A., & Schäfer, H. (2001). Human α-defensin 1 (HNP-1) inhibits adenoviral infection *in vitro*. *Regulatory Peptides*, *101*, 157-161.

[25] Belaid, A., Aouni, M., Khelifa, R., Trabelsi, A., Jemmali, M. & Hani, K. (2002). *In vitro* antiviral activity of dermaseptins against herpes simplex virus type 1. *Journal of Medical Virology*, *66*, 229-234.

[26] Bergsson, G., Agerberth, B., Jörnvall, H. & Gudmundsson, G.H. (2005). Isolation and identification of antimicrobial components from the epidermal mucus of Atlantic cod (*Gadus morhua*). *The FEBS journal*, *272*, 4960-4969

[27] Birkemo, G.A., Lüders, T., Andersen, O., Nes, I.F. & Nissen-Meyer, J. (2003). Hipposin, a histone-derived antimicrobial peptide in Atlantic halibut (*Hippoglossus hippoglossus* L.). *Biochimica et Biophysica Acta (BBA)-Proteins and Proteomics*, *1646*, 207-215.

[28] Biterge, B. & Schneider, R. (2014). Histone variants: Key players of chromatin. *Cell and Tissue Research*, *356*, 457-466.

[29] Boman, H. G. (2003). Antibacterial peptides: Basic facts and emerging concepts. *Journal of Internal Medicine, 254*, 197–215.

[30] Boman, H.G., Agerberth, B. & Boman, A. (1993). Mechanisms of action on *Escherichia coli* of cecropin P1 and PR-39, two antibacterial peptides from pig intestine. *Infection and Immunity*, *61*, 2978-2984.

[31] Boman, H.G., Faye, I., Gudmundsson, G.H., Lee, J.Y. & Lidholm, D.A. (1991). Cell-free immunity in Cecropia. A model system for antibacterial proteins. *European Journal of Biochemistry, 201, 23-31*.

[32] Boumaiza, M., Ezzine, A., Jaouen, M., Sari, M.A. & Marzouki, M.N. (2014). Molecular characterization of a novel hepcidin (HepcD) from *Camelus dromedarius*. Synthetic peptide forms exhibit antibacterial activity. *Journal of Peptide Science*, *20*, 680-688.

[33] Bowdish, D.M., Davidson, D.J. & Hancock, R. (2005). A re-evaluation of the role of host defence peptides in mammalian immunity. *Current Protein and Peptide Science*, *6*, 35-51.

[34] Brewer, D., Hunter, H. & Lajoie, G. (1998). NMR studies of the antimicrobial salivary peptides histatin 3 and histatin 5 in aqueous and nonaqueous solutions. *Biochemistry and Cell Biology*, *76*, 247-256.

[35] Bridle, A., Nosworthy, E., Polinski, M. & Nowak, B. (2011). Evidence of an antimicrobial-immunomodulatory role of Atlantic salmon cathelicidins during infection with Yersinia ruckeri. *PLoS One*, *6*.

[36] Brinkmann, V. & Zychlinsky, A. (2007). Beneficial suicide: why neutrophils die to make NETs. *Nature Reviews Microbiology*, *5*, 577.

[37] Brinkmann, V. & Zychlinsky, A. (2012). Neutrophil extracellular traps: is immunity the second function of chromatin?. *Journal of Cell Biology,198*, 773-783.

[38] Brinkmann, V., Reichard, U., Goosmann, C., Fauler, B., Uhlemann, Y., Weiss, D.S., Weinrauch, Y. & Zychlinsky, A. (2004). Neutrophil extracellular traps kill bacteria. *Science*, *303*, 1532-1535.

[39] Broekman, D.C., Zenz, A., Gudmundsdottir, B.K., Lohner, K., Maier, V.H. & Gudmundsson, G.H. (2011). Functional characterization of codCath, the mature cathelicidin antimicrobial peptide from Atlantic cod (*Gadus morhua*). *Peptides*, *32*, 2044–2051.

[40] Brogden, K.A. (2005). Antimicrobial peptides: Pore formers or metabolic inhibitors in bacteria?. *Nature Reviews Microbiology*, *3*, 238.

[41] Brogden, K.A., Ackermann, M., McCray, P.B. & Tack, B.F. (2003). Antimicrobial peptides in animals and their role in host defences. *International Journal of Antimicrobial Agents*, *22*, 465-478.

[42] Brown, K.L. & Hancock, R.E. (2006). Cationic host defense (antimicrobial) peptides. *Current Opinion in Immunology*, *18*, 24-30.

[43] Browne, M.J., Feng, C.Y., Booth, V. & Rise, M.L. (2011). Characterization and expression studies of Gaduscidin-1 and Gaduscidin-2; paralogous antimicrobial peptide-like transcripts from Atlantic cod (*Gadus morhua*). *Developmental & Comparative Immunology*, *35*, 399-408.

[44] Bulet, P., Stöcklin, R. & Menin, L. (2004). Anti-microbial peptides: from invertebrates to vertebrates. *Immunological Reviews*, *198*, 169-184.

[45] Bulet, P., Urge, L., Ohresser, S., Hetru, C. & Otvos, L. (1996). Enlarged Scale Chemical Synthesis and Range of Activity of Drosocin, an O-Glycosylated Antibacterial Peptide of *Drosophila*. *The FEBS Journal*, *238*, 64-69.

[46] Buonocore, F., Randelli, E., Casani, D., Picchietti, S., Belardinelli, M.C., de Pascale, D., De Santi, C. & Scapigliati, G. (2012). A piscidin-like antimicrobial peptide from the icefish *Chionodraco hamatus* (Perciformes: Channichthyidae): Molecular characterization, localization and bactericidal activity. *Fish & Shellfish Immunology*, *33*, 1183-1191.

[47] Burdick, M.D., Harris, A., Reid, C.J., Iwamura, T. & Hollingsworth, M.A. (1997). Oligosaccharides expressed on MUC1 produced by pancreatic and colon tumor cell lines. *Journal of Biological Chemistry*, *272*, 24198-24202.

[48] Burrowes, O.J., Hadjicharalambous, C., Diamond, G. & Lee, T.C. (2004). Evaluation of antimicrobial spectrum and cytotoxic activity of pleurocidin for food applications. *Journal of Food Science*, *69*.

[49] Bustillo, M. E. (2013). A Modular approach to the characterization of histone H2A-derived antimicrobial peptides (Doctoral dissertation). Retrieved from Honors Thesis Collection, 149, Wellesley College, Wellesley.

[50] Bustillo, M.E., Fischer, A.L., LaBouyer, M.A., Klaips, J.A., Webb, A.C. & Elmore, D.E. (2014). Modular analysis of hipposin, a histone-derived antimicrobial peptide consisting of membrane translocating and membrane permeabilizing fragments. *Biochimica et Biophysica Acta (BBA)-Biomembranes*, *1838*, 2228-2233.

[51] Cabiaux, V., Agerberths, B., Johansson, J., Homble, F., Goormaghtigh, E. & Ruysschaert, J.M. (1994). Secondary Structure and Membrane Interaction of PR-39, a Pro+ Arg-rich Antibacterial Peptide. *The FEBS Journal*, *224*, 1019-1027.

[52] Cai, L., Cai, J.J., Liu, H.P., Fan, D.Q., Peng, H. & Wang, K.J. (2012). Recombinant medaka (*Oryzias melastigmus*) pro-hepcidin: Multifunctional characterization. *Comparative Biochemistry and Physiology* Part B*: Biochemistry and Molecular Biology*, *161*, 140-147.

[53] Campagna, S., Saint, N., Molle, G. & Aumelas, A. ( 2007). Structure and mechanism of action of the antimicrobial peptide piscidin. *Biochemistry*, 46, 1771–1778.

[54] Campos, M.A., Vargas, M.A., Regueiro, V., Llompart, C.M., Albertí, S., & Bengoechea, J.A. (2004). Capsule polysaccharide mediates bacterial resistance to antimicrobial peptides. *Infection and Immunity*, *72*, 7107-7114.

[55] Campoverde, C., Milne, D.J., Estévez, A., Duncan, N., Secombes, C.J. and Andree, K.B. (2017). Ontogeny and modulation after PAMPs stimulation of β-defensin, hepcidin, and piscidin antimicrobial peptides in meagre (*Argyrosomus regius*). *Fish & Shellfish Immunology*, *69*, 200-210.

[56] Carugo, O., Čemažar, M., Zahariev, S., Hudáky, I., Gáspári, Z., Perczel, A. & Pongor, S., (2003). Vicinal disulfide turns. *Protein Engineering*, *16*, 637-639.

[57] Casadei, E., Wang, T., Zou, J., Vecino, J.L.G., Wadsworth, S. & Secombes, C.J. (2009). Characterization of three novel β-defensin antimicrobial peptides in rainbow trout (*Oncorhynchus mykiss*). *Molecular Immunology*, *46*, 3358-3366.

[58] Casteels, P. & Tempst, P. (1994). Apidaecin-type peptide antibiotics function through a nonporeforming mechanism involving stereospecificity. *Biochemical and Biophysical Research Communications*, *199*, 339-345.

[59] Chaithanya, E. R., Philip, R., Sathyan, N. & Anil Kumar, P. R. (2013). Molecular Characterization and Phylogenetic Analysis of a Histone-Derived Antimicrobial Peptide Teleostin from the Marine Teleost Fishes, *Tachysurus jella* and *Cynoglossus semifasciatus*. *ISRN Molecular Biology*, *2013*, 1–7.

[60] Chang, C.I., Pleguezuelos, O., Zhang, Y.A., Zou, J. & Secombes, C.J. (2005). Identification of a novel cathelicidin gene in the rainbow trout, *Oncorhynchus mykiss*. *Infection and Immunity*, *73*, 5053-5064.

[61] Chang, C.I., Zhang, Y.A., Zou, J., Nie, P. & Secombes, C.J. (2006). Two cathelicidin genes are present in both rainbow trout (*Oncorhynchus mykiss*) and atlantic salmon (*Salmo salar*). *Antimicrobial Agents and Chemotherapy*, *50*, 185–195.

[62] Chang, W.T., Pan, C.Y., Rajanbabu, V., Cheng, C.W. & Chen, J.Y. (2011). Tilapia (*Oreochromis mossambicus*) antimicrobial peptide, hepcidin 1–5, shows antitumor activity in cancer cells. *Peptides*, *32*, 342-352.

[63] Chapman, R.W., Mancia, A., Beal, M., Veloso, A., Rathburn, C., Blair, A., Holland, A.F., Warr, G.W., Didinato, G.U.Y., Sokolova, I.M. & Wirth, E.F. (2011). The transcriptomic responses of the eastern oyster, *Crassostrea virginica*, to environmental conditions. *Molecular Ecology*, *20*, 1431-1449.

[64] Chaturvedi, P., Dhanik, M. & Pande, A. (2014). Characterization and structural analysis of hepcidin like antimicrobial peptide from *Schizothorax richardsonii* (Gray). *Protein Journal*, *33*, 1–10.

[65] Chaturvedi, P., Dhanik, M., Pande, V. & Pande, A. (2016). Identification and in-silico analysis of hepcidin from *Tor putitora* (Hamilton). *Indian Journal of Comparative Microbiology, Immunology and Infectious Diseases*, *37*, 67-76.

[66] Chaurasia, M.K., Palanisamy, R., Bhatt, P., Kumaresan, V., Gnanam, A.J., Pasupuleti, M., Kasi, M., Harikrishnan, R. & Arockiaraj, J. (2015). A prawn core histone 4: derivation of N-and C-terminal peptides and their antimicrobial properties, molecular characterization and mRNA transcription. *Microbiological Research*, *170*, 78-86.

[67] Chekmenev, E.Y., Vollmar, B.S., Forseth, K.T., Manion, M.N., Jones, S.M., Wagner, T.J., Endicott, R.M., Kyriss, B.P., Homem, L.M., Pate, M. & He, J. (2006). Investigating molecular recognition and biological function at interfaces using piscidins, antimicrobial peptides from fish. *Biochimica et Biophysica Acta (BBA)-Biomembranes*, *1758*, 1359-1372.

[68] Chen, B., Fan, D.Q., Zhu, K.X., Shan, Z.G., Chen, F.Y., Hou, L., Cai, L. & Wang, K.J. (2015). Mechanism study on a new antimicrobial peptide Sphistin derived from the N-terminus of crab histone H2A identified in haemolymphs of *Scylla paramamosain*. *Fish & Shellfish Immunology*, *47*, 833-846.

[69] Chen, J., Nie, L. & Chen, J. (2017). Mudskipper (*Boleophthalmus pectinirostris*) Hepcidin-1 and Hepcidin-2 Present Different Gene Expression Profile and Antibacterial Activity and Possess Distinct Protective Effect against *Edwardsiella tarda* Infection. *Probiotics and Antimicrobial Proteins*, 1-10.

[70] Chen, J.Y., Lin, W.J. & Lin, T.L. (2009a). A fish antimicrobial peptide, tilapia hepcidin TH2-3, shows potent antitumor activity against human fibrosarcoma cells. *Peptides*, *30*, 1636-1642.

[71] Chen, J.Y., Lin, W.J., Wu, J.L., Her, G.M. &Hui, C.F. (2009b). Epinecidin-1 peptide induces apoptosis which enhances antitumor effects in human leukemia U937 cells. *Peptides*, *30*, 2365–2373.

[72] Chen, L. & Harrison, S. (2007). Cell-penetrating peptides in drug development: enabling intracellular targets. *Biochemical Society Transactions*, *35*, 821-825.

[73] Chen, M.Z., Chen, J., Lu, X.J. & Shi, Y.H. (2010). Molecular cloning, sequence analysis and expression pattern of hepcidin gene in ayu (*Plecoglossus altivelis*). *Zoological Research*, *31*, 595-600.

[74] Chen, S.L., Li, W., Meng, L., Sha, Z.X., Wang, Z.J. & Ren, G.C. (2007). Molecular cloning and expression analysis of a hepcidin antimicrobial peptide gene from turbot (*Scophthalmus maximus*). *Fish & Shellfish Immunology*, *22*, 172–181.

[75] Chen, S.L., Xu, M.Y., Ji, X.S., Yu, G.C. & Liu, Y. (2005). Cloning, characterization, and expression analysis of hepcidin gene from red sea bream (*Chrysophrys major*). *Antimicrobial Agents and Chemotherapy*, *49*, 1608–1612.

[76] Chen, Y., Guarnieri, M.T., Vasil, A.I., Vasil, M.L., Mant, C.T. & Hodges, R.S. (2007). Role of peptide hydrophobicity in the mechanism of action of α-helical antimicrobial peptides. *Antimicrobial Agents and Chemotherapy*, *51*, 1398-1406.

[77] Chen, Y., Guarnieri, M.T., Vasil, A.I., Vasil, M.L., Mant, C.T. & Hodges, R.S. (2007). Role of peptide hydrophobicity in the mechanism of action of alpha-helical antimicrobial peptides. *Antimicrobial Agents and Chemotherapy*, *51*, 1398–1406

[78] Chen, Y., Xu, X., Hong, S., Chen, J., Liu, N., Underhill, C.B., Creswell, K. & Zhang, L. (2001). RGD-Tachyplesin inhibits tumor growth. *Cancer Research*, *61*, 2434-2438.

[79] Chen, Y., Zhao, H., Zhang, X., Luo, H., Xue, X., Li, Z. & Yao, B. (2013). Identification, expression and bioactivity of *Paramisgurnus dabryanus* β-defensin that might be involved in immune defense against bacterial infection. *Fish & Shellfish Immunology*, *35*, 399-406.

[80] Chi, J.R., Liao, L.S., Wang, R.G., Jhu, C.S., Wu, J.L. & Hu, S.Y. (2015). Molecular cloning and functional characterization of the hepcidin gene from the convict cichlid (*Amatitlania nigrofasciata*) and its expression pattern in response to lipopolysaccharide challenge. *Fish Physiology and Biochemistry*, *41*, 449-461.

[81] Chinchar, V.G., Bryan, L., Silphadaung, U., Noga, E., Wade, D. & Rollins-Smith, L. (2004). Inactivation of viruses infecting ectothermic animals by amphibian and piscine antimicrobial peptides. Virology, *323*, 268–275.

[82] Chiou, P. P., Khoo, J., Bols, N. C., Douglas, S. & Chen, T. T. (2006). Effects of linear cationic α-helical antimicrobial peptides on immune-relevant genes in trout macrophages. *Developmental & Comparative Immunology*, 30, 797-806.

[83] Chiou, P.P., Lin, C.M., Bols, N.C. & Chen, T.T. (2007). Characterization of virus/double-stranded RNA-dependent induction of antimicrobial peptide hepcidin in trout macrophages. *Developmental & Comparative Immunology*, *31*, 1297-1309.

[84] Cho, J. & Lee, D.G. (2011). Oxidative stress by antimicrobial peptide pleurocidin triggers apoptosis in *Candida albicans*. *Biochimie*, *93*, 1873-1879.

[85] Cho, J.H., Park, I.Y., Kim, H.S., Lee, W.T., Kim, M.S. & Kim, S.C. (2002a). Cathepsin D produces antimicrobial peptide parasin I from histone H2A in the skin mucosa of fish. *The FASEB Journal*, *16*, 429-431.

[86] Cho, J.H., Park, I.Y., Kim, M.S. & Kim, S.C. (2002b). Matrix metalloproteinase 2 is involved in the regulation of the antimicrobial peptide parasin I production in catfish skin mucosa. *FEBS Letters*, *531*, 459-463.

[87] Cho, J.H., Sung, B.H. & Kim, S.C. (2009). Buforins: histone H2A-derived antimicrobial peptides from toad stomach. *Biochimica et Biophysica Acta (BBA)-Biomembranes*, *1788*, 1564-1569.

[88] Cho, Y.S., Lee, S.Y., Kim, K.H., Kim, S.K., Kim, D.S. & Nam, Y.K. (2009). Gene structure and differential modulation of multiple rockbream (*Oplegnathus fasciatus*) hepcidin isoforms resulting from different biological stimulations. *Developmental & Comparative Immunology*, *33*, 46-58.

[89] Cole, A.M., Darouiche, R.O., Legarda, D., Connell, N. & Diamond, G. (2000). Characterization of a fish antimicrobial peptide: gene expression, subcellular localization, and spectrum of activity. *Antimicrobial Agents and Chemotherapy*, *44*, 2039-2045.

[90] Cole, A.M., Weis, P. & Diamond, G. (1997). Isolation and characterization of pleurocidin, an antimicrobial peptide in the skin secretions of winter flounder. *Journal of Biological Chemistry*, *272*, 12008-12013.

[91] Colorni, A., Ullal, A., Heinisch, G. & Noga, E.J. (2008). Activity of the antimicrobial polypeptide piscidin 2 against fish ectoparasites. *Journal of Fish Diseases*, *31*, 423-432.

[92] Concha, M.I., Molina, S., Oyarzún, C., Villanueva, J. & Amthauer, R. (2003). Local expression of apolipoprotein AI gene and a possible role for HDL in primary defence in the carp skin. *Fish & Shellfish Immunology*, *14*, 259-273.

[93] Concha, M.I., Smith, V.J., Castro, K., Bastías, A., Romero, A. & Amthauer, R.J. (2004). Apolipoproteins A-I and A-II are potentially important effectors of innate immunity in the teleost fish *Cyprinus carpio*. *The FEBS Journal*, *271*, 2984-2990.

[94] Connor, M.A., Jaso-Friedmann, L., Leary III, J.H. & Evans, D.L. (2009). Role of nonspecific cytotoxic cells in bacterial resistance: Expression of a novel pattern recognition receptor with antimicrobial activity. *Molecular Immunology*, *46*, 953-961.

[95] Cory, S. & Adams, J.M. (2002). The Bcl2 family: Regulators of the cellular life-or-death switch. *Nature Reviews Cancer*, *2*, 647.

[96] Cory, S. & Adams, J.M. (2005). Killing cancer cells by flipping the Bcl-2/Bax switch. *Cancer Cell*, 8, 5-6.

[97] Cruciani, R.A., Barker, J.L., Zasloff, M., Chen, H.C. & Colamonici, O. (1991). Antibiotic magainins exert cytolytic activity against transformed cell lines through channel formation. *Proceedings of the National Academy of Sciences*, *88*, 3792-3796.

[98] Cudic, M. & Otvos Jr, L. (2002). Intracellular targets of antibacterial peptides. *Current Drug Targets*, *3*, 101-106.

[99] Cuesta, A., Meseguer, J. & Esteban, M.A. (2008). The antimicrobial peptide hepcidin exerts an important role in the innate immunity against bacteria in the bony fish gilthead seabream. *Molecular immunology*, *45*, 2333-2342.

[100] Cuesta, A., Meseguer, J. & Esteban, M.Á. (2011). Molecular and functional characterization of the gilthead seabream β-defensin demonstrate its chemotactic and antimicrobial activity. *Molecular Immunology*, *48*, 1432-1438.

[101] Cutrona, K.J., Kaufman, B.A., Figueroa, D.M. & Elmore, D.E. (2015). Role of arginine and lysine in the antimicrobial mechanism of histone-derived antimicrobial peptides. *FEBS Letters*, *589*, 3915-3920.

[102] da Silva, B.R., de Freitas, V.A.A., Nascimento-Neto, L.G., Carneiro, V.A., Arruda, F.V.S., de Aguiar, A.S.W., Cavada, B.S. & Teixeira, E.H. (2012). Antimicrobial peptide control of pathogenic microorganisms of the oral cavity: A review of the literature. *Peptides*, *36*, 315-321.

[103] Dathe, M. & Wieprecht, T. (1999). Structural features of helical antimicrobial peptides: their potential to modulate activity on model membranes and biological cells. *Biochimica et Biophysica Acta (BBA)-Biomembranes*, *1462*, 71-87.

[104] Dathe, M., Wieprecht, T., Nikolenko, H., Handel, L., Maloy, W.L., MacDonald, D.L., Beyermann, M. & Bienert, M. (1997). Hydrophobicity, hydrophobic moment and angle subtended by charged residues modulate antibacterial and haemolytic activity of amphipathic helical peptides. *FEBS Letters*, *403*, 208-212.

[105] De Domenico, I., Nemeth, E., Nelson, J.M., Phillips, J.D., Ajioka, R.S., Kay, M.S., Kushner, J.P., Ganz, T., Ward, D.M. & Kaplan, J. (2014). The hepcidin-binding site on ferroportin Is evolutionarily conserved. *Cell Metabolism*, *19*, 1067-1067.

[106] De Lucca, A.J. & Walsh, T.J. (1999). Antifungal peptides: novel therapeutic compounds against emerging pathogens. *Antimicrobial Agents and Chemotherapy*, *43*, 1-11.

[107] De Lucca, A.J., Bland, J.M., Jacks, T.J., Grimm, C. & Walsh, T.J. (1998). Fungicidal and binding properties of the natural peptides cecropin B and dermaseptin. *Medical Mycology*, *36*, 291-298.

[108] De Zoysa, M., Nikapitiya, C., Whang, I., Lee, J.S. & Lee, J. (2009). Abhisin: a potential antimicrobial peptide derived from histone H2A of disk abalone (*Haliotis discus discus*). *Fish & Shellfish Immunology*, *27*, 639-646.

[109] Deivasigamani, B., Subramanian, V. & Sundaresan, A. (2017). Identification of protein from muscle tissue of marine finfish. *International Journal of Current Microbiology and Applied Sciences, 6*, 159-167.

[110] del Castillo, F.J., del Castillo, I. & Moreno, F. (2001). Construction and characterization of mutations at codon 751 of the *Escherichia coli* gyrB gene that confer resistance to the antimicrobial peptide microcin B17 and alter the activity of DNA gyrase. *Journal of Bacteriology*, *183*, 2137-2140.

[111] Dennison, S.R., Harris, F., Bhatt, T., Singh, J. & Phoenix, D.A. (2010). A theoretical analysis of secondary structural characteristics of anticancer peptides. *Molecular and Cellular Biochemistry*, *333*, 129.

[112] Desai, P.N., Shrivastava, N. & Padh, H. (2010). Production of heterologous proteins in plants: Strategies for optimal expression. *Biotechnology Advances*, *28*, 427-435.

[113] Dewson, G.K.R.M. & Kluck, R.M. (2010). Bcl-2 family-regulated apoptosis in health and disease. *Cell Health and Cytoskeleton*, *2*, 9-22.

[114] Dezfuli, B.S., Lui, A., Boldrini, P., Pironi, F. & Giari, L. (2008). The inflammatory response of fish to helminth parasites. *Parasite*, *15*, 426–433.

[115] Diamond, G., Beckloff, N., Weinberg, A. & Kisich, K.O. (2009). The roles of antimicrobial peptides in innate host defense. *Current Pharmaceutical Design*, *15*, 2377-2392.

[116] Dobrzynska, I., Szachowicz-Petelska, B., Sulkowski, S. & Figaszewski, Z. (2005). Changes in electric charge and phospholipids composition in human colorectal cancer cells. *Molecular and Cellular Biochemistry*, *276*, 113-119.

[117] Doenecke, D. & Gallwitz, D. (1982). Acetylation of histones in nucleosomes. *Molecular and Cellular Biochemistry*, *44*, 113-128.

[118] Dondero, F., Dagnino, A., Jonsson, H., Caprì, F., Gastaldi, L. & Viarengo, A. (2006). Assessing the occurrence of a stress syndrome in mussels (*Mytilus edulis*) using a combined biomarker/gene expression approach. *Aquatic Toxicology*, *78*, 13-24.

[119] Dong, F. & Van Holde, K.E. (1991). Nucleosome positioning is determined by the (H3-H4) 2 tetramer. *Proceedings of the National Academy of Sciences*, *88*, 10596-10600.

[120] Dong, J.J., Wu, F., Ye, X., Sun, C.F., Tian, Y.Y., Lu, M.X., Zhang, R. & Chen, Z.H. (2015). Beta-defensin in Nile tilapia (*Oreochromis niloticus*): Sequence, tissue expression, and anti-bacterial activity of synthetic peptides. *Gene, 566*, 23–31.

[121] Douglas, S.E., Patrzykat, A., Pytyck, J. & Gallant, J.W. (2003). Identification, structure and differential expression of novel pleurocidins clustered on the genome of the winter flounder, *Pseudopleuronectes americanus* (Walbaum). *The FEBS Journal*, *270*, 3720-3730.

[122] Droga-Mazovec, G., Bojič, L., Petelin, A., Ivanova, S., Repnik, U., Salvesen, G.S., Stoka, V., Turk, V. & Turk, B. (2008). Cysteine cathepsins trigger caspase-dependent cell death through cleavage of bid and antiapoptotic Bcl-2 homologues. *Journal of Biological Chemistry*, *283*, 19140-19150.

[123] Du Pasquier, L. (2001). The immune system of invertebrates and vertebrates. *Comparative Biochemistry and Physiology* Part B*: Biochemistry and Molecular Biology*, *129*, 1-15.

[124] Duclohier, H. & Wroblewski, H. (2001). Voltage-dependent pore formation and antimicrobial activity by alamethicin and analogues. *The Journal of Membrane Biology*, *184*, 1-12.

[125] Ebralidse, K.K., Grachev, S.A. & Mirzabekov, A.D. (1988). A highly basic histone H4 domain bound to the sharply bent region of nucleosomal DNA. *Nature*, *331*, 365.

[126] Ebran, N., Julien, S., Orange, N., Saglio, P., Lemaître, C. & Molle, G. (1999). Pore-forming properties and antibacterial activity of proteins extracted from epidermal mucus of fish. *Comparative Biochemistry and Physiology* Part A*: Molecular & Integrative Physiology*, *122*, 181-189.

[127] Eisenberg, D., Schwarz, E., Komaromy, M. & Wall, R. (1984). Analysis of membrane and surface protein sequences with the hydrophobic moment plot. *Journal of Molecular Biology*, *179*, 125-142.

[128] Ellis, A.E. (2001). Innate host defense mechanisms of fish against viruses and bacteria. *Developmental & Comparative Immunology*, *25*, 827-839.

[129] Elmore, D. E. (2012). Insights into buforin II membrane translocation from molecular dynamics simulations. *Peptides*, *38,* 357–362.

[130] Epand, R.M. & Vogel, H.J. (1999). Diversity of antimicrobial peptides and their mechanisms of action. *Biochimica et Biophysica Acta (BBA)-Biomembranes*, *1462*, 11-28.

[131] Falanga, A., Lombardi, L., Franci, G., Vitiello, M., Iovene, M.R., Morelli, G., Galdiero, M. & Galdiero, S. (2016). Marine antimicrobial peptides: Nature provides templates for the design of novel compounds against pathogenic bacteria. *International Journal of Molecular Sciences*, *17*, 785.

[132] Falco, A., Chico, V., Marroqui, L., Perez, L., Coll, J.M. & Estepa, A. (2008). Expression and antiviral activity of a β-defensin-like peptide identified in the rainbow trout (*Oncorhynchus mykiss*) EST sequences. *Molecular Immunology*, *45*, 757-765.

[133] Feng, C.Y., Johnson, S.C., Hori, T.S., Rise, M., Hall, J.R., Gamperl, A.K., Hubert, S., Kimball, J., Bowman, S. & Rise, M.L. (2009). Identification and analysis of differentially expressed genes in immune tissues of Atlantic cod stimulated with formalin-killed, atypical *Aeromonas salmonicida*. *Physiological Genomics*, *37*, 149-163.

[134] Fernandes, J. M., Ruangsri, J. & Kiron, V. (2010). Atlantic cod piscidin and its diversification through positive selection. *PLoS One*, *5*.

[135] Fernandes, J.M., Saint, N., Kemp, G.D. & Smith, V.J. (2003). Oncorhyncin III: A potent antimicrobial peptide derived from the non-histone chromosomal protein H6 of rainbow trout, *Oncorhynchus mykiss*. *Biochemical Journal*, *373*, 621.

[136] Fernandes, J.M.O., Kemp, G.D., Molle, M.G. & Smith, V.J. (2002). Anti-microbial properties of histone H2A from skin secretions of rainbow trout, *Oncorhynchus mykiss*. *Biochemical Journal*, *368*, 611.

[137] Fernandes, J.M.O., Molle, G., Kemp, G.D. & Smith, V.J. (2004). Isolation and characterisation of oncorhyncin II, a histone H1-derived antimicrobial peptide from skin secretions of rainbow trout, *Oncorhynchus mykiss. Developmental & Comparative Immunology*, *28*, 127-138.

[138] Fischer, A. (2013). A modular approach to the histone H2A family of antimicrobial peptides (Bachelor's Thesis). Retrieved from Honors Thesis Collection, 149, Wellesley College, Wellesley.

[139] Fischer, W. & Bianchi, G. (1984). *FAO species identification sheets for fishery purposes: Western Indian Ocean (Fishing Area 57).* Food and Agriculture Organization of the United Nations, Rome, Italy.

[140] Frohm, M., Gunne, H., Bergman, A.C., Agerberth, B., Bergman, T., Boman, A., Lidén, S., Jörnvall, H. & Boman, H.G. (1996). Biochemical and antibacterial analysis of human wound and blister fluid. *The FEBS Journal*, *237*, 86-92.

[141] Fry, M.M., Liggett, J.L. & Baek, S.J. (2004). Molecular cloning and expression of canine hepcidin. *Veterinary Clinical Pathology*, *33*, 223-227.

[142] Fu, Y.M., Li, S.P., Wu, Y.F. & Chang, Y.Z. (2007). Identification and expression analysis of hepcidin-like cDNAs from pigeon (*Columba livia*). *Molecular and Cellular Biochemistry*, *305*, 191-197.

[143] Fuchs, T.A., Abed, U., Goosmann, C., Hurwitz, R., Schulze, I., Wahn, V., Weinrauch, Y., Brinkmann, V. & Zychlinsky, A. (2007). Novel cell death program leads to neutrophil extracellular traps. *The Journal of Cell Biology*, *176*, 231-241.

[144] Fujimura, M., Ideguchi, M., Minami, Y., Watanabe, K. and Tadera, K. (2004). Purification, characterization, & sequencing of novel antimicrobial peptides, Tu-AMP 1 and Tu-AMP 2, from bulbs of tulip (*Tulipa gesneriana* L.). *Bioscience, Biotechnology, and Biochemistry*, *68*, 571-577.

[145] Futaki, S., Suzuki, T., Ohashi, W., Yagami, T., Tanaka, S., Ueda, K. & Sugiura, Y. (2001). Arginine-rich peptides:An abundant source of membrane-permeable peptides having potential as carriers for intracellular protein delivery. *Journal of Biological Chemistry*, *276*, 5836-5840.

[146] Gagliardo, B., Faye, A., Jaouen, M., Deschemin, J. C., Canonne-Hergaux, F., Vaulont, S., & Sari, M. A. (2008). Production of biologically active forms of recombinant hepcidin, the iron-regulatory hormone. *FEBS Journal*, *275*, 3793–3803.

[147] Gajski, G. & Garaj-Vrhovac, V. (2013). Melittin: a lytic peptide with anticancer properties. *Environmental Toxicology and Pharmacology*, *36*, 697-705.

[148] Ganz T. (2003). Hepcidin, a key regulator of iron metabolism and mediator of anemia of inflammation. *Blood*, *102*, 783–788.

[149] Gao, Y., Chen, C. F., Li, D. P., Tan, J. J. & Yuan, G. L. (2012). Cloning, expression and antimicrobial activity analysis of hepcidin from Chinese sturgeon (*Acipenser sinensis*). *Acta Hydrobiologica Sinica*, *4*, 027.

[150] Gaspar, D., Veiga, A.S. & Castanho, M.A. (2013). From antimicrobial to anticancer peptides. A review. *Frontiers in Microbiology*, *4*, 294.

[151] Gaspar, D., Veiga, A.S., Sinthuvanich, C., Schneider, J.P. & Castanho, M.A. (2012). Anticancer peptide SVS-1: efficacy precedes membrane neutralization. *Biochemistry*, *51*, 6263-6265.

[152] Gennaro R & Zanetti M. (2000). Structural features and biological activities of the cathelicidin-derived antimicrobial peptides. *Biopolymers*, *55*, 31-49.

[153] Giacometti, A., Cirioni, O., Del Prete, M.S., Barchiesi, F., Fineo, A. & Scalise, G. (2001). Activity of buforin II alone and in combination with azithromycin and minocycline against *Cryptosporidium parvum* in cell culture. *Journal of Antimicrobial Chemotherapy*, *47*, 97-99.

[154] Giacometti, A., Cirioni, O., Del Prete, M.S., Paggi, A.M., D'Errico, M.M. & Scalise, G. (2000). Combination studies between polycationic peptides and clinically used antibiotics against Gram-positive and Gram-negative bacteria. *Peptides*, *21*, 1155-1160.

[155] Giangaspero, A., Sandri, L. & Tossi, A. (2001). Amphipathic α helical antimicrobial peptides. *The FEBS Journal*, *268*, 5589-5600.

[156] Ginsburg, I. & Koren, E. (2008). Are cationic antimicrobial peptides also 'double-edged swords'?. *Expert review of anti-infective therapy*, *6*, 453-462.

[157] Ginsburg, I., van Heerden, P.V. & Koren, E. (2017). From amino acids polymers, antimicrobial peptides, and histones, to their possible role in the pathogenesis of septic shock: A historical perspective. *Journal of inflammation research*, *10*, 7-15.

[158] Gomes, B., Augusto, M.T., Felício, M.R., Hollmann, A., Franco, O.L., Gonçalves, S. & Santos, N.C. (2018). Designing improved active peptides for therapeutic approaches against infectious diseases. *Biotechnology Advances*, *36*, 415-429.

[159] Gomes, B., Santos, N. & Porotto, M. (2017). Biophysical properties and antiviral activities of measles fusion protein derived peptide conjugated with 25-hydroxycholesterol. *Molecules*, *22*, 1869-1882.

[160] Gong, L.C., Wang, H. & Deng, L. (2014). Molecular characterization, phylogeny and expression of a hepcidin gene in the blotched snakehead *Channa maculata*. *Developmental & Comparative Immunology*, *44,* 1-11.

[161] Gonzalez-Romero, R., Méndez, J., Ausió, J. & Eirín-López, J.M. (2008). Quickly evolving histones, nucleosome stability and chromatin folding: all about histone H2A. Bbd. *Gene*, *413*, 1-7.

[162] Gordon, Y.J., Romanowski, E.G. & McDermott, A.M. (2005). A review of antimicrobial peptides and their therapeutic potential as anti-infective drugs. *Current Eye Research*, 30, 505-515.

[163] Guex, N. & Peitsch, M.C. (1997). SWISS MODEL and the Swiss Pdb Viewer: An environment for comparative protein modelling. *Electrophoresis*, *18*, 2714-2723.

[164] Gui, L., Zhang, P., Zhang, Q. & Zhang, J. (2016). Two hepcidins from spotted scat (*Scatophagus argus*) possess antibacterial and antiviral functions *in vitro*. *Fish & Shellfish Immunology*, *50*, 191-199.

[165] Guimaraes-Costa, A.B., Nascimento, M.T., Froment, G.S., Soares, R.P., Morgado, F.N., Conceição-Silva, F. & Saraiva, E.M. (2009). *Leishmania amazonensis* promastigotes induce and are killed by neutrophil extracellular traps. *Proceedings of the National Academy of Sciences*, *106*, 6748-6753.

[166] Guina, T., Eugene, C.Y., Wang, H., Hackett, M. & Miller, S.I. (2000). A PhoP-regulated outer membrane protease of *Salmonella enterica* serovar Typhimurium promotes resistance to alpha-helical antimicrobial peptides. *Journal of Bacteriology*, *182*, 4077-4086.

[167] Gunn, J.S. (2001). Bacterial modification of LPS and resistance to antimicrobial peptides. *Journal of Endotoxin Research*, *7*, 57-62.

[168] Guo, L., Lim, K.B., Poduje, C.M., Daniel, M., Gunn, J.S., Hackett, M. & Miller, S.I. (1998). Lipid A acylation and bacterial resistance against vertebrate antimicrobial peptides. *Cell*, *95,* 189-198.

[169] Guo, M., Wei, J., Huang, X., Huang, Y. & Qin, Q. (2012). Antiviral effects of β-defensin derived from orange-spotted grouper (*Epinephelus coioides*). *Fish & Shellfish Immunology*, *32*, 828-838.

[170] Hancock, R.E. & Sahl, H.G. (2006). Antimicrobial and host-defense peptides as new anti-infective therapeutic strategies. *Nature Biotechnology*, *24*, 1551-1557.

[171] Hancock, R.E. & Scott, M.G. (2000). The role of antimicrobial peptides in animal defenses. *Proceedings of the National Academy of Sciences*, *97*, 8856-8861.

[172] Hancock, R.E. (2001). Cationic peptides: effectors in innate immunity and novel antimicrobials. *The Lancet Infectious Diseases*, *1*, 156-164.

[173] Hancock, R.E., Haney, E.F. & Gill, E.E. (2016). The immunology of host defence peptides: beyond antimicrobial activity. *Nature Reviews Immunology*, *16*, 321.

[174] Haney, E.F., Nazmi, K., Lau, F., Bolscher, J.G. & Vogel, H.J. (2009). Novel lactoferrampin antimicrobial peptides derived from human lactoferrin. *Biochimie*, *91*, 141-154.

[175] Hao, J., Li, Y.W., Xie, M.Q. & Li, A.X. (2012). Molecular cloning, recombinant expression and antibacterial activity analysis of hepcidin from Simensis crocodile (*Crocodylus siamensis*). *Comparative Biochemistry and Physiology* Part B*: Biochemistry and Molecular Biology*, *163*, 309-315.

[176] Harwig, S.S., Swiderek, K.M., Lee, T.D. & Lehrer, R.I. (1995). Determination of disulphide bridges in PG-2, an antimicrobial peptide from porcine leukocytes. *Journal of Peptide Science*, *1*, 207-215.

[177] Hassan, M. A., Mohd, K. S., Azemin, W. A. & Dharmaraj, S. (2015). Cytotoxic effect of Hepcidin (TH1-5) on human breast cancer cellline MCF-7. *Jurnal Teknologi*, *77*, 73-79.

[178] He, X. & Zhang, J. (2005). Rapid subfunctionalization accompanied by prolonged and substantial neofunctionalization in duplicate gene evolution. *Genetics*, *169*, 1157-1164.

[179] Helmerhorst, E.J., Breeuwer, P., van't Hof, W., Walgreen-Weterings, E., Oomen, L.C., Veerman, E.C., Amerongen, A.V.N. & Abee, T. (1999). The cellular target of histatin 5 on *Candida albicans* is the energized mitochondrion. *Journal of Biological Chemistry*, *274*, 7286-7291.

[180] Henzler Wildman, K.A., Lee, D.K. & Ramamoorthy, A. (2003). Mechanism of lipid bilayer disruption by the human antimicrobial peptide, LL-37. *Biochemistry*, *42*, 6545-6558.

[181] Hiemstra, P.S., Eisenhauer, P.B., Harwig, S.S., van den Barselaar, M.T., Van Furth, R. & Lehrer, R.I. (1993). Antimicrobial proteins of murine macrophages. *Infection and Immunity*, *61*, 3038-3046.

[182] Hilchie, A.L., Doucette, C.D., Pinto, D.M., Patrzykat, A., Douglas, S. & Hoskin, D.W. (2011). Pleurocidin-family cationic antimicrobial peptides are cytolytic for breast carcinoma cells and prevent growth of tumor xenografts. *Breast Cancer Research*, *13*, 102.

[183] Hill, C. P., Yee, J., Selsted, M. E., & Eisenberg, D. (1991). Crystal structure of defensin HNP-3, an amphiphilic dimer: Mechanisms of membrane permeabilization. *Science*, *251*, 1481-1485.

[184] Hilton, K.B. & Lambert, L.A. (2008). Molecular evolution and characterization of hepcidin gene products in vertebrates. *Gene*, *415*, 40-48.

[185] Hirono, I., Hwang, J.Y., Ono, Y., Kurobe, T., Ohira, T., Nozaki, R. & Aoki, T. (2005). Two different types of hepcidins from the Japanese flounder *Paralichthys olivaceus*. *The FEBS journal*, *272*, 5257-5264.

[186] Hirsch, J.G. (1958). Bactericidal action of histone. *Journal of Experimental Medicine*, *108*, 925-944.

[187] Hocquellet, A., le Senechal, C. & Garbay, B. (2012). Importance of the disulfide bridges in the antibacterial activity of human hepcidin. *Peptides*, *36*, 303-307.

[188] Hocquellet, A., Odaert, B., Cabanne, C., Noubhani, A., Dieryck, W., Joucla, G., Le Senechal, C., Milenkov, M., Chaignepain, S., Schmitter, J.M. & Claverol, S. (2010). Structure–activity relationship of human liver-expressed antimicrobial peptide 2. *Peptides*, *31*, 58-66.

[189] Horne, W.S., Wiethoff, C.M., Cui, C., Wilcoxen, K.M., Amorin, M., Ghadiri, M.R. & Nemerow, G.R. (2005). Antiviral cyclic d, l-α-peptides: Targeting a general biochemical pathway in virus infections. *Bioorganic & Medicinal Chemistry*, *13*, 5145-5153.

[190] Hoskin, D.W. & Ramamoorthy, A. (2008). Studies on anticancer activities of antimicrobial peptides. *Biochimica et Biophysica Acta (BBA)-Biomembranes*, *1778*, 357-375.

[191] Houyvet, B., Bouchon-Navaro, Y., Bouchon, C., Goux, D., Bernay, B., Corre, E. & Zatylny-Gaudin, C. (2018). Identification of a moronecidin-like antimicrobial peptide in the venomous fish *Pterois volitans*: Functional and structural study of pteroicidin-α. *Fish & Shellfish Immunology*, *72*, 318-324.

[192] Howell, S.J., Wilk, D., Yadav, S.P. & Bevins, C.L. (2003). Antimicrobial polypeptides of the human colonic epithelium. *Peptides*, 24, 1763-1770.

[193] Hsieh, J.C., Pan, C.Y. & Chen, J.Y. (2010). Tilapia hepcidin (TH) 2-3 as a transgene in transgenic fish enhances resistance to *Vibrio vulnificus* infection and causes variations in immune-related genes after infection by different bacterial species. *Fish & Shellfish Immunology*, *29*, 430-439.

[194] Hsu, J.C., Lin, L.C., Tzen, J.T. & Chen, J.Y. (2011). Pardaxin-induced apoptosis enhances antitumor activity in HeLa cells. Peptides, *32*, 1110-1116.

[195] Hu, X., Ward, C., Aono, S., Lan, L., Dykstra, C., Kemppainen, R.J., Morrison, E.E. & Shi, J. (2008). Comparative analysis of *Xenopus tropicalis* hepcidin I and hepcidin II genes. *Gene*, *426*, 91-97.

[196] Huang, H.N., Pan, C.Y., Rajanbabu, V., Chan, Y.L., Wu, C.J. & Chen, J.Y. (2011). Modulation of immune responses by the antimicrobial peptide, epinecidin (Epi)-1, and establishment of an Epi-1-based inactivated vaccine. *Biomaterials*, *32*, 3627-3636.

[197] Huang, H.N., Rajanbabu, V., Pan, C.Y., Chan, Y.L., Wu, C.J. & Chen, J.Y. (2013). Use of the antimicrobial peptide Epinecidin-1 to protect against MRSA infection in mice with skin injuries. *Biomaterials*, *34*, 10319-10327.

[198] Huang, L., Leong, S.S.J. & Jiang, R. (2009). Soluble fusion expression and characterization of bioactive human beta-defensin 26 and 27. *Applied Microbiology and Biotechnology*, *84*, 301-308.

[199] Huang, P.H., Chen, J.Y. & Kuo, C.M. (2007). Three different hepcidins from tilapia, *Oreochromis mossambicus*: analysis of their expressions and biological functions. *Molecular Immunology*, *44*, 1922-1934.

[200] Huang, Y., He, L., Li, G., Zhai, N., Jiang, H. & Chen, Y. (2014). Role of helicity of ??-helical antimicrobial peptides to improve specificity. *Protein & Cell*, *5*, 631–642.

[201] Hunter, H.N., Fulton, D.B., Ganz, T. & Vogel, H.J. (2002). The solution structure of human hepcidin, a peptide hormone with antimicrobial activity that is involved in iron uptake and hereditary hemochromatosis. *Journal of Biological Chemistry*, *277*, 37597-37603.

[202] Hye, J., Young, M., Lee, J., Chang, S. & Hyun, J. (2011). Peptides Enhancement of the cancer targeting specificity of buforin IIb by fusion with an anionic peptide *via* a matrix metalloproteinases-cleavable linker. *Peptides*, *32*, 895–899.

[203] Iger, Y. & Abraham, M. (1990). The process of skin healing in experimentally wounded carp. *Journal of Fish Biology*, *36*, 421-437.

[204] Iijima, N., Tanimoto, N., Emoto, Y., Morita, Y., Uematsu, K., Murakami, T. & Nakai, T. (2003). Purification and characterization of three isoforms of chrysophsin, a novel antimicrobial peptide in the gills of the red sea bream, *Chrysophrys major*. *The FEBS Journal*, *270*, 675-686.

[205] Ilyin, G., Courselaud, B., Troadec, M.B., Pigeon, C., Alizadeh, M., Leroyer, P., Brissot, P. & Loréal, O. (2003). Comparative analysis of mouse hepcidin 1 and 2 genes: Evidence for different patterns of expression and co-inducibility during iron overload 1. *FEBS Letters*, *542*, 22-26.

[206] Ivanov, I.E., Morrison, A.E., Cobb, J.E., Fahey, C.A. & Camesano, T.A. (2012). Creating antibacterial surfaces with the peptide chrysophsin-1. *ACS Applied Materials & Interfaces*, *4*, 5891-5897.

[207] Iwanaga, S. & Lee, B.L. (2005). Recent advances in the innate immunity of invertebrate animals. *BMB Reports*, *38*, 128-150.

[208] Jacobsen, F., Baraniskin, A., Mertens, J., Mittler, D., Mohammadi-Tabrisi, A., Schubert, S., Soltau, M., Lehnhardt, M., Behnke, B., Gatermann, S. & Steinau, H.U. (2005). Activity of histone H1. 2 in infected burn wounds. *Journal of Antimicrobial Chemotherapy*, *55*, 735-741.

[209] Jafari, M., Mehrnejad, F. & Doustdar, F. (2017). Insight into the interactions, residue snorkeling, and membrane disordering potency of a single antimicrobial peptide into different lipid bilayers. *PLoS One,12.*

[210] Janakiraman, V.N., Cabanne, C., Dieryck, W., Hocquellet, A., Joucla, G., Le Senechal, C., Chaignepain, S., Costaglioli, P., Santarelli, X., Garbay, B. & Noubhani, A. (2015). Production and purification of recombinant human hepcidin-25 with authentic N and C-termini. *Journal of Biotechnology*, *195*,89-92.

[211] Jang, J.H., Kim, M.Y., Lee, J.W., Kim, S.C. & Cho, J.H. (2011). Enhancement of the cancer targeting specificity of buforin IIb by fusion with an anionic peptide via a matrix metalloproteinases-cleavable linker. *Peptides*, *32*, 895-899.

[212] Jang, J.H., Kim, Y.J., Kim, H., Kim, S.C. & Cho, J.H. (2015). Buforin IIb induces endoplasmic reticulum stress-mediated apoptosis in HeLa cells. *Peptides*, *69*,144-149.

[213] Jang, S.A., Kim, H., Lee, J.Y., Shin, J.R., Cho, J.H. & Kim, S.C. (2012). Mechanism of action and specificity of antimicrobial peptides designed based on buforin IIb. *Peptides*, *34*, 283-289.

[214] Javadpour, M.M., Juban, M.M., Lo, W.C.J., Bishop, S.M., Alberty, J.B., Cowell, S.M., Becker, C.L. & McLaughlin, M.L. (1996). De novo antimicrobial peptides with low mammalian cell toxicity. *Journal of Medicinal Chemistry*, *39*, 3107-3113.

[215] Jenssen, H., Hamill, P. & Hancock, R.E. (2006). Peptide antimicrobial agents. *Clinical Microbiology Reviews*, *19*, 491-511.

[216] Jin, J.Y., Zhou, L., Wang, Y., Li, Z., Zhao, J.G., Zhang, Q.Y. & Gui, J.F. (2010). Antibacterial and antiviral roles of a fish β-defensin expressed both in pituitary and testis. *PLoS One*, *5*.

[217] John, H., Maronde, E., Forssmann, W., Meyer, M. & Adermann, K. (2008). N-terminal acetylation protects glucagon-like peptide GLP-1-(7-34)-amide from DPP-IV-mediated degradation retaining cAMP-and insulin-releasing capacity. *European Journal of Medical Research*, *13*, 73.

[218] Johnson, D.E. (2000). Noncaspase proteases in apoptosis. *Leukemia*, *14*, 1695.

[219] Jones, E.M., Smart, A., Bloomberg, G., Burgess, L. & Millar, M.R. (1994). Lactoferricin, a new antimicrobial peptide. *Journal of Applied Microbiology*, *77*, 208-214.

[220] Kacprzyk, L., Rydengård, V., Mörgelin, M., Davoudi, M., Pasupuleti, M., Malmsten, M. & Schmidtchen, A. (2007). Antimicrobial activity of histidine-rich peptides is dependent on acidic conditions. *Biochimica et Biophysica Acta (BBA)-Biomembranes*, *1768*, 2667-2680.

[221] Katzenback, B.A. & Belosevic, M. (2009). Isolation and functional characterization of neutrophil-like cells, from goldfish (*Carassius auratus* L.) kidney. *Developmental & Comparative Immunology*, *33*, 601-611.

[222] Kaufmann, S.H. & Earnshaw, W.C. (2000). Induction of apoptosis by cancer chemotherapy. Experimental cell research, *256*, 42-49.

[223] Kawasaki, H. & Iwamuro, S. (2008). Potential roles of histones in host defense as antimicrobial agents. *Infectious Disorders-Drug Targets*, *8*, 195-205.

[224] Kawasaki, H., Isaacson, T., Iwamuro, S. & Conlon, J.M. (2003). A protein with antimicrobial activity in the skin of Schlegel's green tree frog *Rhacophorus schlegelii* (Rhacophoridae) identified as histone H2B. *Biochemical and Biophysical Research Communications*, *312*, 1082-1086.

[225] Ke, F., Wang, Y., Yang, C.S. & Xu, C. (2015). Molecular cloning and antibacterial activity of hepcidin from Chinese rare minnow (*Gobiocypris rarus*). *Electronic Journal of Biotechnology*, *18*, 169-174.

[226] Kelly, G.J., Kia, A.F.A., Hassan, F., O'Grady, S., Morgan, M.P., Creaven, B.S., McClean, S., Harmey, J.H. & Devocelle, M. (2016). Polymeric prodrug combination to exploit the therapeutic potential of antimicrobial peptides against cancer cells. *Organic & Biomolecular Chemistry*, *14*, 9278-9286.

[227] Kemna, E.H., Tjalsma, H., Willems, H.L. & Swinkels, D.W. (2008). Hepcidin: from discovery to differential diagnosis. *Haematologica*, *93*, 90-97.

[228] Khandelia, H. & Kaznessis, Y.N. (2006). Molecular dynamics investigation of the influence of anionic and zwitterionic interfaces on antimicrobial peptides' structure: Implications for peptide toxicity and activity. *Peptides*, *27*, 1192-1200.

[229] Khorasanizadeh, S. (2004). The nucleosome: From genomic organization to genomic regulation. *Cell*, *116*, 259-272.

[230] Kikukawa, T. & Araiso, T. (2002). Changes in lipid mobility associated with alamethicin incorporation into membranes. *Archives of Biochemistry and Biophysics*, *405*, 214-222.

[231] Kim, H. S., Yoon, H., Minn, I., Park, C. B., Lee, W. T., Zasloff, M. & Kim, S. C. (2000). Pepsin-mediated processing of the cytoplasmic histone H2A to strong antimicrobial peptide buforin I. *The Journal of Immunology 165*, 3268–3274.

[232] Kim, H.K., Chun, D.S., Kim, J.S., Yun, C.H., Lee, J.H., Hong, S.K. & Kang, D.K. (2006). Expression of the cationic antimicrobial peptide lactoferricin fused with the anionic peptide in *Escherichia coli*. *Applied Microbiology and Biotechnology*, *72*, 330-338.

[233] Kim, H.S., Cho, J.H., Park, H.W., Yoon, H., Kim, M.S. & Kim, S.C. (2002). Endotoxin-neutralizing antimicrobial proteins of the human placenta. *The Journal of Immunology*, *168*, 2356-2364.

[234] Kim, H.S., Park, C.B., Kim, M.S. & Kim, S.C. (1996). cDNA cloning and characterization of buforin I, an antimicrobial peptide: a cleavage product of histone H2A. *Biochemical and Biophysical Research Communications*, *229*, 381-387.

[235] Kim, J.K., Lee, S.A., Shin, S., Lee, J.Y., Jeong, K.W., Nan, Y.H., Park, Y.S., Shin, S.Y. & Kim, Y. (2010). Structural flexibility and the positive charges are the key factors in bacterial cell selectivity and membrane penetration of peptoid-substituted analog of Piscidin 1. *Biochimica et Biophysica Acta (BBA)-Biomembranes*, *1798*, 1913-1925.

[236] Kim, J.M., Jang, S.A., Yu, B.J., Sung, B.H., Cho, J.H. & Kim, S.C. (2008). High-level expression of an antimicrobial peptide histonin as a natural form by multimerization and furin-mediated cleavage. *Applied Microbiology and Biotechnology*, *78*, 123-130.

[237] Kim, Y.O., Park, E.M., Nam, B.H., Kong, H.J., Kim, W.J. & Lee, S.J. (2008). Identification and molecular characterization of two hepcidin genes from black rockfish (*Sebastes schlegelii*). *Molecular and Cellular Biochemistry*, *315*, 131.

[238] Kleeff, J., Ishiwata, T., Kumbasar, A., Friess, H., Büchler, M.W., Lander, A.D. & Korc, M., (1998). The cell-surface heparan sulfate proteoglycan glypican-1 regulates growth factor action in pancreatic carcinoma cells and is overexpressed in human pancreatic cancer. *The Journal of Clinical Investigation*, *102*, 1662-1673.

[239] Kobayashi, S., Takeshima, K., Park, C.B., Kim, S.C. & Matsuzaki, K. (2000). Interactions of the novel antimicrobial peptide buforin 2 with lipid bilayers: proline as a translocation promoting factor. *Biochemistry*, *39*, 8648-8654.

[240] Konishi, A., Shimizu, S., Hirota, J., Takao, T., Fan, Y., Matsuoka, Y., Zhang, L., Yoneda, Y., Fujii, Y., Skoultchi, A.I. & Tsujimoto, Y. (2003). Involvement of histone H1. 2 in apoptosis induced by DNA double-strand breaks. *Cell*, *114*, 673-688.

[241] Koo, Y.S., Kim, J.M., Park, I.Y., Yu, B.J., Jang, S.A., Kim, K.S., Park, C.B., Cho, J.H. & Kim, S.C. (2008). Structure–activity relations of parasin I, a histone H2A-derived antimicrobial peptide. *Peptides*, *29*, 1102-1108.

[242] Kozlov, S.A., Vassilevski, A.A. & Grishin, E.V. (2008). Antimicrobial peptide precursor structures suggest effective production strategies. *Recent Patents on Inflammation & Allergy Drug Discovery*, *2*, 58-63.

[243] Krause, A., Neitz, S., Mägert, H.J., Schulz, A., Forssmann, W.G., Schulz-Knappe, P. & Adermann, K., (2000). LEAP-1, a novel highly disulfide-bonded human peptide, exhibits antimicrobial activity. *FEBS Letters*, *480*, 147-150.

[244] Krijgsveld, J., Zaat, S.A., Meeldijk, J., van Veelen, P.A., Fang, G., Poolman, B., Brandt, E., Ehlert, J.E., Kuijpers, A.J., Engbers, G.H. & Feijen, J. (2000). Thrombocidins, microbicidal proteins from human blood platelets, are C-terminal deletion products of CXC chemokines. *Journal of Biological Chemistry*, *275*, 20374-20381.

[245] Krusong, K., Poolpipat, P., Supungul, P. & Tassanakajon, A. (2012). A comparative study of antimicrobial properties of crustinPm1 and crustinPm7 from the black tiger shrimp *Penaeus monodon*. *Developmental and Comparative Immunology*, *36*, 208–15.

[246] Kumar, A., Rajendran, V., Sethumadhavan, R. & Purohit, R. (2013). AKT kinase pathway: A leading target in cancer research. *The Scientific World Journal*, *2013*, 1-6.

[247] Kumar, P., Kizhakkedathu, J.N. & Straus, S.K. (2018). Antimicrobial Peptides: Diversity, Mechanism of action and strategies to improve the activity and biocompatibility *in vivo*. *Biomolecules*, *8*, 4.

[248] Kuppulakshmi, C., Prakash, M., Gunasekaran, G., Manimegalai, G. & Sarojini, S. (2008). Antibacterial properties of fish mucus from. *European Review for Medical and Pharmacological Sciences*, *12*, 149-153.

[249] Kuroda, K. & Caputo, G.A. (2013). Antimicrobial polymers as synthetic mimics of host-defense peptides. *Wiley Interdisciplinary Reviews: Nanomedicine and Nanobiotechnology*, *5*, 49-66.

[250] Kuroda, K., Caputo, G.A. & DeGrado, W.F. (2009). The role of hydrophobicity in the antimicrobial and hemolytic activities of polymethacrylate derivatives. *Chemistry-A European Journal*, *15*, 1123-1133.

[251] Kwapisz, J., Slomka, A. & Zekanowska, E. (2009). Hepcidin and its role in iron homeostasis. *EJIFCC*, *20*, 124.

[252] Laquerre, S., Argnani, R., Anderson, D.B., Zucchini, S., Manservigi, R. & Glorioso, J.C., (1998). Heparan sulfate proteoglycan binding by herpes simplex virus type 1 glycoproteins B and C, which differ in their contributions to virus attachment, penetration, and cell-to-cell spread. *Journal of Virology*, *72*, 6119-6130.

[253] Lauth, X., Babon, J.J., Stannard, J.A., Singh, S., Nizet, V., Carlberg, J.M., Ostland, V.E., Pennington, M.W., Norton, R.S. & Westerman, M.E. (2005). Bass hepcidin synthesis, solution structure, antimicrobial activities and synergism, and in vivo hepatic response to bacterial infections. *Journal of Biological Chemistry*, *280*, 9272-9282.

[254] Lauth, X., Shike, H., Burns, J.C., Westerman, M.E., Ostland, V.E., Carlberg, J.M., Van Olst, J.C., Nizet, V., Taylor, S.W., Shimizu, C. & Bulet, P. (2002). Discovery and characterization of two isoforms of moronecidin, a novel antimicrobial peptide from hybrid striped bass. *Journal of Biological Chemistry*, *277*, 5030-5039.

[255] Lawniczak, M.K., Barnes, A.I., Linklater, J.R., Boone, J.M., Wigby, S. & Chapman, T., (2007). Mating and immunity in invertebrates. *Trends in Ecology & Evolution*, *22*(1), pp.48-55.

[256] Lawyer, C., Pai, S., Watabe, M., Borgia, P., Mashimo, T., Eagleton, L. & Watabe, K. (1996). Antimicrobial activity of a 13 amino acid tryptophan-rich peptide derived from a putative porcine precursor protein of a novel family of antibacterial peptides. *FEBS Letters*, *390*, 95-98.

[257] Lazarovici, P., Primor, N. & Loew, L.M. (1986). Purification and pore-forming activity of two polypeptides from the secretion of the Red Sea Moses sole (*Pardachirus marmoratus*). The *Journal of Biological Chemistry*, *261*, 16704–16713.

[258] Lee, D.Y., Huang, C.M., Nakatsuji, T., Thiboutot, D., Kang, S.A., Monestier, M. & Gallo, R.L. (2009). Histone H4 is a major component of the antimicrobial action of human sebocytes. *Journal of Investigative Dermatology*, *129*, 2489-2496.

[259] Lee, H., Hwang, J. S., Lee, J., Kim, J. I. & Lee, D. G. (2015). Scolopendin 2, a cationic antimicrobial peptide from centipede, and its membrane-active mechanism. *Biochimica et Biophysica Acta (BBA)-Biomembranes*, *1848*, 634-642.

[260] Lee, H.S., Park, C.B., Kim, J.M., Jang, S.A., Park, I.Y., Kim, M.S., Cho, J.H. & Kim, S.C. (2008). Mechanism of anticancer activity of buforin IIb, a histone H2A-derived peptide. *Cancer Letters*, *271*, 47-55.

[261] Lee, J., Kim, M., Cho, J. & Kim, S. (2002). Enhanced expression of tandem multimers of the antimicrobial peptide buforin II in *Escherichia coli* by the DEAD-box protein and trxB mutant. *Applied Microbiology and Biotechnology*, *58*, 790-796.

[262] Lee, J.H., Minn, I.L., Park, C.B. & Kim, S.C. (1998). Acidic peptide-mediated expression of the antimicrobial peptide Buforin II as tandem repeats in *Escherichia coli*. *Protein Expression and Purification*, *12*, 53-60.

[263] Lee, J.H., Wan, K.L. & Mohd-Adnan, A. (2012). Molecular characterization of hepcidin in the Asian seabass (*Lates calcarifer*) provides insights into its role in innate immune response. *Aquaculture*, *330*, 8-14.

[264] Lee, K.H., Lee, D.G., Park, Y., Kang, D.I., Shin, S.Y., Hahm, K.S. & Kim, Y. (2006). Interactions between the plasma membrane and the antimicrobial peptide HP (2-20) and its analogues derived from *Helicobacter pylori*. *Biochemical Journal*, *394*, 105-114.

[265] Lee, L.H., Hui, C.F., Chuang, C.M. & Chen, J.Y. (2013). Electrotransfer of the epinecidin-1 gene into skeletal muscle enhances the antibacterial and immunomodulatory functions of a marine fish, grouper (*Epinephelus coioides*). *Fish & Shellfish Immunology*, *35*, 1359-1368.

[266] Lee, S. & Margolin, K. (2011). Cytokines in cancer immunotherapy. *Cancers*, *3*, 3856-3893.

[267] Lee, S.Y., Kim, B.S., Kim, D.S. & Nam, Y.K. (2011). Isolation of Two Hepcidin Paralogs, Hamp1 and Hamp2, from a Euryhaline Javanese Ricefish (*Oryzias javanicus: Beloniformes*). *Fisheries and Aquatic Sciences*, *14*, 93-104.

[268] Lee, Y.K. & Lee, H.K. (2003). Putative histone H2A genes from a red alga, *Griffithsia japonica*. *Algae*, *18*, 191-197.

[269] Lee, Y.T., Kim, D.H., Suh, J.Y., Chung, J.H., Lee, B.L., Lee, Y. & Choi, B.S. (1999). Structural characteristics of tenecin 3, an insect antifungal protein. *International Union of Biochemistry and Molecular Biology-Life*, *47*, 369-376.

[270] Lehrer, R.I., Szklarek, D., Ganz, T. & Selsted, M.E. (1985). Correlation of binding of rabbit granulocyte peptides to *Candida albicans* with candidacidal activity. *Infection and Immunity*, *49*, 207-211.

[271] Leung, L.K. & Wang, T.T. (1999). Differential effects of chemotherapeutic agents on the Bcl-2/Bax apoptosis pathway in human breast cancer cell line MCF-7. *Breast Cancer Research and Treatment*, *55*, 73-83.

[272] Lewis, L.A., Choudhury, B., Balthazar, J.T., Martin, L.E., Ram, S., Rice, P.A., Stephens, D.S., Carlson, R. & Shafer, W.M. (2009). Phosphoethanolamine substitution of lipid A and resistance of *Neisseria gonorrhoeae* to cationic antimicrobial peptides and complement-mediated killing by normal human serum. *Infection and Immunity*, *77*, 1112-1120.

[273] Li, C., Blencke, H.M., Paulsen, V., Haug, T. & Stensvag, K. (2010). Powerful workhorses for antimicrobial peptide expression and characterization. *Bioengineered Bugs*, *1*, 217-220.

[274] Li, C., Song, L., Zhao, J., Zhu, L., Zou, H., Zhang, H., Wang, H. & Cai, Z. (2007). Preliminary study on a potential antibacterial peptide derived from histone H2A in hemocytes of scallop *Chlamys farreri*. *Fish & shellfish immunology*, *22*, 663-672.

[275] Li, G.H., Mine, Y., Hincke, M.T. & Nys, Y. (2007). Isolation and characterization of antimicrobial proteins and peptide from chicken liver. *Journal of Peptide Science*, *13*, 368-378.

[276] Li, H., Zhang, F., Guo, H., Zhu, Y., Yuan, J., Yang, G. & An, L. (2013). Molecular characterization of hepcidin gene in common carp (*Cyprinus carpio* L.) and its expression pattern responding to bacterial challenge. *Fish & Shellfish Immunology*, *35*, 1030-1038.

[277] Li, J. P., Chang, T. M., Wagner, D. & Chey, W. Y. (2001). Pancreatic phospholipase A 2 from the small intestine is a secretin-releasing factor in rats. *American Journal of Physiology-Gastrointestinal and Liver Physiology*, *281*, 526-532.

[278] Li, M. & Fang, Y. (2015). Histone variants: the artists of eukaryotic chromatin. *Science China Life Sciences*, *58*, 232-239.

[279] Li, P., Nijhawan, D., Budihardjo, I., Srinivasula, S.M., Ahmad, M., Alnemri, E.S. & Wang, X. (1997). Cytochrome c and dATP-dependent formation of Apaf-1/caspase-9 complex initiates an apoptotic protease cascade. *Cell*, *91*, 479-489.

[280] Li, Y. & Chen, Z. (2008). RAPD: A database of recombinantly-produced antimicrobial peptides. *FEMS Microbiology Letters*, *289*, 126-129.

[281] Li, Y., Xiang, Q., Zhang, Q., Huang, Y. & Su, Z. (2012). Overview on the recent study of antimicrobial peptides: Origins, functions, relative mechanisms and application. *Peptides*, *37*, 207-215.

[282] Li, Z., Hong, W.S., Qiu, H.T., Zhang, Y.T., Yang, M.S., You, X.X. & Chen, S.X. (2016). Cloning and expression of two hepcidin genes in the mudskipper (*Boleophthalmus pectinirostris*) provides insights into their roles in male reproductive immunity. *Fish & Shellfish Immunology*, *56*, 239-247.

[283] Li, Z., Zhang, S., Gao, J., Guang, H., Tian, Y., Zhao, Z., Wang, Y. & Yu, H. (2013). Structural and functional characterization of CATH_BRALE, the defense molecule in the ancient salmonoid, *Brachymystax lenok*. *Fish & Shellfish Immunology*, *34*, 1–7.

[284] Liang, J.F. & Kim, C. (1999). Not only the nature of peptide but also the characteristics of cell membrane determine the antimicrobial mechanism of a peptide. *Chemical Biology & Drug Design*, *53*, 518-522.

[285] Liang, T., Ji, W., Zhang, G.R., Wei, K.J., Feng, K., Wang, W.M. & Zou, G.W. (2013). Molecular cloning and expression analysis of liver-expressed antimicrobial peptide 1 (LEAP-1) and LEAP-2 genes in the blunt snout bream (*Megalobrama amblycephala*). *Fish & Shellfish Immunology*, *35*, 553-563.

[286] Lim, K.J., Sung, B.H., Shin, J.R., Lee, Y.W., Yang, K.S. & Kim, S.C. (2013). A cancer specific cell-penetrating peptide, BR2, for the efficient delivery of an scFv into cancer cells. *PloS One*, *8*.

[287] Lin, H.J., Huang, T.C., Muthusamy, S., Lee, J.F., Duann, Y.F. & Lin, C.H. (2012). Piscidin-1, an antimicrobial peptide from fish (hybrid striped bass *Morone saxatilis* x *M. chrysops*), induces apoptotic and necrotic activity in HT1080 cells. *Zoological Science*, *29*, 327-332.

[288] Lin, W. J., Chien, Y. L., Pan, C. Y., Lin, T. L., Chen, J. Y., Chiu, S. J. & Hui, C. F. (2009). Epinecidin-1, an antimicrobial peptide from fish (*Epinephelus coioides*) which has an antitumor effect like lytic peptides in human fibrosarcoma cells. *Peptides*, *30*, 283–290.

[289] Lin, W., Liu, S., Hu, L. & Zhang, S. (2014). Characterization and bioactivity of hepcidin-2 in zebrafish: Dependence of antibacterial activity upon disulfide bridges. *Peptides*, *57*, 36-42.

[290] Linde, C.M., Hoffner, S.E., Refai, E. & Andersson, M. (2001). *In vitro* activity of PR-39, a proline-arginine-rich peptide, against susceptible and multi-drug-resistant *Mycobacterium tuberculosis*. *Journal of Antimicrobial Chemotherapy*, *47*, 575-580.

[291] Liu, F., Li, J.L., Yue, G.H., Fu, J.J. & Zhou, Z.F. (2010). Molecular cloning and expression analysis of the liver-expressed antimicrobial peptide 2 (LEAP-2) gene in grass carp. *Veterinary immunology and immunopathology*, *133*, 133-143.

[292] Liu, N., Zhang, R.R., Fan, Z.X., Zhao, X.F., Wang, X.W. & Wang, J.X. (2016). Characterization of a type-I crustin with broad-spectrum antimicrobial activity from red swamp crayfish *Procambarus clarkia*. *Developmental & Comparative Immunology*, *61*, 145-153.

[293] Liu, Q., Zhao, H., Jiang, Y., Wu, M., Tian, Y., Wang, D., Lao, Y., Xu, N. & Li, Z. (2016). Development of a lytic peptide derived from BH3-only proteins. *Cell Death Discovery*, *2*, 16008.

[294] Liu, Q.N., Xin, Z.Z., Zhang, D.Z., Jiang, S.H., Chai, X.Y., Wang, Z.F., Li, C.F., Zhou, C.L. & Tang, B.P. (2017). cDNA cloning and expression analysis of a hepcidin gene from yellow catfish *Pelteobagrus fulvidraco* (Siluriformes: Bagridae). *Fish & Shellfish Immunology*, *60*, 247-254.

[295] Liu, Y., Gong, W., Huang, C.C., Herr, W. & Cheng, X. (1999). Crystal structure of the conserved core of the herpes simplex virus transcriptional regulatory protein VP16. *Genes & development*, *13,* 1692-1703.

[296] Liu, Y., Han, X., Chen, X., Yu, S., Chai, Y., Zhai, T. & Zhu, Q. (2017). Molecular characterization and functional analysis of the hepcidin gene from roughskin sculpin (*Trachidermus fasciatus*). *Fish & Shellfish Immunology*, *68*, 349-358.

[297] Liu, Y., Luo, J., Xu, C., Ren, F., Peng, C., Wu, G. & Zhao, J. (2000). Purification, characterization, and molecular cloning of the gene of a seed-specific antimicrobial protein from pokeweed. *Plant Physiology*, *122*, 1015-1024.

[298] Livak, K.J. & Schmittgen, T.D. (2001). Analysis of relative gene expression data using real-time quantitative PCR and the 2− ΔΔCT method. *Methods*, *25*, 402-408.

[299] Lu, A., Hu, X., Xue, J., Zhu, J., Wang, Y. & Zhou, G. (2012). Gene expression profiling in the skin of zebrafish infected with *Citrobacter freundii*. *Fish & Shellfish Immunology*, *32*(2), pp.273-283.

[300] Lu, X.J., Chen, J., Huang, Z.A., Shi, Y.H. & Lv, J.N. (2011). Identification and characterization of a novel cathelicidin from ayu, *Plecoglossus altivelis*. *Fish & Shellfish Immunology*, *31*, 52–57.

[301] Luders, T., Birkemo, G.A., Nissen-Meyer, J., Andersen, O. & Nes, I.F. (2005). Proline conformation-dependent antimicrobial activity of a proline-rich histone H1 N-terminal peptide fragment isolated from the skin mucus of Atlantic salmon. *Antimicrobial Agents and Chemotherapy*, *49*, 2399-2406.

[302] Ludtke, S. J., He, K., Heller, W. T., Harroun, T. A., Yang, L. & Huang, H. W. (1996). Membrane pores induced by magainin. *Biochemistry, 35*, 13723–13728

[303] Lugardon, K., Raffner, R., Goumon, Y., Corti, A., Delmas, A., Bulet, P., Aunis, D. & Metz-Boutigue, M.H. (2000). Antibacterial and antifungal activities of vasostatin-1, the N-terminal fragment of chromogranin A. *The Journal of Biological Chemistry*, *275*, 10745-10753.

[304] Luger, K., Rechsteiner, T. & Richmond, T. J. (1997). Characterization of nucleosome core particles containing histone proteins made in bacteria. *Journal of Molecular Biology*, *272*, 301–311.

[305] Lynch, M., O'Hely, M., Walsh, B. & Force, A. (2001). The probability of preservation of a newly arisen gene duplicate. *Genetics*, *159*, 1789-1804.

[306] Magnadottir, B. (2006). Innate immunity of fish (overview). *Fish & Shellfish Immunology*, *20*, 137-151.

[307] Mai, J., Tian, X.L., Gallant, J.W., Merkley, N., Biswas, Z., Syvitski, R., Douglas, S.E., Ling, J. & Li, Y.H. (2011). A novel target-specific, salt-resistant antimicrobial peptide against the cariogenic pathogen *Streptococcus mutans*. *Antimicrobial agents and chemotherapy*, *55*, 5205-5213.

[308] Mai, J.C., Mi, Z., Kim, S.H., Ng, B. & Robbins, P.D. (2001). A proapoptotic peptide for the treatment of solid tumors. Cancer Research, *61*, 7709-7712.

[309] Mai, S., Mauger, M.T., Niu, L.N., Barnes, J.B., Kao, S., Bergeron, B.E., Ling, J.Q. & Tay, F.R. (2017). Potential applications of antimicrobial peptides and their mimics in combating caries and pulpal infections. *Acta biomaterialia*, *49*, 16-35.

[310] Maier, V.H., Dorn, K.V., Gudmundsdottir, B.K. & Gudmundsson, G.H. (2008). Characterisation of cathelicidin gene family members in divergent fish species. *Molecular Immunology*, *45*, 3723–3730.

[311] Malmsten, M., Davoudi, M., Walse, B., Rydengård, V., Pasupuleti, M., Mörgelin, M. & Schmidtchen, A. (2007). Antimicrobial peptides derived from growth factors. *Growth Factors*, *25*, 60-70.

[312] Maltseva, A.L., Aleshina, G.M., Kokryakov, V.N. & Krasnodembsky, E.G. (2007). Diversity of antimicrobial peptides in acidic extracts from coelomocytes of starfish *Asterias rubens* L. Vestnik Sankt-Peterburgskogo Universiteta*,* Seriya, *3*, 85-94.

[313] Maltseva, A.L., Aleshina, G.M., Kokryakov, V.N., Krasnodembsky, E.G. & Ovchinnikova, T.V. (2004). New antimicrobial peptides from coelomocytes of sea star *Asterias rubens* L. *Biologiya*, *4*, 101-108.

[314] Mamikonyan, G., Kiyatkin, A., Movsesyan, N., Mkrtichyan, M., Ghochikyan, A., Petrushina, I., Hwang, J., Ichim, T.E., Keledjian, H. & Agadjanyan, M.G. (2008). Detection of the active components of calf thymus nuclear proteins (TNP), histones that are binding with high affinity to HIV-1 envelope proteins and CD4 molecules. *Current HIV research*, *6*, 318-326.

[315] Martin-Antonio, B., Jimenez-Cantizano, R.M., Salas-Leiton, E., Infante, C. and Manchado, M. (2009). Genomic characterization and gene expression analysis of four hepcidin genes in the redbanded seabream (*Pagrus auriga*). *Fish & Shellfish Immunology*, *26*, 483-491.

[316] Marzluff, W.F., Gongidi, P., Woods, K.R., Jin, J. and Maltais, L.J. (2002). The human and mouse replication-dependent histone genes. *Genomics*, *80,* 487-498.

[317] Masso-Silva, J., Diamond, G., Macias-Rodriguez, M. & Ascencio, F. (2011). Genomic organization and tissue-specific expression of hepcidin in the pacific mutton hamlet, *Alphestes immaculatus* (Breder, 1936). *Fish & Shellfish Immunology*, *31*, 1297-1302.

[318] Masso-Silva, J.A. & Diamond, G. (2014). Antimicrobial peptides from fish. *Pharmaceuticals*, *7*, 265-310.

[319] Matsuzaki, K. (1999). Why and how are peptide–lipid interactions utilized for self-defense? Magainins and tachyplesins as archetypes. *Biochimica et Biophysica Acta (BBA)-Biomembranes*, *1462*, 1-10.

[320] Matsuzaki, K., Sugishita, K.I., Harada, M., Fujii, N. & Miyajima, K. (1997a). Interactions of an antimicrobial peptide, magainin 2, with outer and inner membranes of Gram-negative bacteria. *Biochimica et Biophysica Acta (BBA)-Biomembranes*, *1327*, 119-130.

[321] Matsuzaki, K., Yoneyama, S., Fujii, N., Miyajima, K., Yamada, K.-I., Kirino, Y. & Anzai, K. (1997b). Membrane permeabilization mechanisms of a cyclic antimicrobial peptide, tachyplesin I, and its linear analogue. *Biochemistry, 36*, 9799–9806.

[322] Mayer, L. (2003). Mucosal immunity. *Pediatrics*, *111*, 1595-1600.

[323] McCoy, J. & La Ville, E. (2001). Expression and purification of thioredoxin fusion proteins. *Current Protocols in Protein Science*, 6-7.

[324] McPhee, J.B., Scott, M.G. & Hancock, R.E. (2005). Design of host defence peptides for antimicrobial and immunity enhancing activities. *Combinatorial Chemistry & High Throughput Screening*, *8*, 257-272.

[325] Meister, M., Lemaitre, B. & Hoffmann, J.A. (1997). Antimicrobial peptide defense in Drosophila. *BioEssays*, *19*, 1019-1026.

[326] Meneguetti, B.T., Machado, L. dos S., Oshiro, K.G.N., Nogueira, M.L., Carvalho, C.M.E. & Franco, O.L. (2017). Antimicrobial peptides from fruits and their potential use as biotechnological tools—a review and outlook. *Frontiers in Microbiology*, *7*, 1–13.

[327] Mesa, M.A. & Vasquez, G. (2013). NETosis. *Autoimmune diseases*, *2013,*1-7.

[328] Metzler, K.D., Fuchs, T.A., Nauseef, W.M., Reumaux, D., Roesler, J., Schulze, I., Wahn, V., Papayannopoulos, V. & Zychlinsky, A. (2011). Myeloperoxidase is required for neutrophil extracellular trap formation: Implications for innate immunity. *Blood*, *117*, 953-959.

[329] Meyer, E. & Manahan, D.T. (2010). Gene expression profiling of genetically determined growth variation in bivalve larvae (*Crassostrea gigas*). *Journal of Experimental Biology*, *213*, 749-758.

[330] Mihajlovic, M. & Lazaridis, T. (2012). Charge distribution and imperfect amphipathicity affect pore formation by antimicrobial peptides. *Biochimica et Biophysica Acta (BBA)-Biomembranes*, *1818*, 1274-1283.

[331] Miller, B.F., Abrams, R., Dorfman, A. & Klein, M. (1942). Antibacterial properties of protamine and histone. *Science*, *96*, 428-430.

[332] Miller, S.I., Kukral, A.M. & Mekalanos, J.J. (1989). A two-component regulatory system (phoP phoQ) controls *Salmonella typhimurium* virulence. *Proceedings of the National Academy of Sciences*, *86*, 5054-5058.

[333] Miyasaki, K.T. & Lehrer, R.I. (1998). β-sheet antibiotic peptides as potential dental therapeutics1. *International Journal of Antimicrobial Agents*, *9*, 269-280.

[334] Miyashita, T., Krajewski, S., Krajewska, M., Wang, H.G., Lin, H.K., Liebermann, D.A., Hoffman, B. & Reed, J.C. (1994). Tumor suppressor p53 is a regulator of bcl-2 and bax gene expression in vitro and in vivo. *Oncogene*, *9*, 1799-1805.

[335] Moerman, L., Bosteels, S., Noppe, W., Willems, J., Clynen, E., Schoofs, L., Thevissen, K., Tytgat, J., Van Eldere, J., Van Der Walt, J. & Verdonck, F. (2002). Antibacterial and antifungal properties of α-helical, cationic peptides in the venom of scorpions from southern Africa. *The FEBS Journal*, *269*, 4799-4810.

[336] Mohd-Shaharuddin, N., Mohd-Adnan, A., Kua, B.C. & Nathan, S. (2013). Expression profile of immune-related genes in *Lates calcarifer* infected by *Cryptocaryon irritans*. *Fish & Shellfish Immunology*, *34*, 762-769.

[337] Montville, T.J. & Chen, Y., (1998). Mechanistic action of pediocin and nisin: Recent progress and unresolved questions. *Applied Microbiology and Biotechnology*, *50*, 511-519.

[338] Moon, W.J., Hwang, D.K., Park, E.J., Kim, Y.M. & Chae, Y.K. (2007). Recombinant expression, isotope labeling, refolding, and purification of an antimicrobial peptide, piscidin. *Protein Expression and Purification*, *51*, 141-146.

[339] Moore, A.J., Devine, D.A. & Bibby, M.C. (1994). Preliminary experimental anticancer activity of cecropins. *Peptide Research*, *7*, 265-269.

[340] Moore, K.S., Wehrli, S., Roder, H., Rogers, M., Forrest, J.N., McCrimmon, D. & Zasloff, M. (1993). Squalamine: an aminosterol antibiotic from the shark. *Proceedings of the National Academy of Sciences*, *90*, 1354-1358.

[341] Morash, M.G., Douglas, S.E., Robotham, A., Ridley, C.M., Gallant, J.W. & Soanes, K.H. (2011). The zebrafish embryo as a tool for screening and characterizing pleurocidin host-defense peptides as anti-cancer agents. *Disease Models and Mechanisms*, *4*, 622-633.

[342] Munoz, A., Marcos, J.F. & Read, N.D. (2012). Concentration-dependent mechanisms of cell penetration and killing by the de novo designed antifungal hexapeptide PAF26. *Molecular Microbiology*, *85*, 89-106.

[343] Nagashima, Y., Kikuchi, N., Shimakura, K. & Shiomi, K. (2003). Purification and characterization of an antibacterial protein in the skin secretion of rockfish *Sebastes schlegeli*. *Comparative Biochemistry and Physiology* Part C*: Toxicology & Pharmacology*, *136*, 63-71.

[344] Nakayama, K. (1997). Furin: A mammalian subtilisin/Kex2p-like endoprotease involved in processing of a wide variety of precursor proteins. *Biochemical Journal*, *327*, 625.

[345] Nam, B.H., Moon, J.Y., Kim, Y.O., Kong, H.J., Kim, W.J., Lee, S.J. & Kim, K.K. (2010). Multiple β-defensin isoforms identified in early developmental stages of the teleost *Paralichthys olivaceus*. *Fish & Shellfish Immunology*, *28*, 267-274.

[346] Nam, B.H., Seo, J.K., Go, H.J., Lee, M.J., Kim, Y.O., Kim, D.G., Lee, S.J. & Park, N.G. (2012). Purification and characterization of an antimicrobial histone H1-like protein and its gene from the testes of olive flounder, *Paralichthys olivaceus*. *Fish & Shellfish Immunology*, *33*, 92-98.

[347] Nam, Y.K., Cho, Y.S., Lee, S.Y., Kim, B.S. & Kim, D.S. (2011). Molecular characterization of hepcidin gene from mud loach (*Misgurnus mizolepis*; Cypriniformes). *Fish & Shellfish Immunology*, *31*, 1251-1258.

[348] Nemeth, E. & Ganz, T. (2006). Regulation of iron metabolism by hepcidin. *Annual Review of Nutrition*, *26*, 323-42.

[349] Nemeth, E., Tuttle, M.S., Powelson, J., Vaughn, M.B., Donovan, A., Ward, D.M., Ganz, T. & Kaplan, J. (2004). Hepcidin regulates cellular iron efflux by binding to ferroportin and inducing its internalization. *Science*, *306*, 2090-2093.

[350] Neves, J.V., Caldas, C., Vieira, I., Ramos, M.F. & Rodrigues, P.N. (2015). Multiple hepcidins in a teleost fish, *Dicentrarchus labrax*: different hepcidins for different roles. *The Journal of Immunology*, *195*, 2696-2709.

[351] Neves, J.V., Caldas, C., Wilson, J.M. & Rodrigues, P.N.S. (2011). Molecular mechanisms of hepcidin regulation in sea bass (*Dicentrarchus labrax*). *Fish & Shellfish Immunology*, *31,* 1154-1161.

[352] Ng, T.H., Chang, S.H., Wu, M.H. & Wang, H.C. (2013). Shrimp hemocytes release extracellular traps that kill bacteria. *Developmental & Comparative Immunology*, *41*, 644-651.

[353] Nguyen, L.T., Haney, E.F. & Vogel, H.J. (2011). The expanding scope of antimicrobial peptide structures and their modes of action. *Trends in Biotechnology*, *29*, 464-472.

[354] Nicolas, G., Chauvet, C., Viatte, L., Danan, J.L., Bigard, X., Devaux, I., Beaumont, C., Kahn, A. & Vaulont, S. (2002). The gene encoding the iron regulatory peptide hepcidin is regulated by anemia, hypoxia, and inflammation. *The Journal of clinical investigation*, *110*, 1037-1044.

[355] Nijnik, A. & Hancock, R.E.W. (2009). Host defence peptides: antimicrobial and immunomodulatory activity and potential applications for tackling antibiotic-resistant infections. *Emerging Health Threats Journal*, *2*, 7078.

[356] Nikapitiya, C., Dorrington, T. & Gomez-Chiarri, M. (2013). The role of histones in the immune responses of aquatic invertebrates. *International Scientific Journal*, *10*, 94-101.

[357] Nilsson, B.L., Soellner, M.B. & Raines, R.T. (2005). Chemical synthesis of proteins. *Annual Review of Biophysics and Biomolecular Structure, 34*, 91-118.

[358] Nissen-Meyer, J. & Nes, I.F. (1997). Ribosomally synthesized antimicrobial peptides: their function, structure, biogenesis, and mechanism of action. *Archives of Microbiology*, *167*, 67-77.

[359] Niu, S.F., Jin, Y., Xu, X., Qiao, Y., Wu, Y., Mao, Y., Su, Y.Q. & Wang, J. (2013). Characterization of a novel piscidin-like antimicrobial peptide from *Pseudosciaena crocea* and its immune response to *Cryptocaryon irritans*. *Fish & Shellfish Immunology*, *35*, 513-524.

[360] Noga, E.J., Borron, P.J., Hinshaw, J., Gordon, W.C., Gordon, L.J. & Seo, J.K. (2011). Identification of histones as endogenous antibiotics in fish and quantification in rainbow trout (*Oncorhynchus mykiss*) skin and gill. *Fish Physiology and Biochemistry*, *37*, 135-152.

[361] Noga, E.J., Fan, Z. & Silphaduang, U. (2001). Histone-like proteins from fish are lethal to parasitic dinoflagellate *Amyloodinium ocellatum*. *Parasitology, 123*, 57–65.

[362] Noga, E.J., Fan, Z. & Silphaduang, U. (2002). Host site of activity and cytological effects of histone-like proteins against the parasitic dinoflagellate *Amyloodinium ocellatum*. *Diseases of Aquatic Organisms*, *52*, 207–215.

[363] Noga, E.J., Silphaduang, U., Park, N.G., Seo, J.K., Stephenson, J. & Kozlowicz, S. (2009). Piscidin 4, a novel member of the piscidin family of antimicrobial peptides. *Comparative Biochemistry and Physiology* Part B*: Biochemistry and Molecular Biology*, *152*, 299-305.

[364] Noga, E.J., Ullal, A.J., Corrales, J. & Fernandes, J.M. (2011). Application of antimicrobial polypeptide host defenses to aquaculture: Exploitation of downregulation and upregulation responses. *Comparative Biochemistry and Physiology* Part D*: Genomics and Proteomics*, *6*, 44-54.

[365] Oli, M.W., Otoo, H.N., Crowley, P.J., Heim, K.P., Nascimento, M.M., Ramsook, C.B., Lipke, P.N. & Brady, L.J. (2012). Functional amyloid formation by *Streptococcus mutans*. *Microbiology*, *158*, 2903-2916.

[366] Olivieri, C., Buonocore, F., Picchietti, S., Taddei, A.R., Bernini, C., Scapigliati, G., Dicke, A.A., Vostrikov, V.V., Veglia, G. & Porcelli, F. (2015). Structure and membrane interactions of chionodracine, a piscidin-like antimicrobial peptide from the icefish *Chionodraco hamatus*. *Biochimica et Biophysica Acta (BBA)-Biomembranes*, *1848*, 1285-1293.

[367] Onuma, Y., Satake, M., Ukena, T., Roux, J., Chanteau, S., Rasolofonirina, N., Ratsimaloto, M., Naoki, H. & Yasumoto, T. (1999). Identification of putative palytoxin as the cause of clupeotoxism. *Toxicon*, *37*, 55-65.

[368] Orrapin, S. & Intorasoot, S. (2014). Recombinant expression of novel protegrin-1 dimer and LL-37-linker–histatin-5 hybrid peptide mediated biotin carboxyl carrier protein fusion partner. *Protein Expression and Purification*, *93*, 46-53.

[369] Otvos Jr, L., (2000). Antibacterial peptides isolated from insects. *Journal of Peptide Science*, *6*, 497-511.

[370] Ourth, D.D. & Chung, K.T. (2004). Purification of antimicrobial factor from granules of channel catfish peripheral blood leucocytes. *Biochemical and Biophysical Research Communications*, *313*, 28-36.

[371] Palic, D., Andreasen, C.B., Ostojić, J., Tell, R.M. & Roth, J.A. (2007b). Zebrafish (*Danio rerio*) whole kidney assays to measure neutrophil extracellular trap release and degranulation of primary granules. *Journal of Immunological Methods*, *319*, 87-97.

[372] Palic,D., Ostojic, J., Andreasen, C.B. & Roth, J.A. (2007a). Fish cast NETs: Neutrophil extracellular traps are released from fish neutrophils. *Developmental and Comparative Immunology*, *31*, 805–816.

[373] Pan, C.Y., Chen, J.Y., Lin, T.L. & Lin, C.H. (2009). In vitro activities of three synthetic peptides derived from epinecidin-1 and an anti-lipopolysaccharide factor against *Propionibacterium acnes*, *Candida albicans*, and *Trichomonas vaginalis*. *Peptides*, *30*, 1058-1068.

[374] Pan, C.Y., Chen, J.Y., Ni, I.H., Wu, J.L. & Kuo, C.M. (2008). Organization and promoter analysis of the grouper (*Epinephelus coioides*) epinecidin-1 gene. *Comparative Biochemistry and Physiology* Part B*: Biochemistry and Molecular Biology*, *150*, 358–367.

[375] Pan, C.Y., Huang, T.C., Wang, Y.D., Yeh, Y.C., Hui, C.F. & Chen, J.Y. (2012). Oral administration of recombinant epinecidin-1 protected grouper (*Epinephelus coioides*) and zebrafish (*Danio rerio*) from *Vibrio vulnificus* infection and enhanced immune-related gene expressions. *Fish & Shellfish Immunology*, *32*, 947-957.

[376] Pan, C.Y., Peng, K.C., Lin, C.H. & Chen, J.Y. (2011). Transgenic expression of tilapia hepcidin 1-5 and shrimp chelonianin in zebrafish and their resistance to bacterial pathogens. *Fish & Shellfish Immunology*, *31*, 275-285.

[377] Pan, C.Y., Rajanbabu, V., Chen, J.Y., Her, G.M. & Nan, F.H. (2010). Evaluation of the epinecidin-1 peptide as an active ingredient in cleaning solutions against pathogens. *Peptides*, *31*, 1449-1458.

[378] Pandey, B.K., Srivastava, S., Singh, M. & Ghosh, J.K. (2011). Inducing toxicity by introducing a leucine-zipper-like motif in frog antimicrobial peptide, magainin 2. *Biochemical Journal*, *436*, 609-620.

[379] Papagianni, M. (2003). Ribosomally synthesized peptides with antimicrobial properties: Biosynthesis, structure, function, and applications. *Biotechnology Advances*, *21*, 465-499.

[380] Papareddy, P., Rydengård, V., Pasupuleti, M., Walse, B., Mörgelin, M., Chalupka, A., Malmsten, M. & Schmidtchen, A. (2010). Proteolysis of human thrombin generates novel host defense peptides. *PLoS Pathogens*, *6*.

[381] Papo, N. & Shai, Y. (2005). Host defense peptides as new weapons in cancer treatment. *Cellular and Molecular Life Sciences*, *62*, 784-790.

[382] Papo, N. and Shai, Y. (2003). Can we predict biological activity of antimicrobial peptides from their interactions with model phospholipid membranes?. *Peptides*, *24*, 1693-1703.

[383] Parachin, N.S., Mulder, K.C., Viana, A.A.B., Dias, S.C. & Franco, O.L. (2012). Expression systems for heterologous production of antimicrobial peptides. *Peptides*, *38*, 446-456.

[384] Park, C. B., Yi, K. S., Matsuzaki, K., Kim, M. S. & Kim, S. C. (2000). Structure-activity analysis of buforin II, a histone H2A-derived antimicrobial peptide: The proline hinge is responsible for the cell-penetrating ability of buforin II. *Proceedings of the National Academy of Sciences*, *97*, 8245–8250.

[385] Park, C.B., Kim, H.S. & Kim, S.C. (1998). Mechanism of action of the antimicrobial peptide buforin II: buforin II kills microorganisms by penetrating the cell membrane and inhibiting cellular functions. *Biochemical and Biophysical Research Communications, 244*, 253-257.

[386] Park, C.B., Kim, M.S. & Kim, S.C. (1996). A Novel Antimicrobial Peptide from *Bufo bufo gargarizans*. *Biochemical and Biophysical Research Communications*, *218*, 408-413.

[387] Park, C.B., Lee, J.H., Park, I.Y., Kim, M.S. & Kim, S.C. (1997). A novel antimicrobial peptide from the loach, *Misgurnus anguillicaudatus*. *FEBS Letters*, 411, 173–178.

[388] Park, C.H., Valore, E.V., Waring, A.J. & Ganz, T. (2001). Hepcidin, a urinary antimicrobial peptide synthesized in the liver. *The Journal of Biological Chemistry, 276*, 7806–7810.

[389] Park, I.Y., Park, C.B., Kim, M.S. & Kim, S.C. (1998). Parasin I, an antimicrobial peptide derived from histone H2A in the catfish, *Parasilurus asotus*. *FEBS Letters*, *437*, 258-262.

[390] Park, N.G., Silphaduang, U., Moon, H.S., Seo, J.K., Corrales, J. & Noga, E.J. (2011). Structure-activity relationships of piscidin 4, a piscine antimicrobial peptide. *Biochemistry*, *50*, 3288–3299.

[391] Park, Y., Jang, S.H., Lee, D.G. & Hahm, K.S. (2004). Antinematodal effect of antimicrobial peptide, PMAP-23, isolated from porcine myeloid against *Caenorhabditis elegans*. *Journal of Peptide Science*, *10*, 304-311.

[392] Parseghian, M.H. & Luhrs, K.A. (2006). Beyond the walls of the nucleus: the role of histones in cellular signaling and innate immunity. *Biochemistry and Cell Biology*, *84*, 589–604.

[393] Pasupuleti, M., Schmidtchen, A. & Malmsten, M. (2012). Antimicrobial peptides: key components of the innate immune system. *Critical Reviews in Biotechnology*, *32*, 143-171.

[394] Pasupuleti, M., Schmidtchen, A., Chalupka, A., Ringstad, L. & Malmsten, M. (2009). End-tagging of ultra-short antimicrobial peptides by W/F stretches to facilitate bacterial killing. *PLoS One*, *4*.

[395] Patat, S.A., Carnegie, R.B., Kingsbury, C., Gross, P.S., Chapman, R. & Schey, K.L. (2004). Antimicrobial activity of histones from hemocytes of the Pacific white shrimp. *The FEBS Journal*, *271*, 4825-4833.

[396] Patrzykat, A., Gallant, J.W., Seo, J.K., Pytyck, J. & Douglas, S.E. (2003). Novel antimicrobial peptides derived from flatfish genes. *Antimicrobial Agents and Chemotherapy*, *47*, 2464–2470.

[397] Patrzykat, A., Zhang, L., Mendoza, V., Iwama, G.K. & Hancock, R.E.W. (2001). Synergy of histone-derived peptides of coho salmon with lysozyme and flounder pleurocidin. *Antimicrobial Agents and Chemotherapy*, *45*, 1337–1342.

[398] Pavia, K.E., Spinella, S.A. & Elmore, D.E. (2012). Novel histone-derived antimicrobial peptides use different antimicrobial mechanisms. *Biochimica et Biophysica Acta (BBA)-Biomembranes*, *1818*, 869-876.

[399] Pedersen, G.M., Gildberg, A., Steiro, K. & Olsen, R.L. (2003). Histone-like proteins from Atlantic cod milt: Stimulatory effect on Atlantic salmon leucocytes *in vivo* and *in vitro*. *Comparative Biochemistry and Physiology* Part B*: Biochemistry and Molecular Biology*, *134*, 407-416.

[400] Peng, K.C., Lee, S.H., Hour, A.L., Pan, C.Y., Lee, L.H. & Chen, J.Y. (2012). Five different piscidins from Nile tilapia, *Oreochromis niloticus*: Analysis of their expressions and biological functions. *PloS One*, *7*.

[401] Peng, K.C., Pan, C.Y., Chou, H.N. & Chen, J.Y. (2010). Using an improved Tol2 transposon system to produce transgenic zebrafish with epinecidin-1 which enhanced resistance to bacterial infection. *Fish & Shellfish Immunology*, *28*, 905-917.

[402] Pereiro, P., Figueras, A. & Novoa, B. (2012). A novel hepcidin-like in turbot (*Scophthalmus maximus* L.) highly expressed after pathogen challenge but not after iron overload. *Fish & Shellfish Immunology*, *32*, 879-889.

[403] Persson, S., Killian, J.A. & Lindblom, G. (1998). Molecular ordering of interfacially localized tryptophan analogs in ester-and ether-lipid bilayers studied by 2H-NMR. *Biophysical journal*, *75*, 1365-1371.

[404] Pietrantoni, A., M. G. Ammendolia, A. Tinari, R. Siciliano, P. Valenti, & F. Superti. (2006). Bovine lactoferrin peptidic fragments involved in inhibition of Echovirus 6 in vitro infection. *Antiviral Research 69*, 98–106.

[405] Pigeon, C., Ilyin, G., Courselaud, B., Leroyer, P., Turlin, B., Brissot, P. & Loréal, O., (2001). A new mouse liver-specific gene, encoding a protein homologous to human antimicrobial peptide hepcidin, is overexpressed during iron overload. *Journal of Biological Chemistry*, *276*, 7811-7819.

[406] Pijanowski, L., Golbach, L., Kolaczkowska, E., Scheer, M., Verburg-van Kemenade, B.M.L. & Chadzinska, M. (2013). Carp neutrophilic granulocytes form extracellular traps *via* ROS-dependent and independent pathways. *Fish & Shellfish Immunology*, *34*, 1244-1252.

[407] Podda, E., Benincasa, M., Pacor, S., Micali, F., Mattiuzzo, M., Gennaro, R. & Scocchi, M. (2006). Dual mode of action of Bac7, a proline-rich antibacterial peptide. *Biochimica et Biophysica Acta (BBA)-General Subjects*, *1760*, 1732-1740.

[408] Pospisilova, D., Mims, M.P., Nemeth, E., Ganz, T. & Prchal, J.T. (2006). DMT1 mutation: Response of anemia to darbepoetin administration and implications for iron homeostasis. *Blood*, *108*, 404-405.

[409] Prenner, E.J., Lewis, R.N. & McElhaney, R.N. (1999). The interaction of the antimicrobial peptide gramicidin S with lipid bilayer model and biological membranes. *Biochimica et Biophysica Acta (BBA)-Biomembranes*, *1462*, 201-221.

[410] Pridgeon, J.W., Mu, X. & Klesius, P.H. (2012). Expression profiles of seven channel catfish antimicrobial peptides in response to *Edwardsiella ictaluri* infection. *Journal of Fish Diseases*, *35*, 227-237.

[411] Pushpanathan, M., Rajendhran, J., Jayashree, S., Sundarakrishnan, B., Jayachandran, S. & Gunasekaran, P. (2012). Identification of a novel antifungal peptide with chitin-binding property from marine metagenome. *Protein and Peptide Letters*, *19,* 1289-1296.

[412] Qu, H., Chen, B., Peng, H. & Wang, K. (2013). Molecular cloning, recombinant expression, and antimicrobial activity of EC-hepcidin3, a new four-cysteine hepcidin isoform from *Epinephelus coioides*. *Bioscience, Biotechnology, and Biochemistry*, 77, 103-110.

[413] Rakers, S., Gebert, M., Uppalapati, S., Meyer, W., Maderson, P., Sell, A.F., Kruse, C. & Paus, R. (2010). 'Fish matters': The relevance of fish skin biology to investigative dermatology. *Experimental Dermatology*, *19*, 313-324.

[414] Ramey, G., Deschemin, J.C., Durel, B., Canonne-Hergaux, F., Nicolas, G. & Vaulont, S. (2010). Hepcidin targets ferroportin for degradation in hepatocytes. *Haematologica*, *95*, 501-504.

[415] Rao, A.G. (1999). Conformation and antimicrobial activity of linear derivatives of tachyplesin lacking disulfide bonds. *Archives of Biochemistry and Biophysics*, *36*, 127-134.

[416] Rao, X., Hu, J., Li, S., Jin, X., Zhang, C., Cong, Y., Hu, X., Tan, Y., Huang, J., Chen, Z. & Zhu, J. (2005). Design and expression of peptide antibiotic hPAB-β as tandem multimers in *Escherichia coli*. *Peptides*, *26*, 721-729.

[417] Rastogi, S. & Liberles, D.A. (2005). Subfunctionalization of duplicated genes as a transition state to neofunctionalization. *BMC Evolutionary Biology*, *5*, 28.

[418] Ren, G., Shen, W., Li, W. & Zhu, Y. (2014). Molecular characterization and expression pattern of a liver-expressed antimicrobial peptide 2 (LEAP-2) gene in yellow catfish (*Pelteobagrus fulvidraco*). *Journal of Aquaculture Research and Development*, *5*, 229.

[419] Ren, H.L., Wang, K.J., Zhou, H.L. & Yang, M. (2006). Cloning and organisation analysis of a hepcidin-like gene and cDNA from Japan sea bass, *Lateolabrax japonicus*. *Fish & Shellfish Immunology*, *21*, 221-227.

[420] Ren, S.X., Shen, J., Cheng, A.S., Lu, L., Chan, R.L., Li, Z.J., Wang, X.J., Wong, C.C., Zhang, L., Ng, S.S. & Chan, F.L. (2013). FK-16 derived from the anticancer peptide LL-37 induces caspase-independent apoptosis and autophagic cell death in colon cancer cells. *PLoS One 8*.

[421] Richards, R.C., O'Neil, D.B., Thibault, P. & Ewart, K.V. (2001). Histone H1: an antimicrobial protein of Atlantic salmon (*Salmo salar*). *Biochemical and Biophysical Research Communications*, *284*, 549-555.

[422] Robertson, L.S. (2009). Expression in fish of hepcidin, a putative antimicrobial peptide and iron regulatory hormone. In *Proceedings of The Third Bilateral Conference Between the United States and Russia: Aquatic Animal Health,* 284-292, Sheperdstown, West Virginia.

[423] Robinette, D., Wada, S., Arroll, T., Levy, M. G., Miller, W. L. & Noga, E. J. (1998). Antimicrobial activity in the skin of the channel catfish *Ictalurus punctatus*: Characterization of broad- spectrum histone-like antimicrobial proteins. *Cellular and Molecular Life Sciences*, *54*, 467–475.

[424] Robinette, D.W. & Noga, E.J. (2001). Histone-like protein: A novel method for measuring stress in fish. *Diseases of Aquatic Organisms*, *44*, 97-107.

[425] Robinson, W.E., McDougall, B., Tran, D. & Selsted, M.E. (1998). Anti-HIV-1 activity of indolicidin, an antimicrobial peptide from neutrophils. *Journal of Leukocyte Biology*, *63*, 94-100.

[426] Rodrigues, E.G., Dobroff, A.S., Cavarsan, C.F., Paschoalin, T., Nimrichter, L., Mortara, R.A., Santos, E.L., Fázio, M.A., Miranda, A., Daffre, S. & Travassos, L.R. (2008). Effective topical treatment of subcutaneous murine B16F10-Nex2 melanoma by the antimicrobial peptide gomesin. *Neoplasia*, *10*, 61-68.

[427] Rodrigues, P.N., Vázquez-Dorado, S., Neves, J.V. & Wilson, J.M. (2006). Dual function of fish hepcidin: response to experimental iron overload and bacterial infection in sea bass (*Dicentrarchus labrax*). *Developmental and Comparative Immunology*, *30*, 1156-1167.

[428] Rose, F.R.A.J., Bailey, K., Keyte, J.W., Chan, W.C., Greenwood, D. & Mahida, Y.R. (1998). Potential role of epithelial cell-derived histone H1 proteins in innate antimicrobial defense in the human gastrointestinal tract. *Infection and Immunity*, *66*, 3255-3263.

[429] Roux, P. P., & Blenis, J. (2004). ERK & p38 MAPK-activated protein kinases: A family of protein kinases with diverse biological functions. *Microbiology and Molecular Biology Reviews*, *68*, 320-344.

[430] Ruangsri, J., Kitani, Y., Kiron, V., Lokesh, J., Brinchmann, M.F., Karlsen, B.O. & Fernandes, J.M. (2013). A novel beta-defensin antimicrobial peptide in Atlantic cod with stimulatory effect on phagocytic activity. *PLoS One*, *8*.

[431] Ruangsri, J., Salger, S.A., Caipang, C.M., Kiron, V. & Fernandes, J.M. (2012). Differential expression and biological activity of two piscidin paralogues and a novel splice variant in Atlantic cod (*Gadus morhua* L.). *Fish & Shellfish Immunology*, *32*, 396-406.

[432] Saad, T.T. & Atallah, S.T. (2014). Studies on bacterial infection in marine fish. *Journal of the Arabian Aquaculture Society*, *374*, 1-20.

[433] Saad, T.T., Atallah, S.T. & El-Bana, S.A., (2014). Fish diseases and its economic effect on Egyptian fish farms. *Journal of Agriculture and Food Technology, 4*, 1-6.

[434] Saffarzadeh, M., Juenemann, C., Queisser, M.A., Lochnit, G., Barreto, G., Galuska, S.P., Lohmeyer, J. & Preissner, K.T. (2012). Neutrophil extracellular traps directly induce epithelial and endothelial cell death: A predominant role of histones. *PloS One*, *7*.

[435] Saint Jean, K.D., Henderson, K.D., Chrom, C.L., Abiuso, L.E., Renn, L.M. & Caputo, G.A. (2017). Effects of hydrophobic amino acid substitutions on antimicrobial peptide behavior. *Probiotics and Antimicrobial Proteins*, 1-12.

[436] Saint, N., Cadiou, H., Bessin, Y. & Molle, G. (2002). Antibacterial peptide pleurocidin forms ion channels in planar lipid bilayers. *Biochimica et Biophysica Acta (BBA)-Biomembranes*, *1564*, 359-364.

[437] Salerno, G., Parrinello, N., Roch, P. & Cammarata, M. (2007). cDNA sequence and tissue expression of an antimicrobial peptide, dicentracin; a new component of the moronecidin family isolated from head kidney leukocytes of sea bass, *Dicentrarchus labrax*. *Comparative Biochemistry and Physiology* Part B*: Biochemistry and Molecular Biology*, *146*, 521-529

[438] Salger, S.A., Cassady, K.R., Reading, B.J. & Noga, E.J. (2016). A diverse family of host-defense peptides (Piscidins) exhibit specialized anti-bacterial and anti-protozoal activities in fishes. *PloS One*, *11*.

[439] Samakovlis, C., Kylsten, P., Kimbrell, D.A., Engstroëm, A. & Hultmark, D. (1991). The andropin gene and its product, a male-specific antibacterial peptide in *Drosophila melanogaster*. *The EMBO Journal*, *10*, 163-169.

[440] Sang, C., Lin, Y., Jiang, K., Zhang, F. & Song, W. (2015). Molecular cloning and mRNA expression of a hepcidin gene from the spinyhead croaker, *Collichthys lucidus*. *Genetics and Molecular Research*, *14*, 16050-16059.

[441] Sang, Y., Ramanathan, B., Minton, J.E., Ross, C.R. & Blecha, F. (2006). Porcine liver-expressed antimicrobial peptides, hepcidin and LEAP-2: Cloning and induction by bacterial infection. *Developmental & Comparative Immunology*, *30*, 357-366.

[442] Sathyan, N., Philip, R., Chaithanya, E. R. & Anil Kumar, P. R. (2012b). Identification and Molecular characterization of Molluskin, a histone-H2A-derived antimicrobial peptide from molluscs. *ISRN Molecular Biology*,*2012*, 1–6.

[443] Sathyan, N., Philip, R., Chaithanya, E. R., Anil Kumar, P. R. & Antony, S. P. (2012a). Identification of a histone derived, putative antimicrobial peptide Himanturin from round whip ray *Himantura pastinacoides* and its phylogenetic significance. *Results in Immunology*, *2*, 120–124.

[444] Sathyan, N., Philip, R., Chaithanya, E. R., Anil Kumar, P. R., Sanjeevan, V. N. & Singh, I. S. B. (2013). Characterization of histone H2A derived antimicrobial peptides, Harriottins, from sicklefin chimaera *Neoharriotta pinnata* (Schnakenbeck, 1931) and Its Evolutionary Divergence with respect to CO1 and Histone H2A. *ISRN Molecular Biology*, *2013*, 1–10.

[445] Sathyan, N., Philip, R., Chaithanya, E.R., Kumar, P.A., Antony, S.P. & Singh, I.B. (2012c). Identification of a putative antimicrobial peptide sequence, Sunettin from marine clam, *Sunetta scripta*. *Blue Biotechnology Journal*, *1*, 397.

[446] Schein, C.H. & Noteborn, M.H. (1988). Formation of soluble recombinant proteins in *Escherichia coli* is favored by lower growth temperature. *Nature Biotechnology*, *6*, 291.

[447] Schmidt, N., Mishra, A., Lai, G.H. & Wong, G.C. (2010). Arginine-rich cell-penetrating peptides. *FEBS Letters*, *584*, 1806-1813.

[448] Schranz, M., Bakry, R., Creus, M., Bonn, G., Vogel, W. & Zoller, H. (2009). Activation and inactivation of the iron hormone hepcidin: Biochemical characterization of prohepcidin cleavage and sequential degradation to N-terminally truncated hepcidin isoforms. *Blood Cells, Molecules, and Diseases*, *43*, 169-179.

[449] Schwede, T., Kopp, J., Guex, N. & Peitsch, M.C. (2003). SWISS-MODEL: An automated protein homology-modeling server. *Nucleic Acids Research*, *31*, 3381-3385.

[450] Schweizer, F. (2009). Cationic amphiphilic peptides with cancer-selective toxicity. *European Journal of Pharmacology*, *625*, 190-194.

[451] Scocchi, M., Furlan, M., Venier, P. & Pallavicini, A. (2016). Cathelicidins: An ancient family of fish antimicrobial peptides. In *Lessons in Immunity*, 225-237.

[452] Scocchi, M., Pallavicini, A., Salgaro, R., Bociek, K. & Gennaro, R. (2009). The salmonid cathelicidins: a gene family with highly varied C-terminal antimicrobial domains. *Comparative Biochemistry and Physiology* Part B*: Biochemistry and Molecular Biology*, *152*, 376-381.

[453] Scudiero, D.A., Shoemaker, R.H., Paull, K.D., Monks, A., Tierney, S., Nofziger, T.H., Currens, M.J., Seniff, D. & Boyd, M.R. (1988). Evaluation of a soluble tetrazolium/formazan assay for cell growth and drug sensitivity in culture using human and other tumor cell lines. *Cancer Research*, *48*, 4827-4833.

[454] Selsted, M.E., Novotny, M.J., Morris, W.L., Tang, Y.Q., Smith, W. & Cullor, J.S. (1992). Indolicidin, a novel bactericidal tridecapeptide amide from neutrophils. *Journal of Biological Chemistry*, *267*, 4292-4295.

[455] Semreen, M.H., El-Gamal, M.I., Abdin, S., Alkhazraji, H., Kamal, L., Hammad, S., El-Awady, F., Waleed, D. & Kourbaj, L. (2018). Recent updates of marine antimicrobial peptides. *Saudi Pharmaceutical Journal*, *26*, 396-409.

[456] Seo, J.K., Stephenson, J., Crawford, J.M., Stone, K.L. & Noga, E.J. (2010). American oyster, *Crassostrea virginica*, expresses a potent antibacterial histone H2B protein. *Marine Biotechnology*, *12*, 543-551.

[457] Shabir, U., Ali, S., Magray, A.R., Ganai, B.A., Firdous, P., Hassan, T. & Nazir, R. (2017). Fish antimicrobial peptides (AMP's) as essential and promising molecular therapeutic agents: A review. *Microbial Pathogenesis*, *114*, *50-56*.

[458] Shafer, W.M., Qu, X.D., Waring, A.J. & Lehrer, R.I. (1998). Modulation of Neisseria gonorrhoeae susceptibility to vertebrate antibacterial peptides due to a member of the resistance/nodulation/division efflux pump family. *Proceedings of the National Academy of Sciences*, *95*, 1829-1833.

[459] Shai, Y. (1999). Mechanism of the binding, insertion and destabilization of phospholipid bilayer membranes by α-helical antimicrobial and cell non-selective membrane-lytic peptides. *Biochimica et Biophysica Acta (BBA)-Biomembranes*, *1462*, 55-70.

[460] Shai, Y. (2002). Mode of action of membrane active antimicrobial peptides. *Biopolymer*s, *66*, 236–248.

[461] Shamova, O. V Orlov, D.S., Balandin, S.V., Shramova, E.I., Tsvetkova, E.V., Panteleev, P.V., Tagaev, A., Kokryakov, V. & Ovchinnikova, T. (2014). Acipensins – novel antimicrobial peptides from leukocytes of the Russian sturgeon *Acipenser gueldenstaedtii*. , *Acta Naturae*, *6*, 99–109.

[462] Shan, Z., Zhu, K., Peng, H., Chen, B., Liu, J., Chen, F., Ma, X., Wang, S., Qiao, K. & Wang, K. (2016). The new antimicrobial peptide sphyastatin from the mud crab *Scylla paramamosain* with multiple antimicrobial mechanisms and high effect on bacterial infection. *Frontiers in microbiology*, *7*, 1140.

[463] Shen, W., Li, W., Lai, K., Wu, B. & Zhu, Y. (2009). Molecular cloning of an antimicrobial peptide hepcidin gene from yellow catfish (*Pelteobagrus fulvidraco*) and its expression analysis. *Journal of Agricultural Biotechnology*, *17*, 972-978.

[464] Shephard, K.L. (1994). Functions for fish mucus. *Reviews in Fish Biology and Fisheries*, *4*, 401-429.

[465] Shi, J. & Camus, A.C. (2006). Hepcidins in amphibians and fishes: antimicrobial peptides or iron-regulatory hormones?. *Developmental & Comparative Immunology*, *30*, 746-755.

[466] Shike, H., Lauth, X., Westerman, M.E., Ostland, V.E., Carlberg, J.M., Van Olst, J.C., Shimizu, C., Bulet, P. & Burns, J.C. (2002). Bass hepcidin is a novel antimicrobial peptide induced by bacterial challenge. *The FEBS Journal*, *269*, 2232-2237.

[467] Shike, H., Shimizu, C., Lauth, X. & Burns, J.C. (2004). Organization and expression analysis of the zebrafish hepcidin gene, an antimicrobial peptide gene conserved among vertebrates. *Developmental & Comparative Immunology*, *28*, 747-754.

[468] Shin, S.C., Ahn, I.H., Ahn, D.H., Lee, Y.M., Lee, J., Lee, J.H., Kim, H.W. & Park, H. (2017). Characterization of two antimicrobial peptides from antarctic fishes (*Notothenia coriiceps* and *Parachaenichthys charcoti*). *PLoS one 12*.

[469] Shinnar, A.E., Butler, K.L. & Park, H.J. (2003). Cathelicidin family of antimicrobial peptides: Proteolytic processing and protease resistance. *Bioorganic Chemistry*, *31*, 425-436.

[470] Silphaduang, U., Hincke, M.T., Nys, Y. & Mine, Y. (2006). Antimicrobial proteins in chicken reproductive system. *Biochemical and Biophysical Research Communications*, *340*, 648-655.

[471] Silva, O.N.O., Mulder, K.C., Barbosa, A.A., Otero-Gonzalez, A.J., Lopez-Abarrategui, C., Dias, S.C., Rezende, T. & Franco, O.L. (2011). Exploring the pharmacological potential of promiscuous host-defense peptides: from natural screenings to biotechnological applications. *Frontiers in Microbiology*, *2*, 232.

[472] Sim, S., Cutrona, K.J., Beyer, B., Wang, P., Radhakrishnan, M.L. & Elmore, D.E. (2016). Characterization of Nucleic Acid Binding by the Histone-Derived Antimicrobial Peptides Buforin II and DesHDAP1. *Biophysical Journal*, *110*, 560-561.

[473] Singh, B., Arora, S., Agrawal, P. & Gupta, S.K. (2011). Hepcidin: A novel peptide hormone regulating iron metabolism. *Clinica Chimica Acta*, *412*, 823-830.

[474] Sinha, S., Cheshenko, N., Lehrer, R.I. & Herold, B.C. (2003). NP-1, a rabbit α-defensin, prevents the entry and intercellular spread of herpes simplex virus type 2. *Antimicrobial Agents and Chemotherapy*, *47*, 494-500.

[475] Sinthuvanich, C., Veiga, A.S., Gupta, K., Gaspar, D., Blumenthal, R. & Schneider, J.P. (2012). Anticancer β-hairpin peptides: membrane-induced folding triggers activity. *Journal of the American Chemical Society*, *134*, 6210-6217.

[476] Sitaram, N. & Nagaraj, R. (1999). Interaction of antimicrobial peptides with biological and model membranes: Structural and charge requirements for activity. *Biochimica et Biophysica Acta (BBA)-Biomembranes*, *1462*, 29-54.

[477] Skerlavaj, B., Gennaro, R., Bagella, L., Merluzzi, L., Risso, A. & Zanetti, M. (1996). Biological characterization of two novel cathelicidin-derived peptides and identification of structural requirements for their antimicrobial and cell lytic activities. *Journal of Biological Chemistry*, *271*, 28375-28381.

[478] Smith, M.M., (1991). Histone structure and function. *Current Opinion In Cell Biology*, *3*, 429-437.

[479] Smith, V.J. & Fernandes, J.M. (2009). Antimicrobial peptides of the innate immune system. *Fish Defenses*, *1*, 241-275.

[480] Smith, V.J., Desbois, A.P. & Dyrynda, E.A. (2010). Conventional and unconventional antimicrobials from fish, marine invertebrates and micro-algae. *Marine Drugs*, *8*, 1213-1262.

[481] Smith, V.J., Fernandes, J.M., Jones, S.J., Kemp, G.D. & Tatner, M.F. (2000). Antibacterial proteins in rainbow trout, *Oncorhynchus mykiss*. *Fish & Shellfish Immunology*, *10*, 243-260.

[482] Song, B.H., Lee, G.C., Moon, M.S., Cho, Y.H. & Lee, C.H. (2001). Human cytomegalovirus binding to heparan sulfate proteoglycans on the cell surface and/or entry stimulates the expression of human leukocyte antigen class I. *Journal of General Virology*, *82*, 2405-2413.

[483] Sorensen, H.P. & Mortensen, K.K. (2005). Advanced genetic strategies for recombinant protein expression in *Escherichia coli*. *Journal of Biotechnology*, *115*, 113-128.

[484] Sperstad, S.V., Haug, T., Blencke, H.M., Styrvold, O.B., Li, C. & Stensvag, K. (2011). Antimicrobial peptides from marine invertebrates: challenges and perspectives in marine antimicrobial peptide discovery. *Biotechnology Advances*, *29*, 519-530.

[485] Srinivasula, S.M., Ahmad, M., Fernandes-Alnemri, T. & Alnemri, E.S. (1998). Autoactivation of procaspase-9 by Apaf-1-mediated. oligomerization *Molecular Cell*, *1*, 49-957.

[486] Srinivasulu, B., Syvitski, R., Seo, J.K., Mattatall, N.R., Knickle, L.C. & Douglas, S.E. (2008). Expression, purification and structural characterization of recombinant hepcidin, an antimicrobial peptide identified in Japanese flounder, *Paralichthys olivaceus*. *Protein Expression and Purification*, *61*, 36–44.

[487] Srinivasulu, B., Syvitski, R., Seo, J.K., Mattatall, N.R., Knickle, L.C. & Douglas, S.E. (2008). Expression, purification and structural characterization of recombinant hepcidin, an antimicrobial peptide identified in Japanese flounder, *Paralichthys olivaceus*. *Protein Expression and Purification*, *61*, 36-44

[488] Sruthy, K.S., Nair, A., Puthumana, J., Antony, S.P., Singh, I.B. & Philip, R. (2017). Molecular cloning, recombinant expression and functional characterization of an antimicrobial peptide, Crustin from the Indian white shrimp, *Fenneropenaeus indicus*. *Fish & Shellfish Immunology*, *71*, 83-94.

[489] Steinberg, D.A. & Lehrer, R.I. (1997). Designer assays for antimicrobial peptides. In *Antibacterial peptide protocols: Methods In Molecular Biology*. *Humana Press*, *78*, 169-186.

[490] Stewart, E.J., Aslund, F. & Beckwith, J. (1998). Disulfide bond formation in the *Escherichia coli* cytoplasm: An in vivo role reversal for the thioredoxins. *The EMBO journal*, *17*, 5543-5550.

[491] Stromstedt, A.A., Pasupuleti, M., Schmidtchen, A. & Malmsten, M. (2009). Evaluation of strategies for improving proteolytic resistance of antimicrobial peptides by using variants of EFK17, an internal segment of LL-37. *Antimicrobial Agents and Chemotherapy*, *53*, 593-602.

[492] Stromstedt, A.A., Ringstad, L., Schmidtchen, A. & Malmsten, M. (2010). Interaction between amphiphilic peptides and phospholipid membranes. *Current Opinion in Colloid & Interface Science*, *15*, 467-478.

[493] Studencka, M., Konzer, A., Moneron, G., Wenzel, D., Opitz, L., Salinas-Riester, G., Bedet, C., Krüger, M., Hell, S.W., Wisniewski, J.R. & Schmidt, H. (2012). Novel roles of *Caenorhabditis elegans* heterochromatin protein HP1 and linker histone in the regulation of innate immune gene expression. *Molecular and Cellular Biology*, *32*, 251-265.

[494] Stumpe, S., Schmid, R., Stephens, D.L., Georgiou, G. & Bakker, E.P. (1998). Identification of OmpT as the Protease That Hydrolyzes the Antimicrobial Peptide Protamine before It Enters Growing Cells ofEscherichia coli. *Journal of Bacteriology*, *180*, 4002-4006.

[495] Su, Y. (2011). Isolation and identification of pelteobagrin, a novel antimicrobial peptide from the skin mucus of yellow catfish (*Pelteobagrus fulvidraco*). *Comparative Biochemistry and Physiology Part B: Biochemistry and Molecular Biology*, *158*, 149-154.

[496] Subramanian, S., Ross, N.W. & MacKinnon, S.L. (2008). Comparison of the biochemical composition of normal epidermal mucus and extruded slime of hagfish (*Myxine glutinosa* L.). *Fish & Shellfish Immunology*, *25*, 625-632.

[497] Subramanian, S., Ross, N.W. & MacKinnon, S.L. (2009). Myxinidin, a novel antimicrobial peptide from the epidermal mucus of hagfish, *Myxine glutinosa* L. *Marine Biotechnology*, *11*, 748.

[498] Sun, B.J., Xie, H.X., Song, Y. & Nie, P. (2007). Gene structure of an antimicrobial peptide from mandarin fish, *Siniperca chuatsi* (Basilewsky), suggests that moronecidins and pleurocidins belong in one family: the piscidins. *Journal of Fish Diseases*, *30*, 335-343.

[499] Sun, D., Wu, S., Jing, C., Zhang, N., Liang, D. & Xu, A. (2012). Identification, synthesis and characterization of a novel antimicrobial peptide HKPLP derived from *Hippocampus kuda* Bleeker. *The Journal of Antibiotics*, *65*, 117.

[500] Sun, W., Wan, W., Zhu, S., Wang, S., Wang, S., Wen, X., Zheng, H., Zhang, Y. & Li, S. (2015). Characterization of a novel anti-lipopolysaccharide factor isoform (SpALF5) in mud crab, *Scylla paramamosain*. *Molecular Immunology*, *64*, 262-275.

[501] Sung, W.S., Lee, J. & Lee, D.G. (2008a). Fungicidal effect and the mode of action of piscidin 2 derived from hybrid striped bass. *Biochemical and Biophysical Research communications*, *371*, 551-555.

[502] Sung, W.S., Lee, J. & Lee, D.G. (2008b). Fungicidal effect of piscidin on *Candida albicans*: pore formation in lipid vesicles and activity in fungal membranes. *Biological and Pharmaceutical Bulletin*, *31*, 1906-1910.

[503] Svensson, S.L., Pasupuleti, M., Walse, B., Malmsten, M., Mörgelin, M., Sjögren, C., Olin, A.I., Collin, M., Schmidtchen, A., Palmer, R. & Egesten, A. (2010). Midkine and Pleiotrophin have bactericidal properties preserved antibacterial activity in a family of heparin-binding growth factors during evolution. *Journal of Biological Chemistry*, *285*, 16105-16115.

[504] Syvitski, R.T., Burton, I., Mattatall, N.R., Douglas, S.E. & Jakeman, D.L. (2005). Structural characterization of the antimicrobial peptide pleurocidin from winter flounder. *Biochemistry*, *44*, 7282–7293.

[505] Tagai, C., Morita, S., Shiraishi, T., Miyaji, K. & Iwamuro, S. (2011). Antimicrobial properties of arginine-and lysine-rich histones and involvement of bacterial outer membrane protease T in their differential mode of actions. *Peptides*, *32*, 2003-2009.

[506] Takahashi, H., Caputo, G.A., Vemparala, S. & Kuroda, K. (2017). Synthetic random copolymers as a molecular platform to mimic host-defense antimicrobial peptides. *Bioconjugate Chemistry*, *28*, 1340-1350.

[507] Tamamura, H., Ishihara, T., Otaka, A., Murakami, T., Ibuka, T., Waki, M., Matsumoto, A., Yamamoto, N. & Fujii, N. (1996). Analysis of the interaction of an anti-HIV peptide, T22 ([Tyr5, 12, Lys7]-polyphemusin II), with gp 120 and CD4 by surface plasmon resonance. *Biochimica et Biophysica Acta (BBA)-Protein Structure and Molecular Enzymology*, *1298*, 37-44.

[508] Tamamura, H., Waki, M., Imai, M., Otaka, A., Ibuka, T., Waki, K., Miyamoto, K., Matsumoto, A., Murakami, T., Nakashima, H. & Yamamoto, N. (1998). Downsizing of an HIV–cell fusion inhibitor, T22 ([Tyr5, 12, Lys7]-Polyphemusin II), with the maintenance of anti-HIV activity and solution structure1. *Bioorganic & Medicinal Chemistry*, *6*, 473-479.

[509] Tamang, D.G. & Saier Jr, M.H. (2006). The cecropin superfamily of toxic peptides. *Journal of molecular microbiology and biotechnology*, *11*, 94-103.

[510] Tanaka, Y., Tawaramoto-Sasanuma, M., Kawaguchi, S., Ohta, T., Yoda, K., Kurumizaka, H. & Yokoyama, S. (2004). Expression and purification of recombinant human histones. *Methods*, *33*, 3-11.

[511] Tao, R., Tong, Z., Lin, Y., Xue, Y., Wang, W., Kuang, R., Wang, P., Tian, Y. & Ni, L. (2011). Antimicrobial and antibiofilm activity of pleurocidin against cariogenic microorganisms. *Peptides*, *32*, 1748-1754.

[512] Tao, Y., Zhao, D. M., & Wen, Y. (2014). Expression, purification and antibacterial activity of the channel catfish hepcidin mature peptide. *Protein Expression and Purification*, *94*, 73–78.

[513] Teixeira, V., Feio, M.J. & Bastos, M. (2012). Role of lipids in the interaction of antimicrobial peptides with membranes. *Progress in Lipid Research*, *51*, 149-177.

[514] Tennessen, J.A. (2005). Enhanced synonymous site divergence in positively selected vertebrate antimicrobial peptide genes. *Journal of Molecular Evolution*, *61*, 445-455.

[515] Terova, G., Cattaneo, A.G., Preziosa, E., Bernardini, G. & Saroglia, M. (2011). Impact of acute stress on antimicrobial polypeptides mRNA copy number in several tissues of marine sea bass (*Dicentrarchus labrax*). *BMC Immunology*, *12*, 69.

[516] Terras, F.R., Schoofs, H.M., De Bolle, M.F., Van Leuven, F., Rees, S.B., Vanderleyden, J., Cammue, B.P. & Broekaert, W.F. (1992). Analysis of two novel classes of plant antifungal proteins from radish (*Raphanus sativus* L.) seeds. *Journal of Biological Chemistry*, *267*, 15301-15309.

[517] Thatcher, T. H. & Gorovsky, M. A. (1994). Phylogenetic analysis of the core histones H2A, H2B, H3, and H4. *Nucleic Acids Research 22*, 174–179.

[518] Thompson, S.A., Tachibana, K., Nakanishi, K. & Kubota, I. (1986). Melittin-like peptides from the shark-repelling defense secretion of the sole *Pardachirus pavoninus*. *Science*, *233*, 341–343.

[519] Tomasinsig, L. & Zanetti, M. (2005). The cathelicidins-structure, function and evolution. *Current Protein and Peptide Science*, *6*, 23-34.

[520] Tossi, A., D'Este, F., Skerlavaj, B. & Gennaro, R. (2017). Structural and Functional Diversity of Cathelicidins. *Antimicrobial Peptides: Discovery, Design and Novel Therapeutic Strategies*, 20-48.

[521] Tossi, A., Sandri, L. & Giangaspero, A. (2000). Amphipathic, α-helical antimicrobial peptides. *Peptide Science*, *55*, 4-30.

[522] Townes, C.L., Michailidis, G. & Hall, J. (2009). The interaction of the antimicrobial peptide cLEAP-2 and the bacterial membrane. *Biochemical and Biophysical Research Communications*, *387*, 500-503.

[523] Tsai, H. & Bobek, L.A. (1998). Human salivary histatins: Promising anti-fungal therapeutic agents. *Critical Reviews in Oral Biology & Medicine*, *9*, 480-497.

[524] Tsao, H.S., Spinella, S.A., Lee, A.T. & Elmore, D.E. (2009). Design of novel histone-derived antimicrobial peptides. *Peptides*, *30*, 2168-2173.

[525] Uematsu, N. & Matsuzaki, K. (2000). Polar angle as a determinant of amphipathic α-helix-lipid interactions: a model peptide study. *Biophysical Journal*, *79*, 2075-2083.

[526] Urban, C.F., Ermert, D., Schmid, M., Abu-Abed, U., Goosmann, C., Nacken, W., Brinkmann, V., Jungblut, P.R. & Zychlinsky, A. (2009). Neutrophil extracellular traps contain calprotectin, a cytosolic protein complex involved in host defense against *Candida albicans*. *PLoS pathogens*, *5*.

[527] Urban, C.F., Reichard, U., Brinkmann, V. & Zychlinsky, A. (2006). Neutrophil extracellular traps capture and kill *Candida albicans* yeast and hyphal forms. *Cellular Microbiology*, *8*, 668-676.

[528] Utsugi, T., Schroit, A.J., Connor, J., Bucana, C.D. & Fidler, I.J. (1991). Elevated expression of phosphatidylserine in the outer membrane leaflet of human tumor cells and recognition by activated human blood monocytes. *Cancer Research*, *51*, 3062-3066.

[529] Uyterhoeven, E.T., Butler, C.H., Ko, D. & Elmore, D.E. (2008). Investigating the nucleic acid interactions and antimicrobial mechanism of buforin II. *FEBS Letters*, *582*, 1715-1718.

[530] Uzzell, T., Stolzenberg, E.D., Shinnar, A.E. & Zasloff, M. (2003). Hagfish intestinal antimicrobial peptides are ancient cathelicidins. *Peptides*, *24*, 1655-1667.

[531] Valore, E.V. & Ganz, T. (2008). Posttranslational processing of hepcidin in human hepatocytes is mediated by the prohormone convertase furin. *Blood Cells, Molecules, and Diseases*, *40*, 132-138.

[532] van der Weerden, N.L., Hancock, R.E. & Anderson, M.A. (2010). Permeabilization of fungal hyphae by the plant defensin NaD1 occurs through a cell wall-dependent process. *Journal of Biological Chemistry*, *285*, 37513-37520.

[533] Van Muiswinkel, W. & Vervoorn-Van Der Waal, B. (2006). The immune system of fish, In: Woo, P.T.K. (Ed.), *Fish Diseases and Disorders*, 2nd Ed. CAB International,Wallingford, 678–701.

[534] van't Hof W., Veerman E.C., Helmerhorst E.J. & Amerongen A.V. (2001). Antimicrobial peptides: properties and applicability. *The Journal of Biological Chemistry*, *382*, 597-619.

[535] Vassilevski, A.A., Kozlov, S.A., Samsonova, O.V., Egorova, N.S., Karpunin, D.V., Pluzhnikov, K.A., Feofanov, A.V. & Grishin, E.V. (2008). Cyto-insectotoxins, a novel class of cytolytic and insecticidal peptides from spider venom. *Biochemical Journal*, *411*, 687-696.

[536] Vizioli, J. & Salzet, M. (2002). Antimicrobial peptides from animals: Focus on invertebrates. *Trends in Pharmacological Sciences*, *23*, 494-496.

[537] Vogt, T.C. & Bechinger, B. (1999). The interactions of histidine-containing amphipathic helical peptide antibiotics with lipid bilayers: The effects of charges and pH. *Journal of Biological Chemistry*, *274*, 29115-29121.

[538] Wallace, D.F., Jones, M.D., Pedersen, P., Rivas, L., Sly, L.I. & Subramaniam, V.N. (2006). Purification and partial characterisation of recombinant human hepcidin. *Biochimie*, *88*, 31-37.

[539] Wang, D., Li, S., Zhao, J., Liu, H., Lu, T. & Yin, J. (2016). Genomic organization, expression and antimicrobial activity of a hepcidin from taimen (*Hucho taimen,* Pallas). *Fish & Shellfish Immunology*, *56*, 303-309.

[540] Wang, G., Li, J., Zou, P., Xie, H., Huang, B., Nie, P. & Chang, M. (2012). Expression pattern, promoter activity and bactericidal property of beta-defensin from the mandarin fish *Siniperca chuatsi*. *Fish & Shellfish Immunology*, *33*, 522–531.

[541] Wang, H., Wang, H., Zhang, W., Huang, H.J., Liao, W.S. & Fuller, G.N. (2004). Analysis of the activation status of Akt, NFκB, and Stat3 in human diffuse gliomas. *Laboratory Investigation*, *84*, 941.

[542] Wang, K., Dang, W., Yan, J., Chen, R., Liu, X., Yan, W., Zhang, B., Xie, J., Zhang, J. & Wang, R. (2013). Membrane perturbation action mode and structure-activity relationships of Protonectin, a novel antimicrobial peptide from the venom of the neotropical social wasp *Agelaia pallipes pallipes*. *Antimicrobial Agents and Chemotherapy*, *57*, 4632-4639.

[543] Wang, K.J., Cai, J.J., Cai, L., Qu, H.D., Yang, M. & Zhang, M. (2009). Cloning and expression of a hepcidin gene from a marine fish (*Pseudosciaena crocea*) and the antimicrobial activity of its synthetic peptide. *Peptides*, *30*, 638–646.

[544] Wang, K.J., Cai, J.J., Cai, L., Qu, H.D., Yang, M. & Zhang, M. (2009). Cloning and expression of a hepcidin gene from a marine fish (*Pseudosciaena crocea*) and the antimicrobial activity of its synthetic peptide. *Peptides*, *30*, 638-646.

[545] Wang, K.R., Zhang, B.Z., Zhang, W., Yan, J.X., Li, J. & Wang, R. (2008). Antitumor effects, cell selectivity and structure–activity relationship of a novel antimicrobial peptide polybia-MPI. *Peptides*, *29*, 963-968.

[546] Wang, W., Tao, R., Tong, Z., Ding, Y., Kuang, R., Zhai, S., Liu, J. & Ni, L. (2012). Effect of a novel antimicrobial peptide chrysophsin-1 on oral pathogens and *Streptococcus mutans* biofilms. *Peptides*, *33*, 212-219.

[547] Wang, Y.D., Kung, C.W. & Chen, J.Y. (2010). Antiviral activity by fish antimicrobial peptides of epinecidin-1 and hepcidin 1–5 against nervous necrosis virus in medaka. *Peptides*, *31*, 1026-1033.

[548] Ward, R., Bowman, A., El-Mkami, H., Owen-Hughes, T. & Norman, D.G. (2009). Long distance PELDOR measurements on the histone core particle. *Journal of the American Chemical Society*, *131*, 1348-1349.

[549] Wei, O.Y., Xavier, R. & Marimuthu, K. (2010). Screening of antibacterial activity of mucus extract of snakehead fish, *Channa striatus* (Bloch). *European Review for Medical and Pharmacological Sciences*, *14*, 675-681.

[550] Wei, X., Babu, V.S., Lin, L., Hu, Y., Zhang, Y., Liu, X., Su, J., Li, J., Zhao, L. & Yuan, G. (2018). Hepcidin protects grass carp (*Ctenopharyngodon idellus*) against *Flavobacterium columnare* infection *via* regulating iron distribution and immune gene expression. *Fish & Shellfish Immunology*. *75*, 274-283.

[551] Wen, L. L., Zhao, M. L., Chi, H. & Sun, L. (2017). Histones and chymotrypsin-like elastases play significant roles in the antimicrobial activity of tongue sole neutrophil extracellular traps. *Fish & Shellfish Immunology*, *72*, 470-476.

[552] Westerhoff, H.V., Juretić, D., Hendler, R.W. & Zasloff, M. (1989). Magainins and the disruption of membrane-linked free-energy transduction. *Proceedings of the National Academy of Sciences*, *86*, 6597-6601.

[553] Wieprecht, T., Dathe, M., Epand, R.M., Beyermann, M., Krause, E., Maloy, W.L., MacDonald, D.L. & Bienert, M. (1997). Influence of the angle subtended by the positively charged helix face on the membrane activity of amphipathic, antibacterial peptides. *Biochemistry*, *36*, 12869-12880.

[554] Wiesner, J. & Vilcinskas, A. (2010). Antimicrobial peptides: the ancient arm of the human immune system. *Virulence*, *1*, 440-464.

[555] Wolffe, A.P. & Guschin, D. (2000). Chromatin structural features and targets that regulate transcription. *Journal of Structural Biology*, *129*, 102-122.

[556] Wu, D., Gao, Y., Qi, Y., Chen, L., Ma, Y. and Li, Y. (2014). Peptide-based cancer therapy: opportunity and challenge. *Cancer Letters*, *351*, 13-22.

[557] WuDunn, D. & Spear, P.G. (1989). Initial interaction of herpes simplex virus with cells is binding to heparan sulfate. *Journal of Virology*, *63*, 52–58.

[558] Xie, J., Gou, Y., Zhao, Q., Wang, K., Yang, X., Yan, J., Zhang, W., Zhang, B., Ma, C. & Wang, R. (2014). Antimicrobial activities and membrane-active mechanism of CPF-C1 against multidrug-resistant bacteria, a novel antimicrobial peptide derived from skin secretions of the tetraploid frog *Xenopus clivii*. *Journal of Peptide Science*, *20*, 876-884.

[559] Xiong, M. & Waterman, M.S. (1997). A phase transition for the minimum free energy of secondary structures of a random RNA. *Advances in Applied Mathematics*, *18*, 111-132.

[560] Xiong, Y.Q., Bayer, A.S. & Yeaman, M.R. (2002). Inhibition of intracellular macromolecular synthesis in *Staphylococcus aureus* by thrombin-induced platelet microbicidal proteins. *The Journal of Infectious Diseases*, *185*, 348-356.

[561] Xu, P., Bao, B., He, Q., Peatman, E., He, C. & Liu, Z. (2005). Characterization and expression analysis of bactericidal permeability-increasing protein (BPI) antimicrobial peptide gene from channel catfish *Ictalurus punctatus*. *Developmental & Comparative Immunology*, *29*, 865-878.

[562] Xu, Q., Cheng, C.H.C., Hu, P., Ye, H., Chen, Z., Cao, L., Chen, L., Shen, Y. & Chen, L. (2008). Adaptive evolution of hepcidin genes in antarctic notothenioid fishes. *Molecular Biology and Evolution*, *25*, 1099-1112.

[563] Xu, T., Sun, Y., Shi, G. & Wang, R. (2012). Miiuy croaker hepcidin gene and comparative analyses reveal evidence for positive selection. *PLoS One*, *7*(4).

[564] Xu, X., Jin, F., Yu, X., Ji, S., Wang, J., Cheng, H., Wang, C. & Zhang, W. (2007). Expression and purification of a recombinant antibacterial peptide, cecropin, from *Escherichia coli*. *Protein Expression and Purification*, *53*, 293-301.

[565] Xu, Z., Peng, L., Zhong, Z., Fang, X. & Cen, P. (2006). HighLevel Expression of a Soluble Functional Antimicrobial Peptide, Human βDefensin 2, in *Escherichia coli*. *Biotechnology Progress*, *22*, 382-386.

[566] Yadav, D.K., Yadav, N., Yadav, S., Haque, S. & Tuteja, N. (2016). An insight into fusion technology aiding efficient recombinant protein production for functional proteomics. *Archives of Biochemistry and Biophysics*, *612*, 57-77.

[567] Yang, G., Guo, H., Li, H., Shan, S., Zhang, X., Rombout, J.H. & An, L. (2014). Molecular characterization of LEAP-2 cDNA in common carp (*Cyprinus carpio* L.) and the differential expression upon a *Vibrio anguillarum* stimulus; indications for a significant immune role in skin. *Fish & Shellfish Immunology*, *37*, 22-29.

[568] Yang, M., Chen, B., Cai, J.J., Peng, H., Yuan, J.J. &Wang, K.J. (2011). Molecular characterization of hepcidin AS-hepc2 and AS-hepc6 in black porgy (*Acanthopagrus schlegelii*): expression pattern responded to bacterial challenge and in vitro antimicrobial activity. *Comparative Biochemistry and Physiology* Part B*: Biochemistry and Molecular Biology*, *158*, 155-163.

[569] Yang, M., Wang, K.J., Chen, J.H., Qu, H.D. & Li, S.J. (2007). Genomic organization and tissue-specific expression analysis of hepcidin-like genes from black porgy (*Acanthopagrus schlegelii* B.). *Fish & Shellfish Immunology*, *23*, 1060-1071.

[570] Yau, W.M., Wimley, W.C., Gawrisch, K. & White, S.H. (1998). The preference of tryptophan for membrane interfaces. *Biochemistry*, *37*, 14713-14718.

[571] Yeaman, M.R. & Yount, N.Y. (2003). Mechanisms of antimicrobial peptide action and resistance. *Pharmacological Reviews*, *55*, 27-55.

[572] Yeaman, M.R., Bayer, A.S., Koo, S.P., Foss, W. & Sullam, P.M. (1998). Platelet microbicidal proteins and neutrophil defensin disrupt the *Staphylococcus aureus* cytoplasmic membrane by distinct mechanisms of action. *The Journal of Clinical Investigation*, *101*, 178-187.

[573] Yi, G. S., Park, C. B., Kim, S. C. & Cheong, C. (1996). Solution structure of an antimicrobial peptide buforin II. *FEBS Letters*, *398*, 87–90.

[574] Yin, L.M., Edwards, M.A., Li, J., Yip, C.M. & Deber, C.M. (2012). Roles of hydrophobicity and charge distribution of cationic antimicrobial peptides in peptide-membrane interactions. *Journal of Biological Chemistry*, *287*, 7738-7745.

[575] Yokoyama, S., Iida, Y., Kawasaki, Y., Minami, Y., Watanabe, K. & Yagi, F. (2009). The chitin-binding capability of Cy-AMP1 from cycad is essential to antifungal activity. *Journal of Peptide Science*, *15*, 492-497.

[576] Yoshida, K., Mukai, Y., Niidome, T., Takashi, C., Tokunaga, Y., Hatakeyama, T. & Aoyagi, H. (2001). Interaction of pleurocidin and its analogs with phospholipid membrane and their antibacterial activity. *Journal of Peptide Research*, *57*, 119–126.

[577] Yount, N.Y., Bayer, A.S., Xiong, Y.Q. & Yeaman, M.R. (2006). Advances in antimicrobial peptide immunobiology. *Peptide Science*, *84*, 435-458.

[578] Zanetti, M., Gennaro, R. & Romeo, D. (1995). Cathelicidins: a novel protein family with a common proregion and a variable C-terminal antimicrobial domain. *FEBS Letters*, *374*, 1-5.

[579] Zarrinnahad, H., Mahmoodzadeh, A., Hamidi, M. P., Mahdavi, M., Moradi, A., Bagheri, K. P. & Shahbazzadeh, D. (2017). Apoptotic Effect of Melittin Purified from Iranian Honey Bee Venom on Human Cervical Cancer HeLa Cell Line. *International Journal of Peptide Research and Therapeutics*, 1-9.

[580] Zasloff, M. (1987). Magainins, a class of antimicrobial peptides from *Xenopus* skin: Isolation, characterization of two active forms, and partial cDNA sequence of a precursor. *Proceedings of the National Academy of Sciences*, *84*, 5449-5453.

[581] Zasloff, M. (2002). Antimicrobial peptides of multicellular organisms. *Nature*, 415, 389.

[582] Zelezetsky, I. & Tossi, A. (2006). Alpha-helical antimicrobial peptides—using a sequence template to guide structure–activity relationship studies. *Biochimica et Biophysica Acta (BBA)-Biomembranes*, *1758*, 1436-1449.

[583] Zhang, A.S., Xiong, S., Tsukamoto, H. & Enns, C.A. (2004). Localization of iron metabolism–related mRNAs in rat liver indicate that HFE is expressed predominantly in hepatocytes. *Blood*, *103*, 1509-1514.

[584] Zhang, D., Wang, H., He, H., Niu, H. & Li, Y. (2017). Interferon induced transmembrane protein 3 regulates the growth and invasion of human lung adenocarcinoma. *Thoracic Cancer*, *8*, 337-343.

[585] Zhang, G., Fang, X., Guo, X., Li, L., Luo, R., Xu, F., Yang, P., Zhang, L., Wang, X., Qi, H. & Xiong, Z. (2012). The oyster genome reveals stress adaptation and complexity of shell formation. *Nature*, *490*, 49.

[586] Zhang, H., Yuan, Q., Zhu, Y. & Ma, R. (2005). Expression and preparation of recombinant hepcidin in *Escherichia coli*. *Protein Expression and Purification*, *41*, 409-416.

[587] Zhang, J., Yu, L. P., Li, M. F. & Sun, L. (2014). Turbot (*Scophthalmus maximus*) hepcidin-1 and hepcidin-2 possess antimicrobial activity and promote resistance against bacterial and viral infection. *Fish and Shellfish Immunology*, *38*, 127–134.

[588] Zhang, L., Rozek, A. & Hancock, R.E. (2001). Interaction of cationic antimicrobial peptides with model membranes. *Journal of Biological Chemistry*, *276*, 35714-35722.

[589] Zhang, W., Li, J., Liu, L.W., Wang, K.R., Song, J.J., Yan, J.X., Li, Z.Y., Zhang, B.Z. & Wang, R. (2010). A novel analog of antimicrobial peptide Polybia-MPI, with thioamide bond substitution, exhibits increased therapeutic efficacy against cancer and diminished toxicity in mice. *Peptides*, 31, 1832-1838.

[590] Zhang, X.J., Zhang, X.Y., Zhang, N., Guo, X., Peng, K.S., Wu, H., Lu, L.F., Wu, N., Chen, D.D., Li, S. & Nie, P. (2015). Distinctive structural hallmarks and biological activities of the multiple cathelicidin antimicrobial peptides in a primitive teleost fish. *The Journal of Immunology*, *194*, 4974-4987.

[591] Zhang, X.L., Selsted, M.E. & Pardi, A. (1992). NMR studies of defensin antimicrobial peptides. 1. Resonance assignment and secondary structure determination of rabbit NP-2 and human HNP-1. *Biochemistry*, *31*, 11348-11356.

[592] Zhang, Y.A., Zou, J., Chang, C.I. & Secombes, C.J. (2004). Discovery and characterization of two types of liver-expressed antimicrobial peptide 2 (LEAP-2) genes in rainbow trout. *Veterinary Immunology and Immunopathology*, *101*, 259-269.

[593] Zhao, C., Ganz, T. & Lehrer, R.I. (1995). Structures of genes for two cathelin-associated antimicrobial peptides: prophenin-2 and PR-39. *FEBS Letters*, *376*, 130-134.

[594] Zhao, H., Tang, J., Cao, L., Jia, G., Long, D., Liu, G., Chen, X., Cai, J. & Shang, H. (2015). Characterization of bioactive recombinant antimicrobial peptide parasin I fused with human lysozyme expressed in the yeast *Pichia pastoris* system. *Enzyme and Microbial Technology*, *77*, 61-67.

[595] Zhao, J.G., Zhou, L., Jin, J.Y., Zhao, Z., Lan, J., Zhang, Y.B., Zhang, Q.Y. & Gui, J.F. (2009). Antimicrobial activity-specific to Gram-negative bacteria and immune modulation-mediated NF-κB and Sp1 of a medaka β-defensin. *Developmental & Comparative Immunology*, *33*, 624-637.

[596] Zheng, L.B., Mao, Y., Wang, J., Chen, R.N., Su, Y.Q., Hong, Y.Q., Hong, Y.J. & Hong, Y.C. (2018). Excavating differentially expressed antimicrobial peptides from transcriptome of *Larimichthys crocea* liver in response to *Cryptocaryon irritans*. *Fish & Shellfish Immunology*. *75*, 109-114.

[597] Zheng, W., Liu, G., Ao, J. & Chen, X. (2006). Expression analysis of immune-relevant genes in the spleen of large yellow croaker (*Pseudosciaena crocea*) stimulated with poly I: C. *Fish & Shellfish Immunology*, *21*, 414-430.

[598] Zhong, Z., Xu, Z., Peng, L., Huang, L., Fang, X. & Cen, P. (2006). Tandem repeat mhBD2 gene enhance the soluble fusion expression of hBD2 in *Escherichia coli*. *Applied Microbiology and Biotechnology*, *71*, 661-667.

[599] Zhou, J.G., Wei, J.G., Xu, D., Cui, H.C., Yan, Y., Ou-Yang, Z.L., Huang, X.H., Huang, Y.H. & Qin, Q.W. (2011). Molecular cloning and characterization of two novel hepcidins from orange-spotted grouper, *Epinephelus coioides*. *Fish & Shellfish Immunology*, *30*, 559-568.

[600] Zhou, Q.J., Su, Y.Q., Niu, S.F., Liu, M., Qiao, Y. & Wang, J. (2014). Discovery and molecular cloning of piscidin-5-like gene from the large yellow croaker (*Larimichthys crocea*). *Fish & shellfish immunology*, *41*, 417-420.

[601] Zhu, J., Wang, H., Wang, J., Wang, X., Peng, S., Geng, Y., Wang, K., Ouyang, P., Li, Z., Huang, X. & Chen, D. (2017). Identification and characterization of a β-defensin gene involved in the immune defense response of channel catfish, *Ictalurus punctatus*. *Molecular Immunology, 85*, 256-264.

[602] Zhu, S. & Gao, B. (2013). Evolutionary origin of β-defensins. *Developmental & Comparative Immunology*, *39*, 79-84.

[603] Zhuang, Z.R., Yang, X.D., Huang, X.Z., Gu, H.X., Wei, H.Y., He, Y.J. & Deng, L. (2017). Three new piscidins from orange-spotted grouper (*Epinephelus coioides*): Phylogeny, expression and functional characterization. *Fish & Shellfish Immunology*, *66*, 240–253.

[604] Zou, J., Mercier, C., Koussounadis, A. & Secombes, C. (2007). Discovery of multiple beta-defensin like homologues in teleost fish. *Molecular Immunology*, *44*, 638-647.

## GenBank Submissions

1) GenBank accession number **KM034809.** Aishwarya Nair, Swapna P. Antony, Chaitanya, E.R., Naveen Sathyan, Sruthy, K. S., Bright Singh, I.S. and Rosamma Philip. (2014). *Leiognathus equulus* hepcidin mRNA, complete cds.

2) GenBank accession number **KU949385.** Aishwarya Nair, Sruthy, K.S., Bright Singh, I.S. and Rosamma Philip. (2016). *Leiognathus equulus* cytochrome oxidase subunit 1 gene, partial cds, mitochondrial.

3) GenBank accession number **MF966482.** Aishwarya Nair, Naveen Sathyan, Sruthy, K. S., Chaitanya, E.R., Neema Job, Rosamma Philip, Bright Singh, I.S. and Swapna P. Antony. (2017). *Mugil cephalus*, histone H2A mRNA, partial cds.

4) GenBank accession number **MF966483.** Aishwarya Nair, Naveen Sathyan, Sruthy, K. S., Chaitanya, E.R., Swapna P. Antony, Bright Singh, I.S. and Rosamma Philip. (2017). *Etroplus maculatus*, histone H2A mRNA, partial cds.

.....ꕥ.....

# List of Publications

1) **Aishwarya Nair**, Sruthy, K.S., Chaithanya, E.R., Sajeevan, T.P., I. S. Bright Singh, Rosamma Philip. Molecular Characterisation of a Novel Isoform of Hepatic Antimicrobial Peptide, Hepcidin (*Le*-Hepc), from *Leiognathus equulus* and Analysis of Its Functional Properties *In Silico*. Probiotics and antimicrobial proteins, 2017: 9, 473-482.

2) Sruthy, K. S., **Aishwarya Nair**, Jayesh Puthumana, Swapna P. Antony, I. S. Bright Singh, Rosamma Philip. Molecular Cloning, Recombinant Expression and Functional Characterization of an Antimicrobial Peptide, Crustin from the Indian White Shrimp, *Fenneropenaeus indicus*. Fish & Shellfish Immunology, 2017: 71, 83-94.

3) Sruthy K. S., **Aishwarya Nair**, Sherine Sonia Cubelio, I. S. Bright Singh, Rosamma Philip. Molecular Characterization and Phylogenetic Analysis of an Antilipopolysaccharide Factor from the Crucifix Crab, *Charybdis feriatus*, Open access Animal Physiology, 2015: 7, 149-156.

4) Sruthy K. S., Chaithanya E. R., Naveen Sathyan, **Aishwarya Nair**, Swapna P. Antony, I. S. Bright Singh, Rosamma Philip. Molecular Characterization and Phylogenetic Analysis of Novel Isoform of Anti-Lipopolysaccharide Factor from the Mantis Shrimp, *Miyakea nepa*. Probiotics and Antimicrobial Proteins, 2015: *7*, 275-283.